

Inhibition of Heat Shock Protein 90 Reduces Inflammatory Signal Transduction in
Murine J774 Macrophage Cells and Lessens Disease in Autoimmune MRL/lpr Mice:
What *in vitro*, *in vivo*, and *in silico* Models Reveal

Samuel Kline Shimp III

Dissertation submitted to the faculty of the Virginia Polytechnic Institute and State
University in partial fulfillment of the requirements for the degree of

Doctor of Philosophy
In
Biomedical Engineering

M. Nichole Rylander, Committee Co-Chair

Christopher M. Reilly Co-Chair

Yong W. Lee

Luke E. Achenie

David L. Caudell

30 April 2012

Blacksburg, Virginia

Keywords: heat shock protein 90, inflammation, computational models, geldanamycin,
17-DMAG, nuclear factor- κ B

Copyright (2012)

Inhibition of Heat Shock Protein 90 Reduces Inflammatory Signal Transduction in Murine J774 Macrophage Cells and Lessens Disease in Autoimmune MRL/lpr Mice: What *in vitro*, *in vivo*, and *in silico* Models Reveal

Samuel Kline Shimp III

ABSTRACT

Heat shock protein 90 (HSP90) is a molecular chaperone protein that protects proteins from degradation, repairs damaged proteins, and assists proteins in carrying out their functions. HSP90 has hundreds of clients, many of which are inflammatory signaling kinases. The mechanism by which HSP90 enables inflammatory pathways is an active area of investigation. The HSP90 inhibitors such as geldanamycin (GA) and its derivative 17-dimethylaminoethylamino-17-demethoxygeldanamycin (17-DMAG) have been shown to reduce inflammation. It was hypothesized that inhibiting HSP90 would reduce inflammatory signal cascade levels.

To test this, J774 mouse macrophage cells were treated with 17-DMAG and immune-stimulated with lipopolysaccharide (LPS). 17-DMAG treatment reduced nitric oxide (NO) production and the expression of pro-inflammatory cytokines interleukin (IL)-6, IL-12, and TNF- α . Inhibition of HSP90 also prevented nuclear translocation of NF- κ B.

To investigate the anti-inflammatory effects of HSP90 inhibition *in vivo*, MRL/lpr lupus mice were administered 5 mg/kg 17-DMAG for six weeks via intraperitoneal injection. Mice treated with 17-DMAG were found to have reduced proteinuria and reduced splenomegaly. Flow cytometric analysis of splenocytes showed that 17-DMAG decreased double negative T (DNT) cells. Renal expression of HSP90 was also measured and found to be increased in MRL/lpr mice that did not receive 17-DMAG.

The mechanistic interactions between HSP90 and the pro-inflammatory nuclear factor- κ B (NF- κ B) pathway were studied and a computational model was developed. The model predicts cellular response of inhibitor of κ B kinase (IKK) activation and NF- κ B activation to LPS stimulation. Model parameters were fit to IKK activation data. Parameter sensitivity was assessed through simulation studies and showed a strong dependence on IKK-HSP90 binding. The model also accounts for the effect of a general HSP90 inhibitor to disrupt the IKK-HSP90 interaction for reduced activation of NF- κ B. Model simulations were validated with experimental data.

In conclusion, HSP90 facilitates inflammation through multiple signal pathways including Akt and IKK. Inhibition of HSP90 by 17-DMAG reduced disease in the MRL/lpr lupus mouse model. A computational model supported the hypothesis that HSP90 is required for IKK to activate the NF- κ B pathway. Taken together, HSP90 is a prime target for therapeutic regulation of many inflammatory processes and warrants further study to understand its mechanism of regulating cell signaling cascades.

DEDICATION

The toilsome hours that went into this work are completely dedicated to my wife, Kela. Without her patient and loving support I could not have completed any of this. When I was ready to give up, she was there to encourage me and lift me up. When experiments weren't working out, she was there to listen to my frustrations. When there were obstacles her kind and loving advice helped me overcome them, even if I didn't listen at first. I could not have asked for a better companion for this undertaking.

I am also happy to have shared this experience with my three wonderful sons, two of which joined our family during this time. They kept me grounded in the reality that exists outside of the research lab and reminded that this work is for their future. They also provided me with insightful artwork, as shown below in a diagram of a cell.

This work is also dedicated to the many people who suffer from autoimmune diseases such as lupus. My efforts have been to bring the world closer to a treatment, or even better, a cure.

HUMAN BODY

THE INSIDE OF
A CELL IS PACKED
WITH A KIND OF
LIVING JELLY CALLED CYTOPLASM.



The inside of a cell, as drawn by Kline, Age 5. Note the inclusion of structures such as nucleus, endoplasmic reticulum, mitochondria, etc.

ACKNOWLEDGEMENTS

This work could not have been completed without the wonderful help and support of many colleagues. Dr. Rylander's efforts to secure funding for this work were one of the greatest contributions. As my principle advisor, Dr. Rylander has also been a great source of encouragement and optimism.

Dr. Reilly has been not only a great advisor in the realm of immunology and autoimmune disease; he has been a great friend. I am grateful to have been able to work with him and learn from him.

I thank my wonderful committee for their patience and help. Dr. Lee, Dr. Caudell, and Dr. Achenie have all provided invaluable and timely advice that made this project possible.

I thank all of my colleagues in the lab, Cara, Chris S, Chris A, Jon, Bryce, Kristen, Matt, Alana, Cristen, Nicole, Sarah, Alicia, and Abby. They have all been a great source of support and help in the conduct of science and the preparation of these manuscripts.

I also thank the help of the several excellent undergraduates that worked with me over the years, Caitlin, Morgan, Carl, and Molly.

TABLE OF CONTENTS

| | |
|---|-----------------|
| ABSTRACT | II |
| DEDICATION..... | IV |
| ACKNOWLEDGEMENTS..... | VI |
| TABLE OF CONTENTS..... | VII |
| LIST OF FIGURES..... | XIV |
| LIST OF TABLES | XVII |
| LIST OF ABBREVIATIONS..... | XVIII |
| ATTRIBUTION..... | XXII |
| CHAPTER 1. INTRODUCTION..... | 1 |
| <i>1.1 MOTIVATION FOR RESEARCH.....</i> | <i>1</i> |
| <i>1.2 BACKGROUND.....</i> | <i>1</i> |
| <i>1.2.1 Systemic lupus erythematosus.....</i> | <i>3</i> |
| <i>1.2.2 Heat shock protein 90</i> | <i>6</i> |
| <i>1.2.3 Modeling.....</i> | <i>8</i> |
| <i>1.3 HYPOTHESIS</i> | <i>9</i> |
| REFERENCES | 12 |

**CHAPTER 2. HSP90 INHIBITION BY 17-DMAG REDUCES
INFLAMMATION IN J774 MACROPHAGES THROUGH
SUPPRESSION OF AKT AND NUCLEAR FACTOR- κ B
PATHWAYS..... 27**

ABSTRACT..... 27

2.1 INTRODUCTION 28

2.2 METHODS..... 30

2.3 RESULTS..... 33

 2.3.1 17-DMAG reduced viability in immune-stimulated cells..... 33

 2.3.2 17-DMAG decreases Akt and IKK α expression 35

 2.3.3 Translocation of NF- κ B was inhibited in cells treated with 17-DMAG.
 38

 2.3.4 HSP70 expression increased, HSP90 expression was unchanged in
 LPS/IFN- γ stimulated cells treated with 17-DMAG..... 40

 2.3.5 Immune-stimulated NO production and IL-6 expression were
 reduced in response to treatment with 17-DMAG 43

2.4 DISCUSSION 46

2.5 ACKNOWLEDGEMENTS 51

REFERENCES 52

| | |
|---|-----------|
| CHAPTER 3. HEAT SHOCK PROTEIN 90 INHIBITION BY 17-DMAG LESSENS DISEASE IN THE MRL/LPR MOUSE MODEL OF SYSTEMIC LUPUS ERYTHEMATOSUS..... | 62 |
| ABSTRACT..... | 62 |
| 3.1 INTRODUCTION | 63 |
| 3.2 MATERIALS AND METHODS..... | 65 |
| 3.2.1 Mesangial Cell Culture | 65 |
| 3.2.2 In Vitro Inhibition of HSP90 using Geldanamycin..... | 65 |
| 3.2.3 Cytokine ELISA and Griess assay | 65 |
| 3.2.4 Mice..... | 66 |
| 3.2.5 Treatment of mice with 17-DMAG | 66 |
| 3.2.6 Histology of the Kidney..... | 67 |
| 3.2.7 Measurement of Proteinuria | 67 |
| 3.2.8 Anti-dsDNA ELISA | 68 |
| 3.2.9 Flow cytometry | 68 |
| 3.2.10 Statistics..... | 69 |
| 3.3 RESULTS..... | 69 |
| 3.3.1 HSP90 inhibition reduced inflammatory mediator production in stimulated mesangial cells | 69 |
| 3.3.2 Proteinuria was reduced in mice treated with 17-DMAG..... | 72 |
| 3.3.3 Treatment with HSP90 inhibitor 17-DMAG reduced serum anti-dsDNA antibodies but not total IgG | 74 |

| | |
|--|-----------|
| 3.3.4 Renal deposition of IgG and C3 were unaffected by 17-DMAG treatment..... | 74 |
| 3.3.5 HSP90 expression increased in untreated MRL/lpr mice, compared to MRL/lpr mice treated with 17-DMAG and untreated C57BL/6 mice. | 77 |
| 3.3.6 Reduction of splenomegaly by 17-DMAG | 79 |
| 3.3.7 17-DMAG altered splenocyte profiles in MRL/lpr lupus mice | 80 |
| 3.4 DISCUSSION..... | 87 |
| 3.5 ACKNOWLEDGEMENTS | 93 |
| REFERENCES..... | 94 |

CHAPTER 4. COMPUTATIONAL MODEL OF NF- κ B: INHIBITION OF HEAT SHOCK PROTEIN 90 REDUCES CHRONIC ACTIVATION OF NUCLEAR FACTOR- κ B BY PREVENTING HEAT SHOCK PROTEIN CHAPERONING OF INHIBITOR OF κ B KINASE

..... **108**

| | |
|--|------------|
| ABSTRACT..... | 108 |
| 4.1 BACKGROUND..... | 109 |
| 4.2 MODEL DESCRIPTION | 112 |
| 4.2.1 Notation Guide | 113 |
| 4.2.2 Model Equations | 114 |
| 4.3 MATERIALS AND METHODS..... | 121 |
| 4.4 RESULTS AND DISCUSSION..... | 124 |

| | |
|--|------------|
| 4.4.1 IKK activation profile sensitive to HSP90 binding rate..... | 124 |
| 4.4.2 Parameters were fit using experimental data from mouse embryonic fibroblasts..... | 133 |
| 4.4.3 Sensitivity of I_{HSP90} parameters was assessed..... | 136 |
| 4.4.4 Simulated IKK ρ , I κ B α , and NF- κ B profiles agree with experimentally measured data | 139 |
| 4.5 CONCLUSIONS..... | 142 |
| REFERENCES | 144 |
| CHAPTER 5. SUMMARY AND FUTURE WORK | 152 |
| 5.1 CONCLUSIONS..... | 152 |
| 5.1.1 What we learned about HSP90 and inflammation from <i>in vitro</i> studies..... | 152 |
| 5.1.2 How does HSP90 affect inflammation and autoimmunity in an <i>in vivo</i> model? | 153 |
| 5.2 FUTURE WORK..... | 154 |
| 5.2.1 Revisiting <i>in vitro</i> work to validate the current model and extend it to include cytokine production | 154 |
| 5.2.2 Studying the effects of HSP70 on inflammation | 155 |
| 5.2.3 Linking HSP90 to T cell activation..... | 155 |
| 5.2.4 Other potential research directions | 156 |
| 5.3 FINAL REMARKS..... | 156 |
| REFERENCES | 157 |

| | |
|--|------------|
| APPENDICES..... | 159 |
| APPENDIX A. DEVELOPMENT OF TOTAL IGG ELISA FOR ANALYZING MOUSE | |
| SERUM..... | 160 |
| APPENDIX B. COMPLETE MODEL RESPONSE FOR INITIAL PARAMETER | |
| SENSITIVITY STUDY..... | 164 |
| APPENDIX C. COMPLETE MODEL RESPONSE FOR HSP90 INHIBITOR | |
| PARAMETRIC STUDY | 175 |
| APPENDIX D. COMPLETE MODEL RESPONSE FOR VALIDATION STUDY ... | 179 |
| APPENDIX E. MODEL VALIDATION DATA..... | 181 |
| APPENDIX F. MATLAB CODE..... | 182 |
| <i>Appendix F.1 HSP90_TD_ODE.m – A Matlab function containing the set</i> | |
| <i>of ODEs for the HSP90-IKK-NFκB model.</i> | <i>182</i> |
| <i>Appendix F.2 LPSfun.m – A function that generates the LPS profile and</i> | |
| <i>the time delay for IKK activation.....</i> | <i>184</i> |
| <i>Appendix F.3 INHfun.m – function that generates total HSP90 inhibitor</i> | |
| <i>concentration a time t using a logistic function.</i> | <i>185</i> |
| <i>Appendix F.4 HSP90_inhib_Model_Params.m – an m-file script developed</i> | |
| <i>to iteratively simulate the model with a different parameter value for each</i> | |
| <i>simulation run. This was used to generate the data for the parameter</i> | |
| <i>sensitivity study.</i> | <i>186</i> |

| | |
|--|------------|
| <i>Appendix F.5 ParamFit.m – a Matlab m-file script that estimates parameters for the model. Uses the cost function HSP90_error.m. Optimizes using the sqp algorithm in the fmincon function.</i> | <i>188</i> |
| <i>Appendix F.6 HSP90_error.m – The function that calculates the cost function for estimating parameters in the model.....</i> | <i>192</i> |
| <i>Appendix F.7 HSP90_inhib_Model_InhibParams.m – A Matlab m-file script that runs model simulations for multiple values of the inhibitor parameters and for multiple concentrations ratios of inhibitor.</i> | <i>194</i> |
| <i>Appendix F.8 Validate.m – An m-file script that runs model simulations and compares the simulation data to the measured NF-κB data.....</i> | <i>197</i> |

LIST OF FIGURES

| | |
|--|-----------|
| FIGURE 1.1. DEVELOPMENT OF SLE HAS BEEN LINKED TO DYSREGULATION OF B CELLS, T CELLS, AND INNATE IMMUNE CELLS IN ADDITION TO SOME CORRELATION TO ENVIRONMENTAL FACTORS..... | 3 |
| FIGURE 1.2. HSP90 CHAPERONES OF KEY INFLAMMATORY AND APOPTOTIC PROTEINS. THIS CHAPERONE EFFECT CAN BE INHIBITED BY HSP90 INHIBITORS SUCH AS 17-DMAG..... | 5 |
| FIGURE 2.1. 17-DMAG REDUCED VIABILITY AND INDUCED APOPTOSIS AND NECROSIS IN J774 CELLS STIMULATED WITH LPS/IFN-γ. | 34 |
| FIGURE 2.2. 17-DMAG REDUCED AKT AND IKKα EXPRESSION. CELLS WERE TREATED FOR 24-HOURS WITH 17-DMAG THEN STIMULATED FOR ANOTHER 24 HOURS WITH LPS/IFN-γ. | 36 |
| FIGURE 2.3. 17-DMAG REDUCED INITIAL PHOSPHORYLATION OF IKB AND AKT IN LPS/IFN-γ STIMULATED CELLS. | 37 |
| FIGURE 2.4. NUCLEAR TRANSLOCATION OF NF-κB IN IMMUNE-STIMULATED CELLS PRETREATED WITH 17-DMAG SHOWN BY IMMUNOFLUORESCENCE. | 39 |
| FIGURE 2.5. TREATMENT WITH 17-DMAG INCREASED HSP70 EXPRESSION BUT DID NOT CHANGE HSP90 EXPRESSION. | 41 |
| FIGURE 2.6. HSF1 TRANSLOCATION INCREASED IN RESPONSE TO 17-DMAG TREATMENT. | 42 |
| FIGURE 2.7. 17-DMAG REDUCED EXPRESSION OF NO, IL-6 AND TNF-A. | 45 |
| FIGURE 3.1. INHIBITING HSP90 REDUCED IMMUNE STIMULATED NO, IL-6 AND IL-12 EXPRESSION. | 71 |

| | |
|---|------------|
| FIGURE 3.2. TREATMENT WITH 17-DMAG DECREASED PROTEINURIA..... | 73 |
| FIGURE 3.3. HSP90 INHIBITOR 17-DMAG REDUCED SERA ANTI-DSDNA BUT NOT TOTAL IgG. | 74 |
| FIGURE 3.4. RENAL HISTOPATHOLOGY SHOWED NO SIGNIFICANT DIFFERENCES IN RENAL HISTOPATHOLOGY BETWEEN THE CONTROL AND TREATED GROUPS..... | 76 |
| FIGURE 3.5. COMPARISON OF RENAL HSP90 AND HSP70 EXPRESSION IN C57BL/6 MICE AND MRL/LPR MICE WITH AND WITHOUT 17-DMAG..... | 78 |
| FIGURE 3.6. TREATMENT WITH 17-DMAG REDUCED SPLENOMEGALY.. | 79 |
| FIGURE 3.7. 17-DMAG INCREASED CD8+ T CELLS AND REDUCED DNT CELLS (CD4- CD8-). | 81 |
| FIGURE 3.8. CD3+ FOXP3- PHENOTYPES WERE AFFECTED BY 17-DMAG TREATMENT IN MRL/LPR MICE..... | 84 |
| FIGURE 3.9. MICE TREATED WITH 17-DMAG SHOWED A DECREASE IN CD19+ CD21- CD23+ B CELL POPULATIONS..... | 86 |
| FIGURE 4.1 DIAGRAM NF-KB REACTIONS WITH THE INCLUSION OF HSP90-IKK BINDING AND AN HSP90 INHIBITOR. | 113 |
| FIGURE 4.2. HSP90-IKK ASSOCIATION PARAMETER K_{1A} VARIED FROM 0.0001 TO 1 MM^{-1} S^{-1}..... | 128 |
| FIGURE 4.3. MODEL RESPONSE WHEN IKK ACTIVATION PARAMETER K_{2A} WAS TESTED AT VALUES FROM 0.0001 TO 1 $MM^{-1}S^{-1}$..... | 130 |
| FIGURE 4.4. MODEL RESPONSE WHEN IKKK ACTIVATION PARAMETER K_{I3K} WAS TESTED AT VALUES FROM 0.0001 TO 1 $MM^{-1}S^{-1}$..... | 131 |

FIGURE 4.5. THE SIMULATED IKK β RESPONSE MATCHES THE RESPONSE OF IKK β AS MEASURED IN MEF CELLS. 135

FIGURE 4.6. REDUCTION IN NF- κ B RESPONSE REQUIRES HIGH CONCENTRATION OF HSP90 INHIBITOR AND HIGH BINDING AFFINITY. 138

FIGURE 4.7. EXPERIMENTAL NF- κ B DATA SUPPORTS THE MODELED HSP90-IKK INTERACTIONS IN THE NF- κ B MODEL. 140

LIST OF TABLES

| | |
|--|------------|
| TABLE 4.1. PARAMETERS AND RANGES TESTED IN PARAMETER SENSITIVITY STUDY FOR IKKK, IKK, AND HSP90 REACTIONS. | 125 |
| TABLE 4.2. PARAMETERS ESTIMATED THROUGH FITTING IKKp PROFILE TO EXPERIMENTAL DATA..... | 134 |

LIST OF ABBREVIATIONS

| | |
|---------------|---|
| 17-AAG | 17-allylamino-17-demethoxygeldanamycin |
| 17-DMAG | 17-dimethylaminoethylamino-17-demethoxygeldanamycin |
| AnnV | Annexin V-FITC |
| anti-GBM | Anti-glomerular basement membrane |
| APC | Allophycocyanin |
| ATP | Adenosine tri-phosphate |
| C/EBP β | CCAAT/enhancer-binding protein- β |
| C1q | Complement component 1, q subcomponent |
| DMEM | Dulbecco's Modified Eagle's Medium |
| DNT | Double-negative T |
| dsDNA | Double stranded DNA |
| EGCG | Epigallocatechin-3-gallate |
| ELISA | Enzyme linked immunosorbent assay |
| FBS | Fetal bovine serum |
| FDA | Food and Drug Administration |
| FITC | Fluorescein–isothiocyanate |
| FoxP3 | Forkhead box P3 |
| GA | geldanamycin |
| GN | Glomerulonephritis |
| gp96 | Glycoprotein 96 |
| GPM1 | (S)-methyl 2-(4,6-dimethoxypyrimidine-2-ylloxy)-3-methylbutanoate |
| H&E | Hematoxylin and eosin |

| | |
|---------------|---|
| HRP | Horseradish peroxidase |
| HSF1 | Heat Shock Factor 1 |
| HSP27 | Heat shock protein 27 |
| HSP70 | Heat shock protein 70 |
| HSP90 | Heat shock protein 90 |
| HSPs | Heat shock proteins |
| IC | immune complex |
| IFN- γ | Interferon γ |
| IKK | Inhibitor of κ B kinase |
| IKKK | IKK kinase |
| IL | Interleukin |
| iNOS | inducible nitric oxide synthase |
| IRFs | Interferon regulatory factors |
| I κ B | Inhibitor of κ B |
| JAK | Janus acting kinase |
| LAT | Linker for activation of T cells |
| Lck | Lymphocyte-specific protein tyrosine kinase |
| lpr | Lymphoproliferative |
| LPS | lipopolysaccharide |
| MAPK | Mitogen-activated protein kinase |
| MRL/lpr | MRL/Mp- <i>Fas</i> ^{lpr} / <i>Fas</i> ^{lpr} |
| mRNA | Messenger RNA |
| mTOR | Mammalian target of rapamycin |

| | |
|----------------|--|
| NF-IL-6 | Nuclear factor IL-6 |
| NF- κ B | Nuclear factor- κ B |
| NO | Nitric oxide |
| NZB/W | New Zealand Black/White F1 |
| ODE | Ordinary differential equation |
| p-Akt | Phosphorylated Akt |
| PAS | Periodic acid-Schiff |
| PE | Phycoerythrin |
| PI | Propidium Iodide |
| PI3K | Phosphatidylinositol 3-kinase |
| p-I κ B | Phosphorylated I κ B |
| PP2A | Protein phosphatase 2A |
| PVDF | Polyvinylidene Difluoride |
| RANKL | Receptor activator NF- κ B ligand |
| RBC | Red blood cell |
| ROS | Reactive oxygen species |
| SEM | Standard error of the mean |
| SLE | Systemic lupus erythematosus |
| sqp | Sequential quadratic programming |
| STAT | Signal transducers and activators of transcription |
| TCR | T-cell receptor |
| TLR | Toll-like receptor |
| TMB | 3,3',5,5'-Tetramethylbenzidine |

| | |
|------------------|--|
| TNFR | Tumor necrosis factor receptor |
| TNF- α | Tumor necrosis factor- α |
| TRAF6 | Tumor necrosis factor receptor-associated factor 6 |
| T _{reg} | T regulatory cells |

ATTRIBUTION

Chapter 2 contains the manuscript entitled “HSP90 inhibition by 17-DMAG reduces inflammation in J774 macrophages through suppression of Akt and Nuclear Factor- κ B pathways.” This manuscript is published in *Inflammation Research*, May 2012, 61(5):521-33. This publication was co-authored by C.D. Parson, N.L. Regna, A.N. Thomas, C.B. Chafin, C.M. Reilly, and M.N. Rylander. All experiments were planned by me. Experimental results were analyzed by me. C.D. Parson contributed, N.L. Regna, A.N. Thomas, and C.B. Chafin all contributed to the work by performing some of the laboratory experiments. C.M. Reilly and M.N. Rylander advised the analysis of the experimental results and provided input for the organization of the document. The text and images were created by me with editorial proof reading and suggestions provided by all the co-authors.

Chapter 3 contains the manuscript entitled “Heat shock protein 90 inhibition by 17-DMAG lessens disease in the MRL/lpr mouse model of systemic lupus erythematosus.” This manuscript is published in *Cellular and Molecular Immunology*, May 2012, 9(3): 255-66. The manuscript is co-authored by C.B. Chafin, N.L. Regna, S.E. Hammond, M.A. Read, D.L. Caudell, M.N. Rylander, and C.M. Reilly. *In vitro* experiments were planned and carried out by me, under the direction and advisement of M.N. Rylander and C.M. Reilly. *In vivo* experiments were planned and carried out by me, under the direction and advisement of C.M. Reilly. C.B. Chafin assisted in animal handling and collection of animal tissue. N.L. Regna prepared the tissue slides with immunostaining for C3 and IgG. S.E. Hammond and C.M. Reilly conducted blinded assessment and scoring of disease progression in all immunostained slides. D. L. Caudell

performed assessment and pathological assessment of PAS slides. All other assays and experiments were planned and performed by me, under the advisement of C.M. Reilly and/or M.N. Rylander. The text and images were created by me with editorial proof reading and suggestions provided by all authors.

Chapter 4 contains the manuscript entitled, “Computational model of NF- κ B: Inhibition of heat shock protein 90 reduces chronic activation of nuclear factor- κ B by preventing heat shock protein chaperoning of Inhibitor of κ B kinase.” This manuscript is still in preparation and will be submitted for publication in the near future. S.E. Hammond and N.L. Regna each provided assistant in the conduct of laboratory assays. L. Achenie provided significant technical guidance in the development and simulation of the computational model. Y.W. Lee provided guidance in the selection of assays for experimental validation studies as well as subject matter expertise for NF- κ B signaling pathway mechanisms. M.N. Rylander provided general guidance for the conduct of experimental assays and modeling work. Model development, simulation, and matlab coding was performed exclusively by me. The text and images for the manuscript were created by me, under the advisement of L. Achenie, C.M. Reilly, and M.N. Rylander. Editorial proof reading and suggestions for organization of content was provided by Y.W. Lee, L. Achenie, C.M. Reilly, and M.N. Rylander.

CHAPTER 1.

INTRODUCTION

1.1 Motivation for research

Inflammation is a non-specific immune response that is used by an organism to react to injury. Under normal conditions the inflammatory response is well regulated and self-limiting in its role to provide a protective role for an organism in response to harmful stimuli such as tissue injury, pathogens, chemicals, and other phenomenon [1]. However, when the inflammatory response does not resolve properly, prolonged or chronic inflammation may result. This leads to a progressive shift in the cell type at the inflammation site and is characterized by simultaneous destruction and healing of the tissue from the inflammatory process. Chronic inflammation can lead to numerous diseases including: atherosclerosis, cancer, and autoimmunity [2-4]. Understanding inflammation and its regulatory signal networks can enable development of improved treatments for chronic inflammatory conditions.

1.2 Background

Inflammation, an integral part of the innate immune system, is a complex response that can affect any tissue and cell type in the body. Inflammation is considered part of the innate immune response. When innate immunity recognizes a threat it responds instantly by deploying antimicrobial peptides and phagocytes as well as activating the complement cascades, all in order to contain the infection and limit tissue damage [5]. This is in contrast to the adaptive immune response that involves T cells, B cells and antibodies that proliferate and attack the foreign

antigens. The adaptive immune system may take days to build a sufficiently strong response to the invading pathogens [5].

Inside the cell, the innate immune response activates a myriad of signal transduction pathways such as the Toll-like receptor (TLR), tumor necrosis factor receptor (TNFR), Akt (protein kinase B), Janus acting kinase/Signal Transducers and Activators of Transcription (JAK/Stat), the inhibitor of κ B kinase (IKK), and others [6]. These signal transduction pathways are upstream of nuclear factor- κ B (NF- κ B) and interferon regulatory factors (IRFs) which enter the nucleus of the cell to promote production of inflammatory cytokines [7]. Increased activation of pro-inflammatory transcription factors leads to expression of pro-inflammatory molecules such as tumor necrosis factor- α (TNF- α), interleukins, type I and II interferons and increased production of nitric oxide (NO) [8, 9].

Inflammatory responses can be initiated and regulated by diverse intracellular signaling networks, including the TLR network. In particular, TLR4 selectively recognizes microbial lipopolysaccharide (LPS) as well as many host metabolites and lipids including saturated fatty acids [10, 11]. Activation of the TLR4 signaling network initiates multiple cascades of inflammatory processes [12, 13]. At a molecular level, TLR4 activation leads to expression of pro-inflammatory cytokines and mediators including TNF α , interleukin 6 (IL-6), and inducible nitric oxide synthase (iNOS) [14]. At a cellular level, TLR4 activation leads to enhanced macrophage phagocytosis, exacerbated immune cell activation, and increased cross-talk between innate and adaptive immune cells [15]. Collectively, exacerbated TLR4 signaling processes can lead to pathogenesis of autoimmune diseases including lupus [12].

1.2.1 Systemic lupus erythematosus

Systemic lupus erythematosus (SLE) is a chronic inflammatory autoimmune disorder that can affect nearly every organ in the body [16]. It is an autoimmune disease in which the immune system attacks the body's own cells and tissue. The result of the autoimmune attack is chronic inflammation and tissue damage [17]. SLE may manifest in skin, joints, kidneys, heart, lungs, blood vessels, brain, and other organs [18]. Recent studies indicate that inflammation associated with SLE leads to atherosclerosis and accelerated coronary artery disease [19]. For example, women with SLE under age 40 are nearly five times more likely to have atherosclerosis than their healthy, same-age peers, independent of conventional risk factors (smoking, high cholesterol, advanced age, high blood pressure, obesity, and diabetes) [20-22].

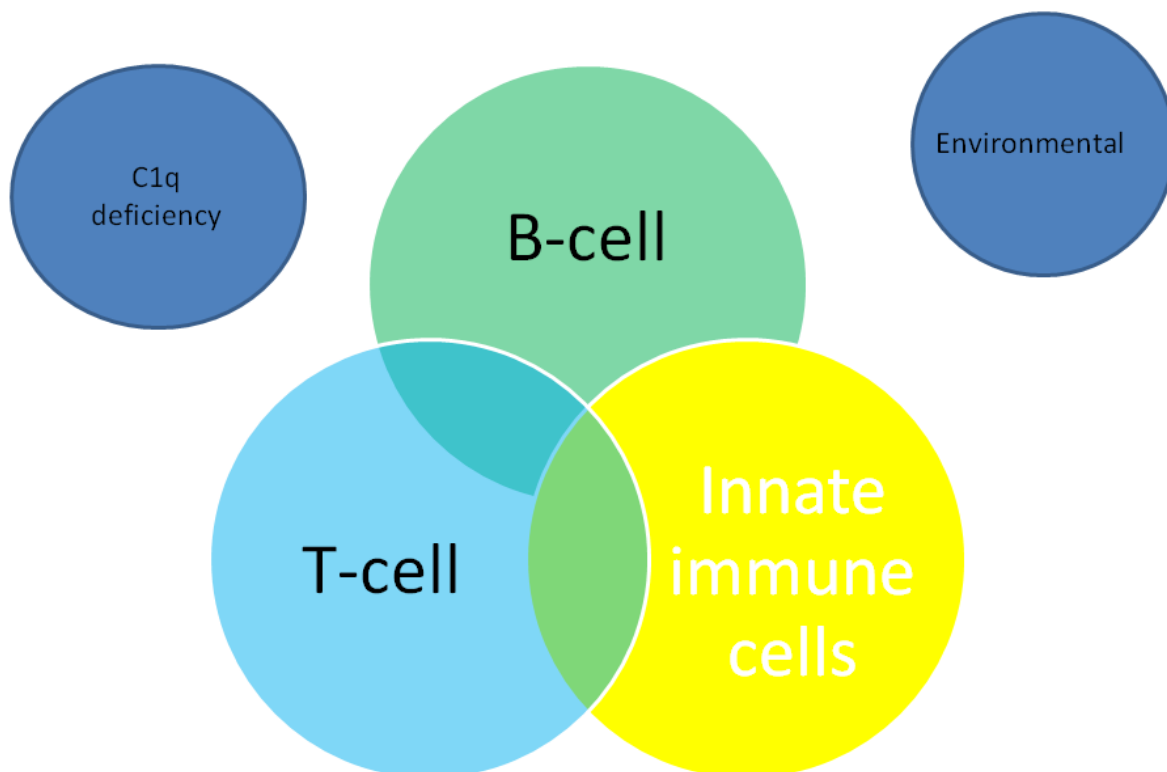


Figure 1.1. Development of SLE has been linked to dysregulation of B cells, T cells, and innate immune cells in addition to some correlation to environmental factors.

The mechanisms underlying the development of SLE are still not understood. Presently, the data suggests correlations between SLE and B cells, or SLE and T cells, or SLE and innate immune cells [23-26]. In addition, there is data suggesting environmental factors and deficiency of the complement component 1, q subcomponent (C1q) can determine susceptibility to developing SLE [18, 27]. It is likely that SLE development is determined by a combination of all of these factors, as is represented in the diagram in Figure 1.1. The notion that SLE development lies in dysregulation of any one of B cells, T cells, or innate immune cells finds support in the literature that shows therapeutic success in targeting B cells, T cells or even extracellular cytokines [23, 26, 28, 29]. The most recent drug approved by the Food and Drug Administration (FDA, March 2011) for treatment of lupus was Belimumab (or LymphoStat-B), a monoclonal antibody that inhibits B-cell activating factor (BAFF) for a net effect called B cell depletion [30]. The difficulty in identifying viable therapies for SLE is highlighted by the fact that Belimumab is the first drug in 56 years to be approved by the FDA for the treatment of SLE [31].

Research has shown that the severity of SLE can also be diminished through down-regulation of the inflammatory pathway comprising phosphatidylinositol 3-kinase (PI3K), Akt, and mammalian target of rapamycin (mTOR) (PI3K/Akt/mTOR) [32, 33]. Recently, several studies have linked modulation of Akt as a potential target for the treatment of SLE [33-35]. Autoimmunity and inflammation are also associated with activation of the NF- κ B pathway [36]. The up-regulation of many pro-inflammatory cytokines and mediators such as TNF- α and interleukins (IL-6, IL-8 etc.) and NO are linked to NF- κ B activation as was discussed by Hacker and Karin [37] and illustrated in Figure 1.2. Numerous other reports show that severity of glomerular nephritis in New Zealand Black/White F1 (NZB/W) mice is attenuated by rapamycin [38]. Rapamycin is a potent immunosuppressive compound [39] that acts by inhibiting mTOR, which is involved with cell cycle progression [40].

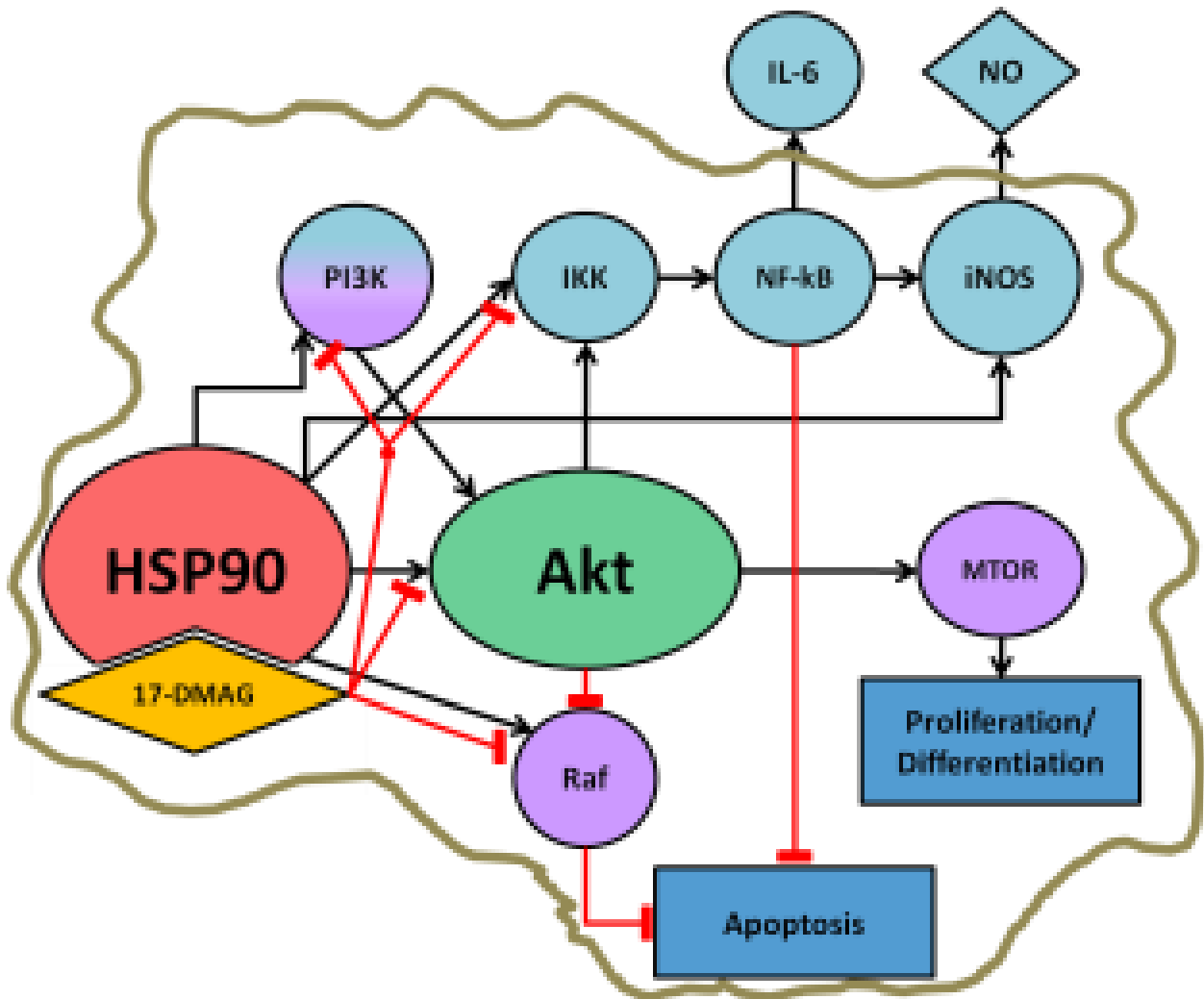


Figure 1.2. HSP90 chaperones of key inflammatory and apoptotic proteins. This chaperone effect can be inhibited by HSP90 inhibitors such as 17-DMAG.

To study SLE, mouse models have provided a valuable tool to understand and test the mechanisms responsible for the human disease [41]. There are several mouse models of lupus nephritis with the three most well recognized being the MRL/lpr model, NZB/W model, and the anti-glomerular basement membrane (anti-GBM) sera induced animal model [41-43]. The MRL/lpr lupus model originates from a mixture of strains where a recessive mutation of the Fas gene implicated in the programmed cell death pathway of auto-reactive thymic T cells appeared spontaneously [44]. In this disease model, mice show glomerulonephritis (GN), vasculitis,

arthritis, increased serum antibodies to double stranded DNA (dsDNA), and increased serum IgG and IgM [44].

In summary, SLE is a complex disease with many factors affecting its development. There is a broad range of approaches to treating the disease that includes targeting specific immune cells. Nevertheless, the overarching approach to SLE therapies, regardless of cellular target, is to suppress the immune system and/or the inflammatory response.

1.2.2 Heat shock protein 90

Heat shock protein 90 (HSP90) is a homo-dimeric molecular chaperone comprising greater than 3% of total cellular protein [45]. HSP90 has a prominent role in folding and conformational regulation of numerous client proteins [46, 47]. The active process of HSP90 chaperone functions is associated with cycles of adenosine tri-phosphate (ATP) binding and hydrolysis [48, 49].

The list of signal transduction client proteins for HSP90 is long, and known to include over 100 proteins including PI3K and Akt [46, 50-52]. This chaperone-client relationship leads to activation and subsequent downstream production of inflammatory mediators. HSP90 has also been linked to SLE with an as yet, unknown role in the disease [53-56].

HSP90 readily binds ATP at its N-terminal domain causing conformational change in HSP90, making it “clamp down” on its client protein [46, 50]. Compounds referred to as “HSP90 inhibitors”, such as radicicol, geldanamycin (GA), and derivatives of GA, 17-allylamino-17-demethoxygeldanamycin (17-AAG) and 17-dimethylaminoethylamino-17-demethoxygeldanamycin (17-DMAG) function by out-competing with ATP to bind to HSP90. Inhibitors binding to HSP90 result in deactivation, destabilization and degradation of client proteins [46, 49, 57]. HSP90 inhibitors suppress immune stimulated release of IL-6, IL-12, TNF-

α , NO [58]. Inhibition of HSP90 is characterized by up-regulation of heat shock regulator mechanisms by activating Heat Shock Factor 1 (HSF1), leading to increased expression of HSP70 [52, 59-61]. The well characterized inhibitor of HSP90, GA, inhibits HSP90 by binding to the N-terminus and preventing proper HSP90-client binding [46, 62-64]. The GA derived HSP90 inhibitor 17-DMAG has been shown to prolong survival while attenuating inflammation and reducing lung injury in induced murine sepsis [65]. Of the GA derivatives, 17-DMAG has shown low toxicity and enhanced water solubility and is currently in clinical trials for the treatment of cancer [66].

Another HSP90 domain associated with ATP binding is the carboxyl domain (C-terminal). Several HSP90 inhibitors are known to produce their inhibitory effect by binding to the C-terminus [46]. The active compound in green tea, epigallocatechin-3-gallate (EGCG) directly binds to the C-terminus of HSP90 [50]. Similar to other HSP90 inhibitors, this HSP90 carboxyl domain binding agent exerts anti-inflammatory effects in animals and humans [67-69].

The literature discussed shows that HSP90 plays an important role in inflammation and HSP90 has been linked to SLE [53-55, 70, 71]. Nevertheless, the mechanistic role that HSP90 plays in SLE continues to be studied. Most studies on HSP90 are performed in cancer cell lines with limited data on the role of HSP90 in immune cells and *in vivo* inflammatory models. To date, there have been no published studies showing the effect of HSP90 inhibition on *in vivo* SLE models. Testing HSP90 inhibitors in a mouse model for SLE would inform us of the extent to which the *in vitro* anti-inflammatory effects of HSP90 inhibition extend to the *in vivo* domain. Furthermore, HSP90 inhibition may be used therapeutically to treat chronic inflammatory diseases such as SLE.

1.2.3 Modeling

Understanding the structure and dynamics of complex intercellular interactions that create and regulate the cellular environment is a key challenge in biology and medicine in the 21st century [72]. Computational and predictive models are becoming increasingly useful in the clinical setting. An example of this comes from using data from microarrays in pathology diagnosis and interpreting that data with well-developed models of the complex cellular networks to see how cell signaling pathways are pathologically altered in disease [72, 73].

A number of computational models have been developed to predict the molecular pathways involved with inflammation. Previous studies have created computational models to elucidate some of the signaling pathways in apoptosis [74, 75], inflammation [76], and heat shock protein responses [74, 77, 78]. Experimental measurements have been integrated with computational methods for the creation of computational models that predict inflammatory response of cartilage in response to compressive loads [79].

Developmental work has also been presented for computational treatment planning models for predicting and optimizing the cellular and tissue response including cell death and heat shock protein expression associated with laser therapy alone or in combination with nanoparticles [80-94]. Empirical and mechanistic molecular pathway models for thermal induction of HSP27, HSP70 and HSP90 expression was investigated. Another research report presented a computational model as a virtual prototype for the mechanism of cdc37 assisted protein client binding to HSP90 [95]. In this study, the ATP binding cycle of HSP90 was modeled as a way to explore theoretical responses. In the computational models of cell signal pathways that depend on HSP90, there has yet to be an inclusion of terms for the chaperone effect of HSP90. Modeling

provides a theoretical rationale to mathematically predict how reducing inflammation by inhibiting HSP90 might simultaneously affect other, non-inflammatory cellular processes.

Of the many pathways dependent on HSP90, the NF- κ B pathway has been well characterized through computational modeling. Originally described by Hoffmann and colleagues, the NF- κ B model has been verified and expanded by numerous other investigators [78]. Early modeling efforts focused on predicting NF- κ B activation in response to assumed or measured IKK activity [96-98]. Later models began to incorporate signaling components upstream of IKK. Most models have focused on TNF- α signaling, however there have been a few mathematical models that have incorporated LPS activation or IL-1 β activation of NF- κ B [99-102]. Nevertheless, efforts have focused on NF- κ B and I κ B dynamics and in many studies, IKK is used as an input. IKK is a well-known client of HSP90 [103-105]. Taken together, IKK's role in NF- κ B dynamics and its dependence on HSP90 make it an excellent candidate for development of a computational model that includes HSP90 in cell signaling dynamics.

In summary, computational modeling offers a virtual environment in which to test hypotheses regarding cellular signaling. The interest in HSP90 as a potential mediator for inflammatory signals is motivation to develop a model that includes the dependence on HSP90 for propagating inflammatory signals. Furthermore, the computational models that have characterized the response of NF- κ B provide an excellent basis on which to build a useful predictive model.

1.3 Hypothesis

Taken together, HSP90 plays a prominent role in inflammation and that inhibition of HSP90 attenuates the inflammatory response. The exact mechanism for this effect is unknown but it is **hypothesized that inhibition of HSP90 may, in part, reduce the activity of Akt**

and/or IKK. We hypothesize that this interruption occurs by the prevention of the client proteins from binding to HSP90. In other words, Akt and or IKK must be bound to HSP90 in order to propagate the signaling cascade. Furthermore, we propose that when the interaction between HSP90 and IKK or HSP90 and Akt is interrupted, there is a subsequent attenuation of inflammatory processes of *in vitro* inflammatory models as well as *in vivo* SLE models. To test these hypotheses, the effect of HSP90 in inflammation was studied according to the following three specific aims:

Specific Aim 1: Determine the *in vitro* mechanistic effects of HSP90 inhibition on the Akt and NF- κ B pro-inflammatory signal cascades. This will expand understanding of the role of HSP90 in inflammation and will highlight the effect of HSP90 inhibition on reduction of inflammation.

Specific Aim 2: Mathematically model the cellular response to immune stimulation and HSP90 inhibition. *In silico* models will provide quantitative predictions of cytokine and inflammatory mediator production in terms of cellular mechanisms.

Specific Aim 3: Test the *in vivo* effectiveness of HSP90 inhibition as a potential treatment for SLE. This proof of concept study will explore the effect of HSP90 inhibition on disease pathogenesis in MRL/lpr mice and will explore the *in vivo* mechanisms of HSP90 in SLE.

These specific aims guided the exploration of the effects of HSP90 inhibition on inflammation. It was found that inhibition of HSP90 reduced Akt activity with a net effect of reducing production of inducible NO and expression of IL-6, IL-12, and TNF- α . A mathematical model was developed to explore the role of HSP90 among the complex inflammatory signal cascades. Analysis of the model showed that IKK activation was highly sensitive to the HSP90 binding rate and that in the presence of HSP90 inhibitors the activation of NF- κ B was reduced. Perhaps the most significant contribution of this work comes from the results of the *in vivo* study

of specific aim 3. This work provides evidence that HSP90 inhibition may reduce disease. We found that HSP90 inhibition significantly affected splenocyte T cell profiles. This suggests that targeting HSP90 may have efficacy in the treatment of SLE through inhibition of T cell activation.

REFERENCES

1. Ferrero-Miliani, L., et al., *Chronic inflammation: importance of NOD2 and NALP3 in interleukin-1 β generation*. *Clinical & Experimental Immunology*, 2007. **147**(2): p. 227-235.
2. Grivennikov, S.I., F.R. Greten, and M. Karin, *Immunity, Inflammation, and Cancer*. *Cell*, 2010. **140**(6): p. 883-899.
3. Hansson, G.K., *Inflammation, Atherosclerosis, and Coronary Artery Disease*. *New England Journal of Medicine*, 2005. **352**(16): p. 1685-1695.
4. Abou-Raya, A. and S. Abou-Raya, *Inflammation: a pivotal link between autoimmune diseases and atherosclerosis*. *Autoimmun Rev*, 2006. **5**(5): p. 331-7.
5. Medzhitov, R. and C. Janeway, *Innate Immunity*. *New England Journal of Medicine*, 2000. **343**(5): p. 338-344.
6. Guha, M. and N. Mackman, *LPS induction of gene expression in human monocytes*. *Cell Signal*, 2001. **13**(2): p. 85-94.
7. Agresti, C., et al., *Synergistic stimulation of MHC class I and IRF-1 gene expression by IFN-gamma and TNF-alpha in oligodendrocytes*. *Eur J Neurosci.*, 1998. **10**(9): p. 2975-83.
8. Mogensen, T.H., *Pathogen recognition and inflammatory signaling in innate immune defenses*. *Clin Microbiol Rev*, 2009. **22**(2): p. 240-73, Table of Contents.

9. Mackay, I.R., et al., *Innate Immunity*. N Engl J Med, 2000. **343**(5): p. 338-344.
10. Yamashita, A., et al., *DNA microarray analyses of genes expressed differentially in 3T3-L1 adipocytes co-cultured with murine macrophage cell line RAW264.7 in the presence of the toll-like receptor 4 ligand bacterial endotoxin*. Int J Obes (Lond), 2008. **32**(11): p. 1725-9.
11. Lapaque, N., et al., *Differential inductions of TNF-alpha and IIGP, IIGP by structurally diverse classic and non-classic lipopolysaccharides*. Cell Microbiol, 2006. **8**(3): p. 401-13.
12. Sibia, J., *Novel concepts and treatments for autoimmune disease: ten focal points*. Joint Bone Spine, 2004. **71**(6): p. 511-7.
13. Hasko, G., et al., *Shaping of monocyte and macrophage function by adenosine receptors*. Pharmacol Ther, 2006.
14. Bassaganya-Riera, J., et al., *Long-term influence of lipid nutrition on the induction of CD8(+) responses to viral or bacterial antigens*. Vaccine, 2002. **20**(9-10): p. 1435-44.
15. Barr, T.A., et al., *TLR-mediated stimulation of APC: Distinct cytokine responses of B cells and dendritic cells*. Eur J Immunol, 2007. **37**(11): p. 3040-53.
16. Manson, J. and A. Rahman, *Systemic lupus erythematosus*. Orphanet Journal of Rare Diseases, 2006. **1**(1): p. 6.

17. James, W.D., T. Berger, and D. Elston, *Andrews' Diseases of the Skin: Clinical Dermatology*. 10 ed. 2005: Saunders. 1210.
18. Rahman, A. and D.A. Isenberg, *Systemic Lupus Erythematosus*. *New England Journal of Medicine*, 2008. **358**(9): p. 929-939.
19. Escarcega, R.O., et al., *Insulin resistance, chronic inflammatory state and the link with systemic lupus erythematosus-related coronary disease*. *Autoimmun Rev*, 2006. **6**(1): p. 48-53.
20. Alves, J.D. and P.R. Ames, *Atherosclerosis, oxidative stress and auto-antibodies in systemic lupus erythematosus and primary antiphospholipid syndrome*. *Immunobiology*, 2003. **207**(1): p. 23-8.
21. Asanuma, Y., et al., *Premature coronary-artery atherosclerosis in systemic lupus erythematosus*. *N Engl J Med*, 2003. **349**(25): p. 2407-15.
22. Hahn, B.H., *Systemic lupus erythematosus and accelerated atherosclerosis*. *N Engl J Med*, 2003. **349**(25): p. 2379-80.
23. Sanz, I. and F.E. Lee, *B cells as therapeutic targets in SLE*. *Nat Rev Rheumatol*, 2010. **6**(6): p. 326-37.
24. Liu, K. and C. Mohan, *Altered B-cell signaling in lupus*. *Autoimmunity Reviews*, 2009. **8**(3): p. 214-218.

25. La Cava, A., *The busy life of regulatory T cells in systemic lupus erythematosus*. *Discov Med*, 2009. **8**(40): p. 13-7.
26. Crispin, J.C., et al., *T cells as therapeutic targets in SLE*. *Nat Rev Rheumatol*, 2010. **6**(6): p. 317-325.
27. Julkunen, H., S. Ekblom-Kullberg, and A. Miettinen, *Nonrenal and renal activity of systemic lupus erythematosus: a comparison of two anti-C1q and five anti-dsDNA assays and complement C3 and C4*. *Rheumatology Int*, 2011: p. 1-7.
28. Karim, M.Y., C.N. Pisoni, and M.A. Khamashta, *Update on immunotherapy for systemic lupus erythematosus--what's hot and what's not!* *Rheumatology (Oxford)*, 2009. **48**(4): p. 332-41.
29. Ronnblom, L. and K.B. Elkon, *Cytokines as therapeutic targets in SLE*. *Nat Rev Rheumatol*, 2010. **6**(6): p. 339-347.
30. Baker, K.P., et al., *Generation and characterization of LymphoStat-B, a human monoclonal antibody that antagonizes the bioactivities of B lymphocyte stimulator*. *Arthritis Rheum*, 2003. **48**(11): p. 3253-65.
31. AssociatedPress, *FDA approves first new drug for lupus in 56 years*, in *USA Today*. 2011: McLean, VA.

32. Patel, R.K. and C. Mohan, *PI3K/AKT signaling and systemic autoimmunity*. Immunol Res, 2005. **31**(1): p. 47-55.
33. Wu, T. and C. Mohan, *The AKT axis as a therapeutic target in autoimmune diseases*. Endocr Metab Immune Disord Drug Targets, 2009. **9**(2): p. 145-50.
34. Patel, R. and C. Mohan, *PI3K/AKT signaling and systemic autoimmunity*. Immunologic Research, 2005. **31**(1): p. 47-55.
35. Weichhart, T. and M.D. Saemann, *The PI3K/Akt/mTOR pathway in innate immune cells: emerging therapeutic applications*. Ann Rheum Dis, 2008. **67**(Suppl_3): p. iii70-74.
36. Karin, M., *NF-kappaB as a critical link between inflammation and cancer*. Cold Spring Harb Perspect Biol, 2009. **1**(5): p. a000141.
37. Hacker, H. and M. Karin, *Regulation and Function of IKK and IKK-Related Kinases*. Sci. STKE, 2006. **2006**(357): p. re13-.
38. Lui, S.L., et al., *Rapamycin attenuates the severity of established nephritis in lupus-prone NZB/W F1 mice*. Nephrol Dial Transplant, 2008. **23**(9): p. 2768-76.
39. Kahan, B.D., *Sirolimus: a comprehensive review*. Expert Opin Pharmacother, 2001. **2**(11): p. 1903-17.

40. Sehgal, S.N., *Rapamune® (RAPA, rapamycin, sirolimus): mechanism of action immunosuppressive effect results from blockade of signal transduction and inhibition of cell cycle progression*. *Clinical Biochemistry*, 1998. **31**(5): p. 335-340.
41. Du, Y., Y. Fu, and C. Mohan, *Experimental anti-GBM nephritis as an analytical tool for studying spontaneous lupus nephritis*. *Arch Immunol Ther Exp (Warsz)*, 2008. **56**(1): p. 31-40.
42. Andrews, B.S., et al., *Spontaneous murine lupus-like syndromes. Clinical and immunopathological manifestations in several strains*. *Journal of Experimental Medicine*, 1978. **148**(5): p. 1198-215.
43. Godfrey, D.G., et al., *Effects of dietary supplementation on autoimmunity in the MRL/lpr mouse: a preliminary investigation*. *Ann Rheum Dis*, 1986. **45**(12): p. 1019-24.
44. Santiago-Raber, M.-L., et al., *Genetic basis of murine lupus*. *Autoimmunity Reviews*, 2004. **3**(1): p. 33-39.
45. Neidle, S., ed. *Cancer Drug Design and Discovery*. 1 ed., ed. S. Neidle. 2008, Elsevier: New York, New York.
46. Blagg, B.S. and T.D. Kerr, *Hsp90 inhibitors: small molecules that transform the Hsp90 protein folding machinery into a catalyst for protein degradation*. *Med Res Rev*, 2006. **26**(3): p. 310-38.

47. Kone, B.C., *Protein-protein interactions controlling nitric oxide synthases*. Acta Physiologica Scandinavica, 2000. **168**(1): p. 27-31.
48. Peng, X., et al., *Heat shock protein 90 stabilization of ErbB2 expression is disrupted by ATP depletion in myocytes*. J Biol Chem, 2005. **280**(13): p. 13148-52.
49. Sharp, S., et al., *Inhibitors of the HSP90 Molecular Chaperone: Current Status*, in *Advances in Cancer Research*. 2006, Academic Press. p. 323-348.
50. Palermo, C.M., C.A. Westlake, and T.A. Gasiewicz, *Epigallocatechin gallate inhibits aryl hydrocarbon receptor gene transcription through an indirect mechanism involving binding to a 90 kDa heat shock protein*. Biochemistry, 2005. **44**(13): p. 5041-52.
51. Pratt, W.B. and D.O. Toft, *Regulation of signaling protein function and trafficking by the hsp90/hsp70-based chaperone machinery*. Exp Biol Med (Maywood), 2003. **228**(2): p. 111-33.
52. Whitesell, L. and S.L. Lindquist, *HSP90 and the chaperoning of cancer*. Nat Rev Cancer, 2005. **5**(10): p. 761-72.
53. Dhillon, V.B., et al., *Differential heat shock protein overexpression and its clinical relevance in systemic lupus erythematosus*. Ann Rheum Dis, 1993. **52**(6): p. 436-442.
54. Dhillon, V.B., et al., *Elevation of the 90 kDa heat-shock protein in specific subsets of systemic lupus erythematosus*. Q J Med, 1994. **87**(4): p. 215-22.

55. Latchman, D.S. and D.A. Isenberg, *The role of hsp90 in SLE*. *Autoimmunity*, 1994. **19**(3): p. 211-8.
56. Faulds, G., et al., *Increased levels of antibodies to heat shock proteins with increasing age in Mrl/Mp-lpr/lpr mice*. *Br J Rheumatol*, 1995. **34**(7): p. 610-5.
57. Donnelly, A. and B.S. Blagg, *Novobiocin and additional inhibitors of the Hsp90 C-terminal nucleotide-binding pocket*. *Curr Med Chem*, 2008. **15**(26): p. 2702-17.
58. Zhu, F.G. and D.S. Pisetsky, *Role of the heat shock protein 90 in immune response stimulation by bacterial DNA and synthetic oligonucleotides*. *Infect Immun*, 2001. **69**(9): p. 5546-52.
59. Neckers, L., *Heat shock protein 90: the cancer chaperone*. *J Biosci*, 2007. **32**(3): p. 517-30.
60. Workman, P., *Auditing the Pharmacological Accounts for Hsp90 Molecular Chaperone Inhibitors: Unfolding the Relationship between Pharmacokinetics and Pharmacodynamics I*. *Molecular Cancer Therapeutics*, 2003. **2**(2): p. 131-138.
61. Yu, Y., et al., *Geldanamycin induces production of heat shock protein 70 and partially attenuates ototoxicity caused by gentamicin in the organ of Corti explants*. *Journal of Biomedical Science*, 2009. **16**(1): p. 79.

62. Clark, C.B., et al., *Role of oxidative stress in geldanamycin-induced cytotoxicity and disruption of Hsp90 signaling complex*. Free Radic Biol Med, 2009.
63. Hadden, M.K., D.J. Lubbers, and B.S. Blagg, *Geldanamycin, radicicol, and chimeric inhibitors of the Hsp90 N-terminal ATP binding site*. Curr Top Med Chem, 2006. **6**(11): p. 1173-82.
64. Shen, G., et al., *Design, synthesis, and structure--activity relationships for chimeric inhibitors of Hsp90*. J Org Chem, 2006. **71**(20): p. 7618-31.
65. Chatterjee, A., et al., *Heat Shock Protein 90 Inhibitors Prolong Survival, Attenuate Inflammation, and Reduce Lung Injury in Murine Sepsis*. Am. J. Respir. Crit. Care Med., 2007. **176**(7): p. 667-675.
66. Eiseman, J.L., et al., *Pharmacokinetics and pharmacodynamics of 17-demethoxy 17-[[2-(dimethylamino)ethyl]amino]geldanamycin (17DMAG, NSC 707545) in C.B-17 SCID mice bearing MDA-MB-231 human breast cancer xenografts*. Cancer Chemother Pharmacol, 2005. **55**(1): p. 21-32.
67. Ahmed, S., et al., *Green tea polyphenol epigallocatechin-3-gallate inhibits the IL-1 beta-induced activity and expression of cyclooxygenase-2 and nitric oxide synthase-2 in human chondrocytes*. Free Radic Biol Med, 2002. **33**(8): p. 1097-105.

68. Le Marchand, L., *Cancer preventive effects of flavonoids--a review*. Biomed Pharmacother, 2002. **56**(6): p. 296-301.
69. Singh, A.K., et al., *Green tea constituent epigallocatechin-3-gallate inhibits angiogenic differentiation of human endothelial cells*. Arch Biochem Biophys, 2002. **401**(1): p. 29-37.
70. Ripley, B.J.M., D.A. Isenberg, and D.S. Latchman, *Elevated Levels of the 90 kDa Heat Shock Protein (hsp90) in SLE Correlate with Levels of IL-6 and Autoantibodies to hsp90*. J Autoimmun, 2001. **17**(4): p. 341-346.
71. Stephanou, A., D.S. Latchman, and D.A. Isenberg, *The regulation of heat shock proteins and their role in systemic lupus erythematosus*. Seminars in Arthritis and Rheumatism, 1998. **28**(3): p. 155-162.
72. Barabasi, A.-L. and Z.N. Oltvai, *Network biology: understanding the cell's functional organization*. Nat Rev Genet, 2004. **5**(2): p. 101-113.
73. Alizadeh, A.A., et al., *Distinct types of diffuse large B-cell lymphoma identified by gene expression profiling*. Nature, 2000. **403**(6769): p. 503-511.
74. Rieger, T.R., R.I. Morimoto, and V. Hatzimanikatis, *Mathematical Modeling of the Eukaryotic Heat-Shock Response: Dynamics of the hsp70 Promoter*. 2005. **88**(3): p. 1646-1658.

75. Sheppard, P.W., et al. *A Computational Model of Apoptosis and Inflammation Signaling in Microglia*. in *THE EIGHTH INTERNATIONAL CONFERENCE ON SYSTEMS BIOLOGY 2007*. Long Beach, California, USA
76. Hua, F., et al., *Effects of Bcl-2 Levels on Fas Signaling-Induced Caspase-3 Activation: Molecular Genetic Tests of Computational Model Predictions*. *J Immunol*, 2005. **175**(2): p. 985-995.
77. El-Samad, H., et al., *Surviving heat shock: Control strategies for robustness and performance*. *Proceedings of the National Academy of Sciences of the United States of America*, 2005. **102**(8): p. 2736-2741.
78. Hoffmann, A., et al., *The IkappaB-NF-kappaB signaling module: temporal control and selective gene activation*. *Science*, 2002. **298**(5596): p. 1241-5.
79. Nam, J., et al., *Biomechanical Thresholds Regulate Inflammation through the NF-kappaB Pathway: Experiments and Modeling*. *PLoS ONE*, 2009. **4**(4): p. e5262.
80. Feng, Y., et al., *Optimal Design of Laser Surgery for Cancer Treatment Through Nanoparticle-Mediated Hyperthermia Therapy*, in *NSTI-Nanotech 2005*. 2005, NSTI.org: Anaheim, CA.
81. Rylander, M.N., et al., *Correlation of HSP70 expression and cell viability following thermal stimulation of bovine aortic endothelial cells*. *J Biomech Eng*, 2005. **127**(5): p. 751-7.

82. Rylander, M.N., et al., *Coordinated Modeling of Thermal Stress Induced Cell Injury and Heat Shock Protein Expression*. *Annals of New York Academy of Science*, 2005(1066): p. 222-242.
83. Oden, J.T., et al., *Development of a Computational Paradigm for Laser Treatment of Cancer*, in *Computational Science – ICCS 2006*. 2006. p. 530-537.
84. Rylander, M.N., et al., *Optimizing heat shock protein expression induced by prostate cancer laser therapy through predictive computational models*. *Journal of Biomedical Optics*, 2006. **11**(4): p. 041113-16.
85. Oden, J.T., et al., *Dynamic data-driven finite element models for laser treatment of cancer*. *Numerical Methods for Partial Differential Equations*, 2007. **23**(4): p. 904-922.
86. Rylander, M.N., et al., *Heat shock protein expression and injury optimization for laser therapy design*. *Lasers in Surgery and Medicine*, 2007. **39**(9): p. 731-746.
87. Feng, Y., J.T. Oden, and M.N. Rylander, *A Two-State Cell Damage Model Under Hyperthermic Conditions: Theory and In Vitro Experiments*. *Journal of Biomechanical Engineering*, 2008. **130**(4): p. 041016-10.
88. Fisher, J.W. and M.N. Rylander, *Effective cancer laser-therapy design through the integration of nanotechnology and computational treatment planning models*. *Proceedings of the SPIE*, 2008. **6869**: p. 68690D-68690D-11.

89. Wang, S., et al., *HSP70 kinetics study by continuous observation of HSP-GFP fusion protein expression on a perfusion heating stage*. *Biotechnology and Bioengineering*, 2008. **99**(1): p. 146-154.
90. Burke, A., et al., *Long-term survival following a single treatment of kidney tumors with multiwalled carbon nanotubes and near-infrared radiation*. *Proceedings of the National Academy of Sciences*, 2009. **106**(31): p. 12897-12902.
91. Feng, Y., et al., *Nanoshell-mediated laser surgery simulation for prostate cancer treatment*. *Engineering with Computers*, 2009. **25**(1): p. 3-13.
92. Feng, Y., et al., *Optimization and real-time control for laser treatment of heterogeneous soft tissues*. *Computer Methods in Applied Mechanics and Engineering*, 2009. **198**(21-26): p. 1742-1750.
93. Fisher, J.W., et al., *Effective Laser Cancer Therapy Design Through the Integration of Multi-walled Carbon Nanotubes*. *Cancer Research*, 2009. **In review**.
94. Sarkar, S., C.G. Rylander, and M.N. Rylander, *Photothermal Response of Tissue Phantoms Containing Multi-walled Carbon Nanotubes* *Journal of Biomechanical Engineering*, 2009. **In Press**.
95. Vali, S., et al., *Virtual prototyping study shows increased ATPase activity of Hsp90 to be the key determinant of cancer phenotype*. *Syst Synth Biol*, 2010. **4**(1): p. 25-33.

96. Cheong, R., et al., *Transient IkappaB kinase activity mediates temporal NF-kappaB dynamics in response to a wide range of tumor necrosis factor-alpha doses.* J Biol Chem, 2006. **281**(5): p. 2945-50.
97. Kearns, J.D., et al., *IkBε provides negative feedback to control NF-κB oscillations, signaling dynamics, and inflammatory gene expression.* The Journal of Cell Biology, 2006. **173**(5): p. 659-664.
98. Werner, S.L., D. Barken, and A. Hoffmann, *Stimulus Specificity of Gene Expression Programs Determined by Temporal Control of IKK Activity.* Science, 2005. **309**(5742): p. 1857-1861.
99. Basak, S., et al., *A fourth IkappaB protein within the NF-kappaB signaling module.* Cell, 2007. **128**(2): p. 369-81.
100. Covert, M.W., et al., *Achieving stability of lipopolysaccharide-induced NF-kappaB activation.* Science, 2005. **309**(5742): p. 1854-7.
101. Lipniacki, T., et al., *Single TNFalpha trimers mediating NF-kappaB activation: stochastic robustness of NF-kappaB signaling.* BMC Bioinformatics, 2007. **8**: p. 376.
102. Park, S.G., et al., *The influence of the signal dynamics of activated form of IKK on NF-kappaB and anti-apoptotic gene expressions: a systems biology approach.* FEBS Lett, 2006. **580**(3): p. 822-30.

103. Broemer, M., D. Krappmann, and C. Scheidereit, *Requirement of Hsp90 activity for I[kappa]B kinase (IKK) biosynthesis and for constitutive and inducible IKK and NF-[kappa]B activation*. *Oncogene*, 2004. **23**(31): p. 5378-5386.

104. Li, D., *Selective degradation of the I[kappa]B kinase (IKK) by autophagy*. *Cell Res*, 2006. **16**(11): p. 855-856.

105. Chen, G., P. Cao, and D.V. Goeddel, *TNF-Induced Recruitment and Activation of the IKK Complex Require Cdc37 and Hsp90*. *Molecular Cell*, 2002. **9**(2): p. 401-410.

CHAPTER 2.

HSP90 INHIBITION BY 17-DMAG REDUCES INFLAMMATION IN J774 MACROPHAGES THROUGH SUPPRESSION OF AKT AND NUCLEAR FACTOR- κ B PATHWAYS

Shimp III, S. K., Parson, C., Regna, N., Chafin, C., Reilly, C. M., Rylander, M. N.,
“HSP90 inhibition by 17-DMAG reduces inflammation in J774 macrophages through
suppression of Akt and NF- κ B pathways”, *Inflamm Res*, 2012 May; 61(5):521-533.

ABSTRACT

Objective:

This study was designed to determine whether inhibition of Heat Shock Protein 90 (HSP90) reduces pro-inflammatory mediator production by decreasing the Nuclear Factor (NF)- κ B and Akt signaling pathways in immune-stimulated macrophages.

Methods:

J774A.1 murine macrophages were treated with the HSP90 inhibitor 17-DMAG (0.01, 0.1 or 1 μ M) prior to immune stimulation with lipopolysaccharide and interferon- γ . Expression of Akt, inhibitor of κ B kinase (IKK), and heat shock proteins were measured in whole cell lysates by Western blot. Phosphorylated Akt and Inhibitor of κ B (I κ B) were measured in whole cell lysates by ELISA. Cell supernatants were analyzed for interleukin (IL)-6, tumor necrosis factor (TNF)- α and nitric oxide (NO). Translocation of NF- κ B and heat shock factor (HSF)-1 was assessed by immunofluorescence.

Results:

Treating cells with 17-DMAG reduced expression of Akt and IKK in immune-stimulated cells. 17-DMAG reduced nuclear translocation of NF- κ B and reduced immune-stimulated production of IL-6, TNF- α and NO, but did not decrease inducible nitric oxide synthase expression.

Conclusions:

Our studies show that the immune mediated NF- κ B inflammatory cascade is blocked by the HSP90 inhibitor 17-DMAG. Due to the broad interaction of HSP90 with many pro-inflammatory kinase cascades, inhibition of HSP90 may provide a novel approach to reduce chronic inflammation.

2.1 Introduction

Heat shock proteins (HSPs) are chaperone proteins that bind to and stabilize many signaling kinases involved with various physiological and pathophysiological cellular functions. One such protein that has been linked to inflammatory conditions is Heat Shock Protein 90 (HSP90). HSP90 is a homo-dimeric molecular chaperone comprising 1-2% of total cellular protein [1]. HSP90 has a prominent role in folding and conformational regulation of many proteins ranging from kinases to transcription factors [2-4]. The extensive list of HSP90 client proteins includes the pro-inflammatory kinase Akt [5-11]. Dissociation of HSP90 from its client proteins is associated with client protein degradation [2]. Inhibition of HSP90 has been shown to exert anti-inflammatory effects through various mechanisms [12]. HSP90 inhibition has been shown to deactivate Akt and reduce the response of the Phosphatidylinositol-3 Kinase (PI3K)/Akt inflammatory cascade [5-7, 13-15].

Given that HSP90 plays a role in inflammatory conditions, controlling HSP90 function and/or expression experimentally may provide a novel mechanism to inhibit the inflammatory cascade. Geldanamycin (GA) and its analogue 17-demethylaminoethylamino-17-demethoxygeldanamycin (17-DMAG or alvespimycin) are inhibitors of HSP90. They function by binding to HSP90 at the N-terminal ATP binding pocket preventing chaperone-client binding [4, 12, 16, 17]. 17-DMAG has been reported to be more soluble and elicit less toxicity compared to the parent compound GA [16, 17]. Due to its improved solubility and lower hepatotoxicity than GA, 17-DMAG is currently being investigated in clinical trials as an anti-cancer therapeutic [18]. It was recently reported that inhibition of HSP90 by 17-DMAG prevented activation of the Nuclear Factor (NF)- κ B pathway in chronic lymphoid leukemia cells [19]. HSP90 inhibition has been reported to decrease inflammatory mediators and cytokines including interleukin (IL)-1 β , IL-6, tumor necrosis factor (TNF)- α , and nitric oxide (NO) [20-22]. Because of the lower toxicity and clinical relevance of HSP90 inhibition, we selected 17-DMAG as the HSP90 inhibitor for this study.

Pro-inflammatory signaling proteins including Akt, Inhibitor of κ B Kinase (IKK), and NF- κ B have all been found to interact with HSP90 [19, 23-28]. Lipopolysaccharide (LPS) and Interferon (IFN)- γ synergistically stimulate inflammatory mediator production in macrophages by binding to their respective receptors and stimulating various cell signaling cascades [29, 30]. Immune stimulation leads to signal transduction by the activation of pathways including Akt/Mammalian Target of Rapamycin (mTOR), IKK/NF- κ B, and others. This results in the production of pro-inflammatory cytokines and mediators including TNF- α , IL-6, and NO [31]. The purpose of this study was to define the mechanism by which 17-DMAG reduces inflammation by inhibiting HSP90.

2.2 Methods

J774 Mouse Macrophage Cell Culture: Mouse macrophages (J774A.1, ATCC, Manassas, VA) were cultured in DMEM media supplemented with 4 mM L-glutamine, 4.5 g/L glucose, 1.5 g/L sodium bicarbonate, 10% fetal bovine serum (FBS), and 1% penicillin/streptomycin. Prior to treatment, the media was changed to 1% FBS. Cells were seeded in 6 well cell culture treated dishes (ThermoFisher Scientific, Waltham, MA) at a density of 2×10^5 cells per cm^2 of growth area. To measure the effect of HSP90 inhibition on inflammatory pathway activation, cells were cultured in 0.01 μM or 0.1 μM 17-DMAG for 1 hour and then stimulated for 15, 30, 60 or 120 minutes with LPS (1 $\mu\text{g}/\text{ml}$; Sigma, St. Louis, MO) and IFN- γ (300 units/ml; Accurate Chemical, Westbury, NY). To measure the effect of HSP90 inhibition on protein expression, cells were treated with 17-DMAG (0.01, 0.1, 1, or 10 μM) for 24 hours followed by 24 hours of stimulation with LPS/IFN- γ . 17-DMAG concentrations were selected based on prior published reports showing that 0.01 to 1 μM of 17-DMAG inhibited HSP90 function without cellular toxicity [19, 32].

Nitrite Production: Media was collected at the indicated times and analyzed for nitrite concentration (a stable metabolite of NO) as previously described [33]. Briefly, supernatants were analyzed by mixing an equal volume of sample with Griess reagents (1% sulfanilamide and 0.1% naphthylethylenediamene in 2.5% H_3PO_4) in a 96 well plate. Absorbance was determined by a microplate reader reading at a wavelength of 550 nm.

Cell Lysis: At the indicated times cells were collected and lysed in the following manner: the media was removed from the cells and replaced with PBS. Cells were scraped from the culture dish and the resulting suspension was pelleted by centrifugation at 120xg for 5 minutes. The supernatant was removed and the pellet was suspended in RIPA lysis buffer (Santa Cruz

Biotechnology, Santa Cruz, CA) and mixed by vortexing. The suspension was placed on ice for 40 minutes with additional mixing occurring after 20 minutes and at the end of the incubation. The suspension was centrifuged at 10,000xg for 10 minutes and the supernatant was collected and stored at -80°C until analysis.

Western Blot: Total cellular protein concentrations of cell lysates were measured by Pierce BCA assay (ThermoFisher Scientific, Waltham, MA) according to the manufacturer's protocol. Cell lysates were diluted to achieve uniform total protein concentrations across samples. Samples were boiled in Laemmli Buffer for 5 minutes and resolved with 10% SDS-PAGE. The proteins were transferred to a Polyvinylidene Difluoride (PVDF) membrane and probed with antibodies against HSP70 and HSP90 (Enzo Life Sciences, Farmingdale, NY); iNOS (Cell Signaling, Boston, MA); and β -Actin (Santa Cruz Biotechnology, Santa Cruz, CA). Densitometric analysis of Western blot images was performed using ImageJ (NIH, Bethesda, MD).

ELISA: Supernatants were collected at the indicated times and analyzed for IL-6 and TNF- α levels by ELISA per the manufacturer's instructions (eBioscience, San Diego, CA). Cell lysates were analyzed by ELISA for phosphorylated Akt (p-Akt) (Cell Signaling, Boston, MA), phosphorylated I κ B (p-I κ B), and total I κ B (Millipore, Billerica, MA) per the manufacturers' instructions.

Apoptosis Assay: Cells were pretreated for 24 hours with 17-DMAG (0.1 and 1 μ M) and stimulated with LPS/IFN- γ for 2 hours. To collect samples, media was removed and the cells were detached using trypsin (Invitrogen, Carlsbad, CA), and pelleted by centrifugation at 120xg for 5 minutes and the cells were suspended in growth media. Cell suspensions were pelleted by centrifugation at 120xg for five minutes and were suspended in binding buffer containing Annexin V-FITC (AnnV) and Propidium Iodide (PI) following the manufacturer's instructions

(Biovision, Mountain View, CA). Cells were analyzed by flow cytometry using a FACS Aria 1 flow cytometer (BD Biosciences, San Jose, CA) and data were analyzed by FlowJo software (Tree Star, Ashland, OR).

Immunofluorescence Microscopy: Cells were seeded on Lab-Tek II slides (Nalge Nunc International, Rochester, NY) at a density of 1×10^5 cells/cm². Cells were treated with 0.1 μ M of 17-DMAG for 1 hour prior to stimulation with LPS/IFN- γ . After 30 minutes, cells were fixed with HistoChoiceMB fixative (Amresco, Solon, OH) and permeabilized using 0.5% Triton-X. Fixed cells were incubated for 1 hour in PBS with 2% BSA and 1% Tween for blocking. Cells were stained with rabbit anti-NF- κ B (Cell Signaling, Boston, MA) and rat anti-HSF1 (Abcam, Cambridge, MA) as primary antibodies, followed by incubation with anti-rabbit-AlexaFluor 488 (Invitrogen, Carlsbad, CA) and anti-rat-rhodamine red-x (Jackson ImmunoResearch, West Grove, PA). Cells were counterstained with DAPI nuclear stain using VectaShield mounting media with DAPI (Vector Labs, Burlingame, CA).

Statistical Analysis: Values are expressed as means plus or minus the standard error of the mean (SEM). One-way ANOVA with Tukey's multiple comparison post-test was used to assess the statistical significance of the effect of 17-DMAG concentration (Figures 1, 2, 5, and 7). Two-way ANOVA with Bonferroni post-tests was used to assess the statistical significance of time and 17-DMAG concentration data (Figure 3). For 95% confidence intervals, p values less than 0.05 were considered significant.

2.3 Results

2.3.1 17-DMAG reduced viability in immune-stimulated cells

17-DMAG has been shown to induce apoptosis [19]. To determine the optimal concentration for decreasing cell activation without toxicity, we measured cellular viability and cell death by apoptosis (Figure 1). To perform this test cells were treated with 17-DMAG (0.1 or 1 μ M) for 24 hours then stimulated cells with LPS/IFN- γ for an additional 2 hours. We found no reduction in viability from cells receiving 0.1 μ M 17-DMAG either with or without stimulation by LPS/IFN- γ (Figure 1A). However, 1 μ M 17-DMAG reduced cell viability when combined with LPS/IFN- γ stimulation ($p < 0.01$; Figure 1A).

Apoptotic and necrotic populations were also assessed to elucidate further the mechanism of cell death (Figure 1B, C, and D). There was no increase in apoptosis or necrosis in cells treated with 0.1 μ M 17-DMAG (with or without LPS/IFN- γ). The combination of 1 μ M 17-DMAG and LPS/IFN- γ resulted in increased apoptosis ($p < 0.05$ vs. non-stimulated control) and increased necrosis ($p < 0.05$ vs. non-stimulated control).

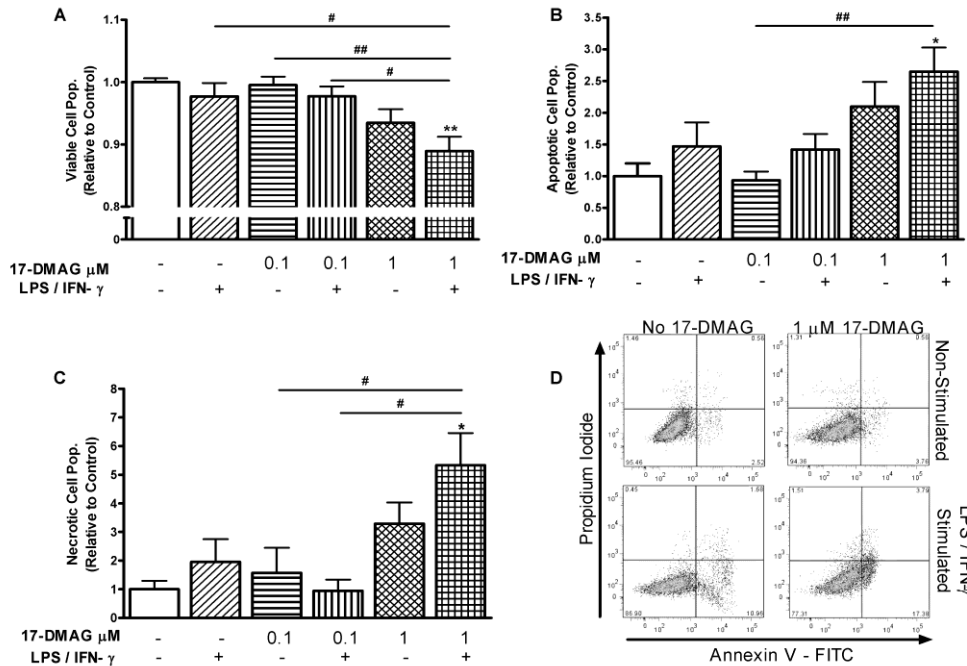


Figure 2.1. 17-DMAG reduced viability and induced apoptosis and necrosis in J774 cells stimulated with LPS/IFN- γ . Cells were pre-treated with 0.1 or 1 μ M 17-DMAG for 24 hours, stimulated for 2 hours with LPS/IFN- γ , and analyzed by flow cytometry for Annexin V and propidium iodide staining. A) There was no significant reduction of cell viability in cells treated with 0.1 μ M 17-DMAG with or without LPS/IFN- γ . Treatment with 1 μ M 17-DMAG alone did not reduce viability but 1 μ M 17-DMAG with LPS/IFN- γ showed reduced cell viability. B) Cells treated with 0.1 μ M of 17-DMAG did not show an increase in apoptosis. In contrast, 1 μ M of 17-DMAG with LPS/IFN- γ stimulation exhibited an increase in apoptosis. C) 17-DMAG (0.1 μ M) did not induce necrosis with or without LPS/IFN- γ . Treatment with 1 μ M 17-DMAG and LPS/IFN- γ stimulation induced necrosis. D) Representative flow cytometry data for cells treated with or without 1 μ M of 17-DMAG and with or without LPS/IFN- γ . One-way ANOVA with Tukey's multi-comparison post-test: * $p < 0.05$, ** $p < 0.01$, non-treated, non-stimulated control; # $p < 0.05$, ## $p < 0.01$ vs. indicated samples. The results represent four independent experiments performed in duplicate.

2.3.2 17-DMAG decreases Akt and IKK α expression

To determine the mechanism by which 17-DMAG inhibits the pro-inflammatory signaling cascade, total expression of IKK- α and Akt were measured by Western blot (Figure 2). Cells were treated for 24 hours with 17-DMAG (0.1 μ M) and then stimulated with LPS/IFN- γ for an additional 24 hours. Total Akt expression was not significantly affected in cells treated for 24 hours with 17-DMAG alone. Treatment with 17-DMAG and LPS/IFN- γ showed a significant reduction in total Akt expression ($p < 0.01$ vs. non-stimulated control; $p < 0.05$ vs. LPS/IFN- γ control). Total IKK was reduced by treatment with 17-DMAG alone ($p < 0.01$ vs. non-treated control) or with 17-DMAG and LPS/IFN- γ ($p < 0.001$ vs. non-treated control; $p < 0.01$ vs. LPS/IFN- γ control),

To test if HSP90 inhibition altered the phosphorylation of Inhibitor of κ B (I κ B), we treated cells with 17-DMAG for one hour, followed by stimulation with LPS/IFN- γ . Cell lysates were collected at 15, 30, 60 and 120 minutes and analyzed for total and phosphorylated I κ B (p-I κ B) (Figure 3A and C). We found that one-hour treatment with 17-DMAG significantly decreased LPS/IFN- γ stimulated p-I κ B expression prior to and after 15 minutes of stimulation ($p < 0.001$). However, p-I κ B was not affected by 17-DMAG at 30, 60 and 120 minutes, suggesting that the 17-DMAG inhibitory effect on p-I κ B was transient. We also found that total I κ B was reduced prior to stimulation ($p < 0.01$) and 15 minutes after stimulation ($p < 0.05$). We found no effect of 17-DMAG on total I κ B after 30, 60 and 120 minutes of LPS/IFN- γ stimulation.

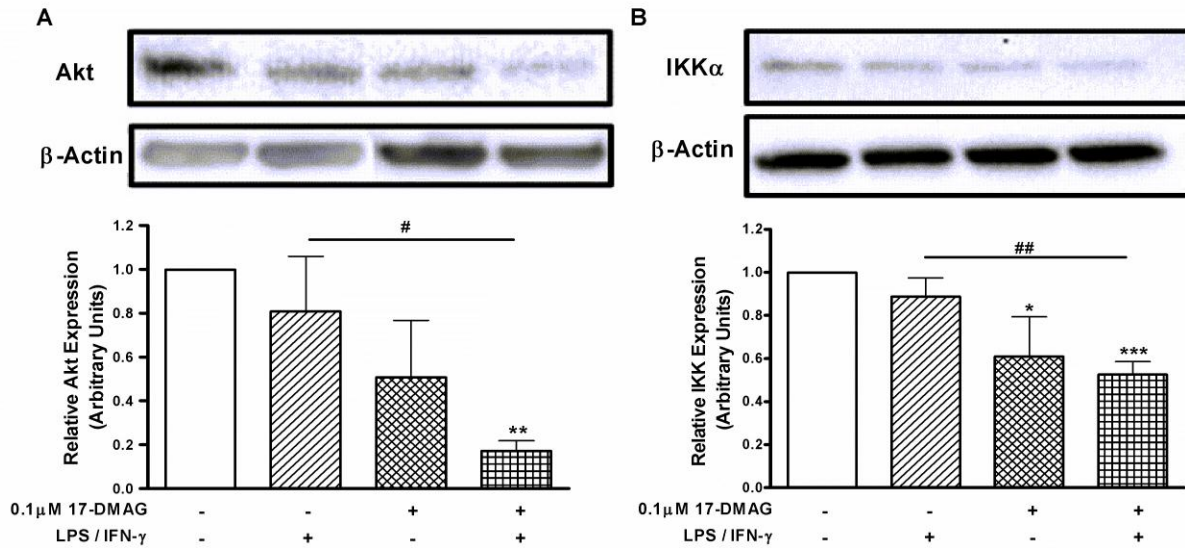


Figure 2.2. 17-DMAG reduced Akt and IKK α expression. Cells were treated for 24-hours with 17-DMAG then stimulated for another 24 hours with LPS/IFN- γ . Cell lysates were collected and analyzed by Western blot for total IKK α , Akt, and β -Actin expression. A) Representative Western blot and averaged densitometry of Akt normalized to β -actin expression. 17-DMAG and LPS/IFN- γ stimulation reduced Akt. Treatment with 17-DMAG alone did not significantly affect Akt. B) Representative Western blot and averaged densitometry of IKK α normalized to β -actin expression. 17-DMAG reduced IKK α expression with and without LPS/IFN- γ stimulation. Analysis of densitometry data by one-way ANOVA with Tukey's multi-comparison test: * $p < 0.05$, ** $p < 0.01$ and *** $p < 0.001$ vs. non-treated, non-stimulated control; # $p < 0.05$, ## $p < 0.01$ vs. LPS/IFN- γ control. The results represent three independent experiments performed in duplicate.

To test if Akt activation was affected by 17-DMAG, cells were treated with 17-DMAG for one hour, followed by stimulation with LPS/IFN- γ . At 15, 30, 60 and 120 minutes following stimulation, the cells were collected, lysed, and analyzed for p-Akt expression (Figure 3B). We found phosphorylated Akt (p-Akt) expression was reduced prior to LPS/IFN- γ stimulation ($p <$

0.001) and 15 minutes after LPS/IFN- γ stimulation ($p < 0.01$). Interestingly, p-Akt was increased by 17-DMAG after 30 minutes of stimulation ($p < 0.05$) but was reduced again by 17-DMAG after 120 minutes of stimulation ($p < 0.001$).

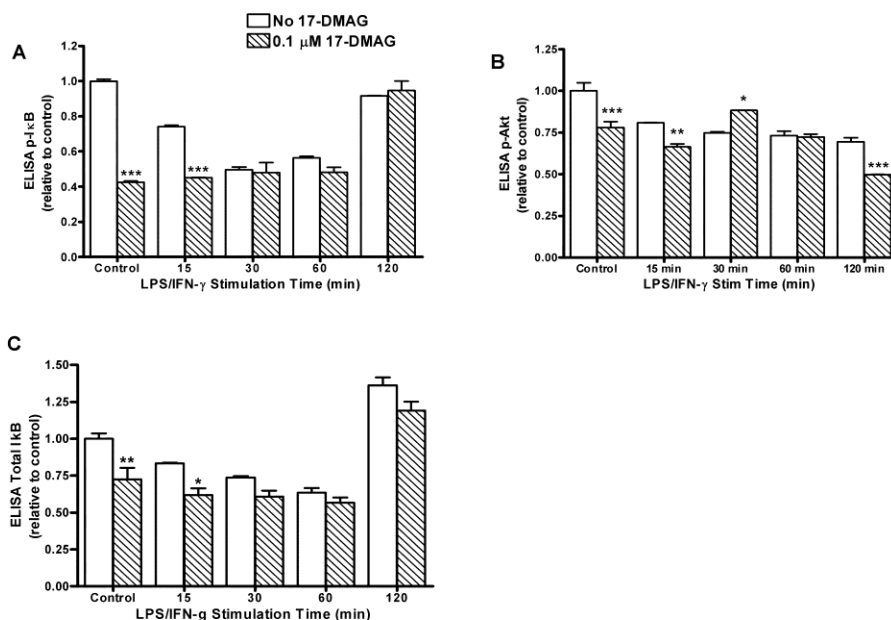


Figure 2.3. 17-DMAG reduced initial phosphorylation of I κ B and Akt in LPS/IFN- γ stimulated cells. Cells were pre-treated for 1 hour with 17-DMAG then stimulated with LPS / IFN- γ . Cell lysates were collected 15, 30, 60, and 120 minutes after stimulation and analyzed by ELISA. A) p-I κ B was reduced prior to and at 15 minutes of LPS/IFN- γ stimulation. 17-DMAG did not affect I κ B phosphorylation at 30, 60 or 120 minutes of LPS/IFN- γ stimulation. B) 17-DMAG reduced p-Akt prior to and at 15 minutes of stimulation. P-Akt was increased in 17-DMAG treated cells at 30 minutes of stimulation, however, p-Akt was reduced by 17-DMAG at 120 minutes of stimulation. C) Total I κ B expression was reduced prior to and at 15 minutes of stimulation. 17-DMAG did not affect total I κ B at any other time point. Analysis by two-way ANOVA with Bonferroni post-tests: * $p < 0.05$, ** $p < 0.01$, *** $p < 0.001$, vs control. Four independent experiments were done in duplicate for $n = 4$, representative experiments shown.

2.3.3 Translocation of NF- κ B was inhibited in cells treated with 17-DMAG.

Having determined that 17-DMAG reduced expression of total Akt and IKK α as well as delaying I κ B phosphorylation, we sought to determine if 17-DMAG would prevent LPS/IFN- γ stimulated NF- κ B translocation (Figure 4). Cells were cultured on microscope slides and treated with 17-DMAG (0.1 or 1 μ M) for 24 hours followed by stimulation with LPS/IFN- γ for 30 minutes. NF- κ B translocation was assessed by immunofluorescence microscopy. We found that 17-DMAG alone did not induce NF- κ B nuclear translocation but reduced overall NF- κ B expression. Stimulation with LPS/IFN- γ alone resulted in strong NF- κ B nuclear localization. In cells treated with 17-DMAG and stimulated with LPS/IFN- γ , nuclear translocation of NF- κ B was abrogated and total NF- κ B expression was reduced.

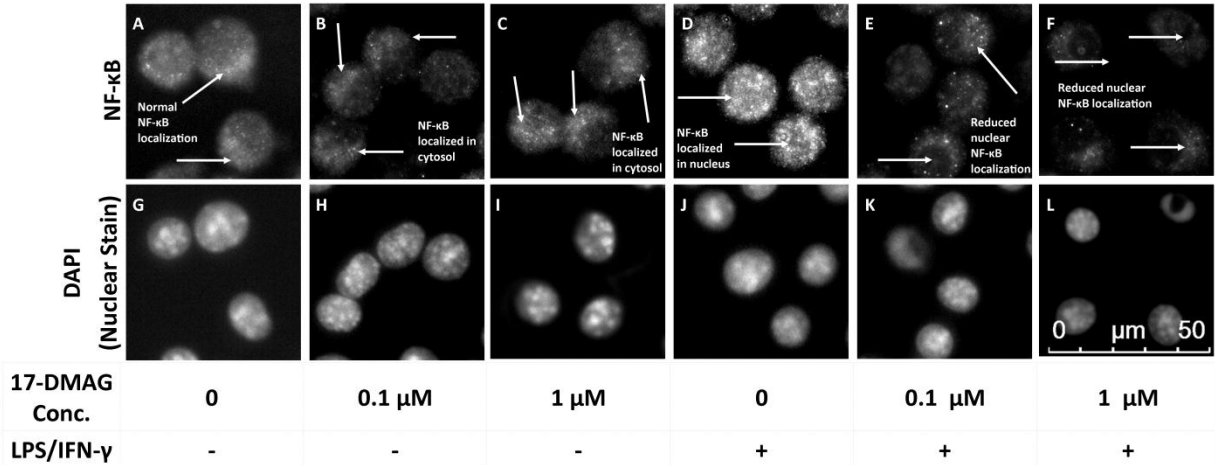


Figure 2.4. Nuclear translocation of NF-κB in immune-stimulated cells pretreated with 17-DMAG shown by immunofluorescence. Cells were cultured on microscopy slides, treated for 24 hours with 0.1 or 1 μM concentrations of 17-DMAG followed by 30 minutes of immune stimulation to activate NF-κB. Background subtraction was performed uniformly for improved image clarity. A-F) AlexaFluor-488 labeled anti-NF-κB. G-L) DAPI nuclear counterstain. A) Cytosolic expression of NF-κB with nominal nuclear translocation in the non-stimulated control. D) Immune stimulation only (no 17-DMAG) increased nuclear translocation of NF-κB. B and C) Decreased NF-κB expression and reduced nuclear translocation in cells treated with 17-DMAG alone. E and F) Decreased expression and reduced nuclear translocation of NF-κB in cells pre-treated with 17-DMAG with LPS/IFN-γ stimulation. Two independent experiments were performed in duplicate, 25 images were taken per slide to verify uniform response. Most representative image is shown. Scale bar is shown for reference.

2.3.4 HSP70 expression increased, HSP90 expression was unchanged in LPS/IFN- γ stimulated cells treated with 17-DMAG

HSP70 protein expression increases in response to HSP90 inhibition and HSP70 expression is frequently used to confirm HSP90 inhibition [34, 35]. Additionally, the heat shock factor 1 (HSF1) protein is known to translocate from the cytosol to the nucleus in response to HSP90 inhibition [34]. To verify that 17-DMAG was exerting its effects through HSP90 inhibition, we assessed HSP70 and HSP90 expression and examined the translocation of HSF1 in response to 17-DMAG treatment.

We treated cells for 24 hours with 17-DMAG followed by stimulation with LPS/IFN- γ for 24 hours. Cell lysates were collected and analyzed by Western blot (Figure 5). We found LPS/IFN- γ stimulation alone did not affect HSP70 expression but cells treated with 17-DMAG and stimulated with LPS/IFN- γ showed elevated HSP70 expression ($p < 0.05$).

To validate further that HSP90 was being inhibited by 17-DMAG, we used immunofluorescence microscopy to examine the translocation of HSF1 (Figure 6). Cells were cultured on microscope slides and treated with 17-DMAG (0.1 and 1 μ M) for 24 hours then stimulated for 30 minutes with LPS/IFN- γ . We found that cells that did not receive 17-DMAG had higher cytosolic localization of HSF1 compared to cells that were treated with 17-DMAG (Figure 6A & D). Cells treated with 17-DMAG exhibited nuclear staining indicative of HSF1 translocation (Figure 6B, C, E, and F). Nuclear translocation of HSF1 occurred equally in immune-stimulated cells and non-immune-stimulated cells treated with 17-DMAG. Furthermore, nuclear localization of HSF1 correlated with increasing concentrations of 17-DMAG administration (Figure 6C & F).

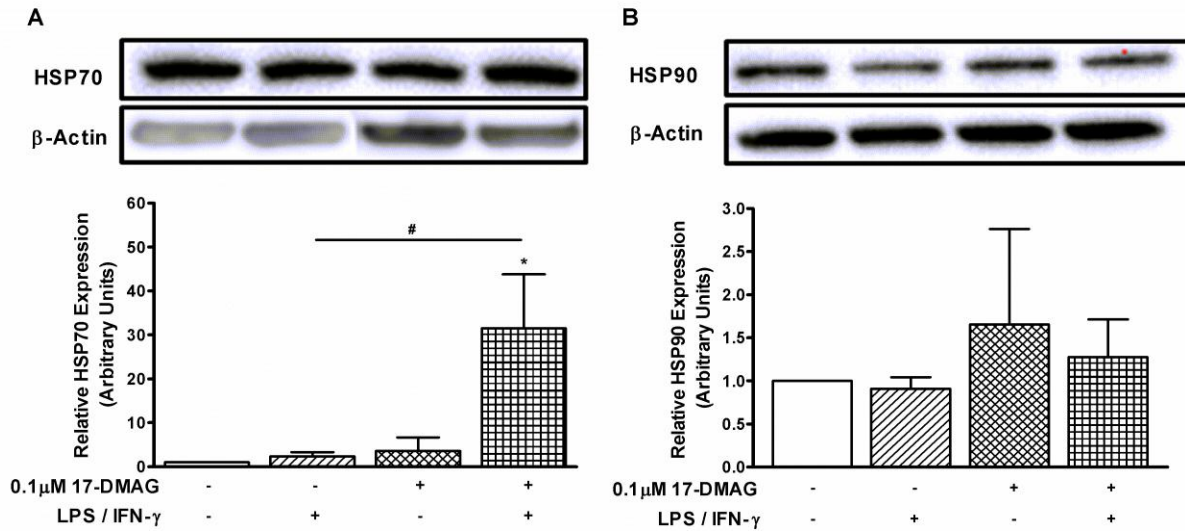


Figure 2.5. Treatment with 17-DMAG increased HSP70 expression but did not change HSP90 expression. Cells were cultured for 24 hours with 17-DMAG then stimulated by LPS/IFN- γ . Cell lysates were collected 24 hours after stimulation and analyzed by Western blot for HSP70, HSP90, and β -Actin expression. A) Representative Western blot and average densitometry is shown. 17-DMAG increased HSP70 expression only in cells stimulated with LPS / IFN- γ . B) Representative Western blot and average densitometry is shown. Neither 17-DMAG nor LPS/IFN- γ stimulation affected HSP90 expression. Analysis of densitometry data by one-way ANOVA with Tukey's multi-comparison test: * $p < 0.05$, vs. non-treated, non-stimulated control; # $p < 0.05$, vs. LPS/IFN- γ control. The results represent three independent experiments performed in duplicate.

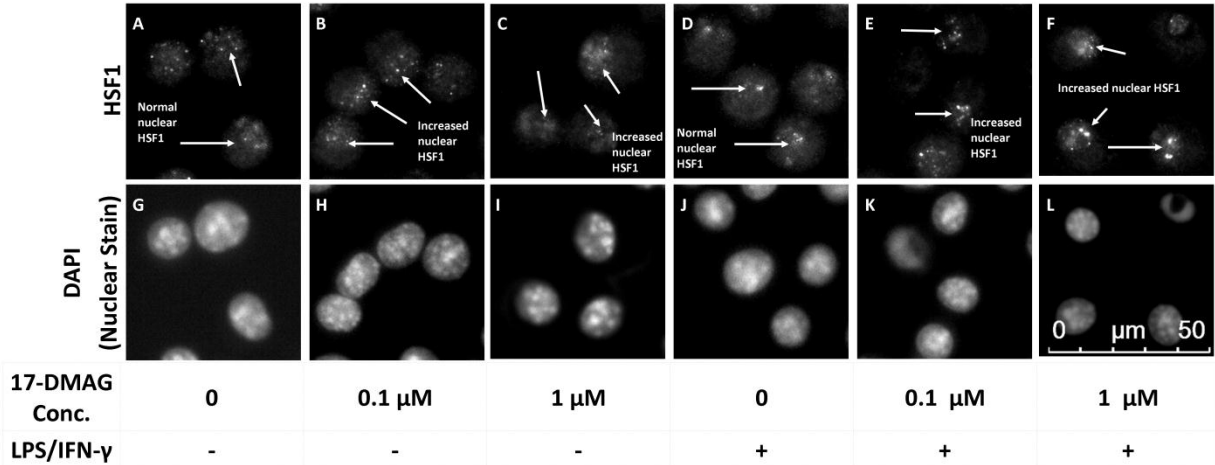


Figure 2.6. HSF1 translocation increased in response to 17-DMAG treatment. A-F) Images of RRX labeled anti-HSF1 stained cells. G-L) Images of DAPI nuclear counterstained cells. A and D) Cytosolic localization of HSF1 is exhibited in cells not treated with 17-DMAG. B, C, E, and F) Cells treated with 17-DMAG showed reduction of cytosolic HSF1 with increased nuclear translocation of HSF1(bright spots) with and without LPS/IFN- γ stimulation. Background subtraction was performed uniformly for improved image clarity. Two independent experiments performed in duplicate, 25 images were taken per slide to verify uniform response. Most representative image is shown. Scale bar is shown for reference.

2.3.5 Immune-stimulated NO production and IL-6 expression were reduced in response to treatment with 17-DMAG

Immune stimulation of macrophages by LPS/IFN- γ induces the release of NO, IL-6, TNF- α , and other cytokines [36]. We tested if HSP90 inhibition would decrease the production of IL-6, TNF- α , and NO in immune-stimulated cells. Cells were treated with 17-DMAG (0.1 or 1 μ M) for 24 hours then stimulated with LPS/IFN- γ . Media was collected 24 hours post stimulation and analyzed by ELISA for IL-6 and TNF- α or by Griess assay for NO (Figure 7).

Production of NO stimulated by LPS/IFN- γ was reduced by treatment with 17-DMAG (Figure 7A). Both concentrations of 17-DMAG that were tested (0.1 and 1 μ M) reduced LPS/IFN- γ stimulated NO production significantly when compared to the LPS/IFN- γ stimulated control ($p < 0.05$, 0.1 μ M; $p < 0.01$, 1 μ M). Next, we sought to determine if 17-DMAG reduced NO production by inhibiting iNOS protein expression. Cell lysates were collected and analyzed by Western blot (Figure 7B). Interestingly, despite the reduction in NO found in cells treated with 17-DMAG, iNOS protein expression was increased with 17-DMAG treatment ($p < 0.05$; Figure 7B).

Media was also analyzed by ELISA for IL-6 production (Figure 7C). As expected, LPS/IFN- γ stimulation increased IL-6 production. Treatment with 17-DMAG reduced immune-stimulated expression of IL-6 in a concentration dependent manner. Treatment with 0.1 μ M 17-DMAG reduced LPS-IFN- γ stimulated IL-6 ($p < 0.001$ vs. LPS/IFN- γ control) but was still elevated above the level of the non-treated, non-stimulated control ($p < 0.001$ vs. control). However, 1 μ M 17-DMAG reduced LPS-IFN- γ stimulated IL-6 to levels comparable to the non-treated, non-stimulated control ($p < 0.001$ vs. LPS/IFN- γ control). Finally, we used ELISA to

analyze the media for TNF- α expression (Figure 7D). We found TNF- α expression was reduced in 17-DMAG treated cells with LPS-IFN- γ stimulation ($p < 0.01$ vs. LPS/IFN- γ control).

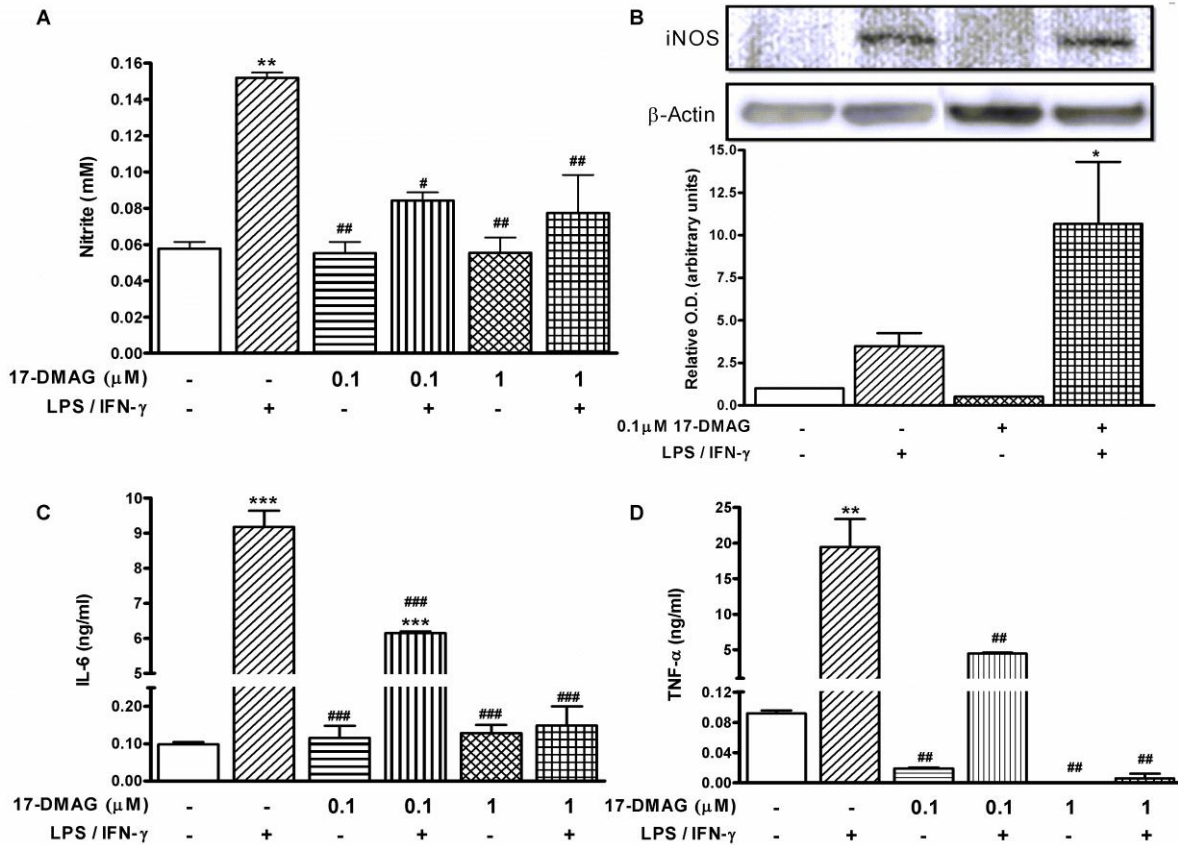


Figure 2.7. 17-DMAG reduced expression of NO, IL-6 and TNF- α . Cells were treated for 24 hours with indicated concentrations of 17-DMAG followed by 24 hours of LPS/IFN- γ stimulation. Media was collected and analyzed by ELISA for IL-6 and TNF- α expression. Media analyzed by Griess assay for NO production. Cell lysates collected and analyzed by Western blot for iNOS and β -Actin expression. A) 17-DMAG reduced immune-stimulated NO expression. B) Representative Western blot and average densitometry showed that 17-DMAG and LPS/IFN- γ stimulation increased iNOS. C) IL-6 expression was reduced by 17-DMAG in LPS/IFN- γ stimulated cells. D) 17-DMAG reduced TNF- α expression in immune-stimulated cells. One-way ANOVA with Tukey's multi-comparison test was performed on ELISA and densitometry data: * $p < 0.05$, ** $p < 0.01$, *** $p < 0.001$, vs. non-stimulated control; # $p < 0.05$, ## $p < 0.01$, ### $p < 0.001$, vs. LPS/IFN- γ stimulated control. Western blot sample loading was normalized by β -actin bands.

2.4 Discussion

Our results show that inhibition of HSP90 by 17-DMAG reduced Akt and IKK expression and decreased NO, IL-6, and TNF- α production in LPS/IFN- γ stimulated macrophages. With more than 100 HSP90-dependent client proteins targeting HSP90 therapeutically, HSP90 inhibition has potential for broad and effective treatment of inflammatory diseases [2]. Activation of macrophages and monocytes in inflammation can prevent apoptosis and lead to prolonged macrophage and monocyte viability [37, 38]. Apoptosis induced by HSP90 inhibitors has shown selectivity for abnormal cells, and recently was shown to be dependent on the activation of specific apoptotic proteins [39]. The HSP90 inhibitor 17-DMAG has been shown to induce apoptosis selectively in chronic lymphoid leukemia cells [19]. In our studies, we found that 1 μ M 17-DMAG induced apoptosis in LPS/IFN- γ stimulated cells but 17-DMAG treatment alone did not induce cell death at any concentration tested. Our data, along with results previously published by other groups [19], suggest that 17-DMAG selectively targets activated macrophage cells in a concentration-dependent manner. To study anti-inflammatory effects of 17-DMAG independent of cell death induction, we used 17-DMAG at concentrations below 1 μ M.

We found that one of the mechanisms for 17-DMAG's anti-inflammatory effects was through reduction of Akt and IKK expression. Akt activation affects cell functions by several mechanisms including protein phosphorylation, inflammatory mediator production, apoptosis, and cell proliferation [40-42]. Activation of Akt pathways increases transcription of several pro-inflammatory cytokines including TNF- α and IL-6 as well as the effector molecule NO. This occurs in part through Akt-associated induction of NF- κ B [40-45].

Akt is a client of HSP90 and known to bind to the middle domain of HSP90 [3, 6]. Inhibition of HSP90 increases Akt degradation which results in decreased Akt expression after 12

hours of exposure to HSP90 inhibitors [5]. HSP90 inhibitors have also been shown to reduce Akt activation [14]. With regard to Akt activation, HSP90 has been found to protect Akt from protein phosphatase 2A (PP2A) mediated dephosphorylation whereas inhibition of HSP90 allows PP2A to deactivate Akt [6]. We found that 24 hour treatment with 17-DMAG reduced total Akt expression in cells stimulated with LPS/IFN- γ . Additionally, we found the reduction in Akt could be achieved at concentrations that did not induce apoptosis. In terms of Akt phosphorylation, our results were mixed. We observed that one hour of treatment with 17-DMAG, Akt phosphorylation induced by LPS/IFN- γ was abrogated for the first 15 minutes. However, at 30 minutes Akt phosphorylation was increased in 17-DMAG treated cells. At 120 minutes of stimulation by LPS/IFN- γ , the 17-DMAG treated cells again showed a reduction in Akt phosphorylation. Our study showed that 24 hour treatment with 17-DMAG does reduce total Akt expression while Akt phosphorylation is only transiently affected by 17-DMAG.

As an intermediate member of the Akt/NF- κ B pathway, IKK is also an HSP90 client protein. In various cell types, IKK-mediated activation of NF- κ B was abrogated by inhibition of HSP90. This suggests that HSP90 is required for IKK to activate NF- κ B [46]. In endothelial cells, enhanced affinity of HSP90 and IKK leads to increased NF- κ B activation and cellular dysfunction [47]. Furthermore, in cardiac cells the HSP90 inhibitor GA prevented HSP90-IKK complex formation, leading to increased IKK α/β degradation [48]. Treatment with HSP90 inhibitors in bladder cancer cells has also been shown to down-regulate expression of IKK, which resulted in reduced NF- κ B activity [49]. Our studies support a role for HSP90 in blocking IKK mediated NF- κ B activation. We found that 17-DMAG reduced IKK expression in LPS/IFN- γ stimulated macrophage cells. To define further how IKK activation is affected by HSP90 inhibition, we examined the downstream protein, I κ B. I κ B is part of the classical NF- κ B pathway. In a recent study, treatment with 17-DMAG for 24 hours reduced I κ B phosphorylation in cancer

cells [19]. I κ B phosphorylation was also reduced in cardiac cells treated with GA and this decrease was attributed to the reduction in IKK expression, and not due to a direct interaction between HSP90 and I κ B [48]. In addition, a four-hour treatment with 17-DMAG prevented I κ B α from being phosphorylated in IL-6/IFN- γ activated human vascular smooth muscle cells [50]. However, we found that a one-hour treatment with 17-DMAG followed by stimulation from LPS/IFN- γ only reduced phosphorylation of I κ B prior to and at 15 minutes stimulation. Our data suggests that HSP90 does not directly affect I κ B activity; however, our data would also suggest that inhibition of I κ B phosphorylation requires 17-DMAG treatment time greater than 1 hour. Upon phosphorylation of I κ B, it dissociates from NF- κ B which allows NF- κ B to translocate to the nucleus and bind to specific inflammatory gene promoters [51]. Recently, 17-DMAG was shown to reduce NF- κ B activation in human macrophage cells by preventing I κ B deactivation [50]. Similarly, our results showed that 17-DMAG reduced nuclear translocation of NF- κ B which we attribute to the degradation of IKK and Akt by inhibition of HSP90.

We showed that Akt and IKK expression and NF- κ B nuclear translocation are reduced by 17-DMAG at concentrations that do not induce cell death. To confirm that these effects were induced by HSP90 inhibition, we tested several markers for HSP90 inhibition. When HSP90 is not bound to a client protein, HSP90 binds to HSF1 and other co-chaperone proteins [52]. When a client protein binds to HSP90 or when HSP90 is inhibited, HSF1 is activated and released from the co-chaperone complex. Activated HSF1 translocates to the nucleus where it initiates the transcription of heat shock responding proteins including heat shock protein 70 (HSP70) [53]. Increased HSP70 and translocation of HSF1 are often used as indicators for the inhibition of HSP90 [34, 35]. There is some disparity in the literature about the effect that HSP90 inhibitors have on the actual expression of HSP90 itself. A report by Clark et. al. showed reduced HSP90 expression following inhibition by GA [54]. Reports by Madrigal-Matute et. al. and Ghoshal et.

al. showed no change in HSP90 expression following inhibition with 17-DMAG [50, 55]. In our studies, we did not observe alterations of HSP90 expression with 17-DMAG regardless of cell activation with LPS/IFN- γ . This would lead us to conclude that 17-DMAG does not affect overall HSP90 protein levels. Nevertheless, we did observe an increase in nuclear translocation of HSF1 which we interpret as an indication of HSP90 inhibition. We also detected an increase in HSP70 in response to treatment with 17-DMAG. We interpreted the increase in HSP70 expression as a marker for HSP90 inhibition. Taken together, these two markers of HSP90 inhibition suggest that the anti-inflammatory mechanism of action that 17-DMAG has on macrophage cells is, in part, due to the inhibition of HSP90.

HSP70 is often negatively associated with suppression of apoptosis and the chaperoning of pro-inflammatory signal proteins [8, 56]. In contrast to this idea, it has also been shown that HSP70 and other HSPs are actively secreted from cancer cells and/or passively lost from necrotic cells as a way to signal tissue stress and destruction to innate and adaptive immune systems [57]. Whether or not this immune signal by HSP70 is a positive or negative effect for inflammation has not been fully determined. It may be that some of the anti-inflammatory effects of HSP90 inhibition are suppressed by the increased expression of HSP70. However, extracellular HSP70 has been associated with anti-inflammatory effects in atherosclerosis as activation of the TLR4 receptor on CD4⁺ CD25⁺ T regulatory cells is believed to increase their suppressive activity in atherosclerosis [58]. Although we did not directly show that HSP70 inhibited IKK activity in our studies, others have shown that HSP70 has a negative feedback effect on NF- κ B signaling activity, possibly by inhibiting IKK activity [59]. Furthermore, HSP70 has been demonstrated to switch off tumor necrosis factor receptor-associated factor 6 (TRAF6) [60]. Taken together, these studies suggest increased HSP70 may have an anti-inflammatory effect and warrants further investigation.

Our investigation of downstream effectors of inflammation included IL-6, TNF- α , and NO. NO production can be induced by immune stimulation [61]. Recently it was shown that HSP70 can function as an inhibitor of iNOS [62]. HSP90 has also been shown to complex with iNOS [63]. Inhibition of iNOS has been achieved with 17-DMAG which is a result of preventing HSP90 from forming a complex with iNOS as well as a result of increased HSP70 which suppresses iNOS activity [64]. We found that 17-DMAG significantly reduced immune-stimulated NO at a concentration (0.1 μ M) that did not reduce cell viability. However, our viability data suggests that at 1 μ M 17-DMAG there may be some effect on NO by the reduction in cell viability. Interestingly, despite the reduction in NO production, iNOS protein levels were not reduced in the 17-DMAG treated immune-stimulated cells. We would expect iNOS expression to be reduced with suppression of NF- κ B translocation [45, 61]. While we did observe reduced NF- κ B translocation with 17-DMAG treatment in immune-stimulated cells, we did not find a reduction in iNOS expression suggesting that inhibiting NF- κ B translocation may not be sufficient to down-regulate iNOS expression. Additionally, these studies suggest alternative HSP90-independent pathways may regulate iNOS.

IL-6 is an inflammatory cytokine that plays a key role in the transition from acute to chronic inflammation. Targeting IL-6 and IL-6 signaling is being actively investigated in clinical trials to treat chronic inflammatory diseases [65]. Nuclear factor (NF)-IL-6, also known as CCAAT/enhancer-binding protein- β (C/EBP β), stimulates expression of HSP90 which suggests a co-stimulatory relationship between IL-6 and HSP90 [66]. The HSP90 inhibitor GA has been shown to reduce expression of several cytokines, including IL-6, without significantly reducing the transcription of IL-6 mRNA [20]. This would suggest a post-translational dependence of pro-inflammatory cytokines on HSP90. This is the mechanism by which down-regulation of IL-6 was achieved by treating human prostate cancer cells with the HSP90 inhibitor 17-AAG [67]. This

same mechanism may be the explanation for the results we observed with 17-DMAG treatment on IL-6 production.

Altogether, our results showed that inhibition of HSP90 by 17-DMAG reduced inflammation by disrupting the Akt/NF- κ B pathway resulting in reduced expression of IL-6 and NO. We found significant reductions of Akt and IKK expression along with reduced nuclear translocation of NF- κ B which diminished expression of IL-6 and NO. Our studies found 17-DMAG reduced Akt activation but had limited effect on I κ B phosphorylation. We found non-toxic concentrations of 17-DMAG reduced production of the pro-inflammatory mediators IL-6, TNF- α , and NO. However, iNOS protein levels in stimulated cells were unaffected. Our studies focused primarily on the Akt/NF- κ B pathway; however, it is likely that crosstalk between other pathways such as the JAK/STAT pathway may be influenced by the chaperone activity of HSP90. Additional investigations into the effect of HSP90 inhibition on these pathways warrants further investigation. Future studies may elucidate how HSP70 expression affects pro-inflammatory cascades or how LPS/IFN- γ stimulated NO production is suppressed by 17-DMAG without a decrease in iNOS expression. Finally, we showed that 17-DMAG altered cytokine release but intracellular RNA levels may be unaffected. Future investigation will examine how mRNA levels are affected by 17-DMAG.

2.5 Acknowledgements

The authors wish to acknowledge the gracious assistance provided by Drs. David Caudell, Luke Achenie, Yong Woo Lee, and Liwu Li in preparation of this manuscript.

REFERENCES

1. Csermely, P., et al., *The 90-kDa Molecular Chaperone Family: Structure, Function, and Clinical Applications. A Comprehensive Review*. Pharmacol Ther, 1998. **79**(2): p. 129-168.
2. Blagg, B.S. and T.D. Kerr, *Hsp90 inhibitors: small molecules that transform the Hsp90 protein folding machinery into a catalyst for protein degradation*. Med Res Rev, 2006. **26**(3): p. 310-38.
3. Neckers, L., *Hsp90 inhibitors as novel cancer chemotherapeutic agents*. Trends Mol Med, 2002. **8**(4): p. S55-S61.
4. Neckers, L., *Heat shock protein 90: the cancer chaperone*. J Biosci, 2007. **32**(3): p. 517-30.
5. Basso, A.D., et al., *Akt forms an intracellular complex with heat shock protein 90 (Hsp90) and Cdc37 and is destabilized by inhibitors of Hsp90 function*. J Biol Chem, 2002. **277**(42): p. 39858-66.
6. Sato, S., N. Fujita, and T. Tsuruo, *Modulation of Akt kinase activity by binding to Hsp90*. Proc Natl Acad Sci U S A, 2000. **97**(20): p. 10832-7.
7. Solit, D.B., et al., *Inhibition of heat shock protein 90 function down-regulates Akt kinase and sensitizes tumors to Taxol*. Cancer Res, 2003. **63**(9): p. 2139-44.

8. Whitesell, L. and S.L. Lindquist, *HSP90 and the chaperoning of cancer*. Nat Rev Cancer, 2005. **5**(10): p. 761-72.
9. Pratt, W.B. and D.O. Toft, *Regulation of signaling protein function and trafficking by the hsp90/hsp70-based chaperone machinery*. Exp Biol Med (Maywood), 2003. **228**(2): p. 111-33.
10. Shen, G., et al., *Design, synthesis, and structure--activity relationships for chimeric inhibitors of Hsp90*. J Org Chem, 2006. **71**(20): p. 7618-31.
11. Francis, L.K., et al., *Combination Mammalian Target of Rapamycin Inhibitor Rapamycin and HSP90 Inhibitor 17-Allylamino-17-Demethoxygeldanamycin Has Synergistic Activity in Multiple Myeloma*. Clin Cancer Res, 2006. **12**(22): p. 6826-6835.
12. Bucci, M., et al., *Geldanamycin, an inhibitor of heat shock protein 90 (Hsp90) mediated signal transduction has anti-inflammatory effects and interacts with glucocorticoid receptor in vivo*. Br J Pharmacol, 2000. **131**(1): p. 13-16.
13. Miao, R.Q., et al., *Dominant-negative Hsp90 reduces VEGF-stimulated nitric oxide release and migration in endothelial cells*. Arterioscler Thromb Vasc Biol, 2008. **28**(1): p. 105-11.
14. Fujita, N., et al., *Involvement of Hsp90 in Signaling and Stability of 3-Phosphoinositide-dependent Kinase-1*. J Biol Chem, 2002. **277**(12): p. 10346-10353.

15. Abramson, J.S., et al., *The heat shock protein 90 inhibitor IPI-504 induces apoptosis of AKT-dependent diffuse large B-cell lymphomas*. *Br J Haematol*, 2009. **144**(3): p. 358-66.
16. Egorin, M., et al., *Pharmacokinetics, tissue distribution, and metabolism of 17-(dimethylaminoethylamino)-17-demethoxygeldanamycin (NSC 707545) in CD2F1 mice and Fischer 344 rats*. *Cancer Chemother Pharmacol*, 2002. **49**(1): p. 7-19.
17. Eiseman, J.L., et al., *Pharmacokinetics and pharmacodynamics of 17-demethoxy 17-[[2-(dimethylamino)ethyl]amino]geldanamycin (17DMAG, NSC 707545) in C.B-17 SCID mice bearing MDA-MB-231 human breast cancer xenografts*. *Cancer Chemother Pharmacol*, 2005. **55**(1): p. 21-32.
18. Holzbeierlein, J., A. Windsperger, and G. Vielhauer, *Hsp90: A Drug Target?* *Curr Oncol Rep*, 2010. **12**(2): p. 95-101.
19. Hertlein, E., et al., *17-DMAG targets the nuclear factor-kappaB family of proteins to induce apoptosis in chronic lymphocytic leukemia: clinical implications of HSP90 inhibition*. *Blood*, 2010. **116**(1): p. 45-53.
20. Wax, S., et al., *Geldanamycin inhibits the production of inflammatory cytokines in activated macrophages by reducing the stability and translation of cytokine transcripts*. *Arthritis Rheum*, 2003. **48**(2): p. 541-550.

21. Mandrekar, P., et al., *Alcohol exposure regulates heat shock transcription factor binding and heat shock proteins 70 and 90 in monocytes and macrophages: implication for TNF- α regulation*. J Leukoc Biol, 2008. **84**(5): p. 1335-1345.
22. Chatterjee, A., et al., *Heat Shock Protein 90 Inhibitors Prolong Survival, Attenuate Inflammation, and Reduce Lung Injury in Murine Sepsis*. Am. J. Respir. Crit. Care Med., 2007. **176**(7): p. 667-675.
23. Ha, T., et al., *Lipopolysaccharide-induced myocardial protection against ischaemia/reperfusion injury is mediated through a PI3K/Akt-dependent mechanism*. Cardiovasc Res, 2008. **78**(3): p. 546-553.
24. Ojaniemi, M., et al., *Phosphatidylinositol 3-kinase is involved in Toll-like receptor 4-mediated cytokine expression in mouse macrophages*. Eur J Immunol, 2003. **33**(3): p. 597-605.
25. Guha, M. and N. Mackman, *LPS induction of gene expression in human monocytes*. Cell Signal, 2001. **13**(2): p. 85-94.
26. Hu, X., et al., *Crosstalk among Jak-STAT, Toll-like receptor, and ITAM-dependent pathways in macrophage activation*. J Leukoc Biol, 2007. **82**(2): p. 237-243.
27. Maira, S.M., P. Finan, and C. Garcia-Echeverria, *From the bench to the bed side: PI3K pathway inhibitors in clinical development*. Curr Top Microbiol Immunol, 2010. **347**: p. 209-39.

28. Shang, L. and T.B. Tomasi, *The Heat Shock Protein 90-CDC37 Chaperone Complex Is Required for Signaling by Types I and II Interferons*. J Biol Chem, 2006. **281**(4): p. 1876-1884.
29. Lin, C.-F., et al., *IFN- γ synergizes with LPS to induce nitric oxide biosynthesis through glycogen synthase kinase-3-inhibited IL-10*. J Cell Biochem, 2008. **105**(3): p. 746-755.
30. Dalpke, A.H. and K. Heeg, *Synergistic and antagonistic interactions between LPS and superantigens*. J Endotoxin Res, 2003. **9**(1): p. 51-54.
31. Takeishi, Y. and I. Kubota, *Role of Toll-like receptor mediated signaling pathway in ischemic heart*. Front Biosci, 2009. **14**: p. 2553-8.
32. Babchia, N., et al., *17-AAG and 17-DMAG-Induced Inhibition of Cell Proliferation through B-Raf Downregulation in WTB-Raf-Expressing Uveal Melanoma Cell Lines*. Invest Ophthalmol Vis Sci., 2008. **49**(6): p. 2348-2356.
33. Gilkeson, G., et al., *Correlation of serum measures of nitric oxide production with lupus disease activity*. J Rheumatol, 1999. **26**(2): p. 318-24.
34. Shen, H.-Y., et al., *Geldanamycin Induces Heat Shock Protein 70 and Protects against MPTP-induced Dopaminergic Neurotoxicity in Mice*. J Biol Chem, 2005. **280**(48): p. 39962-39969.

35. Zhang, H., et al., *Identification of new biomarkers for clinical trials of Hsp90 inhibitors*. Mol Cancer Ther, 2006. **5**(5): p. 1256-1264.
36. Lu, Y.-C., W.-C. Yeh, and P.S. Ohashi, *LPS/TLR4 signal transduction pathway*. Cytokine, 2008. **42**(2): p. 145-151.
37. Marsh, C.B., et al., *Regulation of Monocyte Survival In Vitro by Deposited IgG: Role of Macrophage Colony-Stimulating Factor*. J Immunol, 1999. **162**(10): p. 6217-6225.
38. Ottonello, L., et al., *Dexamethasone -induced apoptosis of human monocytes exposed to immune complexes. Intervention of CD95- and XIAP-dependent pathways*. Int J Immunopathol Pharmacol, 2005. **18**(3): p. 403-15.
39. Ayrault, O., et al., *Inhibition of Hsp90 via 17-DMAG induces apoptosis in a p53-dependent manner to prevent medulloblastoma*. Proc Natl Acad Sci U S A, 2009. **106**(40): p. 17037-42.
40. LoPiccolo, J., et al., *Targeting the PI3K/Akt/mTOR pathway: Effective combinations and clinical considerations*. Drug Resist Updat, 2007. **11**(1-2): p. 32-50.
41. Patel, R.K. and C. Mohan, *PI3K/AKT signaling and systemic autoimmunity*. Immunol Res, 2005. **31**(1): p. 47-55.

42. Wu, T. and C. Mohan, *The AKT axis as a therapeutic target in autoimmune diseases*. *Endocr Metab Immune Disord Drug Targets*, 2009. **9**(2): p. 145-50.
43. Sizemore, N., S. Leung, and G.R. Stark, *Activation of Phosphatidylinositol 3-Kinase in Response to Interleukin-1 Leads to Phosphorylation and Activation of the NF-kappa B p65/RelA Subunit*. *Mol. Cell. Biol.*, 1999. **19**(7): p. 4798-4805.
44. Weichhart, T. and M.D. Säemann, *The PI3K/Akt/mTOR pathway in innate immune cells: emerging therapeutic applications*. *Ann Rheum Dis*, 2008. **67**(Suppl 3): p. iii70-iii74.
45. Kleinert, H., et al., *Regulation of the expression of inducible nitric oxide synthase*. *Eur J Pharmacol*, 2004. **500**(1-3): p. 255-266.
46. Broemer, M., D. Krappmann, and C. Scheidereit, *Requirement of Hsp90 activity for I[kappa]B kinase (IKK) biosynthesis and for constitutive and inducible IKK and NF-[kappa]B activation*. *Oncogene*, 2004. **23**(31): p. 5378-5386.
47. Mohan, S., et al., *High glucose-induced IKK-Hsp-90 interaction contributes to endothelial dysfunction*. *Am J Physiol Cell Physiol*, 2009. **296**(1): p. C182-92.
48. Lee, K.H., Y. Jang, and J.H. Chung, *Heat shock protein 90 regulates IkappaB kinase complex and NF-kappaB activation in angiotensin II-induced cardiac cell hypertrophy*. *Exp Mol Med*, 2010. **42**(10): p. 703-11.

49. Karkoulis, P.K., et al., *17-Allylamino-17-demethoxygeldanamycin induces downregulation of critical Hsp90 protein clients and results in cell cycle arrest and apoptosis of human urinary bladder cancer cells*. BMC Cancer, 2010. **10**: p. 481.
50. Madrigal-Matute, J., et al., *Heat shock protein 90 inhibitors attenuate inflammatory responses in atherosclerosis*. Cardiovasc Res, 2010. **86**(2): p. 330-7.
51. Gomard, T., et al., *An NF-kappaB-dependent role for JunB in the induction of proinflammatory cytokines in LPS-activated bone marrow-derived dendritic cells*. PLoS One, 2010. **5**(3): p. e9585.
52. Kim, H.R., H.S. Kang, and H.D. Kim, *Geldanamycin Induces Heat Shock Protein Expression Through Activation of HSF1 in K562 Erythroleukemic Cells*. IUBMB Life, 1999. **48**(4): p. 429-433.
53. Chaudhury, S., Timothy R. Welch, and Brian S.J. Blagg, *Hsp90 as a Target for Drug Development*. ChemMedChem, 2006. **1**(12): p. 1331-1340.
54. Clark, C.B., et al., *Role of oxidative stress in geldanamycin-induced cytotoxicity and disruption of Hsp90 signaling complex*. Free Radic Biol Med, 2009.
55. Ghoshal, S., et al., *Down-regulation of heat shock protein 70 improves arsenic trioxide and 17-DMAG effects on constitutive signal transducer and activator of transcription 3 activity*. Cancer Chemother Pharmacol, 2010. **66**(4): p. 681-689.

56. Mosser, D.D., et al., *Role of the human heat shock protein hsp70 in protection against stress-induced apoptosis*. Mol Cell Biol, 1997. **17**(9): p. 5317-27.
57. Calderwood, S.K., et al., *Extracellular heat shock proteins in cell signaling*. FEBS Lett, 2007. **581**(19): p. 3689-3694.
58. Pockley, A.G., S.K. Calderwood, and G. Multhoff, *The atheroprotective properties of Hsp70: a role for Hsp70-endothelial interactions?* Cell Stress Chaperones, 2009. **14**(6): p. 545-53.
59. de Jong, P.R., et al., *Hsp70 and cardiac surgery: molecular chaperone and inflammatory regulator with compartmentalized effects*. Cell Stress Chaperones, 2009. **14**(2): p. 117-31.
60. Chen, H., et al., *Hsp70 inhibits lipopolysaccharide-induced NF-kappaB activation by interacting with TRAF6 and inhibiting its ubiquitination*. FEBS Lett, 2006. **580**(13): p. 3145-52.
61. Oates, J.C., *The biology of reactive intermediates in systemic lupus erythematosus*. Autoimmunity, 2010. **43**(1): p. 56-63.
62. Howard, M., et al., *Activation of the stress protein response inhibits the STAT1 signalling pathway and iNOS function in alveolar macrophages: role of Hsp90 and Hsp70*. Thorax, 2010. **65**(4): p. 346-353.

63. Antonova, G., et al., *Functional significance of hsp90 complexes with NOS and sGC in endothelial cells*. Clin Hemorheol Microcirc, 2007. **37**(1-2): p. 19-35.
64. Kiang, J.G., J.T. Smith, and N.G. Agravante, *Geldanamycin Analog 17-DMAG Inhibits iNOS and Caspases in Gamma-Irradiated Human T Cells*. Rad Res, 2009. **172**(3): p. 321-330.
65. Gabay, C., *Interleukin-6 and chronic inflammation*. Arthritis Res Ther, 2006. **8**(Suppl 2): p. S3.
66. Stephanou, A., et al., *The nuclear factor interleukin-6 (NF-IL6) and signal transducer and activator of transcription-3 (STAT-3) signalling pathways co-operate to mediate the activation of the hsp90beta gene by interleukin-6 but have opposite effects on its inducibility by heat shock*. Biochem J, 1998. **330**(Pt 1): p. 189-95.
67. Tsui, K.-h., et al., *Expression of interleukin-6 is downregulated by 17-(allylamino)-17-demethoxygeldanamycin in human prostatic carcinoma cells*. Acta Pharmacol Sin, 2008. **29**(11): p. 1334-1341.

CHAPTER 3.

HEAT SHOCK PROTEIN 90 INHIBITION BY 17-DMAG LESSENS DISEASE IN THE MRL/LPR MOUSE MODEL OF SYSTEMIC LUPUS ERYTHEMATOSUS

Shimp III, S. K., Chafin, C. B., Regna, N. L., Hammond, S. E., Read, M. A., Caudell, D. L., Rylander, M. N., Reilly, C. M., “Heat shock protein 90 inhibition by 17-DMAG lessens disease in the MRL/lpr mouse model of systemic lupus erythematosus”, *Cell Mol Immunol*, 2012 May; 9(3): 255-66.

ABSTRACT

Elevated expression of heat shock protein 90 has been found in kidneys and serum of systemic lupus erythematosus (SLE) patients and MRL/Mp-*Fas*^{lpr}/*Fas*^{lpr} (MRL/lpr) autoimmune mice. We investigated if inhibition of HSP90 would reduce disease in MRL/lpr mice. *In vitro*, pretreatment of mesangial cells with HSP90 inhibitor Geldanamycin prior to immune-stimulation showed reduced expression of IL-6, IL-12, and NO. *In vivo*, we found HSP90 expression was elevated in MRL/lpr kidneys when compared to C57BL/6 mice and MRL/lpr mice treated with HSP90 inhibitor 17-DMAG. MRL/lpr mice treated with 17-DMAG showed decreased proteinuria and reduced serum anti-dsDNA antibody production. Glomerulonephritis and glomerular IgG and C3 were not significantly affected by administration of 17-DMAG in MRL/lpr. 17-DMAG increased CD8⁺ T cells, reduced double-negative T cells, decreased the CD4:CD8 ratio, and reduced follicular B cells. These studies suggest that HSP90 may play a role in regulating T cell differentiation and activation and that HSP90 inhibition may reduce inflammation in lupus.

3.1 Introduction

Heat shock protein 90 (HSP90) is increasingly recognized as a potential therapeutic target in various diseases and has been shown to act as a signaling mediator for inducible nitric oxide synthase (iNOS) and interleukin-6 (IL-6) production as well as play a crucial role in modulation of Toll-like Receptor (TLR) activation [1-3]. HSP90 has also been found to be elevated in some subsets of systemic lupus erythematosus (SLE) patients but its role in the disease is still unknown [4-7]. Elevated serum levels of HSP90 have been correlated to elevated levels of IL-6 [8]. Furthermore, the glomeruli of some SLE patients have been found to have deposits of HSP90 [9]. In addition, HSP90 and its endoplasmic reticulum homologue, glycoprotein 96 (gp96), have been linked to autoimmunity [3, 10, 11].

There are several compounds in clinical trials that target HSP90 for the treatment of cancer [12, 13]. The naturally-occurring benzoquinoid ansamycin known as Geldanamycin (GA) has been found to be a potent and specific HSP90 inhibitor. It binds to an ATP binding site unique to HSP90 [14]. This binding prevents conformational changes in HSP90 that are required for chaperone function [15]. Unfortunately, GA has low systemic duration (3-4 hours) and causes acute hepatic necrosis when administered *in vivo* [16]. However, the GA derivative 17-(Dimethylaminoethylamino)-17-demethoxygeldanamycin (17-DMAG) exhibits similar effectiveness at inhibiting HSP90 with significantly reduced hepatotoxicity, increased systemic duration (more than 24 hours) and greater water solubility [17-19]. GA has been shown to reduce the inflammatory response in a murine sepsis model [20]. Recently, GA was also used to reduce inflammation as a treatment for rheumatoid arthritis [21]. In addition to GA and 17-DMAG, HSP90 can also be inhibited by novobiocin, epigallocatechin gallate (EGCG), cisplatin, and others [22, 23]. These alternative inhibitors differ from GA and 17-DMAG in that they exert

additional effects on cellular mechanisms beyond the blockade of HSP90 [24]. Recently, a synthetic HSP90 inhibitor (EC144) was found to decrease disease severity in mouse and rat models of induced arthritis [25]. Also, the gp96 inhibitor, (S)-methyl 2-(4,6-dimethoxypyrimidine-2-ylloxy)-3-methylbutanoate, (GPM1) was shown to reduce the severity of SLE like disease in transgenic mice [11].

MRL/lpr mice serve as a model to study human SLE as they exhibit similar manifestations to the human disease including glomerulonephritis (GN), vasculitis, and arthritis [26]. Mesangial cells isolated from MRL/lpr mice exhibit increased sensitivity when immune-stimulated by inflammatory cytokines and chemokines such as tumor necrosis factor- α (TNF- α), interleukin-1 β (IL-1 β), interferon- γ (IFN- γ) or lipopolysaccharide (LPS) [27-29]. In SLE, increased sensitivity to immune stimulation leads to higher expression of TNF- α , IL-6, IL-12 and increased nitric oxide (NO) production [29-31].

Lupus mice excrete elevated levels of protein in their urine and possess increased serum IgG antibodies to double stranded DNA (anti-dsDNA) or anti-nuclear antibodies [32-37]. Renal histological markers of glomerular lesions and glomerular deposition of IgG and C3 can also indicate disease [36, 38-41]. Splenocyte populations are often altered in autoimmune mice including differences in T cell subtypes (including T regulatory cells (T_{REG})), and also alterations in B cell subtypes [36, 37, 42, 43]. HSP90 has been implicated in studies investigating similar autoimmune diseases and it has been reported that T cells respond to extracellular HSP90 by increasing their anti-inflammatory cytokines [44]. Other recent work has shown that T cell activation by the T-cell receptor (TCR) is dependent on functioning HSP90 [45].

Despite findings suggesting a role for HSP90 in SLE, or the anti-inflammatory effects of HSP90 inhibition, little has been published exploring the effect of HSP90 inhibition in SLE. Based on the evidence that suggests a possible link between HSP90 and lupus, we explored the

relationship of HSP90 and SLE by studying the effect of HSP90 inhibition in the MRL/lpr lupus mouse model.

3.2 Materials and Methods

3.2.1 Mesangial Cell Culture

SV40 MES13 cells (MES13 cells) were purchased from the American Type Culture Collection (Rockville, MD, USA) and cultured in a 3:1 mixture of Dulbecco's Modified Eagle's Medium (DMEM) and Ham's F12 medium with 14 mM HEPES, supplemented with fetal bovine serum and penicillin/streptomycin at a final concentration of 5% and 1%, respectively. MES13 cells between passages 10 and 20 were used for the experiments. Where appropriate, cells were rendered quiescent in DMEM containing 1% serum for a minimum of 2 hours prior to stimulation.

3.2.2 In Vitro Inhibition of HSP90 using Geldanamycin

Cells were pre-treated with GA (Santa Cruz, Santa Cruz, CA) at concentrations of 0.01, 0.1, and 1 μ M for 1 hour prior to stimulation with the combination of 1 μ g/ml LPS (Sigma, St. Louis, MO) and 300 units/ml IFN- γ (Accurate Chemical, Westbury, NY). Cell culture media was collected 24 hours after stimulation.

3.2.3 Cytokine ELISA and Griess assay

Supernatants were collected 24 hours after stimulation and analyzed for IL-6 and NO. IL-6 levels were quantified by ELISA per the manufacturer's instructions (eBioscience, San Diego, CA). Griess assay was used to quantify nitrite concentration (a stable reaction product of NO with oxygen) [46]. Briefly, supernatants were analyzed by mixing an equal volume of sample

with Griess reagents (1% sulfanilamide and 0.1% naphthylethylenediamene in 2.5% H₃PO₄) in a 96 well plate. Absorbance was determined by a microplate reader measuring at a wavelength of 550 nm. The concentration of nitrite was calculated from a standard curve produced by the reaction of known quantities of control NaNO₂ in the assay.

3.2.4 Mice

MRL/Mp-*Fas*^{lpr}/*Fas*^{lpr} (MRL/lpr) mice purchased from Jackson Laboratory (Bar Harbor, ME) were bred and maintained at the Virginia-Maryland Regional College of Veterinary Medicine. Mice were treated in accordance with the Institutional Animal Care and Use Committee guidelines of Virginia Tech. Experiments were conducted in male and female mice. Baseline proteinuria, weight, and blood data were collected at 12-weeks-of-age. Proteinuria and weight were recorded twice weekly and serum was collected every two weeks until mice were euthanized at 18-weeks-of-age.

3.2.5 Treatment of mice with 17-DMAG

I.P. injections of DMSO (control) or 17-DMAG (ChemieTek, Indianapolis, IN) reconstituted in DMSO (Treatment Group) were administered at a frequency of 3 days/week (alternating days). Treatment of mice with 17-DMAG and vehicle began at 12-weeks-of-age and continued until mice exhibited signs of severe lupus at 18-weeks-of-age. While 17-DMAG is soluble in water, it has greater solubility in DMSO and to minimize the volume of vehicle required to treat the mice, we followed the work by Hertlein et. al. and dissolved 17-DMAG in DMSO [47]. Dosage of 5 mg/kg 17-DMAG was administered in a bolus of 50 µl per injection. To control for DMSO effects in the mice, control mice received a 50 µl bolus of DMSO at the same frequency as the 17-DMAG treated mice.

3.2.6 Histology of the Kidney

At the time of euthanasia the mice were weighed; kidneys were removed. One kidney was placed in buffered formalin, embedded in paraffin, sectioned, and stained by Periodic acid-Schiff (PAS). Sections were assessed via light microscopy for glomerular proliferation, inflammation, size, number of nuclei per glomerulus, crescents, necrosis, and fibrosis. Each of these parameters was graded for 0–3+ and an overall glomerular score derived. The pathology and morphometric analysis were performed by a pathologist blinded to the groups (Dr. David Caudell). The other kidney was embedded in OCT media (Miles, Elkhart, IN) and frozen. Frozen kidneys were cut into 3- μ m sections and stained with one of the following: goat anti-mouse IgG-conjugated to fluorescein–isothiocyanate (FITC) diluted 1:100 (Pierce, Rockford, IL), goat anti-mouse C3-FITC diluted 1:100 (Pierce, Rockford, IL), mouse anti-HSP90-DyLight 488 diluted 1:500, or mouse anti-HSP70-DyLight 488 diluted 1:500 (Enzo Life Sciences, Farmingdale, NY). The severity of glomerulonephritis and immune complex deposition was determined in a blind manner. Scores ranged from 0 to 3+, where 0 corresponded to a non-autoimmune healthy mouse and 3+ to the maximal alteration observed in the study.

3.2.7 Measurement of Proteinuria

Urine was collected twice a week and tested for proteinuria by a standard semi-quantitative test using Siemens Uristix dipsticks (Siemens Healthcare, Deerfield, IL). Results were quantified according to the manufacturer's instructions and scored as follows: Dipstick reading of 0 mg/dl = 0, Trace = 1, 30-100 mg/dl = 2, 100-300 mg/dl = 3, 300-2000 mg/dl = 4, and 2000+ mg/dl = 5.

3.2.8 *Anti-dsDNA ELISA*

Serum was collected at 12-weeks-of-age and at the time of euthanasia (18-weeks-of-age). Mice were bled from the retro-orbital sinus following inhalation of isoflurane anesthesia. Serum levels of antibodies to dsDNA were measured by ELISA as described in the literature [48]. Briefly, ELISA plates (Corning Life Sciences, Lowell, MA) were coated with 100 μ L of 5 μ g/mL Calf Thymus DNA (Sigma, St. Louis, MO) and incubated at 37°C overnight. After washing, the plates were blocked with BSA, then incubated sequentially for 45 minutes at room temperature with 1:100 diluted serum followed by HRP-conjugated goat anti-mouse IgG gamma chain specific (1:4000; Southern Biotech, Birmingham, AL), and finally 3,3',5,5'-Tetramethylbenzidine (TMB) was added (Pierce, ThermoScientific, Rockford, IL). A high titer serum was run in serial dilutions on each plate to allow quantification.

3.2.9 *Flow cytometry*

Flow cytometric analysis was performed using monoclonal antibodies of PerCP-CY5.5-conjugated anti-CD25, FITC-conjugated anti-CD21, PerCP-CY5.5 conjugated anti-CD19, phycoerythrin (PE)-conjugated anti-CD23 (BD Pharmingen, San Diego, CA) and/or Allophycocyanin (APC)-conjugated anti-CD3e, anti-CD4-FITC, anti-CD5-APC, eFluor450 (eF450)-conjugated anti-CD8a, anti-FoxP3-PE (eBioscience, San Diego, CA). Splenic cells were isolated as previously described [173]. Briefly, spleen lymphocytes from MRL/lpr mice at 18-weeks-of-age were aseptically dissociated, treated with red blood cell (RBC) lysis buffer to remove erythrocytes, washed and suspended in RPMI media. Cells were stained with monoclonal antibodies and measured for fluorescence on a FACS Aria 1 (BD Biosciences, San Jose, CA). Flow data was analyzed by FlowJo software (Tree Star, Ashland, OR).

3.2.10 Statistics

Statistical analysis was performed using GraphPad Prism 4 software (GraphPad Software Inc.). Values are expressed as means plus or minus the standard error of the mean (SEM) of seven mice. One-way ANOVA was used to compare data among groups and samples. Comparison of differences between groups was performed using paired, one-tailed *t*-tests (any use of unpaired *t*-tests is noted in figure captions). Proteinuria data was analyzed by linear regression. P values less than 0.05 were considered significant.

3.3 Results

3.3.1 HSP90 inhibition reduced inflammatory mediator production in stimulated mesangial cells

Mesangial cells are the resident kidney macrophage and regulate the immune response in the kidney by releasing pro-inflammatory cytokines that recruit other immune cells to migrate to the kidney [49]. Because mesangial cells in lupus mice are hyper-responsive to immune stimulation, they are a valuable model for testing the role of HSP90 in the inflammatory response [50]. Given that HSP90 is a chaperone for multiple proteins involved in the activation of inflammatory signal transduction cascade pathways, we sought to reduce inflammatory cytokine and molecule expression in mesangial cells through the inhibition of the HSP90 chaperone activity. Cultured mesangial cells were treated with GA for 24 hours prior to stimulation with LPS/IFN- γ . Concentrations of 0.01 μ M to 1 μ M GA were used in these experiments based on the literature and our own unpublished observations showing minimal toxicity after 24 hour treatments with concentrations of GA below 5 μ M [51, 52]. After 24 hours of stimulation, supernatants were collected and assayed for NO, IL-6, and IL-12 production (Figure 1).

Our results showed that GA decreased NO production in a concentration-dependent manner. Treatment with GA alone had no effect over baseline. LPS/IFN- γ stimulated NO production as expected (Figure 3.1A). With increasing concentrations of GA, the level of NO decreased. This decrease in NO was significantly different from cells receiving LPS/IFN- γ alone when GA was applied at concentrations of 0.1 μ M and 1 μ M ($P < 0.001$) (Figure 3.1A).

IL-6 expression was also significantly reduced in LPS/IFN- γ stimulated cells pre-treated with GA (Figure 1 B). Compared to the LPS/IFN- γ stimulated cells, we found that IL-6 was reduced by 0.1 μ M and 1 μ M concentrations of GA ($P < 0.001$). GA treatment alone had no effect over baseline. Reductions in IL-12 were also determined to be dependent on GA concentrations and the reductions occurred in all concentrations of GA tested ($P < 0.001$) (Figure 1 C). GA also reduced IL-12 expression below baseline in cells not stimulated with LPS/IFN- γ ($P < 0.01$).

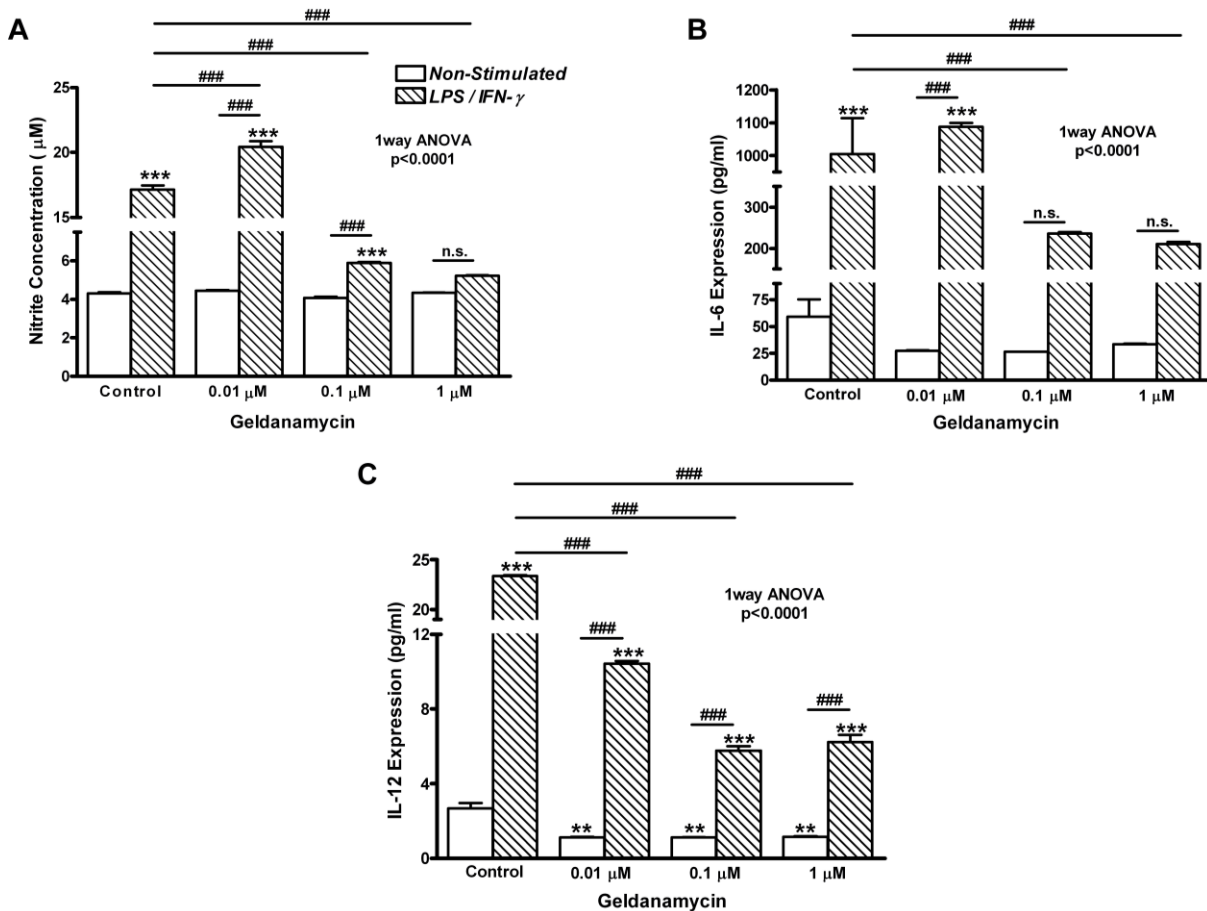


Figure 3.1. Inhibiting HSP90 reduced immune stimulated NO, IL-6 and IL-12 expression.

A) Nitrite concentrations measured by Griess assay show that post-stimulation NO expression was reduced by GA in a concentration dependent manner for concentrations greater than 0.1 μ M. B) IL-6 concentrations measured by ELISA showed that IL-6 expression stimulated by LPS/IFN- γ was reduced by GA in a concentration-dependent manner at concentrations greater than 0.1 μ M. C) Expression of IL-12 was reduced in all samples treated with GA, regardless of LPS/IFN- γ stimulation. One-way ANOVA, Tukey's multi-comparison tests: ** $p < 0.01$, *** $p < 0.001$ for non-stimulated control vs. all other samples; ### $p < 0.001$ for comparisons between samples indicated by connecting bar; n.s. for not significant.

3.3.2 Proteinuria was reduced in mice treated with 17-DMAG

Having found that HSP90 facilitates cytokine and NO expression in mesangial cells *in vitro*, we tested the role of HSP90 in the development of SLE *in vivo*. To perform this test, we inhibited HSP90 in a lupus mouse model by administration of the HSP90 inhibitor 17-DMAG. We selected 17-DMAG over GA as our *in vivo* inhibitor based on published results showing reduced hepatotoxicity *in vivo* when compared to GA or 17-Allylamino-17-demethoxygeldanamycin (17-AAG) [16, 18, 53, 54]. Dosages were selected based on studies showing effective treatment and minimal toxicity at dosages under 15 mg/kg administered three days per week for three weeks [55]. We injected MRL/lpr mice with 17-DMAG three days a week on alternating days for six weeks, beginning at 12-weeks-of-age and lasting until euthanasia at 18-weeks-of-age. Disease progression during the study was measured by total body weight and proteinuria. We found that proteinuria increased with age in the control group whereas the 17-DMAG treated group did not increase in proteinuria (Figure 3.2A). Linear regression of proteinuria showed a statistically significant increase in the control group but no significant increase in the group receiving 17-DMAG ($P < 0.01$, control group; $P < 0.001$, control vs. 17-DMAG). The groups maintained a comparable average weight throughout the study with no significant increase measured by linear regression (data not shown). Total body weight at the end of the study did not differ significantly between the groups at the time of euthanasia (Figure 3.2B).

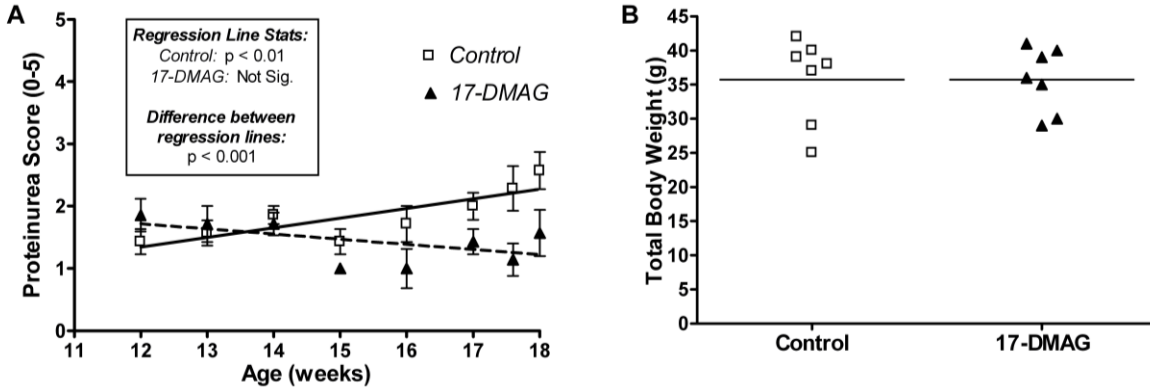


Figure 3.2. Treatment with 17-DMAG decreased proteinuria. A) Linear regression of grouped proteinuria scores showed control mice exhibited increased proteinuria while mice treated with 17-DMAG did not increase in proteinuria. Linear regression for proteinuria in the control group was statistically significant with a p-value less than 0.01. The difference between linear regression of proteinuria in the control and treated groups was also statistically significant (p-value < 0.001). B) Group average total body weight at euthanasia was not statistically different between control and treatment groups.

3.3.3 Treatment with HSP90 inhibitor 17-DMAG reduced serum anti-dsDNA antibodies but not total IgG

We measured autoantibodies and total IgG in sera of MRL/lpr mice treated with 17-DMAG. We found that mice treated with 17-DMAG had a significant reduction in anti-dsDNA antibodies when compared to their own baseline serum levels measured prior to treatment at 12-weeks-of-age ($P < 0.05$, paired one-tail t -test) (Figure 3.3A). However, the difference between the control group and the treated group at 18-weeks-of-age was determined to not be significant. Total IgG in sera was measured at 12 and 18-weeks-of-age and was not found to be statistically significant (Figure 3.3B).

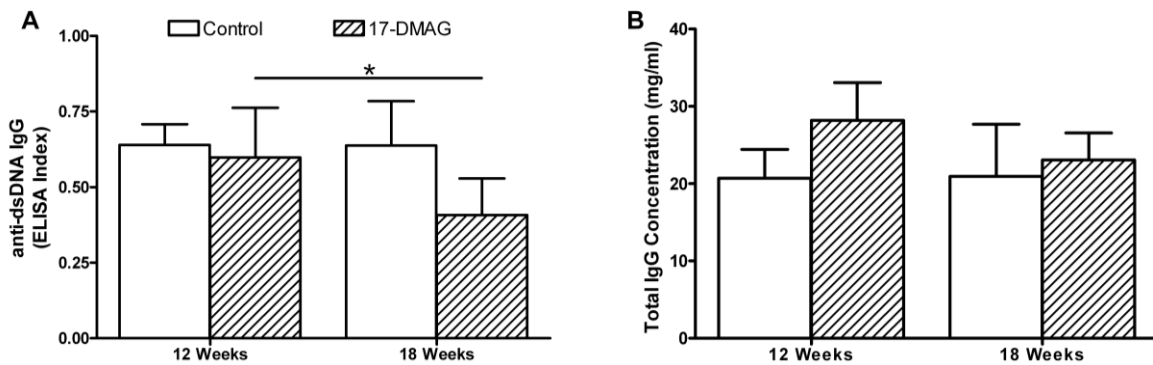


Figure 3.3. HSP90 inhibitor 17-DMAG reduced sera anti-dsDNA but not total IgG. A) Anti-dsDNA antibodies in sera were reduced in the 17-DMAG group at 18-weeks-of-age when compared to the same group at 12-weeks-of-age. * $P < 0.05$ (paired one-tailed t -test). B) 17-DMAG did not have a statistically significant effect on serum IgG.

3.3.4 Renal deposition of IgG and C3 were unaffected by 17-DMAG treatment

Renal histological markers of glomerular lesions by PAS and/or hematoxylin and eosin (H&E) staining and glomerular deposition of IgG and C3 are indications of the severity of GN and lupus in MRL/lpr mice [36, 38-41]. To assess the effect of HSP90 inhibition on renal

pathology, kidneys were taken from MRL/lpr mice at 18 weeks-of-age after being treated with 17-DMAG. For PAS staining, kidneys were formalin-fixed and sections were stained by the PAS method. For C3 and IgG deposition, tissues were frozen in OCT media and 3 μ M sections were stained with FITC-conjugated anti-IgG or anti-C3 antibodies (Figure 4). Histopathology sections were assessed in a blinded fashion and scored according to a rubric described in materials and methods. We found the glomerular pathology scores were not significantly different between the treated and control groups (scoring data not shown; representative images in (Figure 3.4A). We also found that the C3 and IgG fluorescence intensity was not significantly different between treated and control groups as determined by a blinded assessment (scoring data not shown; representative images in Figure 3.4B & C).

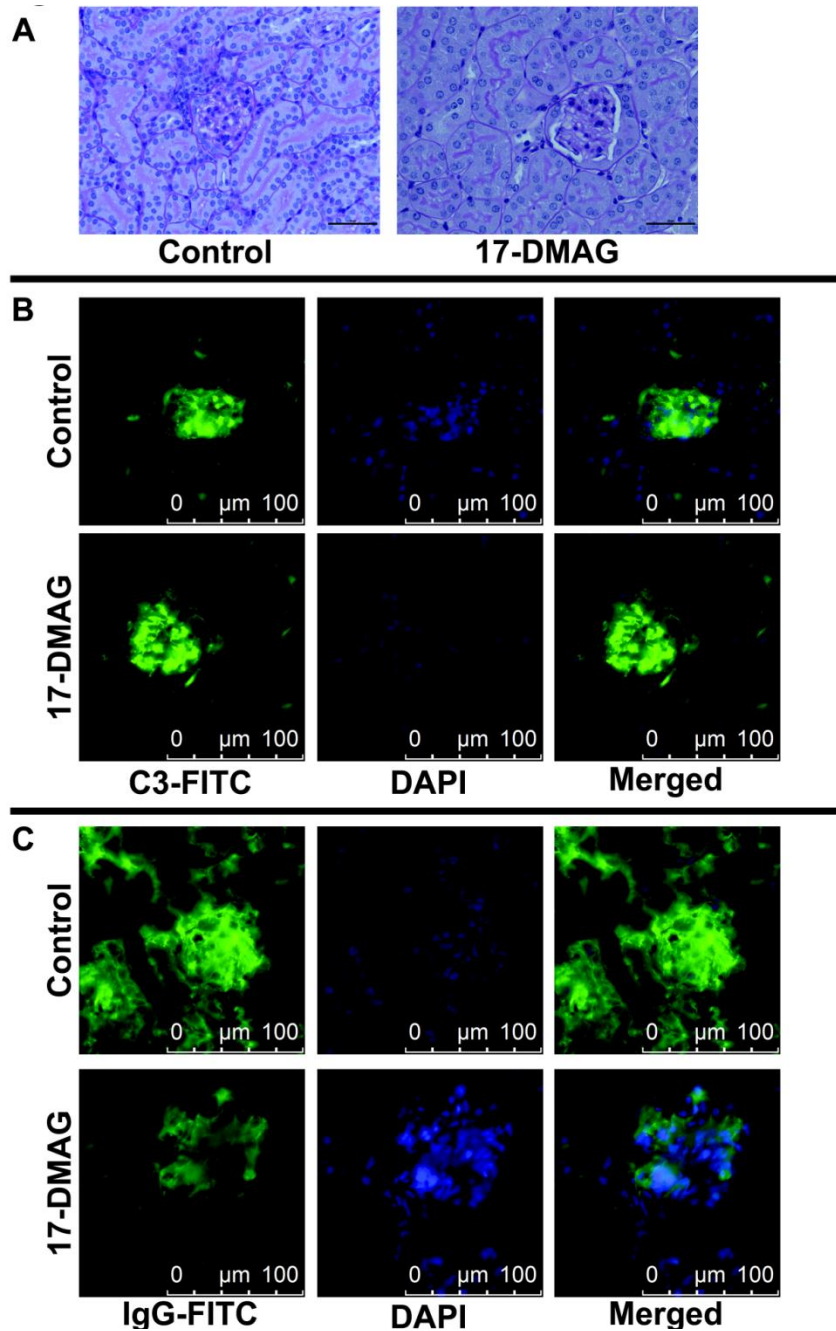


Figure 3.4. Renal histopathology showed no significant differences in renal histopathology between the control and treated groups. Representative images of kidney sections stained with A) PAS for renal histology assessment and GN scoring, B) C3-FITC and DAPI stain, C) IgG and DAPI staining. Representative pictures shown at 400x original magnification.

3.3.5 HSP90 expression increased in untreated MRL/lpr mice, compared to MRL/lpr mice treated with 17-DMAG and untreated C57BL/6 mice.

HSP90 expression has been shown to be altered in SLE patients [9]. To verify that 17-DMAG has pharmacological effects on the murine renal organs, we performed immunofluorescence microscopy of renal tissue sections stained for HSP90 or HSP70. Inhibition of HSP90 by 17-DMAG has been shown to affect HSP90 and HSP70 expression both *in vivo* and clinically [53, 54]. In addition, we questioned if HSP90 expression is altered in MRL/lpr mice compared to other mice strains such as the C57BL/6 strain. To answer these questions, we stained frozen kidney sections with DyLight 488-conjugated anti-HSP90 or anti-HSP70 antibodies and with DAPI nuclear stain. We found that HSP90 was expressed in the kidney at a low level in the C57BL/6 mice strain, but was greatly increased in the tubules and interstitium of untreated MRL/lpr mice; expression only slightly increased in the glomeruli (Figure 3.5A, top 2 rows of frames). In contrast, MRL/lpr mice treated with 17-DMAG exhibited low levels of HSP90 expression in all structures of the kidney, comparable to the C57BL/6 mice (Figure 3.5A, bottom row of frames). Examination of HSP70 expression showed that C57BL/6 mice expressed HSP70 relatively equally in tubules and glomeruli but MRL/lpr mice had decreased HSP70 expression in all renal structures (Figure 3.5B). Interestingly, HSP70 expression was not upregulated in the kidney of MRL/lpr mice treated with 17-DMAG (Figure 3.5B, bottom row of frames).

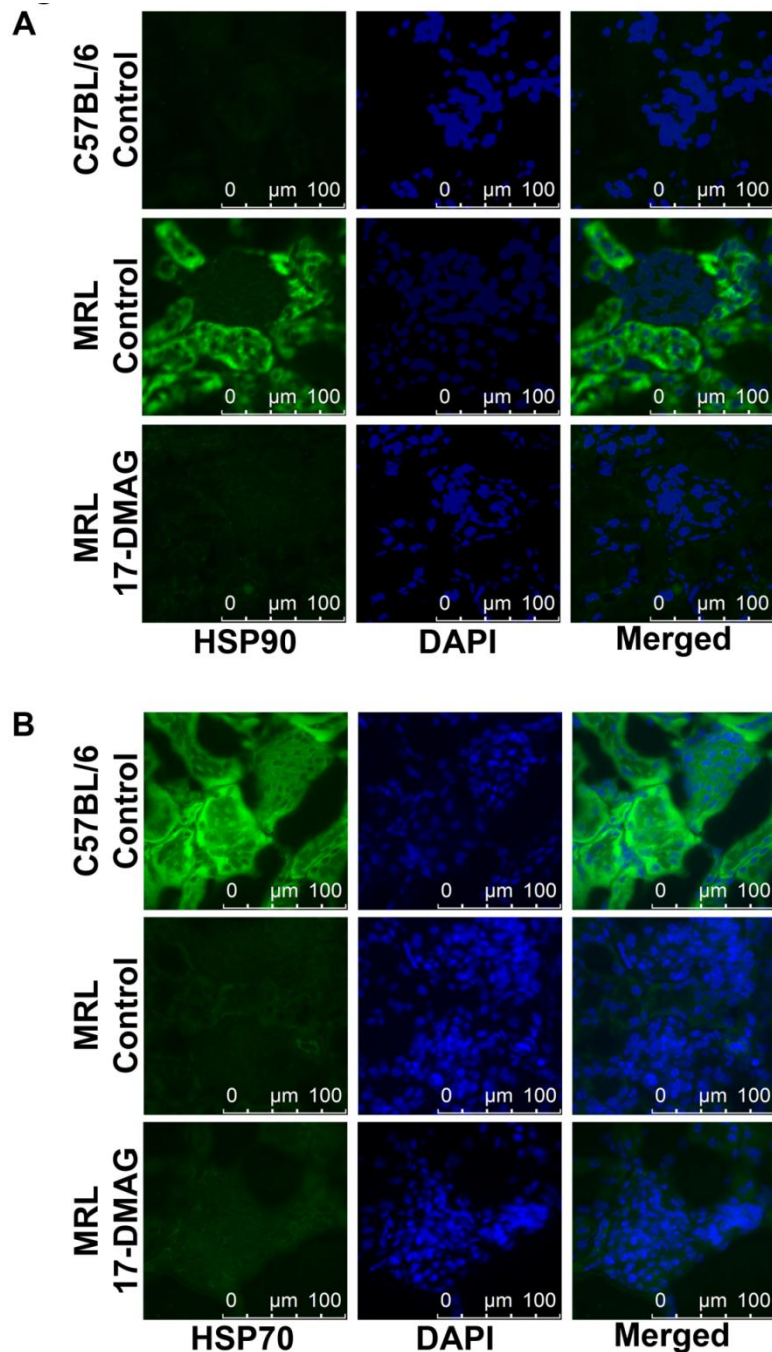


Figure 3.5. Comparison of renal HSP90 and HSP70 expression in C57BL/6 mice and MRL/lpr mice with and without 17-DMAG. Immunofluorescence microscopy of frozen tissue sections stained with DyLight 488-conjugated antibodies to HSP90 or HSP70 and DAPI nuclear stain. A) C57BL/6 mice express low levels of HSP90 in tubules and glomeruli (top row of frames). Expression of HSP90 was increased in tubules but not glomeruli in

diseased MRL/lpr control mice as compared to C57BL/6 mice (middle row of frames). MRL/lpr mice treated with 17-DMAG showed reduced HSP90 expression compared to MRL/lpr controls (bottom row of frames). B) Renal expression of HSP70 was high in tubules and glomeruli C57BL/6 (top row of frames) compared to both groups of MRL/lpr mice (bottom 2 rows of frames). MRL/lpr mice treated with 17-DMAG did not exhibit elevated levels of HSP70 in the tubules or glomeruli of kidney sections. Representative images shown at 400x original magnification.

3.3.6 Reduction of splenomegaly by 17-DMAG

HSP90 inhibition has been shown to reduce cellular proliferation in cancer cells [56, 57]. Splenomegaly is exhibited in the lymphoproliferative (lpr) model of MRL/lpr [58]. To test the effect of HSP90 inhibition on splenomegaly in MRL/lpr mice, spleens were collected and weighed and the average mass of treatment groups was compared. We found a significant difference in spleen weights between the control and treated groups where $P < 0.05$, unpaired one-tailed t -test (Figure 3.6A, B).

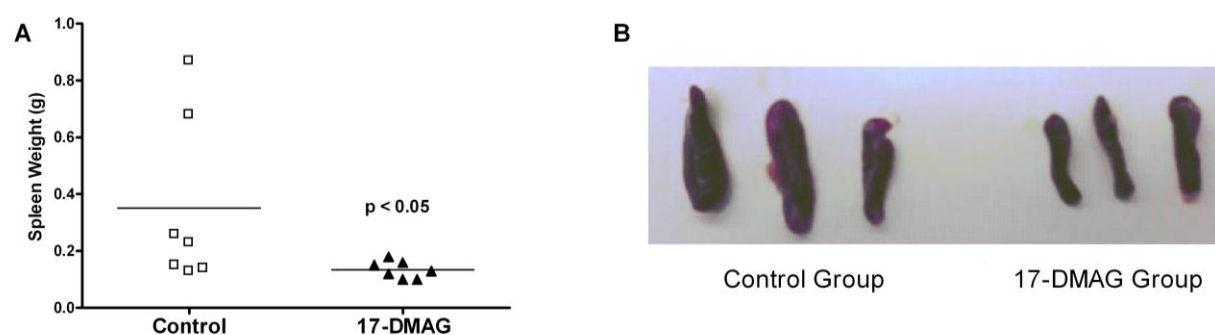


Figure 3.6. Treatment with 17-DMAG reduced splenomegaly A) The grouped average spleen weight was significantly lower for the 17-DMAG group compared to the control group (one-tail unpaired t -test, p -value < 0.05). B) Picture of representative spleens taken from both groups.

3.3.7 17-DMAG altered splenocyte profiles in MRL/lpr lupus mice

In addition to splenomegaly prevalent in MRL/lpr mice, disease pathogenesis of lupus in humans and murine models has been shown to include alterations in many T cell and B cell subtypes [59]. The alterations in T and B cells subtypes has led to the investigation of many T and B cell targeted therapies for the treatment of lupus, as recently reviewed [60, 61]. We tested the effect of HSP90 on T and B cells by quantifying populations of splenocytes expressing markers for specific subtypes of T and B cells shown to be altered in MRL/lpr mice. Splenocytes were collected from 18-week old mice treated with 17-DMAG for six weeks or treated with DMSO for six weeks (control), stained for appropriate markers, and analyzed by flow cytometry.

3.3.7.1 Double-negative T cells decreased and CD8⁺ T cells increased in mice treated with 17-DMAG

First, we assessed CD4 and CD8 splenocyte profiles by staining with fluorescent-tagged antibodies to CD3, CD4, and CD8. We were able to show 17-DMAG decreased CD3⁺ CD4⁻ CD8⁻ or double-negative T (DNT) cells ($P < 0.05$, paired one-tailed *t*-test) (Figure 7 A, F, & G). CD3⁺ CD4⁺ T cells were not significantly different between groups (Figure 3.7B, F, & G). 17-DMAG treatment produced an increase in CD3⁺ CD4⁻ CD8⁺ T cells ($P < 0.05$, paired one-tailed *t*-test) (Figure 3.7C, F, & G) CD3⁺ CD4⁺ CD8⁺ T cells were also not significantly different between groups (Figure 3.7D, F, & G). We compared CD4 and CD8 expressing T cells by computing the ratio between CD3⁺ CD4⁺ CD8⁻ and CD3⁺ CD4⁻ CD8⁺ T cells (CD4:CD8 ratio). We found the CD4:CD8 ratio decreased in mice treated with 17-DMAG ($P < 0.01$, paired one-tailed *t*-test) (Figure 3.7E, F, & G).

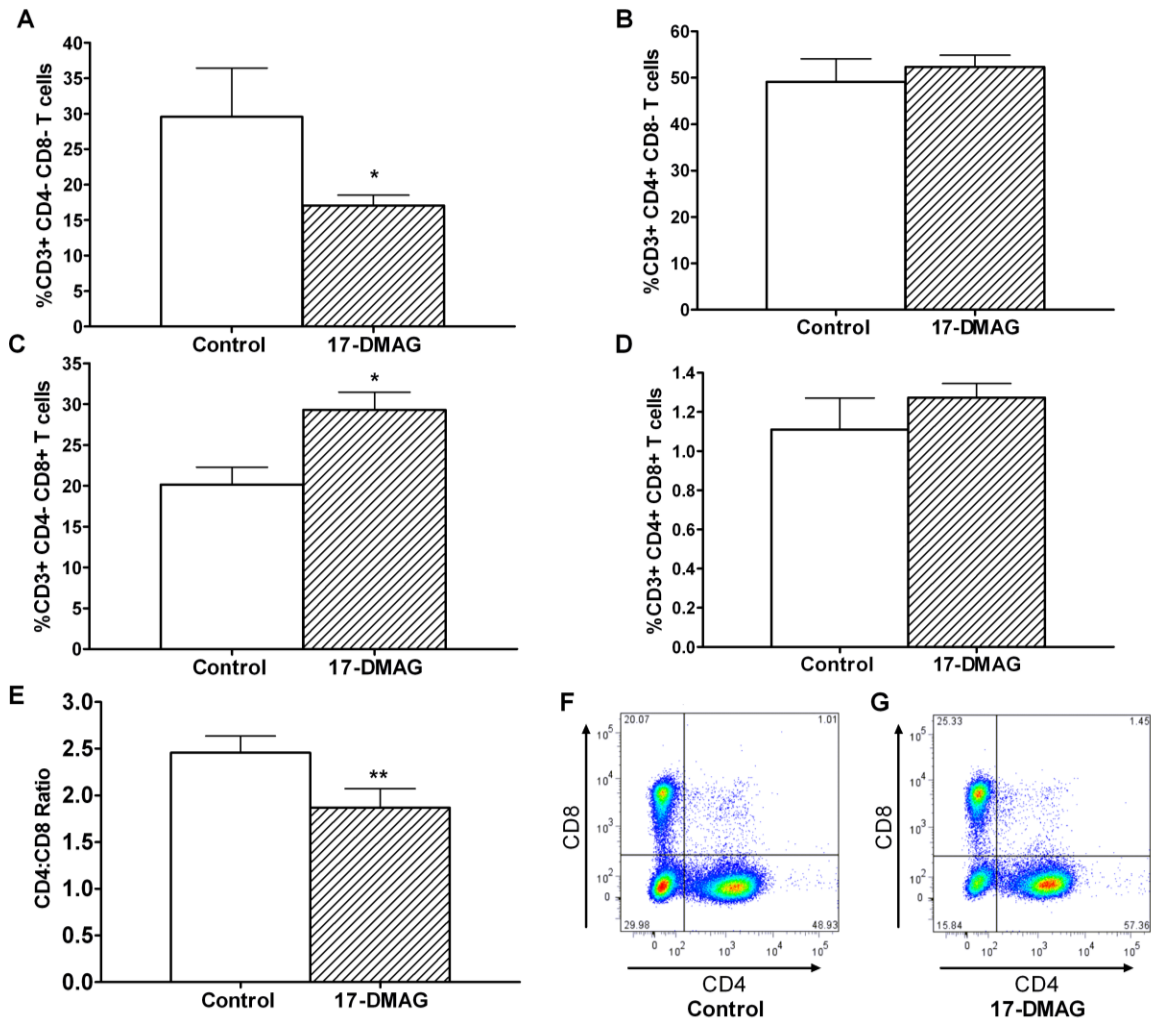


Figure 3.7. 17-DMAG increased CD8⁺ T cells and reduced DNT cells (CD4⁻ CD8⁻). Splenocytes were stained with fluorescent antibodies to CD3, CD4 and CD8 and analyzed by flow cytometry. A) DNT cells were reduced in mice treated with 17-DMAG compared to the control (* p-value < 0.05, paired one-tailed t-test). B) CD3⁺ CD4⁺ CD8⁻ T cells were not significantly affected by 17-DMAG treatment compared to the control. C) CD4⁻ CD8⁺ T cells were increased in mice receiving 17-DMAG treatments. (* p-value < 0.05, paired one-tailed t-test). D) CD4⁺ CD8⁺ T cells were not significantly altered in the group of mice receiving 17-DMAG. E) The ratio of CD4⁺ T cells to CD8⁺ T cells was reduced in mice receiving 17-DMAG (p-value < 0.01, paired one-tailed t-test). F and G) Representative**

images of flow cytometry data showing CD3⁺ gating of CD4 vs. CD8 splenocyte profiles for control and 17-DMAG treatment groups, respectively.

3.3.7.2 17-DMAG affected FoxP3- phenotypes in CD3+ T cell subsets

CD8⁺ T cells and T_{REG} cells CD4⁺ CD25⁺ forkhead box P3⁺ (FoxP3⁺) have been shown to reduce autoimmune reactivity in SLE [62]. We studied the effect of 17-DMAG on regulatory immune cells by profiling CD4, CD8 and FoxP3 expression in CD3⁺ T cells. We found no significant difference in CD4 and FoxP3 expressing populations between the control and treated groups (data not shown). However, CD8 and FoxP3 T cell profiles for the control and 17-DMAG groups did show that CD8 subsets of CD3⁺ FoxP3⁻ T cells were altered (Figure 3.8). 17-DMAG reduced the population of CD3⁺ CD8⁻ FoxP3⁻ T cells ($P < 0.01$, unpaired one-tailed *t*-test) (Figure 3.8A, E, & F). Populations of CD3⁺ CD8⁺ FoxP3⁻ T cells were increased in mice treated with 17-DMAG ($P < 0.05$, unpaired one-tailed *t*-test) (Figure 3.8B, E, & F). No significant difference was found between the groups for CD3⁺ FoxP3⁺ CD8⁻ or CD3⁺ FoxP3⁺ CD8⁺ (Figure 3.8C - F).

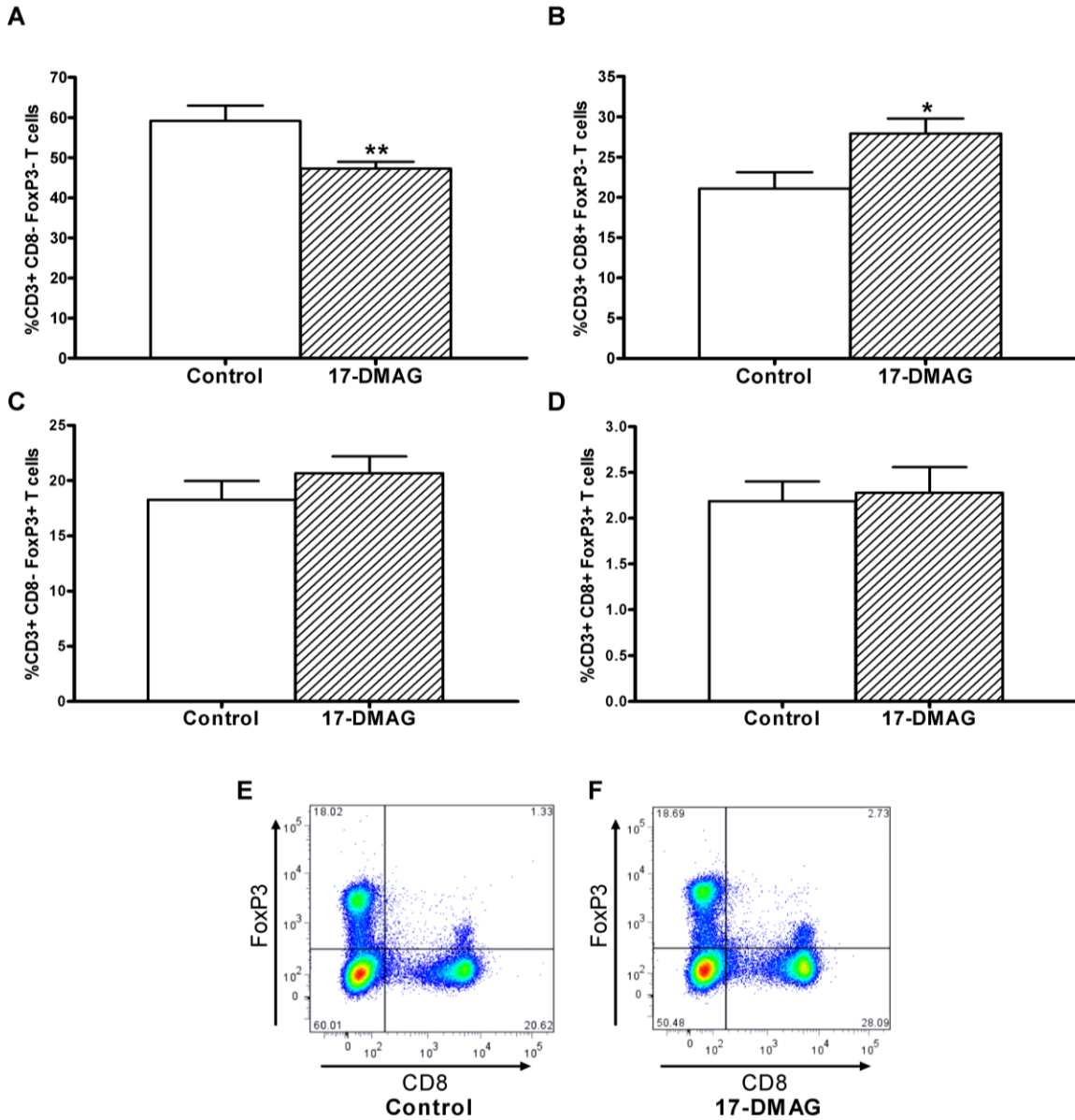


Figure 3.8. CD3⁺ FoxP3⁻ phenotypes were affected by 17-DMAG treatment in MRL/lpr mice. A) A significant decrease in CD3⁺ CD8⁻ FoxP3⁻ T cells was seen in the mice treated with 17-DMAG (* P <0.01, unpaired one-tailed t-test). B) Treatment with 17-DMAG increased CD3⁺ CD8⁺ FoxP3⁻ T cells (P <0.05, unpaired one-tailed t-test). C & D) No significant difference in CD3⁺ CD8⁻ FoxP3⁺ or CD3⁺ CD8⁺ FoxP3⁺ T cells between groups. E & F) Representative images of flow cytometry data showing splenocyte profiles gated on CD3⁺, with axes corresponding to CD8 vs. FoxP3.

3.3.7.3 Mature B cells were decreased in mice treated with 17-DMAG

To test the effect of HSP90 inhibition on B cell populations, we used flow cytometry to examine splenocytes stained with fluorescently-tagged antibodies to CD5, CD19, CD21, and CD23. We found follicular B cells (CD19⁺ CD21⁻ CD23⁺) were decreased in mice treated with 17-DMAG compared to the controls ($P < 0.05$, paired one-tailed *t*-test) (Figure 3.9A, E, & F). In contrast, populations of marginal zone B cells CD19⁺ CD21⁺ CD23⁻ were found to be unchanged in the 17-DMAG group (Figure 3.9B, E, & F). We examined B-1 cell populations and found that 17-DMAG had no effect on either the CD19⁺ CD5⁺ B-1a cells (Figure 3.9C, G, & H) or on the CD19⁺ CD5⁻ B-2a cells (Figure 3.9D, G, & H).

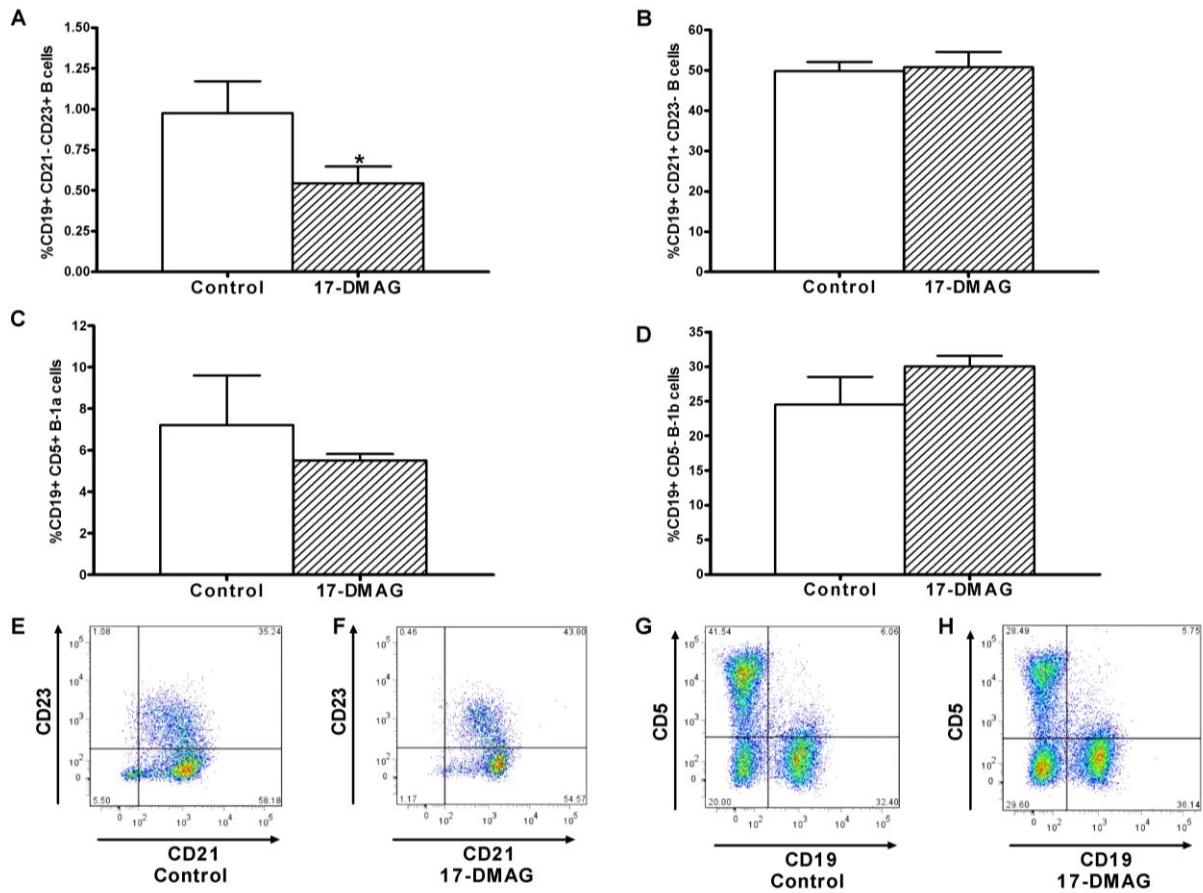


Figure 3.9. Mice treated with 17-DMAG showed a decrease in CD19+ CD21- CD23+ B cell populations. A) CD19+ CD21- CD23+ follicular B cells decreased in mice treated with 17-DMAG ($P < 0.05$, paired one-tailed t-test). B) CD19+ CD21+ CD23- marginal zone B cells were unchanged by 17-DMAG. C) CD19+ CD5+ B-1a cells were not affected by the treatment. D) CD19+ CD5- B-1b cells were not affected by the treatment. E & F) Representative splenocyte flow cytometry gate: CD19+, plotting CD21 vs. CD23. G & H) Representative splenocyte flow cytometry CD19 vs. CD5.

3.4 Discussion

Several reports in the literature have demonstrated a link between HSP90 and lupus including studies showing increased HSP90 expression in SLE patients or antibody reactivity to extracellular HSP90 [63]. Recently investigations into the regulation of HSP90 in lupus has been renewed due to the ability of HSP90 to serve as a client protein for inflammatory signaling molecules such as phosphoinositide 3-kinase (PI3K), mammalian target of rapamycin (mTOR), and Akt (protein kinase B) [64, 65]. Another example of HSP90 dependence in the inflammatory response is in the NF- κ B pathway which depends on functional HSP90 in order for upstream signal molecules to activate NF- κ B [66, 67]. TLR-mediated inflammation is regulated by HSP90 chaperoning of key TLR signal components that promote expression of TNF- α and IL-1 β messenger RNA (mRNA) [2, 68]. It has also been shown that several HSP90 homologs fold multiple TLRs [68]. It has been shown that the severity of SLE can be diminished in mice and humans through down-regulation of many of these HSP90-dependent inflammatory pathways [69-72]. Our current studies were undertaken to determine if modulation of HSP90 would decrease mesangial cell inflammatory mediator production and lessen renal disease in MRL/lpr lupus mice.

Mesangial cells are the principal resident immunoregulatory cells in the kidney. To assess the role of HSP90 in pro-inflammatory cytokine expression, we examined the effect of HSP90 inhibition in immune stimulated mesangial cells by measuring output of several pro-inflammatory cytokines (IL-6, and IL-12 and the mediator NO). Each of these is known to play a role in SLE and known to be linked to HSP90. Mice and SLE patients exhibit elevated IL-6 and inhibition of IL-6 or the IL-6 receptor decreases anti-dsDNA and proteinuria [73-75]. With HSP90 inhibition by GA, IL-6 expression was reduced in macrophages by preventing HSP90

from chaperoning newly transcribed cytokines [76]. HSP90 complexes with iNOS and is required for iNOS to synthesize NO [77]. It has also been found that HSP90 inhibition reduces iNOS function without reducing iNOS expression [78]. Additionally, IL-12 promotes disease in MRL/lpr mice while a deficiency in IL-12 will delay GN in the same MRL mice [31]. HSP90 has been linked to IL-12, with one example being that mature dendritic cells cultured in GA had their IL-12 expression significantly reduced [79]. We have previously shown that HSP90 inhibition by 17-DMAG reduced Inhibitor of κ B Kinase (IKK) expression and decreased NF- κ B translocation to the nucleus in J774 macrophage cells [80]. Our results agree with the literature and we showed that HSP90 inhibition reduced mesangial cell responsiveness to inflammatory stimuli by decreasing NO, IL-6 and IL-12 expression. Changes in these cytokines would suggest the potential for an overall decrease of inflammation in SLE.

For initial *in vitro* experiments, our team focused on determining the mechanistic effects of HSP90 inhibition using the HSP90 inhibitor, GA. Having measured significant effects of HSP90 inhibition by GA, we set out to determine if HSP90 inhibition had *in vivo* effects in MRL/lpr mice. Our studies were focused on mechanism, and based on the *in vivo* toxicity of GA, we opted to use 17-DMAG, a derivative of GA with lower toxicity and similar mechanism of action, for the *in vivo* studies [53]. Others have reported heat shock proteins expressed in glomeruli and tubules of some SLE patients [9]. However, our assessment of HSP90 expression in our control and HSP90 inhibited groups as well as C57BL/6 mouse kidneys showed that the diseased mice exhibited elevated HSP90 in tubules but not in glomeruli. While HSP90 inhibition reduced inflammatory mediator production in mesangial cells *in vitro*, the relatively lower levels of HSP90 in the glomeruli may suggest that the anti-inflammatory effects of HSP90 inhibition in the glomeruli may not be as critical to mesangial cell function as the *in vitro* studies would suggest.

Interestingly, HSP70 in C57BL/6 mice was higher than in either of the MRL/lpr groups we tested. Both 17-AAG and 17-DMAG have been shown to increase HSP70 expression in human macrophages and vascular smooth muscle cells after four hours of treatment and is typically used as a marker for HSP90 inhibition [3, 81]. Early pre-clinical study of 17-DMAG found that short term (24 hour) dosages of 17-DMAG increased renal and liver HSP70 expression. However, we found in our long-term (six week) study that HSP70 did not increase in renal tissue following treatment with an HSP90 inhibitor (17-DMAG) in a lupus mouse model. It is possible that there is a compensation mechanism for HSP70 during long-term *in vivo* treatment with 17-DMAG that was beyond the scope of the present studies. Further work can be done to measure HSP70 expression during long term treatment with HSP90 inhibitors. Understanding HSP70 expression in SLE mice treated with HSP90 inhibitors may be instructive for several reasons. First, it has been shown that extracellular HSP70 is a ligand for TLR2 and TLR4 activation. Second, HSP70 activation of the TLR4 ligand on CD4⁺ CD25⁺ T cells is attributed to an increase in suppressive activity of these T cells in atherosclerosis [82, 83]. Furthermore, HSP70 has been indicated to have a negative feedback effect on NF-κB signaling activity [84]. HSP70 has also been demonstrated to switch off TNF receptor-associated factor 6 (TRAF6) [85].

Active lupus renal disease can be defined clinically or pathologically. As MRL/lpr mice age and disease progresses they develop proteinuria. We report reductions in proteinuria in mice treated with 17-DMAG. Interestingly, we still found elevated levels of IgG and C3 deposition in both groups and the difference between the groups was not significantly different. We also found that there was no significant difference in glomerular pathology between the treated and control groups. Pathological assessment of MRL/lpr kidney sections typically exhibit elevated levels of IgG and C3 deposition in mice with active SLE [86]. Therefore, we would expect to see some difference in C3 and IgG deposition or renal pathology due to the decrease in proteinuria and

decrease in anti-dsDNA. However, it has been previously shown that C3 deposition in glomeruli can be uncoupled from the inflammatory response and that complement activation by immune complexes (ICs) is not sufficient to trigger the inflammatory response [87]. It was somewhat perplexing that proteinuria and glomerulonephritis were not as markedly increased in MRL/lpr mice at 18 weeks-of-age as many others have reported for the strain [88, 89]. Possibly having the treatment regime progress for a longer period of time would have allowed us to determine more significant differences between the treated and the untreated groups. However, the downside of a prolonged treatment could either overshoot the window of therapeutic effects of 17-DMAG or risk the loss of untreated animals due to disease as several reports have shown 50% mortality for MRL/lpr mice after 20 weeks of age, with disease expression by the 14-16 week [32, 89, 90].

Another pathological aspect of MRL/lpr mice is the presence of splenomegaly in mice exhibiting disease [59]. We found that splenomegaly was reduced in mice treated with the HSP90 inhibitor 17-DMAG. We infer from this that HSP90 may be enabling the proliferation of T and B cells. In support of this hypothesis, it was recently reported that cells isolated from draining lymph nodes in experimental epidermolysis bullosa acquisita mice were shown to have significantly reduced proliferation of T cells when treated with 17-DMAG [91]. The increased proliferation of T and B cells in SLE leads to increased expression of serum IgG with high levels of the IgG being antibodies to double stranded DNA (anti-dsDNA). It has been shown that mice treated with 17-DMAG exhibit suppressed autoantibody production [91]. We found that 17-DMAG did reduce anti-dsDNA, but we did not see a significant change in total IgG expression in the serum.

T cell regulation has long been pursued as a potential therapy for lupus. There are a number of altered or distinct T cell subtypes in lupus. The DNT cells are known to be upregulated in lupus mice and it is believed that this contributes to the disease state when they infiltrate target

organs to produce pro-inflammatory cytokines and activate B cell antibody production [59, 60]. CD8⁺ T cells suppress autoimmune reactivity in SLE [62]. Elevated CD4:CD8 ratios have been identified in murine SLE models [92, 93]. We tested CD4 and CD8 profiles of splenic T cells and found that HSP90 inhibition decreased DNT cells, increased CD8⁺ T cells, but did not change CD4⁺ T cells. As a result, we found an overall decrease in the CD4:CD8 ratio. Recently, T cells from mice treated with an HSP90 inhibitor showed reduced responsiveness to activating antigens in the collagen induced arthritis model [25]. Han et. al. found that an inhibitor for the endoplasmic reticulum homologue of HSP90, gp96, reduced both the CD4⁺ memory T cells and activated CD4⁺ T cells in the spleen and lymph nodes [11]. The effects of HSP90 inhibition on T cell populations might be explained by the fact that stimulation of the T cell receptor (TCR) leading to T cell activation requires HSP90 to stabilize lymphocyte-specific protein tyrosine kinase (Lck) in order to initiate activation [45]. Furthermore, it has been shown that HSP90 is an essential regulator for gene expression of Linker for activation of T cells (LAT) and that following inhibition of HSP90, LAT mRNA was decreased, followed by a decrease in total LAT protein. Taken together, HSP90 plays a role in activation of T cells which may be the mechanism behind the changes in T cell subtypes we found in mice treated with an HSP90 inhibitor.

T_{REG} cells are marked by expression of the master T_{REG} transcription factor, FoxP3. These cells are necessary for maintaining an immunological balance due to their suppressive role, but are typically low in SLE patients [60]. Furthermore, T_{REG} cell suppressive functions are reduced in SLE patients and MRL mice and it is thought that this is due to elevated levels of IL-6, which inhibits T_{REG} cell function [42, 94, 95]. T_{REG} cells have significantly higher expression of HSP90 than T cells. The high expression of HSP90 in T_{REG} suggests a role for HSP90 in FoxP3 expression and may explain why we found higher levels of FoxP3 negative CD3⁺ CD8⁺ T cells. However, we also found that CD4⁺ CD25⁺ FoxP3⁺ T_{REG} cells were unaffected by 17-DMAG

treatment. Nevertheless, HSP90 inhibitors have been shown to improve T_{REG} suppressive functions. For example, T_{REG} cells co-cultured with T cells in the presence of HSP90 inhibitors exhibit an increased suppressive function. Furthermore, HSP90 inhibition (17-AAG) decreased homeostatic proliferation of T cells in spleens and lymph nodes after daily injection for a week [96]. Taken together, we propose that HSP90 plays a role in regulating CD8⁺ T cells and DNT proliferation. This likely occurs through an IL-6 and T_{REG} or FoxP3-mediated mechanism. Understanding the role of HSP90 in T_{REG} cells may provide clues to how HSP90 contributes to SLE via a T cell mediated mechanism.

B cells also play an important role in the development of lupus pathology [97-99]. According to a recent review article, B cells act in lupus to present auto-antigens, induce T helper cells, CD8⁺ effector cells, and to inhibit T_{REG} cells [61]. Some B cell therapy approaches being investigated include the therapeutic targeting of HSP90 client proteins such as TLR and PI3K. When inhibited, these signal pathway proteins reduce B cell activation and survival. It should also be noted that targeting IL-6 (an HSP90 dependent cytokine) reduces memory-cell differentiation [61]. The inhibitor for gp96 was shown to reduce populations of mature B cells, B220⁺, and MHC class II⁺ cells [11]. However, it has also been shown that splenic plasma cells and germinal center B cells are unaffected by 17-DMAG treatment [91]. We found that only follicular B cells were affected by the HSP90 inhibition treatment while marginal zone B cells (B1a and B1b) were not significantly affected. Current thinking in lupus literature suggests that follicular B cells are important for pathogenic autoantibody production while the role for marginal zone B cells has yet to be established [100]. B1 cells have been indicated as a possible source or activation of auto-reactive CD4 T cells and autoantibody production in the development of lupus. Taken together, our results suggest that HSP90 does not play a significant role in B cell regulation in lupus.

In summary, we have shown that HSP90 is important for the expression of the key lupus cytokines IL-6, IL-12 and the mediator NO in mesangial cells *in vitro*. Inhibition of HSP90 in the MRL/lpr mouse resulted in decreased proteinuria and decreased spleen size, but did not affect renal histopathology or C3 and IgG deposition. However, we show that HSP90 is upregulated in diseased MRL/lpr mice in the renal tubules while HSP70 is downregulated in MRL/lpr mice, regardless of HSP90 inhibition. Furthermore, our data showed that anti-dsDNA can be decreased with HSP90 inhibition. We also found that DNT cells are down-regulated while CD8⁺ T cells are upregulated in mice treated with 17-DMAG. Some effects were also observed in T_{REG} cells which express high levels of HSP90. Follicular B cells were decreased, but the role of follicular B cells has yet to be determined for lupus. Future work should focus on determining the mechanisms that link HSP90 to T cell activation and T_{REG} suppressive potency. Targeting HSP90 may be an effective treatment for SLE, especially if combined with other targeted therapeutic approaches.

3.5 Acknowledgements

We would like to acknowledge the assistance that Melissa Makris provided with the flow cytometry. We would also like to thank the animal care staff at VMRCVM for their attention to our animals. We are appreciative of the support by the National Institute of Allergy and Infectious Diseases at the National Institutes of Health.

REFERENCES

1. Bandholtz, L., et al., *Hsp90 binds CpG oligonucleotides directly: implications for hsp90 as a missing link in CpG signaling and recognition*. Cell Mol Life Sci, 2003. **60**(2): p. 422-9.
2. De Nardo, D., et al., *A Central Role for the Hsp90-Cdc37 Molecular Chaperone Module in Interleukin-1 Receptor-associated-kinase-dependent Signaling by Toll-like Receptors*. J Biol Chem, 2005. **280**(11): p. 9813-9822.
3. Dello Russo, C., et al., *The heat-shock protein 90 inhibitor 17-allylamino-17-demethoxygeldanamycin suppresses glial inflammatory responses and ameliorates experimental autoimmune encephalomyelitis*. J Neurochem, 2006. **99**(5): p. 1351-62.
4. Dhillon, V.B., et al., *Differential heat shock protein overexpression and its clinical relevance in systemic lupus erythematosus*. Ann Rheum Dis, 1993. **52**(6): p. 436-442.
5. Dhillon, V.B., et al., *Elevation of the 90 kDa heat-shock protein in specific subsets of systemic lupus erythematosus*. Q J Med, 1994. **87**(4): p. 215-22.
6. Latchman, D.S. and D.A. Isenberg, *The role of hsp90 in SLE*. Autoimmunity, 1994. **19**(3): p. 211-8.
7. Faulds, G., et al., *Increased levels of antibodies to heat shock proteins with increasing age in Mrl/Mp-lpr/lpr mice*. Br J Rheumatol, 1995. **34**(7): p. 610-5.

8. Ripley, B.J.M., D.A. Isenberg, and D.S. Latchman, *Elevated Levels of the 90 kDa Heat Shock Protein (hsp90) in SLE Correlate with Levels of IL-6 and Autoantibodies to hsp90*. *J Autoimmun*, 2001. **17**(4): p. 341-346.
9. Kenderov, A., et al., *Lupus-specific kidney deposits of HSP90 are associated with altered IgG idiotypic interactions of anti-HSP90 autoantibodies*. *Clin Exp Immunol*, 2002. **129**(1): p. 169-76.
10. Liu, B., et al., *Cell surface expression of an endoplasmic reticulum resident heat shock protein gp96 triggers MyD88-dependent systemic autoimmune diseases*. *Proc Natl Acad Sci U S A*, 2003. **100**(26): p. 15824-9.
11. Han, J.M., et al., *Identification of gp96 as a novel target for treatment of autoimmune disease in mice*. *PLoS One*, 2010. **5**(3): p. e9792.
12. Taldone, T., et al., *Targeting Hsp90: small-molecule inhibitors and their clinical development*. *Curr Opin Pharmacol*, 2008. **8**(4): p. 370-374.
13. Kim, Y.S., et al., *Update on Hsp90 Inhibitors in Clinical Trial*. *Curr Top Med Chem*, 2009. **9**(15): p. 1479-1492.
14. Söti, C., et al., *Heat shock proteins as emerging therapeutic targets*. *Br J Pharmacol*, 2005. **146**(6): p. 769-780.

15. Garnier, C., et al., *Binding of ATP to Heat Shock Protein 90*. J Biol Chem, 2002. **277**(14): p. 12208-12214.
16. Supko, J.G., et al., *Preclinical pharmacologic evaluation of geldanamycin as an antitumor agent*. Cancer Chemother Pharmacol, 1995. **36**(4): p. 305-15.
17. Blagg, B.S. and T.D. Kerr, *Hsp90 inhibitors: small molecules that transform the Hsp90 protein folding machinery into a catalyst for protein degradation*. Med Res Rev, 2006. **26**(3): p. 310-38.
18. Egorin, M., et al., *Pharmacokinetics, tissue distribution, and metabolism of 17-(dimethylaminoethylamino)-17-demethoxygeldanamycin (NSC 707545) in CD2F1 mice and Fischer 344 rats*. Cancer Chemother Pharmacol, 2002. **49**(1): p. 7-19.
19. Egorin, M.J., et al., *Plasma pharmacokinetics and tissue distribution of 17-(allylamino)-17-demethoxygeldanamycin (NSC 330507) in CD2F1 mice*. Cancer Chemother Pharmacol, 2001. **47**(4): p. 291-302.
20. Chatterjee, A., et al., *Heat Shock Protein 90 Inhibitors Prolong Survival, Attenuate Inflammation, and Reduce Lung Injury in Murine Sepsis*. Am. J. Respir. Crit. Care Med., 2007. **176**(7): p. 667-675.

21. Rice, J.W., et al., *Small molecule inhibitors of Hsp90 potently affect inflammatory disease pathways and exhibit activity in models of rheumatoid arthritis*. *Arthritis Rheum*, 2008. **58**(12): p. 3765-75.
22. Whitesell, L. and S.L. Lindquist, *HSP90 and the chaperoning of cancer*. *Nat Rev Cancer*, 2005. **5**(10): p. 761-72.
23. Zhang, H. and F. Burrows, *Targeting multiple signal transduction pathways through inhibition of Hsp90*. *J Mol Med (Berl)*, 2004. **82**(8): p. 488-99.
24. Donnelly, A. and B.S. Blagg, *Novobiocin and additional inhibitors of the Hsp90 C-terminal nucleotide-binding pocket*. *Curr Med Chem*, 2008. **15**(26): p. 2702-17.
25. Yun, T.J., et al., *EC144, a synthetic inhibitor of heat shock protein 90, blocks innate and adaptive immune responses in models of inflammation and autoimmunity*. *J Immunol*, 2011. **186**(1): p. 563-75.
26. Suzuka, H., et al., *Morphological analysis of autoimmune disease in MRL-lpr,Yaa male mice with rapidly progressive systemic lupus erythematosus*. *Autoimmunity*, 1993. **14**(4): p. 275-82.
27. Ka, S.M., et al., *Mesangial cells of lupus-prone mice are sensitive to chemokine production*. *Arthritis Res Ther*, 2007. **9**(4): p. R67.

28. Theofilopoulos, A.N., et al., *The role of IFN-gamma in systemic lupus erythematosus: a challenge to the Th1/Th2 paradigm in autoimmunity*. Arthritis Res, 2001. **3**(3): p. 136-41.
29. Aringer, M. and J.S. Smolen, *Cytokine expression in lupus kidneys*. Lupus, 2005. **14**(1): p. 13-18.
30. Reilly, C.M., et al., *Prostaglandin J(2) inhibition of mesangial cell iNOS expression*. Clin Immunol, 2001. **98**(3): p. 337-345.
31. Kikawada, E., D.M. Lenda, and V.R. Kelley, *IL-12 deficiency in MRL-Fas(lpr) mice delays nephritis and intrarenal IFN-gamma expression, and diminishes systemic pathology*. J Immunol, 2003. **170**(7): p. 3915-3925.
32. Santiago-Raber, M.-L., et al., *Genetic basis of murine lupus*. Autoimmunity Reviews, 2004. **3**(1): p. 33-39.
33. Theofilopoulos, A.N. and D.H. Kono, *Mechanisms and genetics of autoimmunity*. Annals of the New York Academy of Sciences, 1998. **841**: p. 225-35.
34. Singh, A.K., *Lupus in the Fas lane?* J R Coll Physicians Lond, 1995. **29**(6): p. 475-8.
35. Deng, G.-M., L. Liu, and G.C. Tsokos, *Targeted tumor necrosis factor receptor I preligand assembly domain improves skin lesions in MRL/lpr mice*. Arthritis Rheum, 2010. **62**(8): p. 2424-2431.

36. Ichinose, K., et al., *Suppression of autoimmunity and organ pathology in lupus-prone mice upon inhibition of calcium/calmodulin-dependent protein kinase type IV*. *Arthritis Rheum*, 2011. **63**(2): p. 523-529.
37. Xie, C., et al., *PI3K/AKT/mTOR hypersignaling in autoimmune lymphoproliferative disease engendered by the epistatic interplay of *Sle1b* and *FASlpr**. *Int Immunol*, 2007. **19**(4): p. 509-22.
38. Sekine, H., et al., *Complement component C3 is not required for full expression of immune complex glomerulonephritis in *MRL/lpr* mice*. *J Immunol*, 2001. **166**(10): p. 6444-51.
39. Xie, C., et al., *Strain distribution pattern of susceptibility to immune-mediated nephritis*. *J Immunol*, 2004. **172**(8): p. 5047-55.
40. Xie, C., et al., *Enhanced susceptibility to end-organ disease in the lupus-facilitating NZW mouse strain*. *Arthritis Rheum*, 2003. **48**(4): p. 1080-1092.
41. Du, Y., Y. Fu, and C. Mohan, *Experimental anti-GBM nephritis as an analytical tool for studying spontaneous lupus nephritis*. *Arch Immunol Ther Exp (Warsz)*, 2008. **56**(1): p. 31-40.
42. Divekar, A.A., et al., *Dicer Insufficiency and MicroRNA-155 Overexpression in Lupus Regulatory T Cells: An Apparent Paradox in the Setting of an Inflammatory Milieu*. *J Immunol*, 2011. **186**(2): p. 924-930.

43. Yang, J., et al., *Th17 and natural Treg cell population dynamics in systemic lupus erythematosus*. *Arthritis Rheum*, 2009. **60**(5): p. 1472-1483.
44. Wieten, L., et al., *Cell stress induced HSP are targets of regulatory T cells: A role for HSP inducing compounds as anti-inflammatory immuno-modulators?* *FEBS Lett*, 2007. **581**(19): p. 3716-3722.
45. Giannini, A. and M.J. Bijlmakers, *Regulation of the Src family kinase Lck by Hsp90 and ubiquitination*. *Mol Cell Biol*, 2004. **24**(13): p. 5667-76.
46. Gilkeson, G., et al., *Correlation of serum measures of nitric oxide production with lupus disease activity*. *J Rheumatol*, 1999. **26**(2): p. 318-24.
47. Hertlein, E., et al., *17-DMAG targets the nuclear factor-kappaB family of proteins to induce apoptosis in chronic lymphocytic leukemia: clinical implications of HSP90 inhibition*. *Blood*, 2010. **116**(1): p. 45-53.
48. Gilkeson, G.S., A.M. Pippen, and D.S. Pisetsky, *Induction of cross-reactive anti-dsDNA antibodies in preautoimmune NZB/NZW mice by immunization with bacterial DNA*. *J Clin Invest*, 1995. **95**(3): p. 1398-402.
49. Schwarz, M., et al., *IFN γ induces functional chemokine receptor expression in human mesangial cells*. *Clin Exp Immunol*, 2002. **128**(2): p. 285-294.

50. Teramoto, K., et al., *Microarray analysis of glomerular gene expression in murine lupus nephritis*. J Pharmacol Sci, 2008. **106**(1): p. 56-67.
51. Jeon, Y.K., et al., *The heat-shock protein 90 inhibitor, geldanamycin, induces apoptotic cell death in Epstein–Barr virus-positive NK/T-cell lymphoma by Akt down-regulation*. J Pathol, 2007. **213**(2): p. 170-179.
52. Dey, A. and A.I. Cederbaum, *Geldanamycin, an Inhibitor of Hsp90, Potentiates Cytochrome P4502E1-Mediated Toxicity in HepG2 Cells*. J Pharmacol Exp Ther, 2006. **317**(3): p. 1391-1399.
53. Eiseman, J.L., et al., *Pharmacokinetics and pharmacodynamics of 17-demethoxy 17-[[2-dimethylamino)ethyl]amino]geldanamycin (17DMAG, NSC 707545) in C.B-17 SCID mice bearing MDA-MB-231 human breast cancer xenografts*. Cancer Chemother Pharmacol, 2005. **55**(1): p. 21-32.
54. Ramanathan, R.K., et al., *Phase I pharmacokinetic and pharmacodynamic study of 17-dimethylaminoethylamino-17-demethoxygeldanamycin, an inhibitor of heat-shock protein 90, in patients with advanced solid tumors*. J Clin Oncol, 2010. **28**(9): p. 1520-6.
55. Hollingshead, M., et al., *In vivo antitumor efficacy of 17-DMAG (17-dimethylaminoethylamino-17-demethoxygeldanamycin hydrochloride), a water-soluble geldanamycin derivative*. Cancer Chemother Pharmacol, 2005. **56**(2): p. 115-125.

56. Babchia, N., et al., *17-AAG and 17-DMAG-Induced Inhibition of Cell Proliferation through B-Raf Downregulation in WTB-Raf-Expressing Uveal Melanoma Cell Lines*. Invest Ophthalmol Vis Sci., 2008. **49**(6): p. 2348-2356.
57. Bishop, S.C., J.A. Burlison, and B.S. Blagg, *Hsp90: a novel target for the disruption of multiple signaling cascades*. Curr Cancer Drug Targets, 2007. **7**(4): p. 369-88.
58. Vidal, S., D.H. Kono, and A.N. Theofilopoulos, *Loci predisposing to autoimmunity in MRL-Fas lpr and C57BL/6-Faslpr mice*. J Clin Invest, 1998. **101**(3): p. 696-702.
59. Reilly, C.M., et al., *Modulation of renal disease in MRL/lpr mice by suberoylanilide hydroxamic acid*. J Immunol, 2004. **173**(6): p. 4171-8.
60. Crispin, J.C., et al., *T cells as therapeutic targets in SLE*. Nat Rev Rheumatol, 2010. **6**(6): p. 317-325.
61. Sanz, I. and F.E. Lee, *B cells as therapeutic targets in SLE*. Nat Rev Rheumatol, 2010. **6**(6): p. 326-37.
62. La Cava, A., *The busy life of regulatory T cells in systemic lupus erythematosus*. Discov Med, 2009. **8**(40): p. 13-7.
63. Staub, H.L., et al., *Revisiting anti-hsp90 antibodies in systemic lupus erythematosus*. Clin Exp Rheumatol, 2010. **28**(6): p. 928-928.

64. Neckers, L., *Heat shock protein 90: the cancer chaperone*. J Biosci, 2007. **32**(3): p. 517-30.
65. Neckers, L., *Hsp90 inhibitors as novel cancer chemotherapeutic agents*. Trends Mol Med, 2002. **8**(4): p. S55-S61.
66. Karkoulis, P.K., et al., *17-Allylamino-17-demethoxygeldanamycin induces downregulation of critical Hsp90 protein clients and results in cell cycle arrest and apoptosis of human urinary bladder cancer cells*. BMC Cancer, 2010. **10**: p. 481.
67. Broemer, M., D. Krappmann, and C. Scheidereit, *Requirement of Hsp90 activity for I[κ]B kinase (IKK) biosynthesis and for constitutive and inducible IKK and NF-[κ]B activation*. Oncogene, 2004. **23**(31): p. 5378-5386.
68. Liu, B., et al., *Folding of Toll-like receptors by the HSP90 paralogue gp96 requires a substrate-specific cochaperone*. Nat Commun, 2010. **1**: p. 79.
69. Patel, R.K. and C. Mohan, *PI3K/AKT signaling and systemic autoimmunity*. Immunol Res, 2005. **31**(1): p. 47-55.
70. Wu, T. and C. Mohan, *The AKT axis as a therapeutic target in autoimmune diseases*. Endocr Metab Immune Disord Drug Targets, 2009. **9**(2): p. 145-50.

71. Fernandez, D. and A. Perl, *mTOR signaling: a central pathway to pathogenesis in systemic lupus erythematosus?* Discov Med, 2010. **9**(46): p. 173-8.
72. Liu, J. and D.I. Beller, *Distinct pathways for NF-kappa B regulation are associated with aberrant macrophage IL-12 production in lupus- and diabetes-prone mouse strains.* J Immunol, 2003. **170**(9): p. 4489-96.
73. Finck, B.K., B. Chan, and D. Wofsy, *Interleukin 6 promotes murine lupus in NZB/NZW F1 mice.* J Clin Invest, 1994. **94**(2): p. 585-91.
74. Mihara, M., et al., *IL-6 receptor blockage inhibits the onset of autoimmune kidney disease in NZB/W F1 mice.* Clin Exp Immunol, 1998. **112**(3): p. 397-402.
75. Tsai, C.Y., et al., *Increased excretions of beta2-microglobulin, IL-6, and IL-8 and decreased excretion of Tamm-Horsfall glycoprotein in urine of patients with active lupus nephritis.* Nephron, 2000. **85**(3): p. 207-14.
76. Wax, S., et al., *Geldanamycin inhibits the production of inflammatory cytokines in activated macrophages by reducing the stability and translation of cytokine transcripts.* Arthritis Rheum, 2003. **48**(2): p. 541-550.
77. Antonova, G., et al., *Functional significance of hsp90 complexes with NOS and sGC in endothelial cells.* Clin Hemorheol Microcirc, 2007. **37**(1-2): p. 19-35.

78. Yoshida, M. and Y. Xia, *Heat Shock Protein 90 as an Endogenous Protein Enhancer of Inducible Nitric-oxide Synthase*. J Biol Chem, 2003. **278**(38): p. 36953-36958.
79. Bae, J., et al., *Phenotypic and functional effects of heat shock protein 90 inhibition on dendritic cell*. J Immunol, 2007. **178**(12): p. 7730-7.
80. Shimp III, S.K., et al., *HSP90 inhibition by 17-DMAG reduces inflammation in J774 macrophages through suppression of Akt and NF- κ B pathways*. Inflamm Res, 2012.
81. Madrigal-Matute, J., et al., *Heat shock protein 90 inhibitors attenuate inflammatory responses in atherosclerosis*. Cardiovasc Res, 2010. **86**(2): p. 330-7.
82. Dasu, M.R., et al., *Increased Toll-Like Receptor (TLR) Activation and TLR Ligands in Recently Diagnosed Type 2 Diabetic Subjects*. Diabetes Care, 2010. **33**(4): p. 861-868.
83. Pockley, A.G., S.K. Calderwood, and G. Multhoff, *The atheroprotective properties of Hsp70: a role for Hsp70-endothelial interactions?* Cell Stress Chaperones, 2009. **14**(6): p. 545-53.
84. de Jong, P.R., et al., *Hsp70 and cardiac surgery: molecular chaperone and inflammatory regulator with compartmentalized effects*. Cell Stress Chaperones, 2009. **14**(2): p. 117-31.
85. Chen, H., et al., *Hsp70 inhibits lipopolysaccharide-induced NF-kappaB activation by interacting with TRAF6 and inhibiting its ubiquitination*. FEBS Lett, 2006. **580**(13): p. 3145-52.

86. Julkunen, H., S. Ekblom-Kullberg, and A. Miettinen, *Nonrenal and renal activity of systemic lupus erythematosus: a comparison of two anti-C1q and five anti-dsDNA assays and complement C3 and C4*. *Rheumatology Int*, 2011: p. 1-7.
87. Clynes, R., C. Dumitru, and J.V. Ravetch, *Uncoupling of Immune Complex Formation and Kidney Damage in Autoimmune Glomerulonephritis*. *Science*, 1998. **279**(5353): p. 1052-1054.
88. Sekine, H., et al., *The benefit of targeted and selective inhibition of the alternative complement pathway for modulating autoimmunity and renal disease in MRL/lpr mice*. *Arthritis Rheum*, 2011. **63**(4): p. 1076-1085.
89. Sun, L., et al., *Amelioration of systemic lupus erythematosus by withangulatin A in MRL/lpr mice*. *Journal of Cellular Biochemistry*, 2011. **112**(9): p. 2376-2382.
90. Wenderfer, S.E., et al., *C3a receptor deficiency accelerates the onset of renal injury in the MRL/lpr mouse*. *Mol Immunol*, 2009. **46**(7): p. 1397-404.
91. Kasperkiewicz, M., et al., *Heat-shock protein 90 inhibition in autoimmunity to type VII collagen: evidence that nonmalignant plasma cells are not therapeutic targets*. *Blood*, 2011. **117**(23): p. 6135-42.
92. Sobel, E.S., et al., *Genetic dissection of systemic lupus erythematosus pathogenesis: evidence for functional expression of Sle3/5 by non-T cells*. *J Immunol*, 2002. **169**(7): p. 4025-32.

93. Zhu, J., et al., *T cell hyperactivity in lupus as a consequence of hyperstimulatory antigen-presenting cells*. J Clin Invest, 2005. **115**(7): p. 1869-1878.
94. Linker-Israeli, M., et al., *Elevated levels of endogenous IL-6 in systemic lupus erythematosus. A putative role in pathogenesis*. J Immunol, 1991. **147**(1): p. 117-23.
95. Wan, S., C. Xia, and L. Morel, *IL-6 produced by dendritic cells from lupus-prone mice inhibits CD4⁺CD25⁺ T cell regulatory functions*. J Immunol, 2007. **178**(1): p. 271-9.
96. de Zoeten, E.F., et al., *Histone Deacetylase 6 and Heat Shock Protein 90 Control the Functions of Foxp3⁺ T-Regulatory Cells*. Mol. Cell. Biol., 2011. **31**(10): p. 2066-2078.
97. Madaio, M.P., *B cells and autoantibodies in the pathogenesis of lupus nephritis*. Immunol Res, 1998. **17**(1-2): p. 123-32.
98. Chan, O.T., M.P. Madaio, and M.J. Shlomchik, *The central and multiple roles of B cells in lupus pathogenesis*. Immunol Rev, 1999. **169**: p. 107-21.
99. Theofilopoulos, A.N., et al., *B and T cell antigen receptor repertoires in lupus/arthritis murine models*. Springer Semin Immunopathol, 1989. **11**(3): p. 335-68.
100. Grimaldi, C.M., *Sex and systemic lupus erythematosus: the role of the sex hormones estrogen and prolactin on the regulation of autoreactive B cells*. Curr Opin Rheumatol, 2006. **18**(5): p. 456-61.

CHAPTER 4.

**COMPUTATIONAL MODEL OF NF- κ B: INHIBITION OF
HEAT SHOCK PROTEIN 90 REDUCES CHRONIC ACTIVATION OF
NUCLEAR FACTOR- κ B BY PREVENTING
HEAT SHOCK PROTEIN CHAPERONING OF INHIBITOR OF κ B KINASE**

Shimp III, S. K., Hammond, S. E., Regna, N. L., Achenie, L., Lee, Y. W., Reilly, C. M., Rylander, M. N. “Computational model of NF- κ B: Inhibition of heat shock protein 90 reduces chronic activation of nuclear factor- κ B by preventing heat shock protein chaperoning of inhibitor of κ B kinase”, Manuscript in Preparation for BMC Computational Biology

ABSTRACT

Background: Inflammation is a critical process for healing and combating infection. It is a potent physiological process that if not tightly regulated it can become chronic, leading to more tissue damage instead of healing. Activation of the nuclear factor- κ B (NF- κ B) signaling pathway increases expression of many pro-inflammatory molecules. NF- κ B can be activated by multiple external stimuli to which it responds dynamically and has multiple feedback mechanisms to regulate its activity. The characteristics of the dynamic response of NF- κ B dictate which inflammatory molecules are up-regulated. Heat shock protein 90 (HSP90) has been linked to NF- κ B as a chaperone for inhibitor of κ B kinase (IKK) which is upstream of NF- κ B. Molecules that inhibit HSP90 reduce the activity of many of the inflammatory kinases that HSP90 chaperones, such as IKK. The complex dynamics of NF- κ B have been studied through experimental and computational biology methods.

Results: We sought to explore the interaction between HSP90 and NF- κ B in response to immune-stimulation by lipopolysaccharide (LPS) with and without HSP90 inhibition. A model was constructed containing the core NF- κ B signaling constituents of inhibitor of κ B (I κ B), IKK, NF- κ B, and A20, as well as binding interactions between HSP90, IKK, and a generalized HSP90 inhibitor. Parameter sensitivity was assessed for the parameters regulating HSP90 interactions with IKK. HSP90-IKK binding rate, IKK activation rate, and the rate of A20 deactivation of IKK were all identified as parameters requiring accurate estimation. Parameters were estimated by fitting the model IKKp response to experimental data. A second parameter sensitivity study explored HSP90 inhibitor concentrations and binding rates. Complete blockage of NF- κ B activity by HSP90 inhibition requires a high relative inhibitor concentrations and high binding rates. While NF- κ B activation was difficult to block, longer term NF- κ B activity was reduced by HSP90 inhibition. The model response to LPS stimulation with and without HSP90 inhibition was validated using experimental NF- κ B activity data.

Conclusions: The effect of HSP90 inhibition on the dynamics of NF- κ B activity may alter the genes NF- κ B promotes. This suggests that HSP90 inhibition may provide a therapeutic option to reduce chronic NF- κ B activity for reduction of chronic inflammation.

4.1 Background

Inflammation is a non-specific immune response that is used by an organism to react to injury. Under normal conditions the inflammatory response is well regulated and self-limiting in its role to provide a protective role for an organism in response to harmful stimuli such as tissue injury, pathogens, and chemicals, and other phenomenon [1]. Inflammation that becomes chronic can lead to diseases including atherosclerosis, cancer, and autoimmunity [2-5].

The cellular signaling mechanisms for inflammation involve complicated interactions beginning at cell surface receptors and are transmitted through a series of phosphorylation, ubiquitination, and binding events that eventually lead to upregulation of inflammatory mediators such as TNF- α , IL-6, and NO [6, 7]. Key intracellular pathways for inflammation include NF- κ B, mitogen-activated protein kinases (MAPKs), phosphatidylinositol 3-kinase (PI3K)/Akt, signal transducers and activators of transcription (STATs), and reactive oxygen species (ROS) production [8]. The NF- κ B pathway impacts many disease states such as tumor development, malignant lymphomas, rheumatoid arthritis, and lupus, therefore we elected to focus our modeling to the NF- κ B pathway [6, 9-12]. Amino acid inhibition of NF- κ B was shown to reduce inflammation in atherosclerosis [13]. Targeting the receptor activator NF- κ B ligand (RANKL) is a therapeutic approach currently undergoing multiple clinical trials [14].

NF- κ B in its inactivated form is bound to an inhibitor protein, inhibitor of κ B (I κ B α / β) which prevents NF- κ B from translocating to the nucleus. When the upstream inflammatory signal cascade is initiated, I κ B kinase (IKK) is activated through a phosphorylation reaction and in turn, IKK β phosphorylates I κ B α . Phosphorylation of I κ B α releases the inhibitor from its complex with NF- κ B and NF- κ B translocates to the nucleus and binds to inflammatory gene promoter regions [15, 16].

Further investigation has shown that NF- κ B activation cannot be characterized as simply and on/off switch. Rather NF- κ B has an oscillatory pattern to its activation. The oscillations of NF- κ B are distinct for individual cellular stimuli. For example, in response to tumor necrosis factor (TNF)- α stimulation, NF- κ B will strongly activate (spike) in less than 10 minutes and activation will reduce to near zero within an hour, only to activate again about 30 minutes later. This cycle will repeat each time with decreased amplitude of NF- κ B activation [17]. However, in

response to lipopolysaccharide (LPS) stimulation, NF- κ B activation occurs approximately 30 minutes to an hour after exposure. The activation of NF- κ B very slowly decreases as long as LPS is present [18]. Other inflammatory stimuli are shown to have their own characteristic NF- κ B response. The dynamics of the NF- κ B response ultimately determine the overall cellular response, appropriate for the initial cellular stimuli. Cheong, Hoffmann and Levchenko assert that the dynamic response of NF- κ B enables the cell to use one activation factor, in this case, NF- κ B, while still distinguishing between distinct cellular stimuli [19].

The 90 kD heat shock protein (HSP90) is a homo-dimeric molecular chaperone comprising greater than 3% of total cellular protein [20]. HSP90 has a prominent role in folding and conformational regulation of numerous client proteins including many inflammatory pathway kinases [21-25]. NF- κ B relies on functional HSP90 in order for full activation of the nuclear factor. HSP90 has several small molecule inhibitors that prevent its chaperone activity [21, 26, 27]. Geldanamycin (GA) and its derivatives 17-allylamino-17-demethoxygeldanamycin (17-AAG) and 17-(dimethylaminoethylamino)-17-demethoxygeldanamycin (17-DMAG) have been shown to reduce NF- κ B activity [28, 29].

Having previously shown that HSP90 inhibition reduces NF- κ B activity, these studies sought to show how HSP90 inhibition would alter the dynamic response of NF- κ B. We sought to quantify the effectiveness at which HSP90 inhibition blocks NF- κ B activity in terms of oscillation magnitude, frequency, and duration. We hypothesized that HSP90 inhibition would not only reduce the amplitude of the NF- κ B response, but might also affect the amplitude and period of the subsequent oscillations as a mechanistic explanation for the anti-inflammatory effects of HSP90 inhibitors. A large body of data on NF- κ B dynamics shows extensive use of computational modeling to describe the temporal characteristics [17, 18, 30-44]. We developed a model based on the reduced NF- κ B model developed and analyzed in previously published

reports [36, 38-40] where we incorporated HSP90 interactions with IKK and a generalized HSP90 inhibitor.

In this report we present our model for NF- κ B, including HSP90 chaperoning of IKK and the interaction of HSP90 inhibitors to prevent that chaperoning. We explored the model through parameter sensitivity analysis and discovered several key parameters that significantly influence system response. We estimated new parameter values using experimental data. We also explored the effect of HSP90 inhibitor concentration and binding rates. Experimental data for HSP90 inhibition was used to validate the model.

4.2 Model Description

Investigations into the role of HSP90 in the IKK- NF- κ B pathway have elucidated a mechanism by which HSP90 chaperones the inflammatory pathway. Inhibiting HSP90 decreases IKK expression and kinase activity [45, 46]. Inhibition of HSP90 prevented client proteins such as IKK from binding to HSP90 [47]. Other HSP90 client proteins, such as Akt (protein kinase B) have been shown to rely on HSP90 for protection not only from degradation, but also from deactivation by protein phosphatases such as protein phosphatase 2A (PP2A) [48]. Inhibition of HSP90 resulted in decreased NF- κ B activation by TNF- α , LPS, and other immune-stimulating compounds [29, 49].

To investigate the role of HSP90 in the NF- κ B pathway, we constructed kinetic ordinary differential equations (ODEs) to describe the reactions among HSP90, IKK, and a general HSP90 inhibitor. The model reactions are shown graphically in Figure 4.1. The IKK-I κ B-NF- κ B reactions and parameter values were obtained from the literature [36, 38, 44].

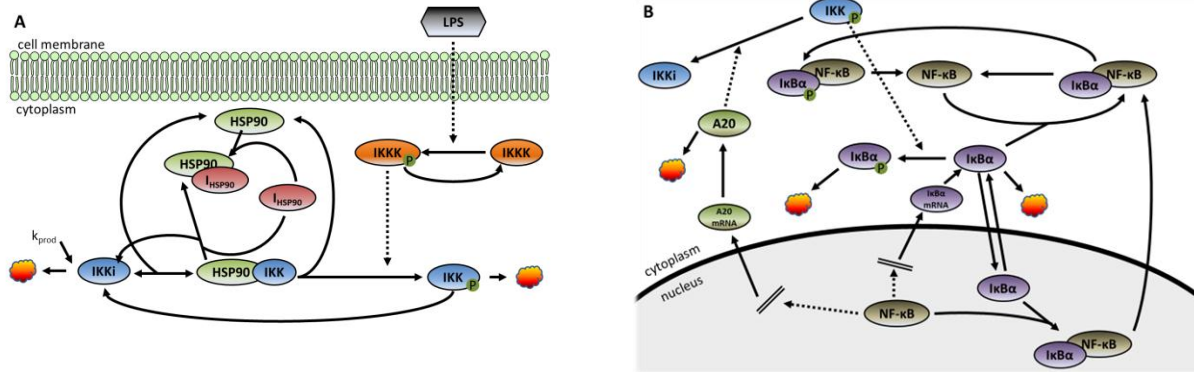


Figure 4.1 Diagram NF-κB reactions with the inclusion of HSP90-IKK binding and an HSP90 inhibitor. A) IKK interactions with IKKK, HSP90, and I_{HSP90}. B) NF-κB activation reactions.

4.2.1 Notation Guide

In this section we give a complete listing of the terms and notation describing the constituent molecules and complexes of the model. Nuclear concentration is represented by the subscript n , while phosphorylated molecules are denoted by the subscript p . Concentration of mRNA transcripts are represented by the subscript t . All other concentrations are cytoplasmic.

- IKKi – cytoplasmic concentration of in-active IKK,
- IKK_p – cytoplasmic concentration of IKK activated through phosphorylation,
- HSP90 – cytoplasmic concentration of the endogenous, unbound HSP90,
- HSP90_IKK – cytoplasmic concentration of the complex formed between HSP90 and IKKi,
- IKKK – cytoplasmic concentration of in-active IKKK,
- IKKK_p – cytoplasmic concentration of IKKK activated through phosphorylation,
- NFκB – cytoplasmic concentration of NF-κB, free and unbound from complexes,
- NFκB_n – Activated or nuclear NF-κB. We assume that NF-κB found in the nucleus, when not complexed with other proteins, is in its activated state,

- A_{20} – cytoplasmic concentration of A20 protein,
- A_{20_t} – concentration of the A20 mRNA transcript, assumed to be a cytoplasmic concentration,
- $I\kappa B\alpha$ – cytoplasmic concentration of $I\kappa B\alpha$,
- $I\kappa B\alpha_n$ – nuclear concentration of $I\kappa B\alpha$,
- $I\kappa B\alpha_p$ – cytoplasmic concentration of phosphorylated $I\kappa B\alpha$,
- $I\kappa B\alpha_t$ – concentration of the $I\kappa B\alpha$ mRNA transcript, assumed to be a cytoplasmic concentration,
- $HSP90_{I_{HSP90}}$ – cytoplasmic concentration of inhibited HSP90,
- I_{HSP90} – cytoplasmic concentration of HSP90 inhibitor not bound to HSP90,
- $I\kappa B\alpha_{NF\kappa B}$ – cytoplasmic concentration of the complexes of $I\kappa B\alpha$ and NF- κB ,
- $I\kappa B\alpha_n-NF\kappa B_n$ – nuclear concentration of the complexes of $I\kappa B\alpha$ and NF- κB ,
- $I\kappa B\alpha_p-NF\kappa B$ – cytoplasmic concentration of the complexes of $I\kappa B\alpha_p$ and NF- κB ,
- $k_v = V/U$ – the ratio of cytoplasmic and nuclear volumes,
- τ – the time delay between introduction of LPS to the cellular environment and actual onset of activity by IKKK.

4.2.2 Model Equations

In this section we discuss the equations of the model following the assumed kinetics. Molecules and complexes are represented as described in the above notation guide.

In-active IKK (IKKi)

In-active IKK represents the endogenous form of the IKK protein, as found generally in the cytoplasm. We assumed that new IKK is inactive until it becomes bound to HSP90 which enables activation of IKK. We also assumed that IKK unbound from HSP90 is inactive [45]. In our model (Eq. 1), the first two terms in describe the production of new IKK and degradation of

unbound IKK. Production is assumed to be continuous and at a level such that under non-stimulated conditions the levels of total IKK do not vary significantly. The third and fourth terms in the first line of the equation describe IKK binding to and unbinding from HSP90. In the second line of the equation, the first term describes deactivation of IKK by endogenous phosphatase while the second term describes deactivation by the IKK inhibitor A20. Finally, the last two terms describe the unbinding of IKK from HSP90 as induced by the HSP90 inhibitor (I_{HSP90}).

$$\begin{aligned} \frac{d}{dt} IKKi(t) = & k_{prod} - k_{deg} IKKi(t) - k_{1a} HSP90(t) IKKi(t) + k_{1b} HSP90_IKK(t) \\ & + k_{4a} IKK_p + k_{A20} IKK_p(t) A20(t) + k_{5a} HSP90_IKK(t) I_{HSP90}(t) \end{aligned} \quad \text{Eq. 1}$$

Activated IKK (IKK_p)

IKK is phosphorylated by several known kinases as well as some yet to be identified kinases. We represent IKK activation kinetics as an interaction between the activated form of the general IKK kinase (we term IKKK). We also assume that the activation of IKK by IKKK_p occurs only to IKK in the HSP90 complex [45, 47]. In the model equations (Eq. 2), we first describe degradation of IKK. The second term describes the activation of IKK bound to HSP90 occurring by IKKK_p. The third term describes the deactivation of IKK by endogenous phosphatases. The final term of the equation describes deactivation of IKK by the IKK inhibitor A20.

$$\begin{aligned} \frac{d}{dt} IKK_p(t) = & -k_{deg} IKK_p(t) + k_{2a} HSP90_IKK(t) IKKK_p(t) \\ & - k_{4a} IKK_p(t) - k_{A20} IKK_p(t) A20(t) \end{aligned} \quad \text{Eq. 2}$$

Free (unbound) HSP90

Free HSP90 is defined for our model as being unbound to IKK or inhibitors. The first two terms of Eq. 3 describe the reversible binding between HSP90 and IKK. The third term (second

line) describes the activation of IKK by IKKKp. Line three describes the reversible binding of HSP90 to the HSP90 inhibitor.

$$\begin{aligned} \frac{d}{dt}HSP90(t) = & -k_{1a}HSP90(t)IKKi(t) + k_{1b}HSP90_IKK(t) \\ & + k_{2a}HSP90_IKK(t)IKKK_p(t) \\ & - k_{5a}HSP90(t)I_{HSP90}(t) + k_{5b}HSP90_I_{HSP90}(t) \end{aligned} \quad \text{Eq. 3}$$

IKK bound to HSP90 IKK (HSP90_IKK)

This constituent is analogous to the neutral IKK presented in previous models [38-40]. Lipniacki et. al. defined neutral IKK as also including a production term and degradation term as well as having a term that described direct conversion to its activated state [38]. However, we assume that HSP90 protects IKK from degradation and have removed the degradation term [50]. We also assume that new IKK (as described by the production term) is inactive, and only after binding to HSP90 does it become active. This assumption is in agreement with the general function of HSP90 as a chaperone that completes protein folding and enables kinase activity. In our model equation (Eq. 4), the first two terms describe the binding and unbinding of HSP90 and IKKi to form HSP90_IKK. The term in the second line describes the activation of HSP90_IKK by IKK kinase (IKKKp). The term in the third line represents the binding of the HSP90 inhibitor (I_{HSP90}) to HSP90_IKK complex when it simultaneously frees IKK from the complex.

$$\begin{aligned} \frac{d}{dt}HSP90_IKK(t) = & k_{1a}HSP90(t)IKKi(t) - k_{1b}HSP90_IKK(t) \\ & - k_{2a}HSP90_IKK(t)IKKK_p(t) \\ & - k_{5a}HSP90_IKK(t)I_{HSP90}(t) \end{aligned} \quad \text{Eq. 4}$$

Neutral IKK kinase (IKKK)

Instead of direct IKK activation by the addition of a stimulant as in other published models [38-40], we created simplified reactions describing kinase activation by LPS upstream of IKK. We based our reaction equations on two other models in which IKK is activated by IKKKp

[40, 44]. In our model equation for IKKK concentration (Eq. 5), the first term of the formula describes dephosphorylation of IKKKp by phosphatases to result in replenishment of neutral IKK. The second term describes LPS activation of IKKK with an assumed time delay.

$$\frac{d}{dt} IKKK = +k_{I3Kphatase} IKKK_p(t) - k_{I3K} LPS(t-\tau) IKKK(t) \quad \text{Eq. 5}$$

Active IKK kinase (IKKKp)

In our model equation describing IKKK activation, we use two terms (Eq. 6). The first describes the time-delayed activation of IKKK as a result of LPS stimulation. The second term describes the decrease in IKKKp as a result of phosphatase activity.

$$\frac{d}{dt} IKKK_p(t) = k_{I3K} LPS(t-\tau) IKKK(t) - k_{I3Kphatase} IKKK_p(t) \quad \text{Eq. 6}$$

Free Cytoplasmic NF-κB:

To describe the concentration of free cytoplasmic NF-κB over time, we used formulas found in [38]. In the equation (Eq. 7), the first term describes the liberation of NF-κB when dissociated from complexes with IκBα. The second term describes the depletion of NF-κB due to the formation of complexes with IκBα. The third term represents the liberation of NF-κB due to the catalytic activity of IKKp when it phosphorylates IκBα. The final term accounts for free NF-κB removed from the cytoplasm when it is transported to the nucleus.

$$\begin{aligned} \frac{d}{dt} NF\kappa B(t) = & c_{6a} I\kappa B\alpha - NF\kappa B(t) - a_1 NF\kappa B(t) I\kappa B\alpha(t) \\ & + t_1 I\kappa B\alpha_p - NF\kappa B(t) - i_1 NF\kappa B(t) \end{aligned} \quad \text{Eq. 7}$$

Active NF-κB (NF-κB_n):

Activation of NF-κB is described as the localization of free NF-κB in the nucleus. Our model equation below (Eq. 8) is derived from that presented in [38-40]. The first term represents the translocation of free NF-κB from the cytoplasm to the nucleus. This transport is adjusted by

the coefficient k_v which accounts for changes in nuclear concentration due to the smaller relative volume of the nucleus. The second term describes depletion of free NF- κ B when it forms a complex with nuclear I κ B α .

$$\frac{d}{dt} NF\kappa B_n(t) = i_1 k_v NF\kappa B(t) - a_1 NF\kappa B_n(t) I\kappa B\alpha_n(t) \quad \text{Eq. 8}$$

A20 protein:

We describe the formation of A20 protein below (Eq. 9) using the equations presented by [38-40]. The first term describes the formation of new A20 protein from the A20 mRNA transcript. Depletion of A20 protein is represented by the second term.

$$\frac{d}{dt} A20(t) = c_4 A20_t(t) - c_5 A20(t) \quad \text{Eq. 9}$$

A20 transcript:

The concentration of A20 mRNA transcripts is described using previously published equations [38-40]. The first term in Eq. 10 describes nominal A20 mRNA production. The second term describes the production of A20 mRNA as induced by NF- κ B activation. The third term describes the degradation of A20 mRNA.

$$\frac{d}{dt} A20_t(t) = c_2 + c_1 NF\kappa B_n(t) - c_3 A20_t(t) \quad \text{Eq. 10}$$

Free Cytoplasmic I κ B α :

Concentrations of free cytoplasmic I κ B α are represented by equations derived from [38-40]. The first term in Eq. 11 describes the depletion of free I κ B α by the catalytic activity of IKK ρ which phosphorylates it. The second term describes the depletion of I κ B α by the formation of complexes with NF- κ B. The third term represents the formation of new I κ B α from the I κ B α mRNA transcripts. The fourth term shows constitutive degradation of I κ B α . The fifth and sixth terms represent the transport of I κ B α into and out of the nucleus.

$$\begin{aligned} \frac{d}{dt} I\kappa B\alpha(t) = & -a_2 IKK_p(t) I\kappa B\alpha(t) - a_1 I\kappa B\alpha(t) NF\kappa B(t) \\ & + c_4 I\kappa B\alpha_i(t) - c_{5a} I\kappa B\alpha(t) - i_{1a} I\kappa B\alpha(t) + e_{1a} I\kappa B\alpha_n(t) \end{aligned} \quad \text{Eq. 11}$$

Free Nuclear IκBα:

Concentrations of free nuclear IκBα are represented by equations derived from [38-40]. The first term in Eq. 12 represents the depletion of nuclear IκBα from the formation of nuclear complexes of IκBα and NF-κB. The second and third terms represent the transport of IκBα into and out of the nucleus.

$$\frac{d}{dt} I\kappa B\alpha_n(t) = -a_1 I\kappa B\alpha_n(t) NF\kappa B_n(t) + i_{1a} k_v I\kappa B\alpha(t) - e_{1a} k_v I\kappa B\alpha_n(t) \quad \text{Eq. 12}$$

Phospho-IκB

To describe phosphorylated IκBα, we used equations presented in [40]. In Eq. 13 the first term describes IκBα phosphorylation due to catalytic action of IKKp. The second term describes the catalytic degradation of phosphorylated IκBα.

$$\frac{d}{dt} I\kappa B\alpha_p(t) = a_2 IKK_p(t) I\kappa B\alpha(t) - t_1 I\kappa B\alpha_p(t) \quad \text{Eq. 13}$$

IκBα transcript:

The concentration of IκBα mRNA transcripts occurs similar to that of A20. Using equations from [38-40]. In Eq. 14, the first term, we account for nominal IκBα transcript production. The second term represents the induced production of IκBα transcripts by activated NF-κB. The third term describes the constitutive degradation of IκBα transcripts.

$$\frac{d}{dt} I\kappa B\alpha_i(t) = c_2 + c_1 NF\kappa B_n(t) - c_3 I\kappa B\alpha_i(t) \quad \text{Eq. 14}$$

Inhibited HSP90:

The inhibited form of HSP90 is created as HSP90 binds to I_{HSP90} . We account for the dynamic behavior of inhibited HSP90 concentration in Eq. 15. The first two terms represent the binding of and HSP90 inhibitor to HSP90 and the reverse reaction. The third term describes the increase of inhibited HSP90 when I_{HSP90} out competes with IKK to bind to HSP90.

$$\begin{aligned} \frac{d}{dt} HSP90_{-}I_{HSP90}(t) = & k_{5a} HSP90(t)I_{HSP90}(t) - k_{5b} HSP90(t)I_{HSP90}(t) \\ & + k_{5a} HSP90_{-}IKK(t)I_{HSP90}(t) \end{aligned} \quad \text{Eq. 15}$$

HSP90 Inhibitor:

The total concentration of HSP90 inhibitor ($I_{HSP90,total}$) is a known, externally controllable concentration. In order to fix the total HSP90 inhibitor concentration in the model, we compute that the free I_{HSP90} is a function of the total concentration of I_{HSP90} minus the concentration of I_{HSP90} bound to HSP90 as shown in Eq. 16a. In order to represent the intracellular concentration of $I_{HSP90,total}$, we approximate the concentration using a logistic function as presented in Eq. 16b.

$$I_{HSP90}(t) = I_{HSP90,total}(t) - HSP90_{-}I_{HSP90}(t) \quad \text{Eq. 16a}$$

$$I_{HSP90,total}(t) = I_{HSP90,ecell} \left(\frac{1}{1 + e^{-a(t-\tau_2 + 10/a)}} \right) \quad \text{Eq. 16b}$$

Cytoplasmic $I\kappa B\alpha$ _NF- κ B Complexes:

We represent the concentration of cytoplasmic $I\kappa B\alpha$ _NF- κ B in Eq. 17 complexes using the equations found in [38-40]. The first term describes the formation of the complex when $I\kappa B\alpha$ associates with NF- κ B. The second term shows that the complex is depleted due to the catalytic activity of IKKp. The third term describes depletion of the complex due to constitutive $I\kappa B\alpha$ degradation. The fourth term represents the translocation of nuclear complexes of $I\kappa B\alpha$ NF κ B from the nucleus to the cytoplasm.

$$\begin{aligned} \frac{d}{dt} I\kappa B\alpha_{-NF\kappa B}(t) = & a_1 I\kappa B\alpha(t) NF\kappa B(t) - a_3 IKKp(t) I\kappa B\alpha_{-NF\kappa B}(t) \\ & - c_{6a} I\kappa B\alpha_{-NF\kappa B}(t) + e_{2a} I\kappa B\alpha_n_{-NF\kappa B_n}(t) \end{aligned} \quad \text{Eq. 17}$$

Nuclear IκBα_n-NF-κB Complexes:

The concentration of nuclear IκBα_n-NF-κB complexes is described in Eq. 18, which is based on equations presented in [38-40]. The first term describes the formation of the complex when IκBα_n associates with NF-κB_n. The second terms describes the transport of the nuclear complex into the cytoplasm.

$$\frac{d}{dt} I\kappa B\alpha_n_{-NF\kappa B_n}(t) = a_1 I\kappa B\alpha_n(t) NF\kappa B_n(t) - e_{2a} k_v I\kappa B\alpha_n_{-NF\kappa B_n}(t) \quad \text{Eq. 18}$$

Phospho-IκBα complexed to NF-κB

We describe the concentration of phosphorylated IκBα in complex with NF-κB in Eq. 19 using equations presented in [40]. The first term describes phosphorylation of IκBα in NF-κB complexes as it occurs by the catalytic action of IKKp. The second term describes the degradation of phosphorylated IκBα (NF-κB is recovered).

$$\frac{d}{dt} I\kappa B\alpha_p_{-NF\kappa B}(t) = a_3 IKK_p(t) I\kappa B\alpha_{-NF\kappa B}(t) - t_1 I\kappa B\alpha_p_{-NF\kappa B}(t) \quad \text{Eq. 19}$$

4.3 Materials and Methods

Model Simulation: Model ODEs were constructed in Matlab and simulations were performed using the ODE solver ode15s in Matlab 2010a (Mathworks, Inc., Natick, MA) to solve the differential equations. All Matlab files are included as supplementary materials in the appendix.

Parameter Estimation: Parameters were estimated using the sequential quadratic programming (sqp) algorithm in the Matlab function “fmincon”. An objective function (J) was

computed and minimized by the “fmincon” optimization routine by adjusting two or three specified parameters until a local minimum was found. The resulting parameters were tested and the accuracy of the response was assessed and key discrepancies in the response were identified and the parameters that most affected those features were then selected for estimation. The optimization routine was repeated until a new local cost function minimum was found. Response was assessed again by identifying key discrepancies. A third round of parameters was selected and the optimization conducted. The objective function (J) minimized by the optimization routine was the sum of the error squared between the model response and the data (Eq. 20).

$$J = \sum_{t=0}^{240} (IKK_{p,sim}(t) - IKK_{p,exp}(t))^2 \quad \text{Eq. 20}$$

Cell Culture: J774 macrophage cells were cultured overnight in 60 mm tissue culture treated dishes at an approximate density of 3.2×10^6 cells/dish. Prior to experiment, cells were rendered quiescent by replacing growth media with low serum media constituted as follows: DMEM (ATCC, Manassas, VA) supplemented with 1% FBS and 1% Penicillin/Streptomycin (Sigma, St. Louis, MO).

Treatment with 17-DMAG and Stimulation with LPS: One hour prior to stimulation, cells were pre-treated with or without 1 μ M of the HSP90 inhibitor, 17-DMAG (ChemieTek, Indianapolis, IN). Cells were stimulated with 1 μ g/ml LPS (Sigma). Following LPS stimulation cells were collected for nuclear lysate extraction at 10, 20, 30, 40, 50, 60, 70, 80, 90, 100, 110, and 120 minutes. Un-stimulated cells were also collected as experimental controls.

Nuclear Extract Preparation: Cytoplasmic and nuclear extracts were prepared using a commercial nuclear extract kit (Active Motif, Carlsbad, CA). Extracts were prepared according to manufacturer instructions. In brief, cells were rinsed with PBS containing phosphatase inhibitors (PBS/pi) and then cells were suspended in PBS/pi followed by centrifugation at 500 rpm for 5

minutes at 4°C. Supernatant was removed and cells were resuspended in ice-cold hypotonic buffer. Cells were kept in buffer for 15 minutes, after which, detergent was added, cells were vortexed for 10 seconds, and then were pelleted by centrifugation for 30 seconds at 14000 xg at 4°C. Supernatant was collected as the cytoplasmic fraction and stored at -80°C until assay. The remaining pellet (intact nuclei) was resuspended in complete lysis buffer, vortexed for 10 seconds, and then incubated on ice for 30 minutes. Following incubation in lysis buffer, samples were vortexed for 30 seconds and then spun down in a centrifuge at 14000xg for 10 minutes at 4°C. The supernatant was then collected as the nuclear fraction and stored at -80°C until assay. Nuclear and cytoplasmic fractions were analyzed for protein concentration using BCA protein assay (ThermoScientific, Rockford, IL) following manufacturer instructions.

NF-κB ELISA: Cell lysates were analyzed for NF-κB p65 by TransAM ELISA (ActivMotif, Carlsbad, CA) following manufacturer instructions. Briefly, nuclear extracts were diluted in lysis buffer to equalize total protein content of all samples. Diluted samples were incubated in oligonucleotide coated ELISA plates in the presence of binding buffer for one hour. The plate was washed three times using manufacturers wash buffer. The plate was then incubated for one hour with antibody to NF-κB followed by washing of the plate three times with wash buffer. Next, the plate was incubated for one hour with HRP conjugated secondary antibody. Following secondary incubation, the plate was washed four times with wash buffer. The plate was then incubated for five minutes with developing solution provided by manufacturer, followed immediately by addition of stop solution. Absorbance was read on a spectrophotometer plate reader at wavelength of 450 nm. Active NF-κB concentration was computed using a linear curve fit of a prepared standard curve.

4.4 Results and Discussion

To test the model presented in the Model Equations section we first conducted a numerical sensitivity study of parameters that form the HSP90, IKK, and IKKK reaction equations. We performed the study by testing one parameter at a time at discrete intervals over a range of assumed parameter values. Only one parameter was varied for each simulation, and each parameter was tested at 5 discrete values spaced an order of magnitude apart. From this study we obtained a sense for how each parameter affected the overall system response. These studies also identified the parameters to which the system was most sensitive.

Next we used published experimental IKK activation data to determine improved estimates of the parameter values. The data used can be found in the supplemental materials section of [18]. Our third task was to conduct a secondary parameter sensitivity analysis in which we assessed the sensitivity of the model to the parameter values associated with I_{HSP90} . This allowed us to determine an estimated range for the I_{HSP90} associated parameters. The secondary parameter study enabled us to test our hypothesis that an HSP90 inhibitor must out-compete IKK for binding to HSP90. Finally, we validated the model by comparing experimental data to our simulated NF- κ B activity.

4.4.1 IKK activation profile sensitive to HSP90 binding rate

To test the sensitivity of the predicted IKKp profile to model parameters associated with IKKK and IKK activation, we ran simulations in which a single parameter was iteratively varied across a range of values. Only one parameter was varied at a time while all other parameters were held fixed. The parameters we tested and their respective test ranges are shown in Table 4.1. The parameter ranges tested spanned across several orders of magnitude which allowed us to test for singularities at extreme parameters. We found that among the parameters tested, three exhibited

interesting and significant behavior. Those three were, not surprisingly, the HSP90-IKK binding rate (k_{1a}), the IKK activation rate (k_{2a}), and the IKKK activation rate (k_{i3k}). The complete system response for all parameters tested is provided as an appendix.

Table 4.1. Parameters and ranges tested in parameter sensitivity study for IKKK, IKK, and HSP90 reactions.

| Parameter | Range | Units | Description |
|------------------|---------------------|----------------------------------|--|
| k_{1a} | $10^{-4} - 10^0$ | $\mu\text{M}^{-1} \text{s}^{-1}$ | IKK_HSP90 association |
| k_{1b} | $10^{-5} - 10^{-1}$ | s^{-1} | IKK_HSP90 dissociation |
| k_{2a} | $10^{-4} - 10^0$ | $\mu\text{M}^{-1} \text{s}^{-1}$ | IKK activation by IKKKp |
| k_{4a} | $10^{-4} - 10^0$ | s^{-1} | IKKp deactivation by phosphatases |
| $k_{i3kphtase}$ | $10^{-6} - 10^{-2}$ | s^{-1} | Dephosphorylation of IKKK by phosphatases |
| k_{i3k} | $10^{-6} - 10^{-1}$ | $\mu\text{M}^{-1} \text{s}^{-1}$ | IKKK activation (phosphorylation) rate |
| k_{A20} | $10^{-3} - 10^1$ | $\mu\text{M}^{-1} \text{s}^{-1}$ | IKK inactivation by A20 |

To test the parameters, the model was simulated for 1200 hours (simulation time) to ensure the system reached equilibrium values for all model concentrations at each of the parameter values tested. Final concentrations of the steady-state equilibration simulation were used as initial conditions for the parameter sensitivity simulations. To simulate LPS stimulation,

the model was simulated so that two hours after initializing, LPS was “turned on”. We show the LPS stimulation curve in Figure 4.2A, Figure 4.3A, and Figure 4.4A.

Testing the parameter k_{1a} across the range of values illustrated the sensitivity of NF- κ B to any level of IKKp response, shown in Figure 4.2D and G. Neither IKKKp nor IKKK was affected by k_{1a} which was expected as the model does not have a feedback loop to IKKK (Figure 4.2B & C). IKKi exhibited an interesting, non-linear response as shown in Figure 4.2E. For the lowest three values of k_{1a} , the magnitude of the IKKi concentration after LPS stimulation increased as k_{1a} increased. However, for k_{1a} values of 0.1 and 1 $\mu\text{M}^{-1}\text{s}^{-1}$ IKKi magnitudes decreased. Perhaps least surprising is that as k_{1a} increased, the concentration of HSP90_IKK increased. However, while each parameter was an order of magnitude greater than the last, the increase of HSP90_IKK concentration did not increase at the same rate (Figure 4.2F). Finally, free HSP90 was not significantly affected by the variation in the parameter (Figure 4.2H).

Next we tested the activation rate of IKKp, k_{2a} . The LPS stimulation profile, IKKKp, and IKKK are shown in Figure 4.3A-C. IKKp increased in magnitude at the initial response peak and the width of the initial peak increased as k_{2a} increased. The change in magnitude of the peak was most sensitive to the lower parameter values, suggesting an upper bound to the parameter value (Figure 4.3D). IKKi also exhibited interesting behavior in that not only did it increase in concentration, but for higher parameter values (0.1 and 1 $\mu\text{M}^{-1}\text{s}^{-1}$) the response peaked just after stimulation, then fell to a steady value (Figure 4.3E). HSP90_IKK concentrations decrease dramatically just after stimulation, with the sharpest declines occurring as k_{2a} increased (Figure 4.3F). NF- κ B was not as significantly affected by k_{2a} as it was by k_{1a} . That is likely due in part to the fact that the changes in IKKp magnitude were smaller for k_{2a} than the changes were for k_{1a} . Again it was seen that lower k_{2a} values produce more oscillatory behavior in NF- κ B (Figure 4.3G). Free HSP90, shown in Figure 4.3H was not significantly affected by k_{2a} .

We tested k_{i3k} across a broader range of parameter values as the system seemed highly sensitive to this parameter. Figure 4.4B and C show that IKKKp is indeed sensitive to the activation rate, however, the higher activation rates did not have an effect on increasing IKKK activity as all the free IKKK was depleted. Lower parameter values exhibited great variations in the response of IKKKp. IKKp was sensitive to k_{i3k} , especially at the lower values which caused a decrease in the magnitude of the IKKp and IKKi responses (Figure 4.4D and E). HSP90_IKK showed sharp changes in concentration for larger k_{i3k} values (Figure 4.4F). With IKKp sensitive to k_{i3k} , that sensitivity propagated to NF- κ B activity which responded to the parameter changes with its own changes in oscillatory frequency and magnitude (Figure 4.4G). Free HSP90 was again not significantly affected by the parameter (Figure 4.4H).

In constructing the model, we assumed the initial parameter values describing interactions between HSP90 and IKK based on constraints determined by findings in the literature. As HSP90 is typically bound to IKK [51, 52], we assumed that HSP90 and IKK would preferentially bind and any reverse reaction would occur at a slower rate, thus $k_{1a} > k_{1b}$. We also assumed that the rate at which HSP90 and IKK form a complex should not reduce the rate at which IKK is activated under normal (non-HSP90 inhibited) conditions, thus, $k_{1a} \geq k_{2a}$.

We found that despite changing HSP90 binding rates across 5 orders of magnitude, NF- κ B activity still responded strongly to the smallest of IKKp activity profiles. This is in agreement with previous studies showing how NF- κ B activity is highly sensitive to IKK activation [34]. In summary, the system was sensitive to parameters that directly impact IKKp activity and that sensitivity was propagated to NF- κ B activity. With the parameter sensitivity results, we were able to prioritize which parameters to fit to experimental data.

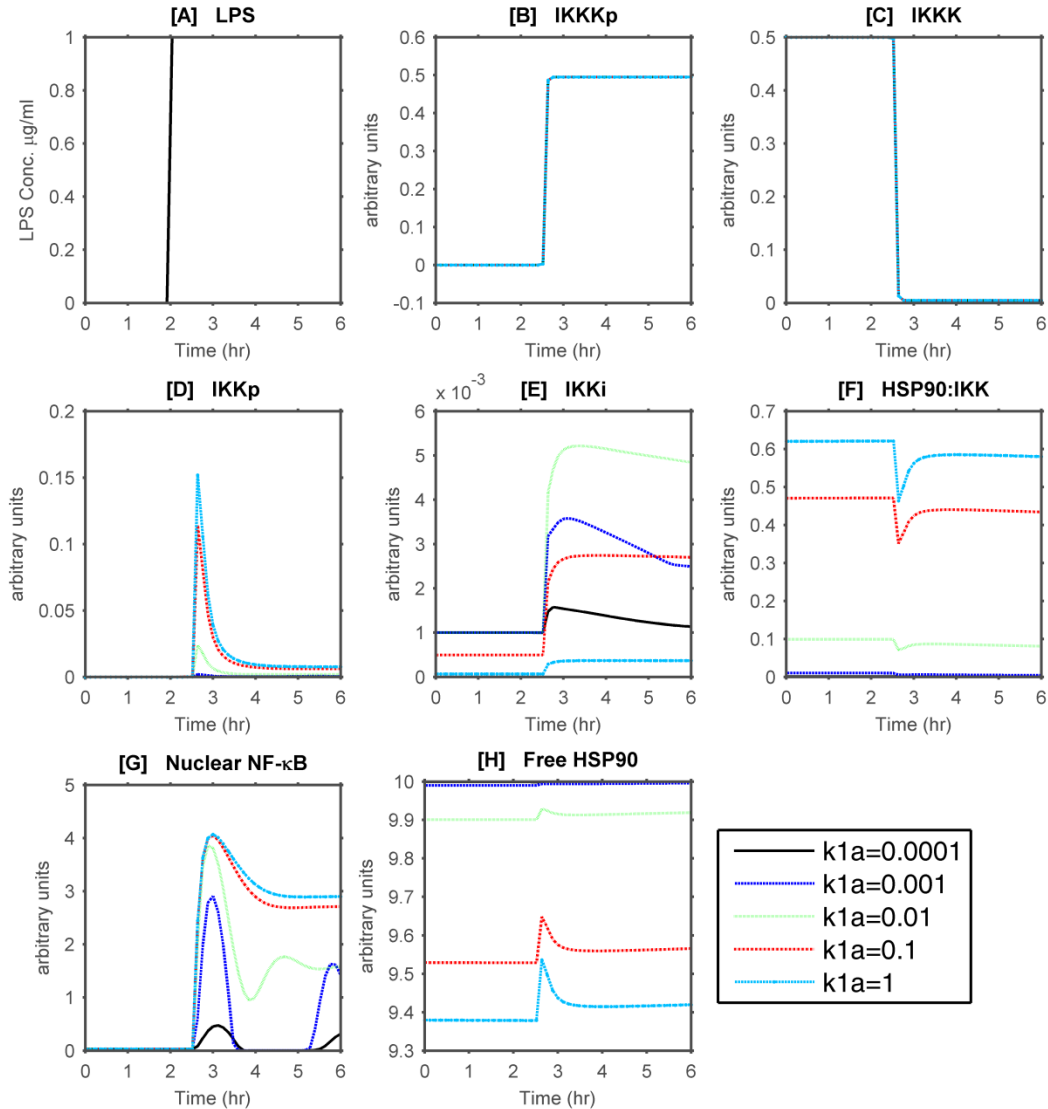


Figure 4.2. HSP90-IKK association parameter k_{1a} varied from 0.0001 to 1 $\mu\text{M}^{-1}\text{s}^{-1}$. A) Model was allowed to equilibrate for 2 hours before LPS stimulation began. B and C) IKKKp and IKKK are unaffected by k_{1a} . D) IKKp activity increases as the HSP90 binding rate increases with an order of magnitude difference in IKKp profile for the middle range of parameter values. E) IKKi has a non-linear response to the change in k_{1a} as seen by the fact that the middle parameter value (0.01 $\mu\text{M}^{-1}\text{s}^{-1}$) reached the highest concentration while the highest parameter value (1 $\mu\text{M}^{-1}\text{s}^{-1}$) was the lowest concentration. F) HSP90:IKK complex concentrations show some variation, though it is interesting to note that the equilibration

values were affected by the parameter. G) NF- κ B activity increases as a result of an increased rate of binding between HSP90 and IKK. H) Free HSP90 was not significantly affected by the change in binding rate.

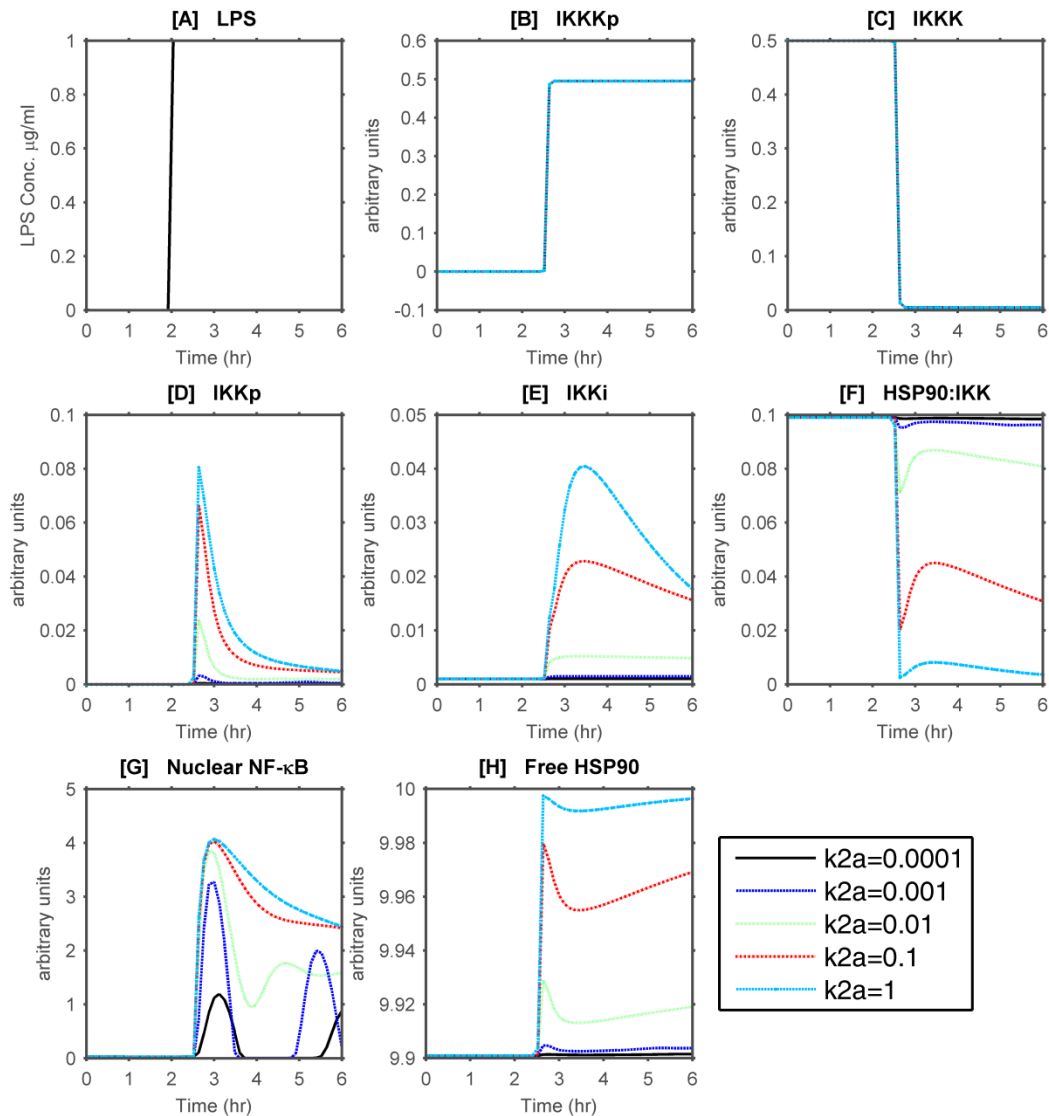


Figure 4.3. Model response when IKK activation parameter k_{2a} was tested at values from 0.0001 to 1 $\mu\text{M}^{-1}\text{s}^{-1}$. A) Model was allowed to equilibrate for 2 hours before LPS stimulation began. B and C) IKKKp and IKKK are unaffected by k_{2a} . D) Magnitude and duration of IKKp activity increased as k_{2a} increased. E) IKKi Concentration increased as k_{2a} increased. IKKi also exhibited a pronounced peak for higher values of k_{2a} . F) HSP90:IKK complex concentrations decreased as k_{2a} increased. G) NF- κ B activity increased in response to increased k_{2a} . NF- κ B activity also had less oscillatory behavior as k_{2a} increased. H) The magnitude of the free HSP90 concentration was not significantly affected by the change k_{2a} .

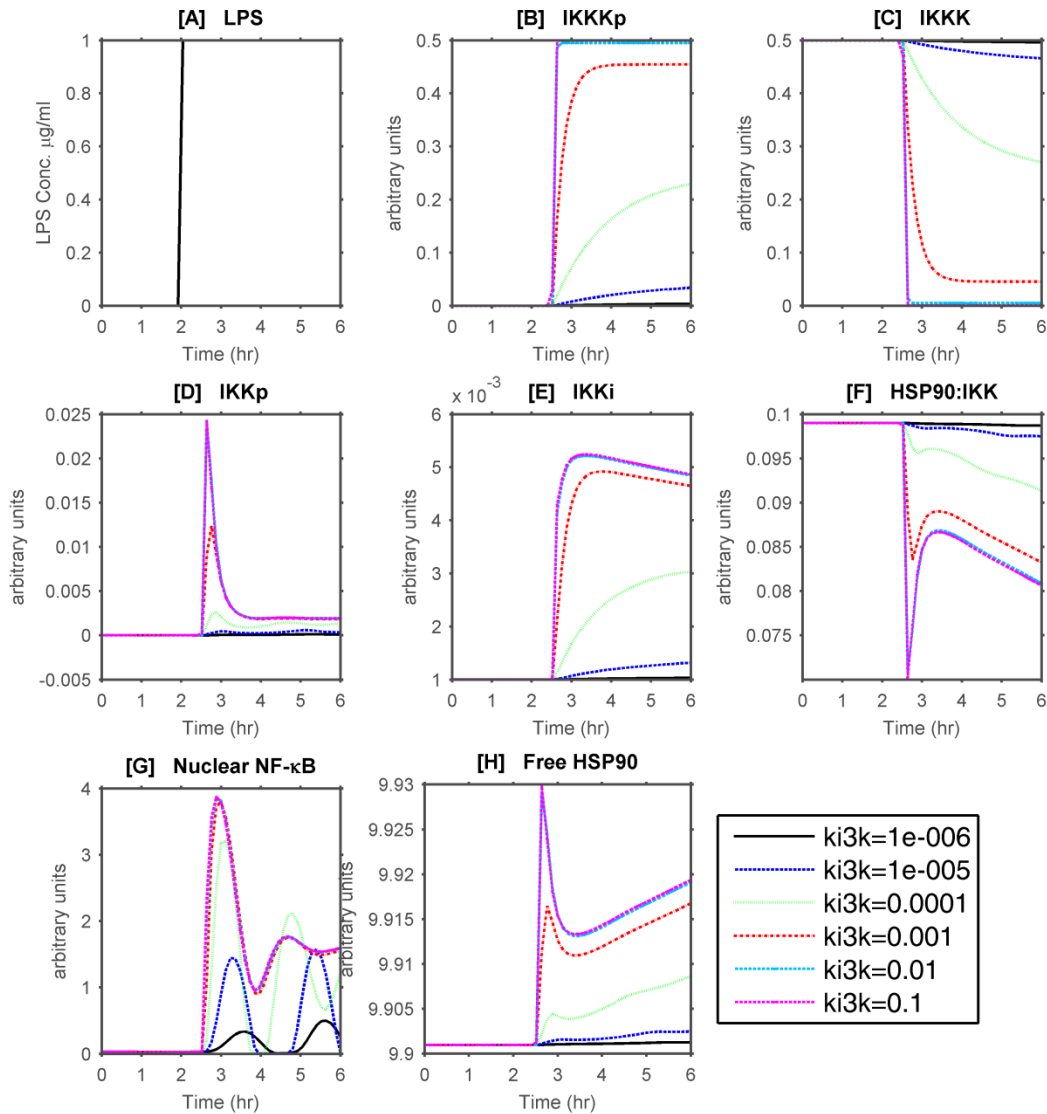


Figure 4.4. Model response when IKKK activation parameter k_{i3k} was tested at values from 0.0001 to 1 $\mu\text{M}^{-1}\text{s}^{-1}$. A) Model was allowed to equilibrate for 2 hours before LPS stimulation began. B) IKKKp response was slow and a lower magnitude for the k_{i3k} at 0.0001 and 0.001 $\mu\text{M}^{-1}\text{s}^{-1}$ whereas IKKKp response was fast and higher in magnitude for k_{i3k} at the higher parameter values. IKKKp response was not sensitive to changes in k_{i3k} at the larger parameter values. C) IKKK was only sensitive to the smaller k_{i3k} parameter values. D) The magnitude of IKKp activity increased as k_{i3k} increased, but the system was not sensitive to k_{i3k} parameter values greater than 0.01. E) IKKi Concentration increased as k_{i3k} increased.

F) HSP90:IKK complex concentrations exhibited sharp changes in concentration in when k_{i3k} was set to a larger value. G) NF- κ B activity was only slightly affected by the parameter change from 0.0001 to 0.001 $\mu\text{M}^{-1}\text{s}^{-1}$. NF- κ B exhibited stronger oscillations for the lower k_{i3k} value. H) Other than small but sharp changes in concentration, the magnitude of the free HSP90 concentration was not significantly affected by the change k_{i3k} .

4.4.2 Parameters were fit using experimental data from mouse embryonic fibroblasts.

Based on our parameter sensitivity results, we proceeded to estimate model parameters by fitting the model IKKp response to an existing data set provided in the supplemental materials section in [18]. The data provided was obtained by stimulating mouse embryonic fibroblasts (MEFs) with a 45 minute pulse of 0.1 $\mu\text{g/ml}$ LPS. IKKp data was collected for 120 minutes and was normalized such that the nominal, un-stimulated value for IKKp at the initial time point is unity. Given that the experimental data is normalized, it does not represent an absolute concentration for IKKp but rather provides a relative trend. As stated in [38], the concentrations of the simulated system are also arbitrary and only represent qualitative concentrations. Therefore, in order to use the IKKp experimental dataset, we were required to scale our simulated IKKp profile using a scaling factor of 1000 and offset the baseline by +1. This put our initial IKKp concentration within an order of magnitude of the measured data.

The data was fit in a semi-manual manner. First, the fitting algorithm was used to adjust k_{1a} , k_{2a} , and k_{i3k} simultaneously. We constrained the fitting algorithm to find parameter values within a specified range. We found that the fitting algorithm obtained a result that approached the experimental data but did not seem to capture the rate at which IKKp decreased after the initial spike. A review of the parameter sensitivity data led us to believe that k_{A20} could be re-estimated to provide a better fit the experimental data. We repeated the parameter estimation for k_{i3k} and k_{A20} . We then conducted a third round of fitting was performed in which we re-estimated k_{1a} and also estimated k_{4a} . We found the model and experimental data in good agreement. The final estimates for the parameters are given in Table 4.2. A comparison of the predicted response to the experimental data used for fitting is provided in Figure 4.5.

Table 4.2. Parameters estimated through fitting IKKp profile to experimental data.

| Symbol | Initial Estimate | Fitted Value | Units |
|------------------------|-------------------------|---------------------|---|
| k_{1a} | 0.01 | 0.005 | $\mu\text{M}^{-1}\text{s}^{-1}$ |
| k_{2a} | 0.01 | 0.073 | $\mu\text{M}^{-1}\text{s}^{-1}$ |
| k_{4a} | 0.01 | 0.0099 | s^{-1} |
| k_{i3k} | 0.01 | 0.000848 | $\mu\text{M}^{-1}\text{s}^{-1}$ |
| k_{A20} | 0.1 | 0.001 | $\mu\text{M}^{-1}\text{s}^{-1}$ |

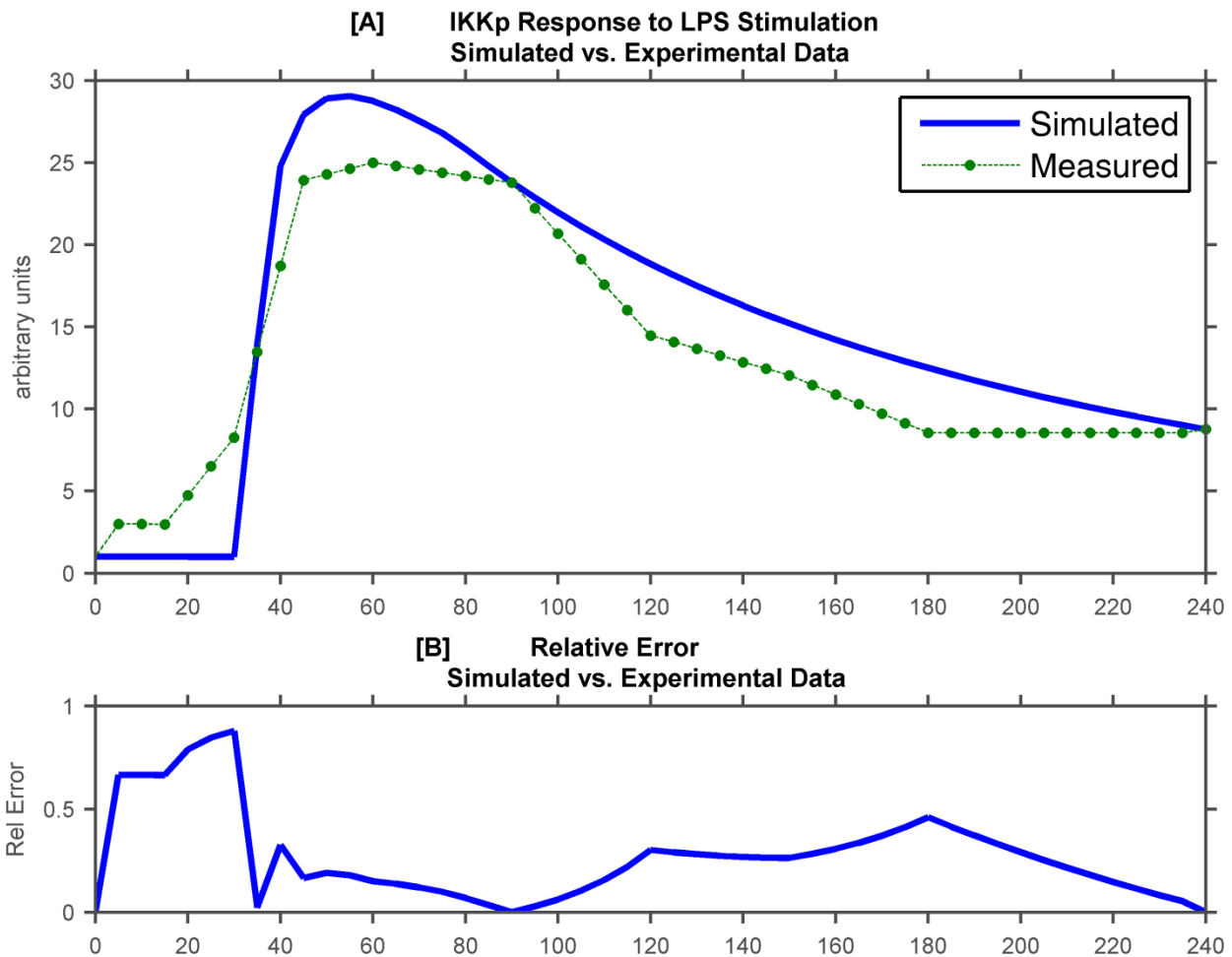


Figure 4.5. The simulated IKKp response matches the response of IKKp as measured in MEF cells. A) Comparison of the simulated IKKp profile to the measured IKKp profile shows qualitatively how well the parameters fit. B) The relative error between the measured data and simulated data quantifies how well the model fits the data over time. Parameters k_{1a} , k_{2a} , k_{4a} , k_{i3k} , and k_{A20} were estimated using the “sqp” algorithm in the fmincon function in Matlab.

4.4.3 Sensitivity of I_{HSP90} parameters was assessed

Once the model parameters for the HSP90, IKK, and IKKK interactions were adequately estimated, we tested the effect that inhibitor concentration and inhibitor binding rate would have on activation of IKK, NF- κ B and total I κ B α . We performed the simulations by fixing the I_{HSP90} concentration as a ratio of total HSP90 concentration. Ratios of HSP90 to I_{HSP90} of 0.9, 1, and 1.1 were each tested across a range of I_{HSP90} binding rate (k_{5a}) values. The range of k_{5a} values were selected to be either 10x, 1x, or 0.1x the fitted value for HSP90-IKK binding rate (k_{1a}). Linking the range of k_{5a} to the HSP90-IKK binding rate allowed us to test the sensitivity of the model to the assumption that the inhibitor binds competitively to HSP90. Figure 4.6 shows that IKKp is relatively sensitive to k_{5a} for inhibitor concentrations near the total HSP90 concentration. Figure 4.6A-C shows that for k_{5a} set to a value 1/10 of k_{1a} the IKKp activation was reduced. This reduction was relatively equal across the range of concentration ratios tested. When k_{5a} is increased to 10 times that of k_{1a} we found that for the inhibitor concentration ratio of 0.9, IKKp was reduced by approximately 1/5. For the same parameter value tested in the model with the concentration ratio of 1.1 the IKKp activity was all but eliminated.

Interestingly, NF- κ B activity was less sensitive to the reduction in IKKp activation (Figure 4.6D-E) in that the smallest increase in IKKp elicited an induction of NF- κ B activity. However, NF- κ B activity died out more rapidly in the presence of an inhibitor.

From this simulation data, we see that NF- κ B activation was not completely blocked by the lower dose of HSP90 inhibitor but it did show that after initial NF- κ B activation, the level of activity was not sustained. Taken from another viewpoint, IKKp activity is amplified in NF- κ B as the slightest activation of IKKp induces NF- κ B activity. Taking into consideration the more rapid decrease in activity that was seen with HSP90 inhibition, over the long term, an HSP90 inhibitor

may prevent chronic activation of NF- κ B. This has implications for chronic diseases where NF- κ B activity is elevated for long periods of time, such as lupus. We recently reported that in MRL/lpr mice treatment with 17-DMAG over 6 weeks reduced proteinuria and anti-dsDNA but did not elicit significant differences in renal tissue pathology [53]. In other words, inflammation was reduced but not eliminated. We also infer from this data that to reduce NF- κ B activity, IKK activation must be completely eliminated and to do so by interrupting HSP90 would require an inhibitor with either a high binding affinity for HSP90, and/or a concentration much larger than the total HSP90. It has been reported that several HSP90 inhibitors, such as Geldanamycin or 17-DMAG have increased affinity for HSP90 produced by tumor cell lines [54].

Figure 4.6G-I we see that total I κ B still responds to the LPS stimulation, even in the presence of an HSP90 inhibitor. Nevertheless, the highest concentration of inhibitor and largest k_{5a} value, the fluctuations in I κ B α were prevented. In order for NF- κ B to be activated, I κ B α must be phosphorylated and degraded. Therefore, in order for NF- κ B to be sensitive to IKKp it is required that I κ B α be sensitive to IKKp. The simulated responses of the other concentrations can be found in the appendix.

We see from the model that NF- κ B activation dynamics are affected by HSP90. Changing NF- κ B activation magnitudes as well as frequency of oscillation through HSP90 inhibition effect which genes get upregulated by NF- κ B [19, 34]. It may be possible to externally control NF- κ B dynamics using HSP90 inhibitors combined with other NF- κ B therapeutics, and external cell stimuli.

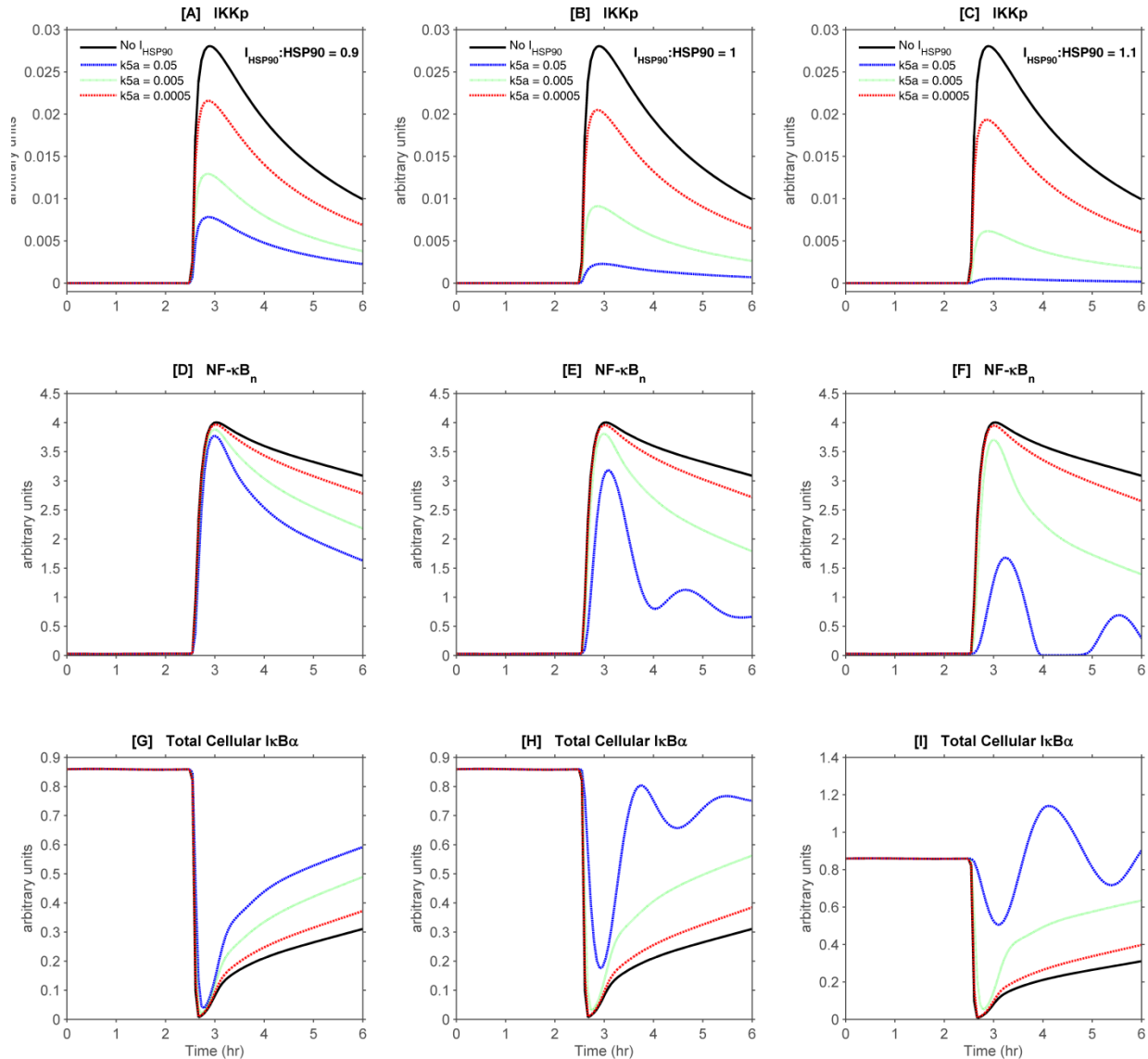


Figure 4.6. Reduction in NF- κ B response requires high concentration of HSP90 inhibitor and high binding affinity. Simulations were performed in which the cells were treated with various inhibitor concentrations fixed as a ratio to total HSP90 ($I_{\text{HSP90}}:\text{HSP90}$). Three ratios of the concentration ratio were tested: 0.9 (A, D, & G), 1 (B, E, & H), and 1.1 (C, F, & I). For each concentration ratio tested, the binding rate parameter, k_{5a} was varied across a range spanning from 5×10^{-4} to 5×10^{-2} . A-C) IKKp response for each value of k_{5a} and concentration ratio tested. D-F) Nuclear NF- κ B for each value of k_{5a} and concentration ratio tested. G-H) Total Cellular I κ B α for each value of k_{5a} and concentration ratio tested.

4.4.4 Simulated IKK ρ , I κ B α , and NF- κ B profiles agree with experimentally measured data

Based on our parameter sensitivity results, we determined to experimentally determine the effectiveness of an HSP90 inhibitor, 17-DMAG, at reducing the activity of NF- κ B. There have been several studies that have published results indicating that 17-DMAG and other HSP90 inhibitors reduce NF- κ B activity in various cell types [45, 46, 51, 55, 56]. However, much of this data is presented for single time points, most often 30-60 minutes post stimulation. In order to obtain time domain data on NF- κ B activity, we conducted an experiment in which we treated J774 macrophage cells with 1 μ M 17-DMAG for 1 hour, followed by immune-stimulation with 1 μ g/ml of LPS. These concentrations were selected based on previous work that showed 1 μ M 17-DMAG having significant anti-inflammatory effects on J774 cells when stimulated with 1 μ g/ml LPS [29]. At the time points indicated, cells were collected and lysed for nuclear extracts. The nuclear extracts were analyzed by ELISA for NF- κ B activity.

The simulations mimicked the experimental conditions by introducing an HSP90 inhibitor 1 hour into simulation time followed by LPS at the 2 hour mark. We fixed the inhibitor concentration ratio at a value of 2:1 to total HSP90. The k_{5a} parameter was fixed at a value of 0.01 ($2 \times k_{1a}$) as guided by our sensitivity results. The model predicted results for NF- κ B activity in response to LPS stimulation. Predicted responses of the model with and without 17-DMAG were compared qualitatively to the experimental data (Figure 4.7A). We see that for the inhibitor:HSP90 ratio and the parameters used, the model predicts the qualitative trend for NF- κ B activation and the relative error between the experimental data and the model data supports this (Figure 4.7B). We do note that for later time points, the model appears to lose accuracy as the

experimental NF- κ B activity data begins to decrease at a higher rate than the model. We also see that the model does capture the slight increase in NF- κ B activity for the 17-DMAG set.

One explanation for the difference at the later time points is that the model parameters were estimated using data from MEF cells. Our validation data came from J774 macrophage cells. It is likely that these cell types respond differently. As more time series experimental data becomes available, it will be possible to find better estimates for the parameters to account for the more rapid decrease in NF- κ B. It is also important to note the fluctuations in NF- κ B for the HSP90 inhibited data set. As NF- κ B is sensitive to the least IKK activation, it may be that some IKKp is still being transiently activated and thereby activating NF- κ B.

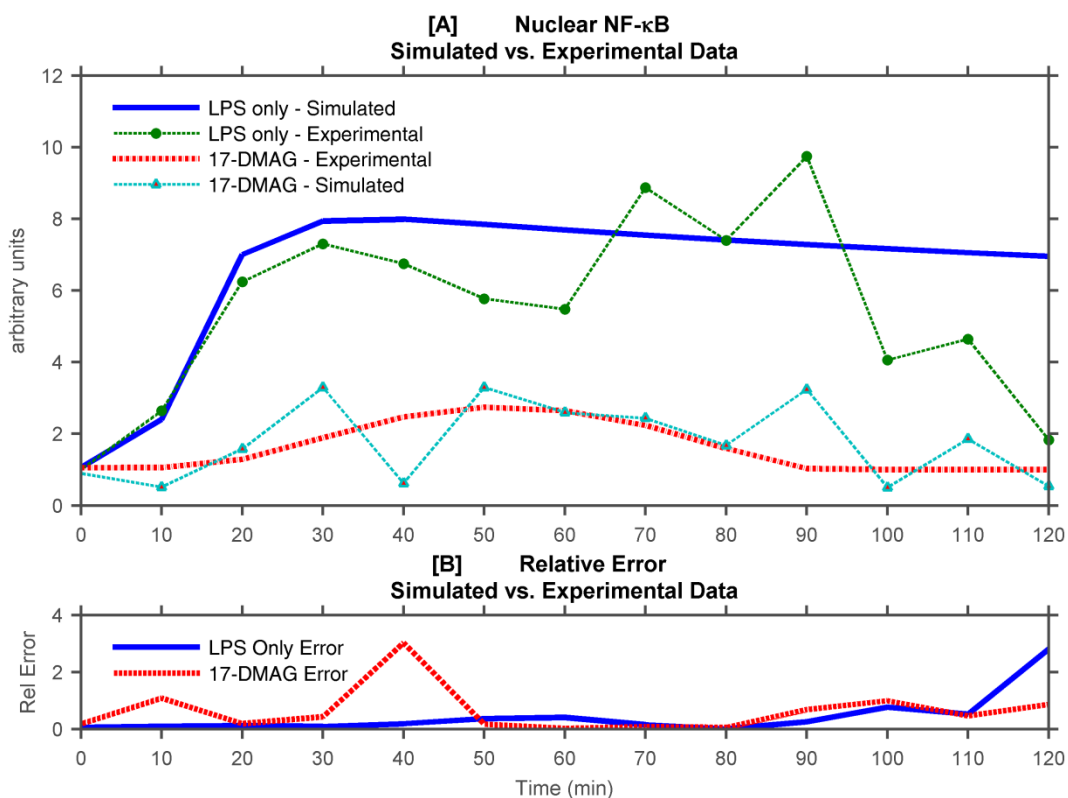


Figure 4.7. Experimental NF- κ B data supports the modeled HSP90-IKK interactions in the NF- κ B model. Experimental data was obtained by treating J774 cells with or without 17-DMAG for 1 hour followed by immune-stimulation with LPS. Samples were collected at 10 minute intervals and analyzed by ELISA for quantification of NF- κ B activity. Model was

simulated to receive 17-DMAG 1 hour before LPS. A) Simulated NF- κ B activity in response to LPS stimulation without HSP90 inhibition (solid, blue curve) and with HSP90 inhibition (dashed, red curve) are compared to experimentally measured NF- κ B activity in cells cultured without HSP90 inhibition (green circles) or with HSP90 inhibition (baby blue triangles). The NF- κ B simulation data was linearly scaled by a factor of 1.75 to facilitate qualitative comparison in figure. B) The relative error between the experimental and simulation data for LPS only (solid blue line) and for HSP90 inhibitor treated (dashed, red line) shows relative agreement between the model and the experimental data.

4.5 Conclusions

Previous models of NF- κ B included IKK activation as the input to the model and illustrated the important role of IKK activation in NF- κ B activation. In fact, the dynamic behavior of IKK activation determines the response time and magnitude of NF- κ B activity as well as the duration of the activity. NF- κ B activity can be reduced by the anti-inflammatory and pro-apoptotic HSP90 inhibitors. To explore the anti-inflammatory effects of HSP90 inhibition on NF- κ B activation, we employed the use of computational modeling techniques to predict the response of IKK activation to interference by HSP90 inhibitors and then apply that response to the downstream activity of NF- κ B. We modified an existing model by adding the reactions that describe the interactions between HSP90 and IKK.

We tested the sensitivity of the model to parameter variation and prioritized model parameters for estimation. Model parameters were successfully estimated using published data on IKKp in response to a 45-minute pulse of LPS. Model sensitivity to HSP90 inhibition parameters was also tested. We found that IKKp was sensitive to fluctuations in concentration ratio and inhibitor binding rates. We also saw that NF- κ B greatly amplified IKKp and that HSP90 inhibition did not stop the initial NF- κ B activity; it did reduce the longer term activation levels. The effect on chronic NF- κ B activity has implications in the treatment of chronic inflammatory diseases.

Future work should focus on elucidating the pathway between the TLR and IKK. It is likely that other HSP90 clients up stream of IKK are involved and contribute to the reduction in NF- κ B. It will be critical to identify any additional HSP90 clients in said pathway. Identification of the specific IKKK proteins would also allow greater fidelity in the model. Future efforts in

evaluating HSP90 inhibitors could use this model to estimate HSP90 binding rates and/or affinities.

REFERENCES

1. Ferrero-Miliani, L., et al., *Chronic inflammation: importance of NOD2 and NALP3 in interleukin-1 β generation*. *Clinical & Experimental Immunology*, 2007. **147**(2): p. 227-235.
2. Grivennikov, S.I., F.R. Greten, and M. Karin, *Immunity, Inflammation, and Cancer*. *Cell*, 2010. **140**(6): p. 883-899.
3. Hansson, G.K., *Inflammation, Atherosclerosis, and Coronary Artery Disease*. *New England Journal of Medicine*, 2005. **352**(16): p. 1685-1695.
4. Abou-Raya, A. and S. Abou-Raya, *Inflammation: a pivotal link between autoimmune diseases and atherosclerosis*. *Autoimmun Rev*, 2006. **5**(5): p. 331-7.
5. Goldbach-Mansky, R. and D.L. Kastner, *Autoinflammation: The prominent role of IL-1 in monogenic autoinflammatory diseases and implications for common illnesses*. *Journal of Allergy and Clinical Immunology*, 2009. **124**(6): p. 1141-1149.
6. Karin, M., *NF-kappaB as a critical link between inflammation and cancer*. *Cold Spring Harb Perspect Biol*, 2009. **1**(5): p. a000141.
7. Geller, D.A. and T.R. Billiar, *Molecular biology of nitric oxide synthases*. *Cancer & Metastasis Reviews*, 1998. **17**(1): p. 7-23.

8. Tas, S.W., et al., *Signal transduction pathways and transcription factors as therapeutic targets in inflammatory disease: towards innovative antirheumatic therapy*. *Curr Pharm Des*, 2005. **11**(5): p. 581-611.
9. Karin, M., Y. Yamamoto, and Q.M. Wang, *The IKK NF-kappa B system: a treasure trove for drug development*. *Nat Rev Drug Discov*, 2004. **3**(1): p. 17-26.
10. Karin, M., et al., *NF-kappaB in cancer: from innocent bystander to major culprit*. *Nat Rev Cancer*, 2002. **2**(4): p. 301-10.
11. van Loo, G. and R. Beyaert, *Negative regulation of NF-kappaB and its involvement in rheumatoid arthritis*. *Arthritis Res Ther*, 2011. **13**(3): p. 221.
12. Kurylowicz, A. and J. Nauman, *The role of nuclear factor-kappaB in the development of autoimmune diseases: a link between genes and environment*. *Acta Biochim Pol*, 2008. **55**(4): p. 629-47.
13. Hasegawa, S., et al., *Cysteine, histidine and glycine exhibit anti-inflammatory effects in human coronary arterial endothelial cells*. *Clin Exp Immunol*, 2012. **167**(2): p. 269-74.
14. Helo, S., J.P. Manger, and T.L. Krupski, *Role of denosumab in prostate cancer*. *Prostate Cancer Prostatic Dis*, 2012.

15. Gomard, T., et al., *An NF-kappaB-dependent role for JunB in the induction of proinflammatory cytokines in LPS-activated bone marrow-derived dendritic cells*. PLoS One, 2010. **5**(3): p. e9585.
16. Komives, E.A., *Consequences of fuzziness in the NFkappaB/IkappaBalpa interaction*. Adv Exp Med Biol, 2012. **725**: p. 74-85.
17. Cheong, R., et al., *Transient IkappaB kinase activity mediates temporal NF-kappaB dynamics in response to a wide range of tumor necrosis factor-alpha doses*. J Biol Chem, 2006. **281**(5): p. 2945-50.
18. Werner, S.L., D. Barken, and A. Hoffmann, *Stimulus Specificity of Gene Expression Programs Determined by Temporal Control of IKK Activity*. Science, 2005. **309**(5742): p. 1857-1861.
19. Cheong, R., A. Hoffmann, and A. Levchenko, *Understanding NF-kappaB signaling via mathematical modeling*. Mol Syst Biol, 2008. **4**: p. 192.
20. Neidle, S., ed. *Cancer Drug Design and Discovery*. 1 ed., ed. S. Neidle. 2008, Elsevier: New York, New York.
21. Blagg, B.S. and T.D. Kerr, *Hsp90 inhibitors: small molecules that transform the Hsp90 protein folding machinery into a catalyst for protein degradation*. Med Res Rev, 2006. **26**(3): p. 310-38.

22. Kone, B.C., *Protein-protein interactions controlling nitric oxide synthases*. Acta Physiologica Scandinavica, 2000. **168**(1): p. 27-31.
23. Xiao, L., X. Lu, and D.M. Ruden, *Effectiveness of hsp90 inhibitors as anti-cancer drugs*. Mini Rev Med Chem, 2006. **6**(10): p. 1137-43.
24. Pearl, L.H., *Hsp90 and Cdc37 - a chaperone cancer conspiracy*. Current Opinion in Genetics & Development, 2005. **15**(1): p. 55-61.
25. Pearl, L.H. and C. Prodromou, *Structure and mechanism of the Hsp90 molecular chaperone machinery*. Annu Rev Biochem, 2006. **75**: p. 271-94.
26. Kim, Y.S., et al., *Update on Hsp90 Inhibitors in Clinical Trial*. Curr Top Med Chem, 2009. **9**(15): p. 1479-1492.
27. Taldone, T., et al., *Targeting Hsp90: small-molecule inhibitors and their clinical development*. Curr Opin Pharmacol, 2008. **8**(4): p. 370-374.
28. Madrigal-Matute, J., et al., *Heat shock protein 90 inhibitors attenuate inflammatory responses in atherosclerosis*. Cardiovasc Res, 2010. **86**(2): p. 330-7.
29. Shimp III, S.K., et al., *HSP90 inhibition by 17-DMAG reduces inflammation in J774 macrophages through suppression of Akt and NF- κ B pathways*. Inflamm Res, 2012.

30. Basak, S., et al., *A fourth IkappaB protein within the NF-kappaB signaling module*. Cell, 2007. **128**(2): p. 369-81.
31. Covert, M.W., et al., *Achieving stability of lipopolysaccharide-induced NF-kappaB activation*. Science, 2005. **309**(5742): p. 1854-7.
32. Foteinou, P.T., et al., *Multiscale model for the assessment of autonomic dysfunction in human endotoxemia*. Physiol Genomics, 2010. **42**(1): p. 5-19.
33. Foteinou, P.T., et al., *A physiological model for autonomic heart rate regulation in human endotoxemia*. Shock, 2011. **35**(3): p. 229-39.
34. Hoffmann, A., et al., *The IkappaB-NF-kappaB signaling module: temporal control and selective gene activation*. Science, 2002. **298**(5596): p. 1241-5.
35. Ihekwaba, A.E.C., et al., *Bridging the gap between in silico and cell-based analysis of the nuclear factor- κ B signaling pathway by in vitro studies of IKK2*. FEBS Journal, 2007. **274**(7): p. 1678-1690.
36. Joo, J., et al., *Sensitivity Analysis of a Computational Model of the IKK–NF- κ B–I κ B α –A20 Signal Transduction Network*. Annals of the New York Academy of Sciences, 2007. **1115**(1): p. 221-239.

37. Kearns, J.D., et al., *I κ B ϵ provides negative feedback to control NF- κ B oscillations, signaling dynamics, and inflammatory gene expression*. The Journal of Cell Biology, 2006. **173**(5): p. 659-664.
38. Lipniacki, T., et al., *Mathematical model of NF-kappaB regulatory module*. J Theor Biol, 2004. **228**(2): p. 195-215.
39. Lipniacki, T., et al., *Stochastic regulation in early immune response*. Biophys J, 2006. **90**(3): p. 725-42.
40. Lipniacki, T., et al., *Single TNFalpha trimers mediating NF-kappaB activation: stochastic robustness of NF-kappaB signaling*. BMC Bioinformatics, 2007. **8**: p. 376.
41. Moss, B.L., et al., *Identification of a ligand-induced transient refractory period in nuclear factor-kappaB signaling*. J Biol Chem, 2008. **283**(13): p. 8687-98.
42. Nelson, D.E., et al., *Oscillations in NF-kappaB signaling control the dynamics of gene expression*. Science, 2004. **306**(5696): p. 704-8.
43. O'Dea, E.L., et al., *A homeostatic model of IkappaB metabolism to control constitutive NF-kappaB activity*. Mol Syst Biol, 2007. **3**: p. 111.

44. Park, S.G., et al., *The influence of the signal dynamics of activated form of IKK on NF-kappaB and anti-apoptotic gene expressions: a systems biology approach*. FEBS Lett, 2006. **580**(3): p. 822-30.
45. Broemer, M., D. Krappmann, and C. Scheidereit, *Requirement of Hsp90 activity for I[kappa]B kinase (IKK) biosynthesis and for constitutive and inducible IKK and NF-[kappa]B activation*. Oncogene, 2004. **23**(31): p. 5378-5386.
46. Hinz, M., et al., *Signal Responsiveness of Ikb Kinases Is Determined by Cdc37-assisted Transient Interaction with Hsp90*. Journal of Biological Chemistry, 2007. **282**(44): p. 32311-32319.
47. Chen, G., P. Cao, and D.V. Goeddel, *TNF-Induced Recruitment and Activation of the IKK Complex Require Cdc37 and Hsp90*. Molecular Cell, 2002. **9**(2): p. 401-410.
48. Sato, S., N. Fujita, and T. Tsuruo, *Modulation of Akt kinase activity by binding to Hsp90*. Proc Natl Acad Sci U S A, 2000. **97**(20): p. 10832-7.
49. Zhang, L., et al., *Gambogic acid inhibits Hsp90 and deregulates TNF-alpha/NF-kappaB in HeLa cells*. Biochem Biophys Res Commun, 2010. **403**(3-4): p. 282-7.
50. Li, D., *Selective degradation of the I[kappa]B kinase (IKK) by autophagy*. Cell Res, 2006. **16**(11): p. 855-856.

51. Lee, K.H., Y. Jang, and J.H. Chung, *Heat shock protein 90 regulates IkappaB kinase complex and NF-kappaB activation in angiotensin II-induced cardiac cell hypertrophy*. *Exp Mol Med*, 2010. **42**(10): p. 703-11.
52. Qing, G., P. Yan, and G. Xiao, *Hsp90 inhibition results in autophagy-mediated proteasome-independent degradation of I[kappa]B kinase (IKK)*. *Cell Res*, 2006. **16**(11): p. 895-901.
53. Shimp III, S.K., et al., *Heat shock protein 90 inhibition by 17-DMAG lessens disease in the MRL/lpr mouse model of systemic lupus erythematosus*, in *Cell Mol Immunol*. In Press.
54. Kamal, A., et al., *A high-affinity conformation of Hsp90 confers tumour selectivity on Hsp90 inhibitors*. *Nature*, 2003. **425**(6956): p. 407-10.
55. Karkoulis, P.K., et al., *17-Allylamino-17-demethoxygeldanamycin induces downregulation of critical Hsp90 protein clients and results in cell cycle arrest and apoptosis of human urinary bladder cancer cells*. *BMC Cancer*, 2010. **10**: p. 481.
56. Wieten, L., et al., *Cell stress induced HSP are targets of regulatory T cells: A role for HSP inducing compounds as anti-inflammatory immuno-modulators?* *FEBS Lett*, 2007. **581**(19): p. 3716-3722.

CHAPTER 5.

SUMMARY AND FUTURE WORK

5.1 Conclusions

The inflammatory response can be a lifesaving process as it enables the body to respond rapidly and decisively to foreign pathogens and tissue damage. Some disease models have shown that quick and decisive response is the only way to contain the most serious of epidemics [1]. Yet if that quick and decisive mechanism becomes unbalanced, the process can become life threatening. In extreme cases, such as septic shock, the inflammatory response is so extremely out of control that organs simply fail [2]. In less extreme cases, chronic inflammation contributes to and amplifies disease pathogenesis of atherosclerosis, cancer, and autoimmunity [3-5]. The studies presented in this work contribute to the understanding of the regulation of inflammation and inflammatory signaling within the cell and should be applied to the development of therapies to treat chronic and unregulated inflammation.

5.1.1 What we learned about HSP90 and inflammation from in vitro studies

In the *in vitro* study of HSP90 inhibition, it was shown that inhibiting HSP90 with 17-DMAG reduced inflammation by disrupting the Akt/NF- κ B pathway. Investigating for mechanistic explanations for the reduction in cytokines and inflammatory mediators, it was found that in the presence of HSP90 inhibitors for 24 hours or more, Akt and IKK expression were reduced in the J774 cells. In addition, it was also shown in the results that nuclear translocation of NF- κ B was reduced. It was inferred from this data that the reduction in NF- κ B activity resulted in the diminished expression of IL-6 and NO. One hour pre-treatment, with a relatively low dose of 0.1 μ M 17-DMAG showed reduced Akt activation but had limited effect on I κ B phosphorylation.

Looking to the computational model for answers, it can be seen that I κ B phosphorylation is highly sensitive to even the smallest level of IKK activation. The parameter sensitivity studies for the HSP90 inhibitor showed a strong dependence on high concentrations of 17-DMAG in order to sufficiently block I κ B phosphorylation. Therefore, it is likely that with a higher concentration of 17-DMAG the I κ B phosphorylation would be significantly reduced.

Despite the fact that 0.1 μ M 17-DMAG had little effect on I κ B activity, it was shown that this concentration still reduced production of the pro-inflammatory mediators IL-6, TNF- α , and NO. It was interesting that iNOS protein levels in stimulated cells were unaffected. At the time of publication of this manuscript the lack of an effect on iNOS was attributed to be due to crosstalk between other pathways such as the JAK/STAT pathway as the JAK/STAT pathway plays an important role in iNOS transcription. In light of more recent modeling studies showing that HSP90 inhibition does not block the NF- κ B activity, only reduce its long term activation, it must also be considered that the lack of an effect on iNOS transcription may be due to insufficient treatment concentration. Perhaps this warrants further *in vitro* study in which higher HSP90 inhibitor concentrations are used, or perhaps an inhibitor with a larger binding rate could be used.

5.1.2 How does HSP90 affect inflammation and autoimmunity in an *in vivo* model?

The effect of HSP90 inhibition in the MRL/lpr lupus mouse model was studied. Typical markers for disease severity and pathology were assessed to determine if HSP90 inhibition would reduce disease in the mouse. Splenocytes and serum were examined for clues to mechanistic explanations for any measured effects. *In vitro* tests of HSP90 inhibition in mesangial cells resulted in reduced expression of the key lupus cytokines IL-6, IL-12, and the mediator NO. Inhibition of HSP90 in the MRL/lpr mouse decreased proteinuria. Spleens from the 17-DMAG treated mice were smaller, suggesting an attenuation of splenomegaly as a result of the HSP90

inhibition. But, HSP90 inhibition did not affect renal histopathology or C3 and IgG deposition. It is interesting to find from immunofluorescence staining that HSP90 was upregulated in the renal tubules of diseased MRL/lpr mice. Immunofluorescence staining for HSP70 expression in the kidneys showed that HSP70 was downregulated in both the MRL/lpr control and 17-DMAG MRL/lpr mice, as compared to C57BL/6 mice kidneys. Data showed that anti-dsDNA decreased within the 17-DMAG treatment group. It was also found that with 17-DMAG treatment, DNT cells were down-regulated while CD8⁺ T cells were upregulated. Some effects were also observed in T_{REG} cells which express high levels of HSP90.

5.2 Future Work

5.2.1 Revisiting in vitro work to validate the current model and extend it to include cytokine production

It was mentioned above that a testing higher concentrations of HSP90 inhibitors to and measuring the response of I κ B phosphorylation would be beneficial. If these experiments were repeated, they would confirm what the computational model shows, that a concentration of HSP90 inhibitor greater than 0.1 μ M 17-DMAG, or a more potent inhibitor than 17-DMAG, would have a significant effect in the reduction of I κ B phosphorylation. This work could be further extended by measuring how cytokine mRNA levels would be altered by treatment with 17-DMAG. Experiments should be conducted in which mRNA expression and NF- κ B activation are each measured at discrete time points following LPS and/or TNF- α stimulation. This time-domain data would then be used to develop modeling equations that would be implemented in the existing NF- κ B model. The benefit of extending the model beyond NF- κ B activation into the

realm of transcription and translation, is that the effects of autocrine signaling could then be addressed.

5.2.2 Studying the effects of HSP70 on inflammation

The exciting results of the *in vitro* study opened up additional questions. Future efforts should examine how HSP70 expression affects pro-inflammatory cascades. Interest in HSP70 and inflammation comes for the following reasons. It has been shown that extracellular HSP70 is a ligand for TLR2 and TLR4 activation. Second, HSP70 activation of the TLR4 ligand on CD4⁺ CD25⁺ T cells is attributed to an increase in suppressive activity of these T cells in atherosclerosis [6, 7]. Furthermore, HSP70 has been indicated to have a negative feedback effect on NF- κ B signaling activity [8]. HSP70 has also been demonstrated to switch off TNF receptor-associated factor 6 (TRAF6) [9]. And finally, increased HSP70 suppresses iNOS activity [10]. These studies would be conducted with the use of siRNA for HSP70 downregulation or over-expression vectors to artificially increase HSP70 expression. With HSP70 regulated such, the cells would be analyzed for the response of NF- κ B activity, iNOS expression, upregulation of TNF- α , IL-6, and NO production. Given the negative feedback effect that HSP70 may have on NF- κ B signaling, it would be valuable to develop some modeling equations to describe the possible mechanistic interactions, and then test the model in parallel with the experiments to validate the mechanistic hypotheses.

5.2.3 Linking HSP90 to T cell activation

Given the interesting results of the splenocyte profiles in the *in vivo* study, work should be done to determine the mechanisms that link HSP90 to T cell activation and T_{REG} suppressive potency. Considering the interesting results of [11], it would be worth the effort to explore how

HSP90 inhibition affects T_{regs} and how HSP90 may be linked to histone deacetylases. Based on the results of the modeling study, targeting HSP90 to reduce chronic activation of inflammatory signals may be an effective treatment for SLE. Exploration of T cells and T_{regs} would aid in understanding how the HSP90 inhibitors would alter T cell populations.

5.2.4 Other potential research directions

Several other ideas that may warrant future studies include the exploration of the NF- κ B pathway upstream of IKK. This would enhance the model by accounting for any HSP90 interactions with other proteins. The model would also be enhanced by experimentally determining HSP90 binding parameters, obtained from measurement of HSP90 IKK binding affinity with and without an HSP90 inhibitor. This may be achieved by immune precipitation. The author is unaware of any NF- κ B models that incorporate cross-talk with other signal pathways. This could be achieved by exploring the JAK/Stat pathway in the presence of HSP90 inhibitor and developing models to describe the interactions.

5.3 Final Remarks

Taking the results of the entire body of work together, HSP90 may be a worthy therapeutic target for combating chronic inflammation. The challenge is that HSP90 presents itself as a regulator of many complex cellular mechanisms and parsing out the role of HSP90 is complicated. Inhibiting HSP90 in any therapeutic application will have far reaching consequences. Part of the complexity is that HSP90 can be both beneficial and detrimental to cellular function. As the computational models improve, the picture of HSP90 and its role in the cell will likely become clearer and enable the development of therapeutics that target HSP90 for suppression or perhaps even utilize HSP90 for enhancing other therapeutics.

REFERENCES

1. Munz, P., et al., *When Zombies Attack!: Mathematical Modelling of an Outbreak of Zombie Infection*, in *Infectious Disease Modelling Research Progress*, J.M. Tchenche and C. Chiyaka, Editors. 2009, Nova Publishers. p. 133-150.
2. Nguyen, H.B., et al., *Severe Sepsis and Septic Shock: Review of the Literature and Emergency Department Management Guidelines*. *Annals of Emergency Medicine*, 2006. **48**(1): p. 54.e1.
3. Grivennikov, S.I., F.R. Greten, and M. Karin, *Immunity, Inflammation, and Cancer*. *Cell*, 2010. **140**(6): p. 883-899.
4. Hansson, G.K., *Inflammation, Atherosclerosis, and Coronary Artery Disease*. *New England Journal of Medicine*, 2005. **352**(16): p. 1685-1695.
5. Abou-Raya, A. and S. Abou-Raya, *Inflammation: a pivotal link between autoimmune diseases and atherosclerosis*. *Autoimmun Rev*, 2006. **5**(5): p. 331-7.
6. Dasu, M.R., et al., *Increased Toll-Like Receptor (TLR) Activation and TLR Ligands in Recently Diagnosed Type 2 Diabetic Subjects*. *Diabetes Care*, 2010. **33**(4): p. 861-868.
7. Pockley, A.G., S.K. Calderwood, and G. Multhoff, *The atheroprotective properties of Hsp70: a role for Hsp70-endothelial interactions?* *Cell Stress Chaperones*, 2009. **14**(6): p. 545-53.

8. de Jong, P.R., et al., *Hsp70 and cardiac surgery: molecular chaperone and inflammatory regulator with compartmentalized effects*. *Cell Stress Chaperones*, 2009. **14**(2): p. 117-31.
9. Chen, H., et al., *Hsp70 inhibits lipopolysaccharide-induced NF-kappaB activation by interacting with TRAF6 and inhibiting its ubiquitination*. *FEBS Lett*, 2006. **580**(13): p. 3145-52.
10. Kiang, J.G., J.T. Smith, and N.G. Agravante, *Geldanamycin Analog 17-DMAG Inhibits iNOS and Caspases in Gamma-Irradiated Human T Cells*. *Rad Res*, 2009. **172**(3): p. 321-330.
11. de Zoeten, E.F., et al., *Histone Deacetylase 6 and Heat Shock Protein 90 Control the Functions of Foxp3+ T-Regulatory Cells*. *Mol. Cell. Biol.*, 2011. **31**(10): p. 2066-2078.

APPENDICES

Appendix A. Development of Total IgG ELISA for analyzing mouse serum

Results

For a range of standards as high as 100 ng/ml down to 1.5625 ng/ml, it was found that detection antibody dilution of 1:16000 or greater was sufficient produce non-saturated O.D. data.

Figure A.1 shows the resulting O.D. data for the standard curve tested.

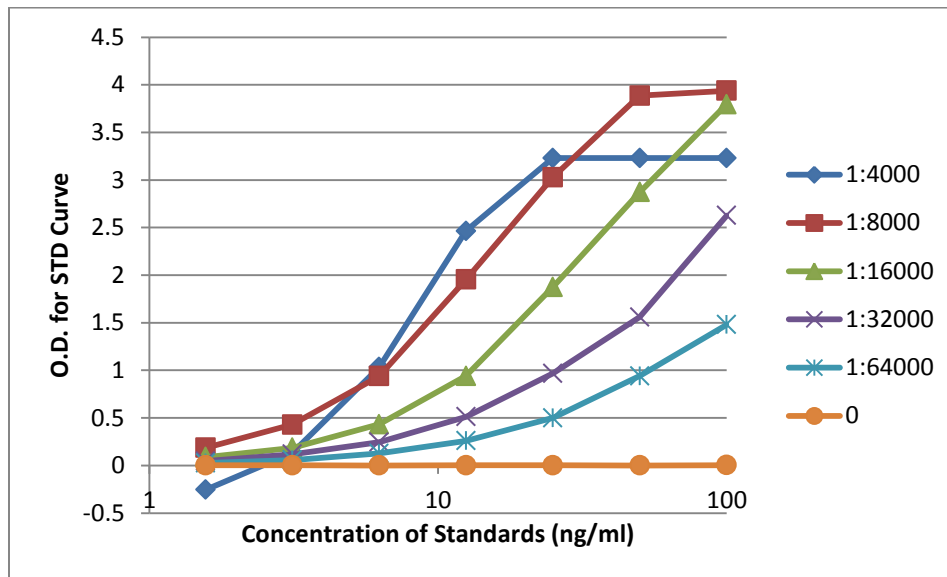


Figure A.1 - Detection Antibody dilutions were tested at several concentrations of known standards. Data shows that 1:4000 and 1:8000 had high levels of saturation for the range of detection antibody tested.

For mouse serum, a dilution of 1:10000 to 1:64000 produced the best results when detected with detection antibody diluted 1:32000 or higher. The 1:32000 dilution of detection AB produced some saturation, but it also produced a very low O.D. value for the highest serum concentration Figure A.2. This data was obtained using serum from an untreated MRL/LPR mouse whose other indications for lupus were severe.

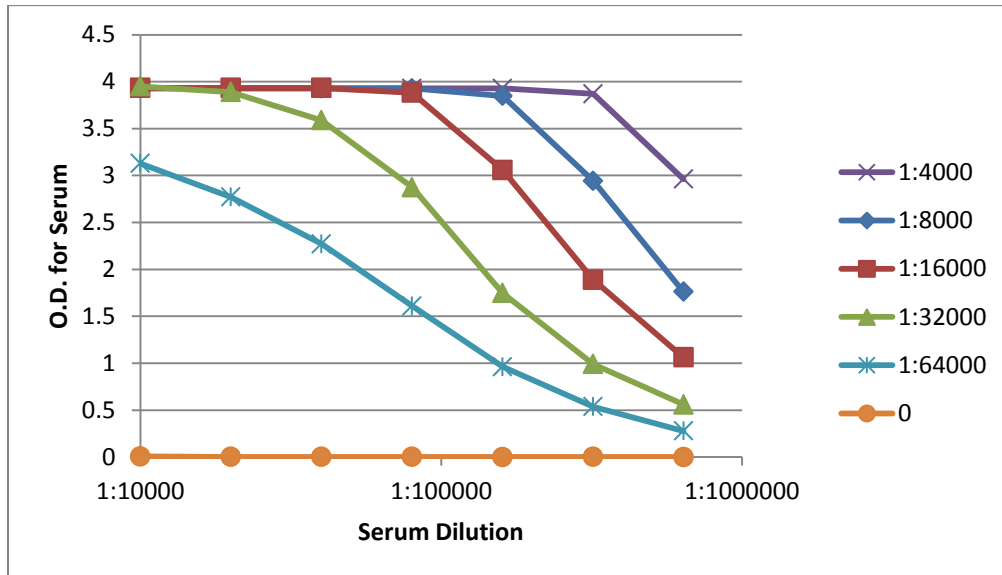


Figure A.2 Detection antibody dilutions were tested at several dilutions of serum taken from an MRL/LPR control mouse. An optimum range of serum and detection antibody can be determined from this data.

Table A.1 Serum optimization layout.

| | 1 | 2 | 3 | 4 | 5 | 6 | 7 | 8 | 9 | 10 | 11 | 12 |
|----------|-------------|--|---|---------|---------|---|---------|---------------|---------|---|---------|----|
| Det AB | 1:4000 | 1:8000 | 1:16000 | 1:32000 | 1:64000 | 0 | 1:4000 | 1:8000 | 1:16000 | 1:32000 | 1:64000 | 0 |
| A | 100 ng/ml | 1:2 Dilutions: Start with 250µl stock at top, and 125µl diluent in the others. | | | | | 1:10000 | R3-5 Endpoint | | | | |
| B | 50 ng/ml | 125ul | Stock Dilution: 5mg/ml Dilute 1:500 (10ul in 5ml) => 10ug/ml Dilute again 1:100 (10ul in 1ml) => 100ng/ml | | | | | 1:20000 | 125ul | 1:2 Dilutions: Start with 250µl stock at top and 125 diluent in the others. | | |
| C | 25 ng/ml | 125ul | | | | | | 1:40000 | 125ul | Dilute 1:10000 (2ul in 20ml) and use this to create top | | |
| D | 12.5 ng/ml | 125ul | | | | | | 1:80000 | 125ul | | | |
| E | 6.25 ng/ml | 125ul | | | | | | 1:160000 | 125ul | | | |
| F | 3.125 ng/ml | 125ul | | | | | | 1:320000 | 125ul | | | |
| G | 15625 ng/ml | 125ul | | | | | | 1:640000 | 125ul | | | |
| H | 0 ng/ml | | | | | | | 1:1280000 | 125ul | | | |

Conclusions

Based on the optimization performed, Serum dilution from 1:10000 and higher, combined with a secondary dilution of 1:32000 worked well. Because of the strong, readable signal, it must be assumed that the previous, low signal error must be the result of an incorrect dilution of capture or detection antibody. It is most likely that capture antibody was diluted incorrectly. As for the saturated signal, this data shows that the serum and detection antibody dilutions were too strong.

For the official protocol I will use the following concentrations and dilutions:

- Capture: 1 $\mu\text{g/ml}$
- Serum: Will be serial diluted 1:2 starting at 1:10000 and increasing dilution to 1:1280000
- Standard Curve: Will be serial diluted 1:2 starting at 500 ng/ml and decreasing in concentration to 7.8125 ng/ml.
- Detection antibody will be diluted 1:30000.
- All incubation times will be kept as is, and serum will be prepared/diluted prior to the beginning of the blocking step so as not to overblock the plate.

Appendix B. Complete Model Response for Initial Parameter Sensitivity Study

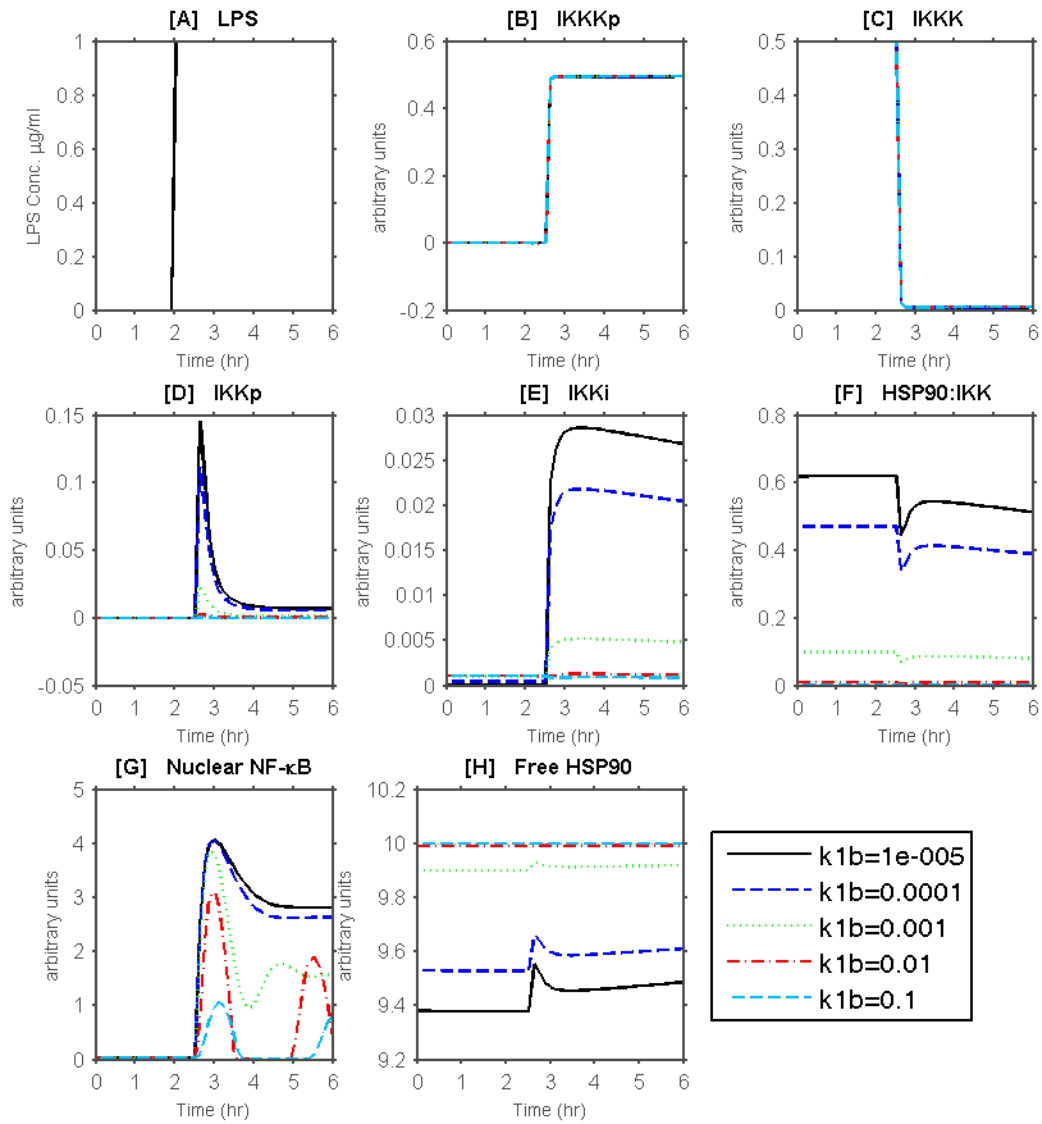


Figure B.1 Response of model when k_{1b} is varied (Part 1 of 2).

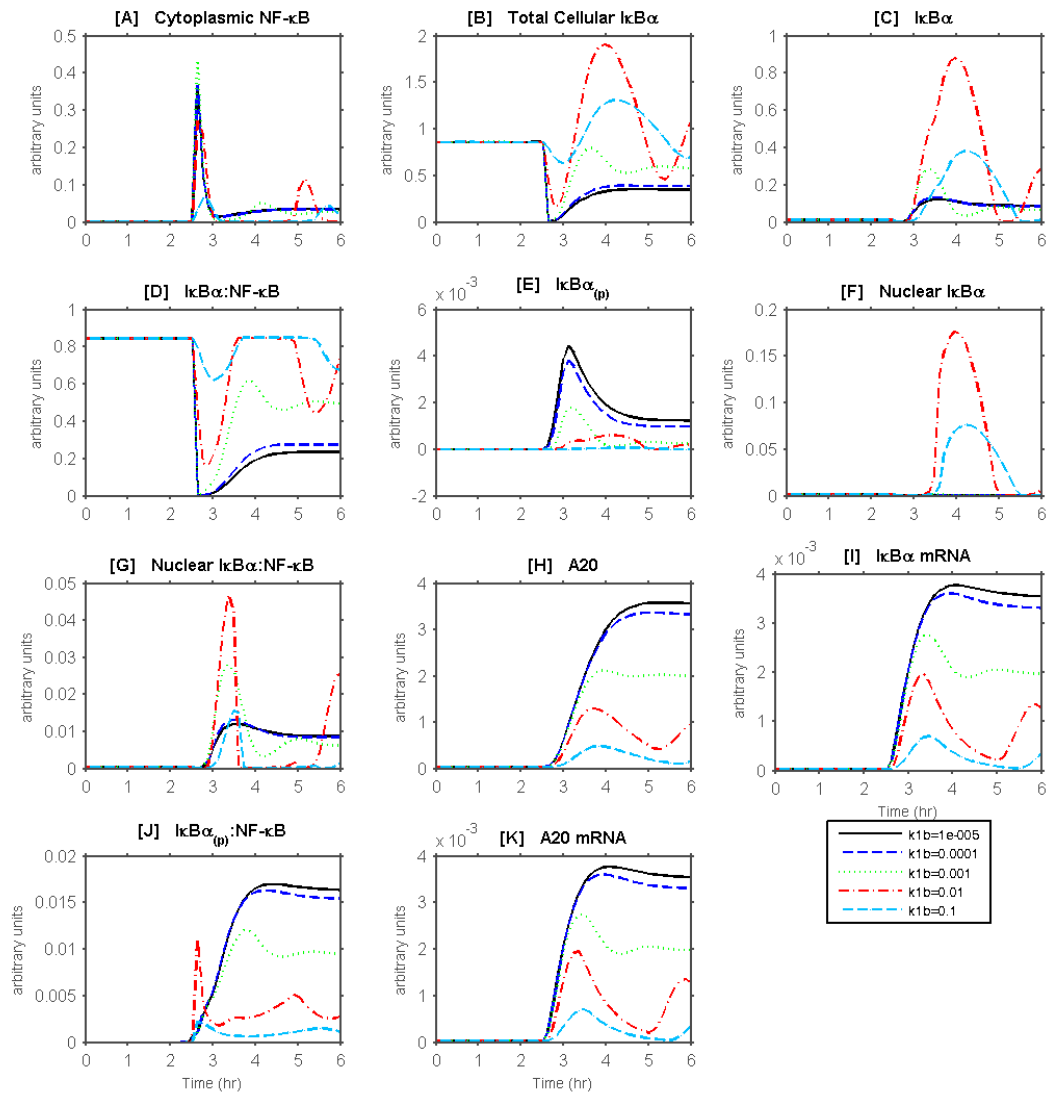


Figure B.2 Response of model when k_{1b} is varied (Part 2 of 2).

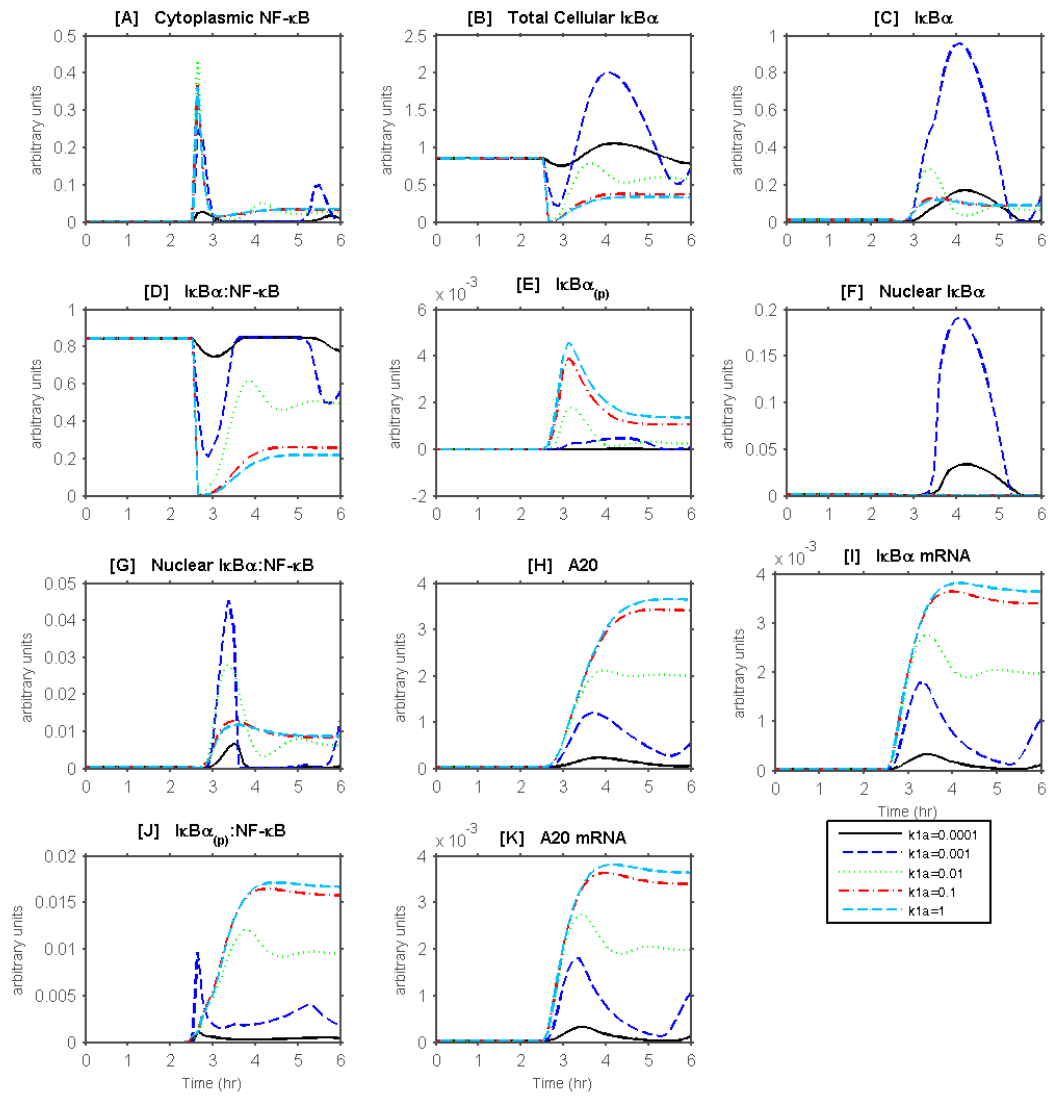


Figure B.3 Response of model when k_{1a} is varied.

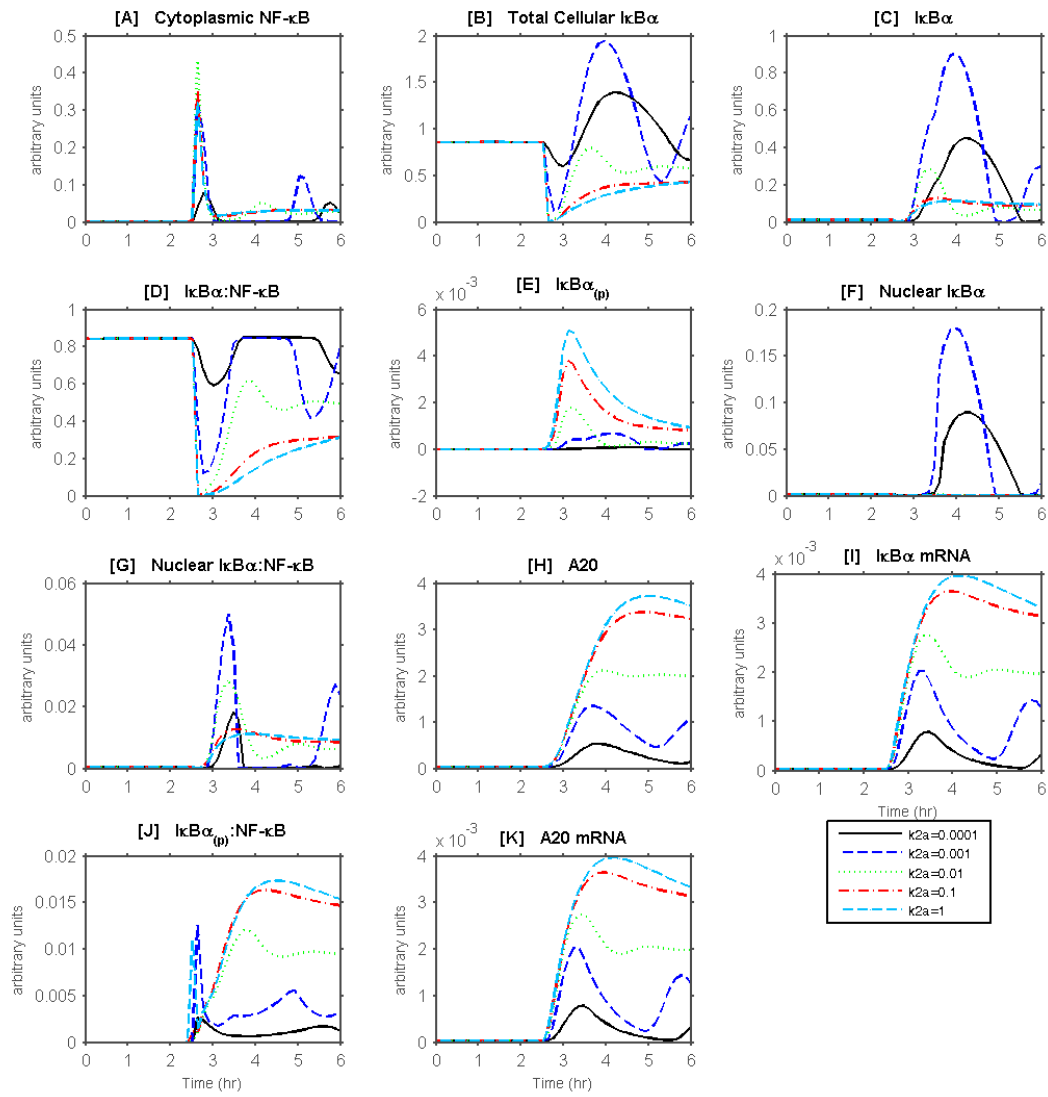


Figure B.4 Response of model when k_{2a} is varied.

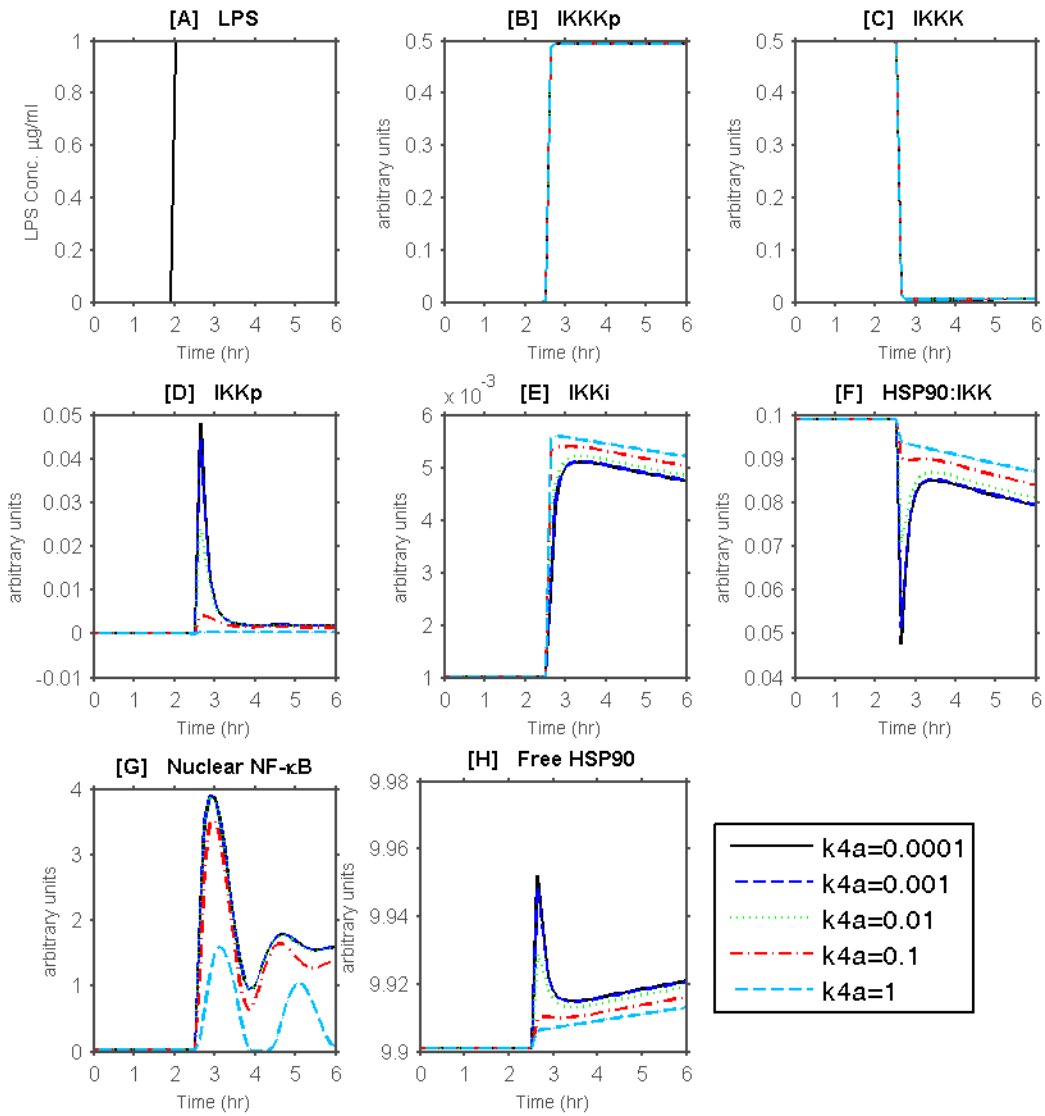


Figure B.5 Response of model when k_{4a} is varied (Part 1 of 2).

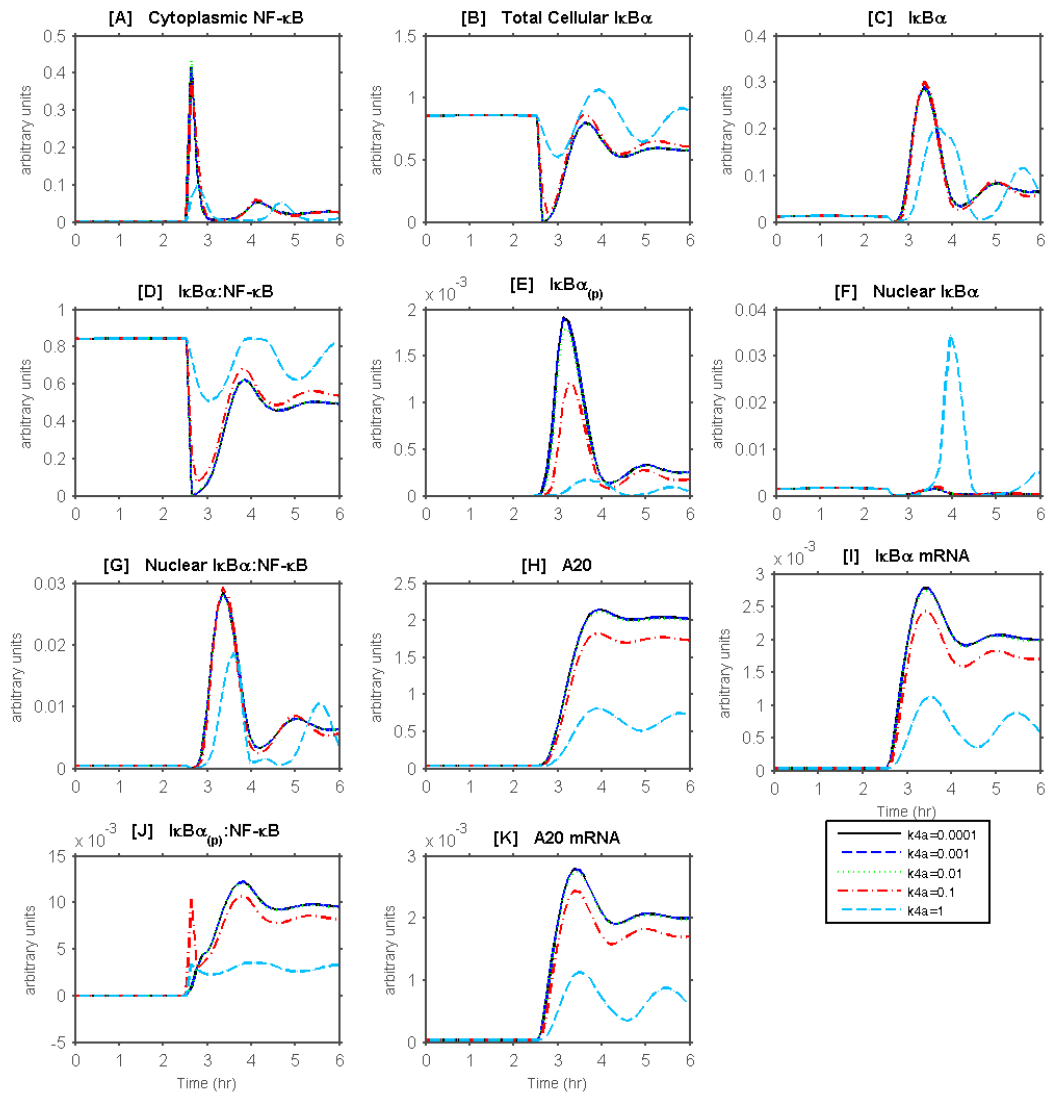


Figure B.6 Response of model when k_{4a} is varied (Part 2 of 2).

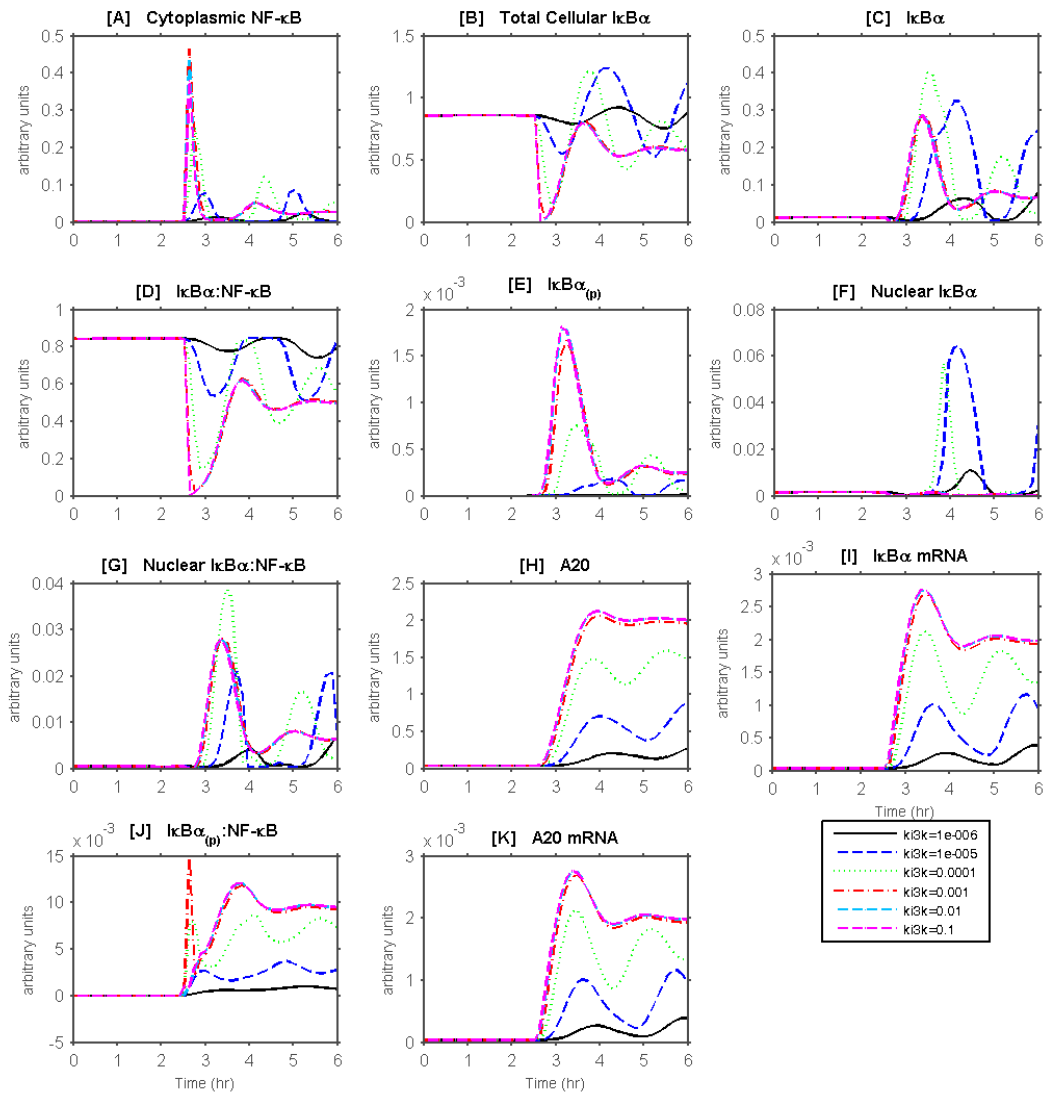


Figure B.7 Response of model when $ki3k$ is varied.

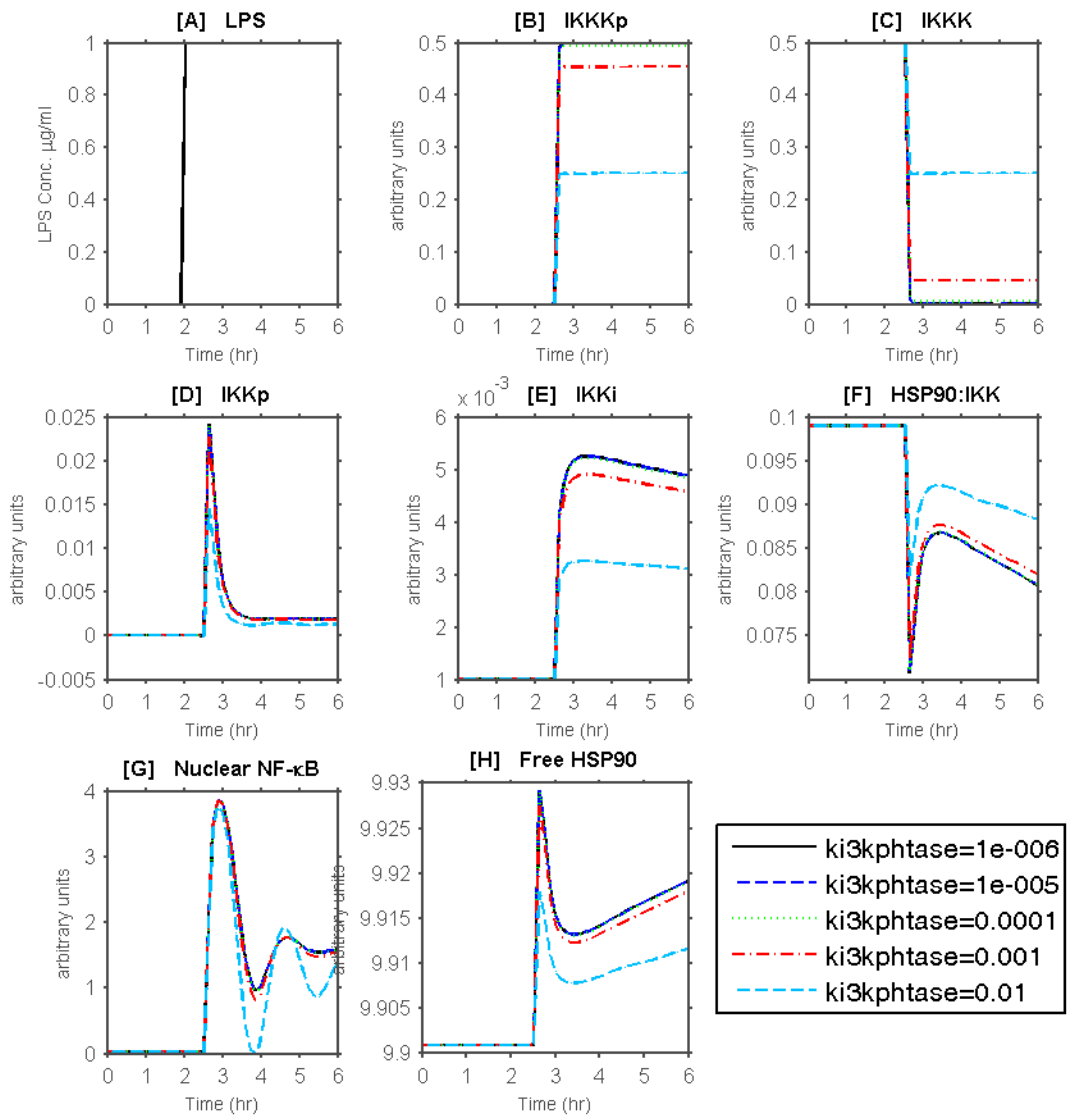


Figure B.8 Response of model when $ki3kphtase$ is varied (Part 1 of 2).

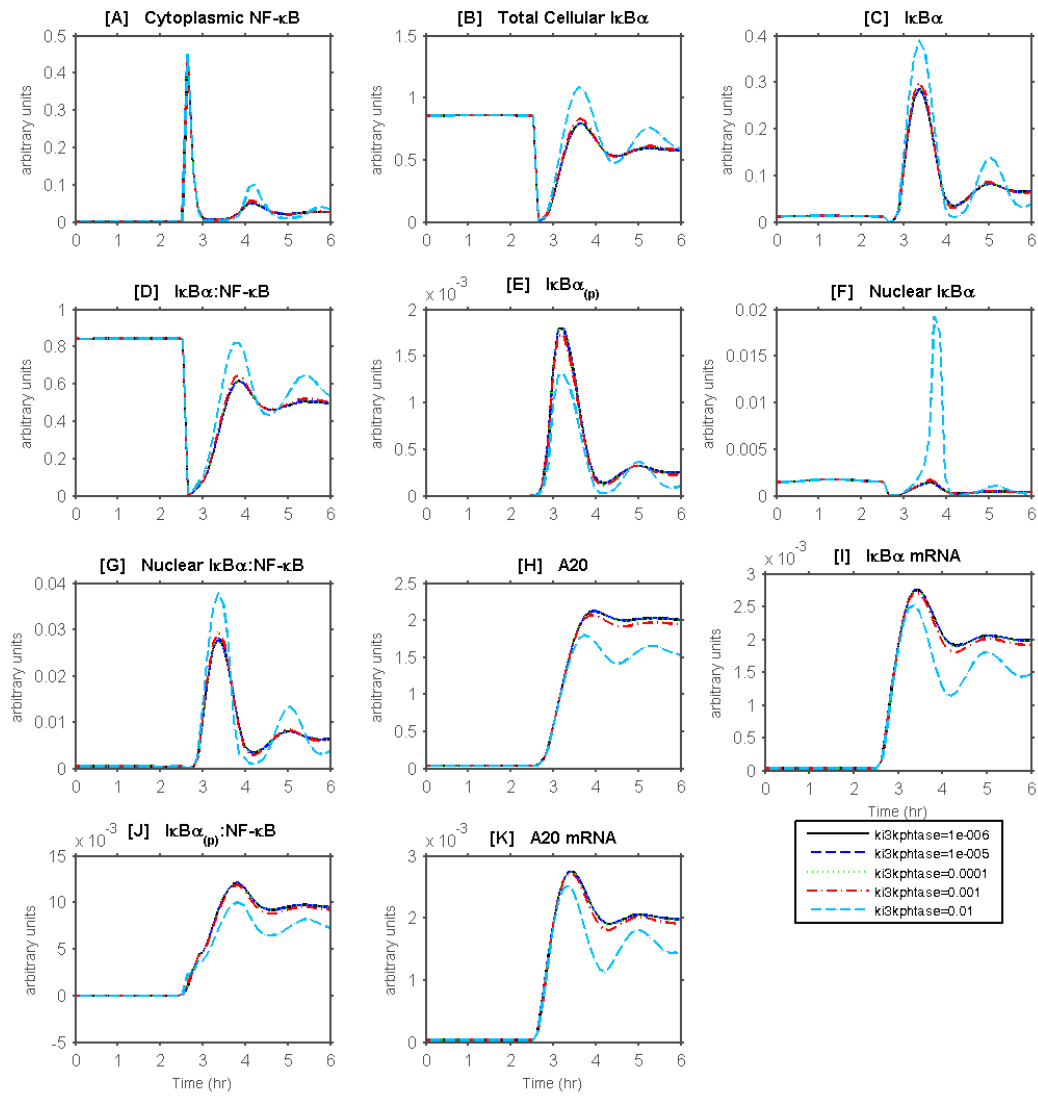


Figure B.9 Response of model when $ki3kptase$ is varied (Part 2 of 2).

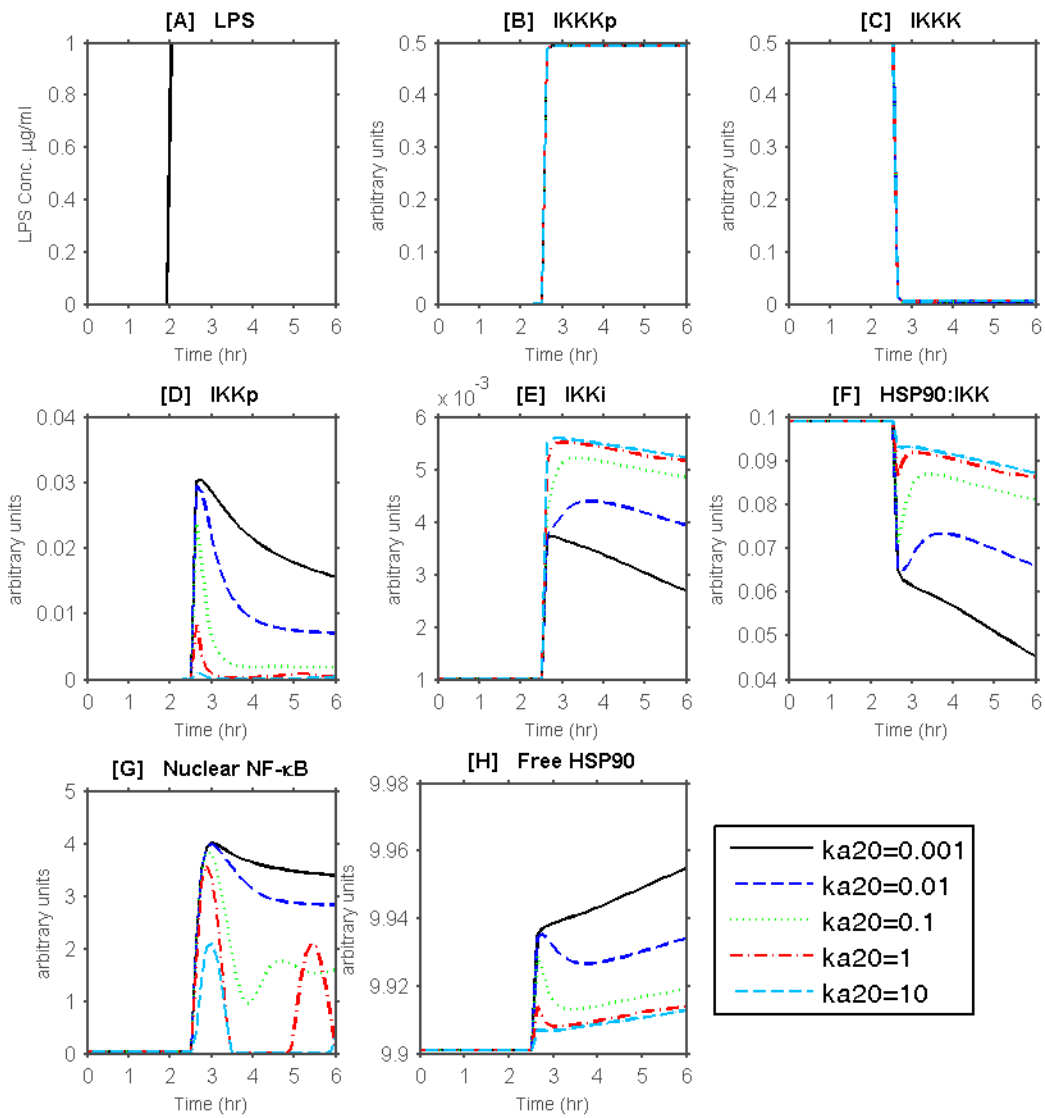


Figure B.10 Response of model when k_{a20} is varied (Part 1 of 2).

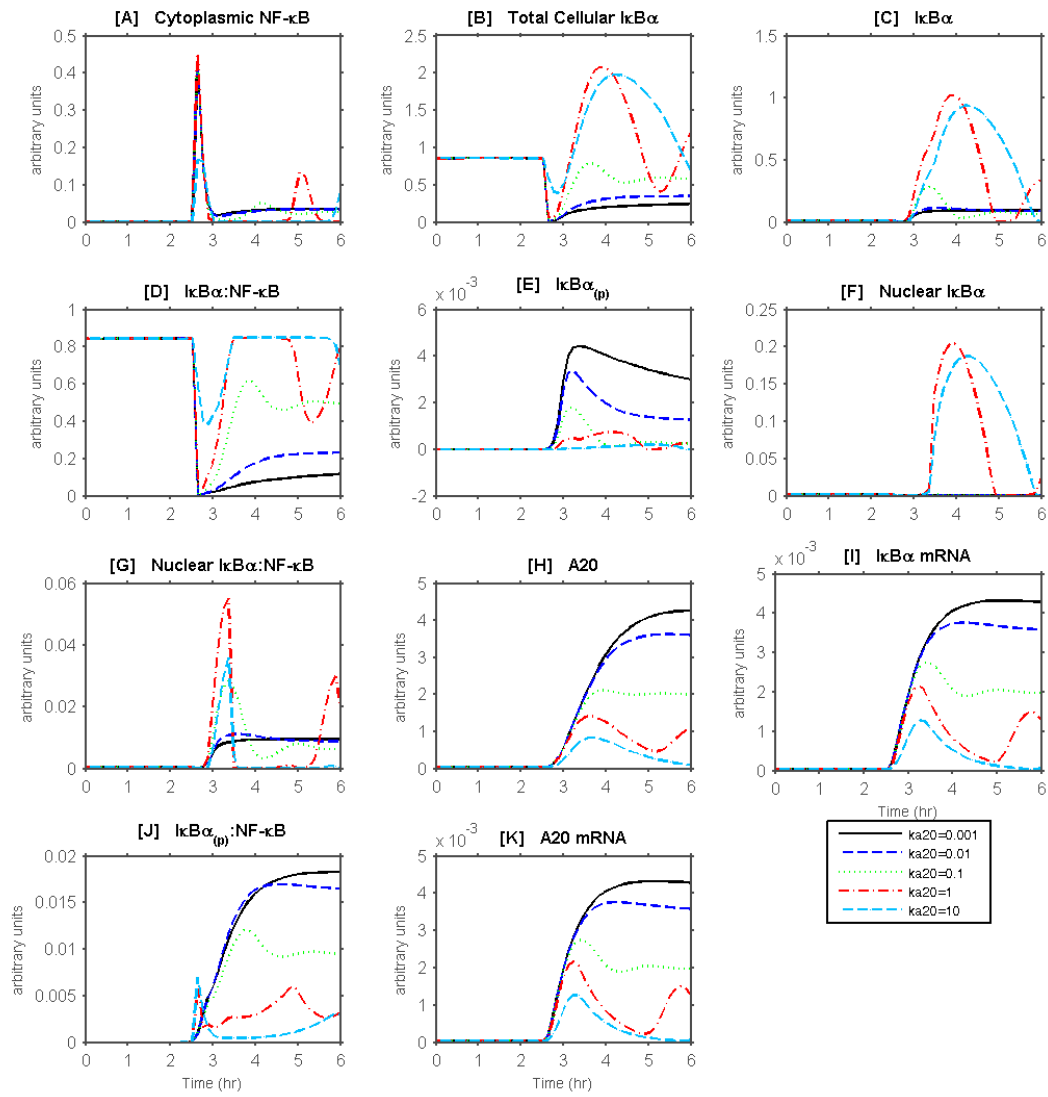


Figure B.11 Response of model when k_{a20} is varied (Part 2 of 2).

Appendix C. Complete Model Response for HSP90 Inhibitor Parametric Study

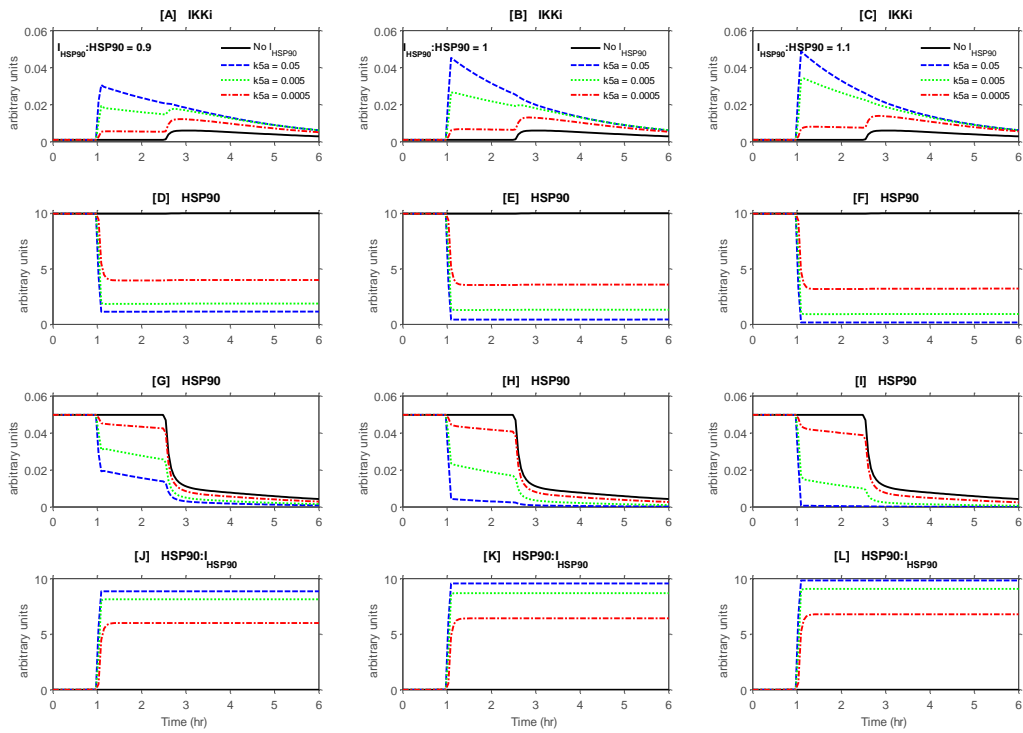


Figure C.1 Response of model to variations in HSP90 inhibitor parameters. A-C) IKKi. D-F) HSP90. G-I) HSP90_IKK. J-L) HSP90_IHSP90.

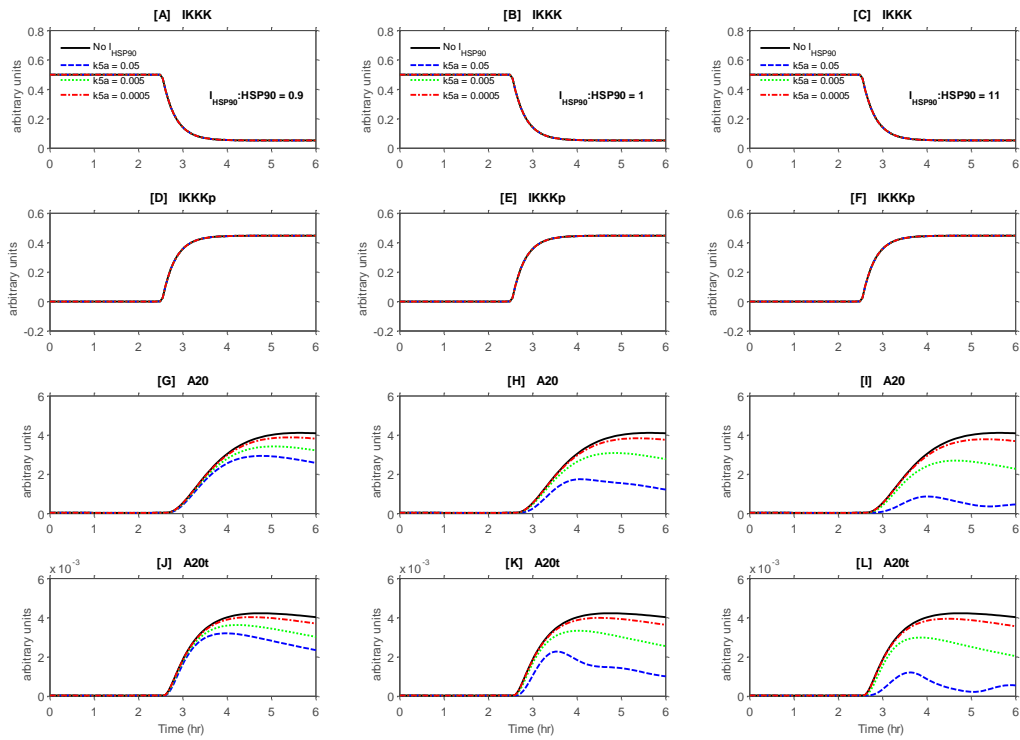


Figure C.2 Response of model to variations in HSP90 inhibitor parameters. A-C) IKKK. D-F) IKKKp. G-I) A20 protein. J-L) A20 mRNA.

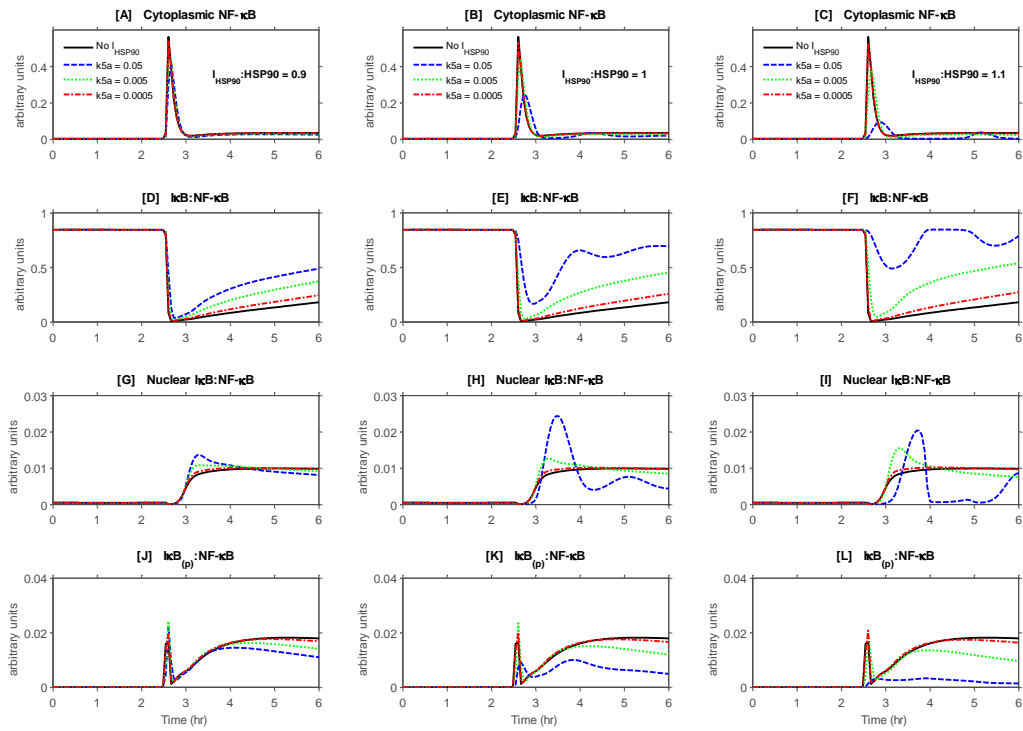


Figure C.3 Response of model to variations in HSP90 inhibitor parameters. A-C) Cytoplasmic NF- κ B. D-F) I κ B-NF κ B. G-I) Nuclear I κ B-NF κ B. J-L) I κ B_p-NF κ B.

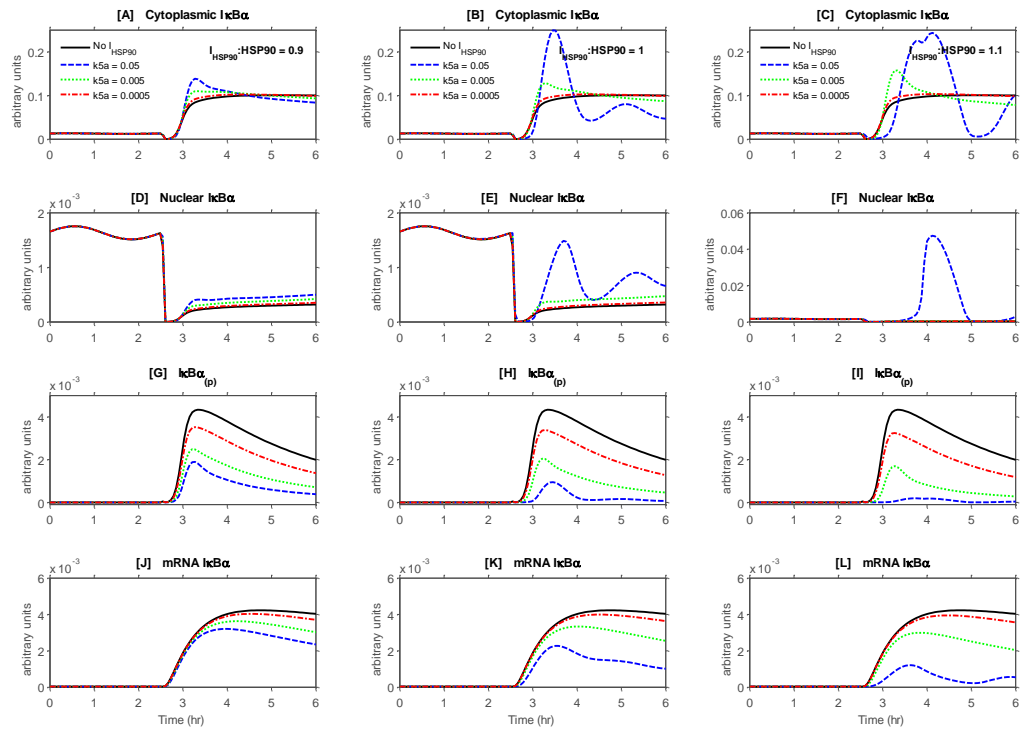


Figure C.4 Response of model to variations in HSP90 inhibitor parameters. A-C) Cytoplasmic IκB. D-F) Nuclear IκB. G-I) IκBp. J-L) IκB mRNA.

Appendix D. Complete Model Response for Validation Study

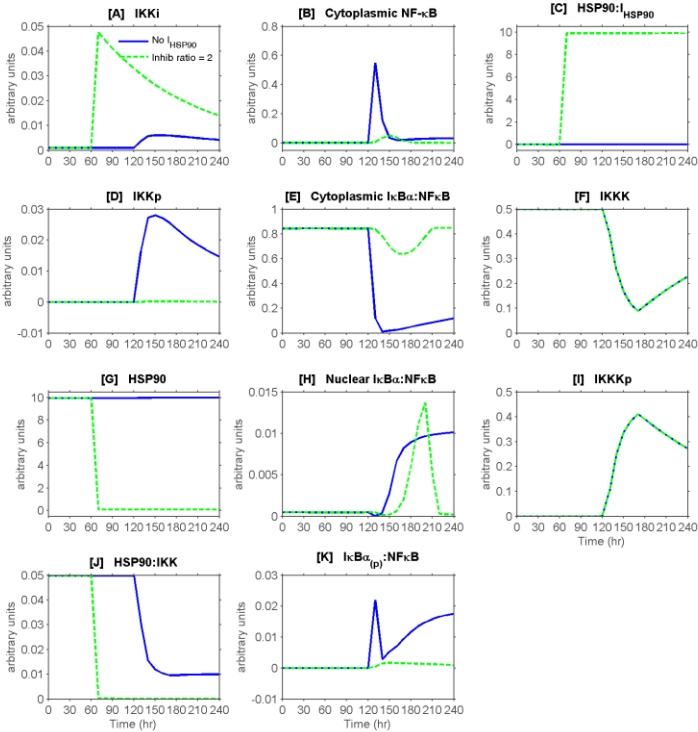


Figure D.1 Complete response of model for validation simulations (Part 1 of 2).

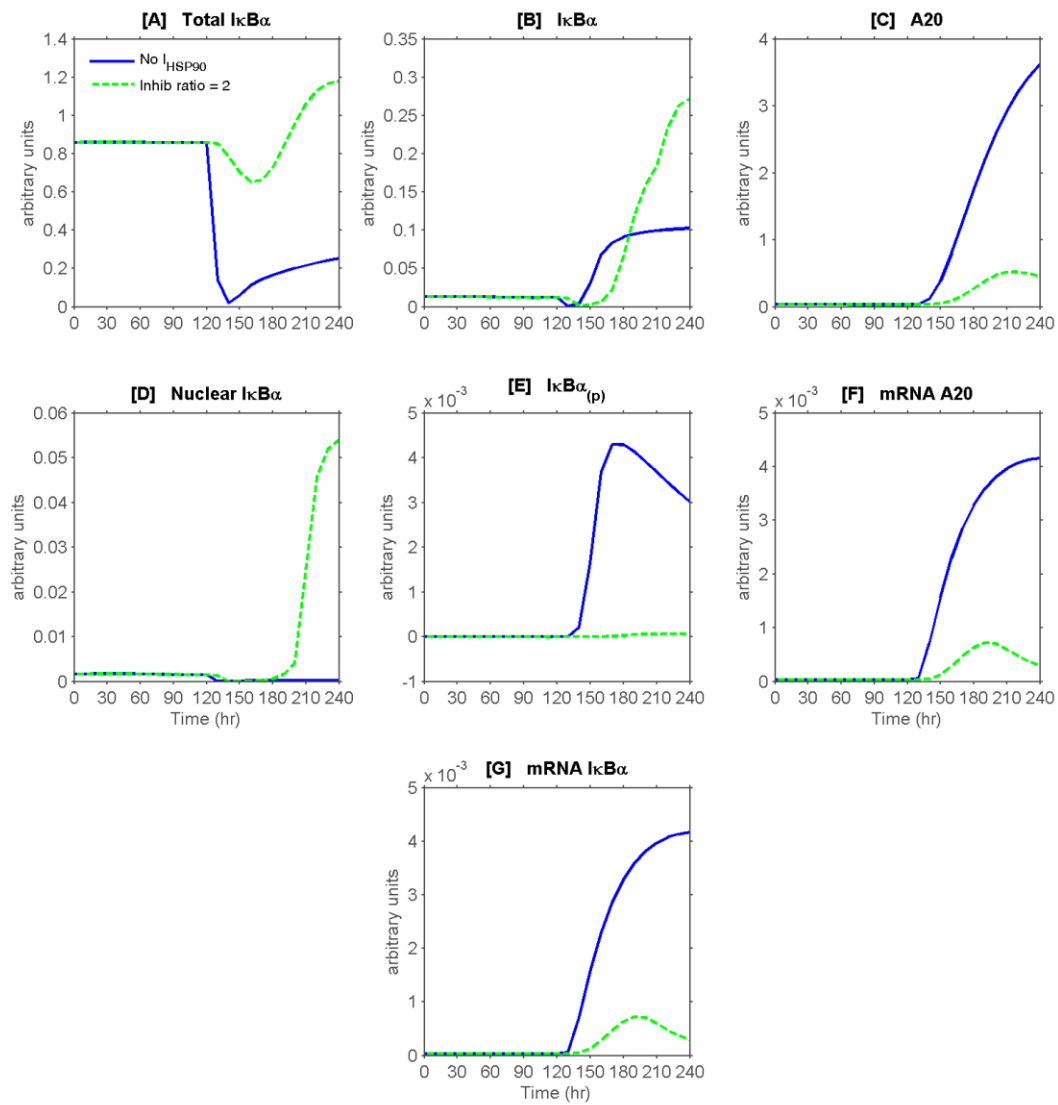


Figure D.2 Complete response of model to validation simulations (Part 2 of 2).

Appendix E. Model Validation data

| Time (min) | LPS (1µg/ml) | 17-DMAG (1µM) + LPS (1µg/ml) | Time (min) | LPS (1µg/ml) | 17-DMAG (1µM) + LPS (1µg/ml) | Time (min) | LPS (1µg/ml) | 17-DMAG (1µM) + LPS (1µg/ml) |
|------------|--------------|------------------------------|------------|--------------|------------------------------|------------|--------------|------------------------------|
| 0 | 1 | 0.898195 | 80 | 1 | 0.898195 | 170 | 5.766238 | 3.294117 |
| 10 | 1 | 0.898195 | 90 | 1 | 0.898195 | 180 | 5.473626 | 2.593503 |
| 20 | 1 | 0.898195 | 100 | 1 | 0.898195 | 190 | 8.871107 | 2.437203 |
| 30 | 1 | 0.898195 | 120 | 1 | 0.898195 | 200 | 7.397175 | 1.676776 |
| 40 | 1 | 0.898195 | 130 | 2.639719 | 0.898195 | 210 | 9.741172 | 3.238887 |
| 50 | 1 | 0.898195 | 140 | 6.240964 | 0.509956 | 220 | 4.055193 | 0.502285 |
| 60 | 1 | 0.898195 | 150 | 7.302567 | 1.577482 | 230 | 4.642854 | 1.85376 |
| 70 | 1 | 0.898195 | 160 | 6.749331 | 3.291877 | 240 | 1.828002 | 0.537183 |

Appendix F. Matlab Code

Appendix F.1 HSP90_TD_ODE.m – A Matlab function containing the set of ODEs for the HSP90-IKK-NFκB model.

```
HSP90_TD_ODE.m

%% Set of ODE equatoins that describe HSP90 and IKK interactions
% 1/18/2012
% By Samuel Shimp

function [outputs t] = HSP90_TD_ODE(t,x,tau,p,LPSpar,inhpar)

% define concentrations
IKKi = x(1);    IKKp = x(2);
HSP90 = x(3);  HSP90_IKK = x(4);
IKKK = x(5);   IKKKp = x(6);
NFkBcyto = x(7); NFkBnuc = x(8);

A20 = x(9);    A20t = x(10);
IkBa = x(11);  IkBanuc = x(12);
IkBap = x(13); IkBat = x(14);
inhib = x(15); HSP90_inhib = x(16);

IkBa_NFkB = x(17);
IkBa_NFkBnuc = x(18);
IkBap_NFkB = x(19);

%% Define Parameters

% IKK Synthesis/Degradation reactions
kprod = p(1);  kdeg = p(2);

% HSP90_IKK Binding
k1a = p(3);    k1b = p(4);

% IKK Activation with HSP90
k2a = p(5);

% Phtase reaction parameters
k4a = p(6);

% HSP90 inhibitor
k5a = p(7);    k5b = p(8);

%IKKK Phtase
ki3kphtase = p(9);  ki3k = p(10);

%A20 and IKK interaction
ka20 = p(11);
```

```

% Ikb params
a1 = p(12);      a2 = p(13);      a3 = p(14);
t1 = p(15);      i1 = p(16);      i1a = p(17);
e1a = p(18);     e2a = p(19);

% A20 parameters
c1 = p(20);      c2 = p(21);      c3 = p(22);
c4 = p(23);      c5 = p(24);      c5a = p(25);
c6a = p(26);

kv = 5; % kc = V/U -- the ratio of cytoplasmic and nuclear volumes

% LPS function
[LPS LPSlag] = LPSfun(t,tau,LPSpar(1),LPSpar(2),LPSpar(3));

% HSP90 inhibitor function
inhibtot = INHfun(t,inhpar(1),inhpar(2));
inhib = inhibtot - HSP90_inhib;

%% Define ODEs

dIKKi = kprod - kdeg*IKKi...
        - (k1a * HSP90 * IKKi) + (k1b * HSP90_IKK) ...
        + (k4a * IKKp) + (ka20 * IKKp * A20) ...
        + (k5a * HSP90_IKK * inhib);

dIKKp = - (kdeg * IKKp) + (k2a * HSP90_IKK * IKKp) ...
        - (k4a * IKKp) - (ka20 * IKKp * A20);

dHSP90 = -(k1a * HSP90 * IKKi) + (k1b * HSP90_IKK) ...
        + (k2a * HSP90_IKK * IKKp) ...
        - (k5a * HSP90 * inhib) + (k5b * HSP90_inhib);

dHSP90_IKK = (k1a * HSP90 * IKKi) - (k1b * HSP90_IKK) ...
        - (k2a * HSP90_IKK * IKKp) - (k5a * HSP90_IKK * inhib);

dIKKK = ki3kphtase * IKKp - ki3k * LPSlag * IKKK;

dIKKKp = ki3k * LPSlag * IKKK - ki3kphtase * IKKKp;

dNFkBcyto = (c6a * IkBa_NFkB) - (a1 * IkBa * NFkBcyto) ...
        + (t1 * IkBap_NFkB) - (i1 * NFkBcyto);

dNFkBnuc = (i1 * kv * NFkBcyto) - (a1 * NFkBnuc * IkBanuc);

dA20 = (c4 * A20t) - (c5 * A20);

dA20t = c2 + (c1 * NFkBnuc) - (c3 * A20t);

dIkBa = - (a2 * IKKp * IkBa) - (a1 * IkBa * NFkBcyto) ...

```

```

+ (c4 * IkBat) - (c5a * IkBa)...
- (ila * IkBa) + (e1a * IkBanuc);

dIkBanuc = - (a1 * NFkBnuc * IkBanuc) + (ila * kv * IkBa)...
- (e1a * kv * IkBanuc);

dIkBap = (a2 * IKKp * IkBa) - (t1 * IkBap);

dIkBat = c2 + (c1 * NFkBnuc) - (c3 * IkBat);

dHSP90_inhib = (k5a * HSP90 * inhib) - (k5b * HSP90_inhib)...
+ (k5a * HSP90_IKK * inhib);

dinhib = 0;

dIkBa_NFkB = + (a1 * IkBa * NFkBcyto)...
- (c6a * IkBa_NFkB)...
- (a3 * IKKp * IkBa_NFkB)...
+ (e2a * IkBa_NFkBnuc);

dIkBa_NFkBnuc = a1 * NFkBnuc * IkBanuc...
- (e2a * kv * IkBa_NFkBnuc);

dIkBap_NFkB = (a3 * IKKp * IkBa_NFkB) - (t1 * IkBap_NFkB);

outputs = [dIKKi, dIKKp, dHSP90, dHSP90_IKK,...
dIKKK, dIKKKp, dNFkBcyto, dNFkBnuc,...
dA20, dA20t, dIkBa, dIkBanuc, dIkBap, dIkBat,...
dinhib, dHSP90_inhib, dIkBa_NFkB, dIkBa_NFkBnuc, dIkBap_NFkB]';

end

```

Appendix F.2 LPSfun.m – A function that generates the LPS profile and the time delay for IKK activation.

```

function [LPS LPSlag] = LPSfun(t,taul,stmtm,LPSmax,dur)
%%%%%%%%%%%%%%%%%%%%%%%%%%%%%%%%%%%%%%%%%%%%%%%%%%%%%%%%%%%%%%%%%%%%%%%%
% This function computes the LPS concentration and the time-delayed LPS
% concentration for use in the HSP90_IKK ode functions.
%
% The function returns the LPS concentration and lagged LPS concentratoin
% LPSlag at time t.
%
% Inputs for the function are
% t, the time in seconds
% taul, the LPS lag time in seconds
% stmtm, time of stimulation in seconds
% LPSmas, the LPS stimulation concentration (uM)

```

```

% dur, the duration of the LPS stimulation in seconds
%
% Created by Samuel Shimp
% 4/16/2012
%%%%%%%%%%%%%%%%%%%%%%%%%%%%%%%%%%%%%%%%%%%%%%%%%%%%%%%%%%%%%%%%%%%%%%%%

%% Extracellular LPS concentration is a step function

LPS = 0;    % LPS concentration defaults to 0
if t > stmtm && t < stmtm + dur
    LPS = LPSmax;
end

%% LPS lag is a logistic function

a = 0.1;    % define logistic function slope

LPSlag = LPSmax.*(1./(1 + exp(-a.*(t - stmtm - 10/a) - tau1))));

if t-tau1 > stmtm + dur
    LPSlag = LPSmax.*(1./(1 + exp(a.*(t - stmtm - 10/a - dur) - tau1))));
end

return

```

Appendix F.3 INHfun.m – function that generates total HSP90 inhibitor concentration a time t using a logistic function.

```

function inhibtot = INHfun(t,trttm,trtcon)
%%%%%%%%%%%%%%%%%%%%%%%%%%%%%%%%%%%%%%%%%%%%%%%%%%%%%%%%%%%%%%%%%%%%%%%%
% This function computes the total HSP90 inhibitor concentration for use in
% HSP90_IKK ode functions.
%
% The function returns the total inhibitor concentration at time t.
%
% Inputs for the function are
% t, the time in seconds
% trttm, the time of treatment in seconds
% trtcon, treatment concentration in uM
%
% Created by Samuel Shimp
% 4/16/2012
%%%%%%%%%%%%%%%%%%%%%%%%%%%%%%%%%%%%%%%%%%%%%%%%%%%%%%%%%%%%%%%%%%%%%%%%
%% Total HSP90 inhibitor is represented by a logistic function

a = 0.1;    % define logistic function slope

inhibtot = trtcon.*(1./(1 + exp(-a.*(t - trttm - 10/a))));

return

```

Appendix F.4 HSP90_inhib_Model_Params.m – an m-file script developed to iteratively simulate the model with a different parameter value for each simulation run. This was used to generate the data for the parameter sensitivity study.

```

% HSP90_inhib_Model_Params.m

%%%%%%%%%%%%%%%%%%%%%%%%%%%%%%%%%%%%%%%%%%%%%%%%%%%%%%%%%%%%%%%%%%%%%%%%
% This m-file sets up and runs a simulation of the HSP90_TD_ODE assumingLPS
% stimulation at a specified point and for various levels of HSP90
% inhibition.
%
% Created: 3/27/12
% By: Samuel Shimp
%%%%%%%%%%%%%%%%%%%%%%%%%%%%%%%%%%%%%%%%%%%%%%%%%%%%%%%%%%%%%%%%%%%%%%%%

clear all; clc; clf;

%% Define Parameters
% IKK Synthesis/Degradation reactions
kprod = 1.250e-7;   kdeg = 1.250e-4;

% HSP90_IKK Binding
k1a = 1.0e-2;   k1b = 1.0e-3;
% k1a = 3e-3; %fitted

% IKK Activation with HSP90
k2a = 1.0e-2;
% k2a = 7.3e-2;   %fitted

% Phtase reaction parameters
k4a = 1.0e-2;

% HSP90 inhibitor
k5a = 1.0e-1;   k5b = 5.0e-2;

%IKKKp
ki3kphtase = 1e-4;   ki3k = 1e-2;
% ki3k = 8.48e-4; %fitted

%A20 and IKK interaction
ka20 = 0.1;
% ka20 = 0.001; %fitted

% Ikb params
a1 = 0.5;   a2 = 0.2;   a3 = 1;
t1 = 0.1;   i1 = 0.0025; i1a = 0.001;
e1a = 0.005; e2a = 0.01;

% A20 parameters
c1 = 5e-7;   c2 = 0.0;   c3 = 0.0004;
c4 = 0.5;   c5 = 0.0005; c5a = 0.0001;

```

```

c6a = 0.00002;

params = [kprod,kdeg,k1a,k1b,k2a,k4a,k5a,k5b,...
          ki3kphtase,ki3k,ka20,a1,a2,a3,t1,i1,ila,ela,e2a,...
          c1,c2,c3,c4,c5,c5a,c6a];

%% Simulate model response for HSP90_ODE with LPS stimulation
% This simulates the cellular response for the HSP90_ODE
% model under the with LPS stimulation and various levels of HSP90
% inhibition.

% Setup ODE solver parameters for LPS stimulation
tspan = 0:6*3600/250:6*3600; % Spanning 6 hours

% LPS function
tau = 30*60; % LPS time delay
stmtm = 2*3600; % Stimulate with LPS at time point
LPSmax = 1; % 0 or 1
dur = tspan(end);
LPSpar = [stmtm,LPSmax,dur];

%% Simulate HSP90_ODE
% Initial Conditions
IKKi_0 = 0.001; IKKp_0 = 0;
HSP90_0 = 9.9; HSP90_IKK_0 = 0.1;
IKKK_0 = 0.5; IKKKp_0 = 0;
NFkBcyto_0 = 0; NFkBnuc_0 = 0;

A20_0 = 0; A20t_0 = 0;
IkBa_0 = 0.009; IkBanuc_0 = 0.001;
IkBap_0 = 0; IkBat_0 = 0;
inhib_0 = 0; HSP90_inhib_0 = 0;

IkBa_NFkB_0 = 0.85; IkBa_NFkBnuc_0 = 0.01;
IkBap_NFkB_0 = 0;

%% Parameter sensitivity
% pertvar = 'ki3k';
% pert = [1e-2,1e-1,1e0,1e1,1e2,1e3]*1e-2 *eval(pertvar);

% Enter name of variable for pertvar
pertvar = 'ka20';
pert = [1e-2,1e-1,1e0,1e1,1e2]*1e0 *eval(pertvar);

% Cycle through parameter values
for count = 1:length(pert)

    IC = [IKKi_0,IKKp_0,...
          HSP90_0, HSP90_IKK_0,...
          IKKK_0,IKKKp_0,...
          NFkBcyto_0,NFkBnuc_0,...
          A20_0,A20t_0,IkBa_0,IkBanuc_0,IkBap_0,IkBat_0,...
          inhib_0,HSP90_inhib_0,IkBa_NFkB_0,IkBa_NFkBnuc_0,IkBap_NFkB_0];

    % Simulate for steady state initials
    disp('Now computing HSP90 NT/NS solution'); tic;

```

```

% redefine parameter vector
eval([pertvar, '=pert(count);']);
params = [kprod, kdeg, k1a, k1b, k2a, k4a, k5a, k5b, ...
ki3kptase, ki3k, ka20, a1, a2, a3, t1, i1, i1a, e1a, e2a, ...
c1, c2, c3, c4, c5, c5a, c6a];

% HSP90 inhibitor Concentration function
trttm = 1*3600; % Treat with inhibitor 1 hour into stimulation
trtcon = 0; % Treatment concentration, 0 or 1
inhpar = [trttm, trtcon];

LPSpar(2) = 0; % 0 or 1
tspan = [0, 1200*3600]; % Spanning 1200 hours
[HSPtout, HSPfout] = ode15s(@HSP90_TD_ODE, tspan, IC, [], ...
tau, params, LPSpar, inhpar); toc;

% Define new ICs
IC = HSPfout(end, :);
clear HSPtout;

%%%%%%%%%%%%%%%%%%%%%%%%%%%%%%%%%%%%%%%%%%%%%%%%%%%%%%%%%%%%%%%%%%%%%%%%
% Simulate for Stimulated, Non-Treated Solution
disp('Now computing HSP90 NT/S solution'); tic;

LPSpar(2) = 1; % LPS_max = 0 or 1;
tspan = 0:6*3600/50:6*3600; % Spanning 6 hours
[HSPtout, HSPfout] = ode15s(@HSP90_TD_ODE, tspan, IC, [], ...
tau, params, LPSpar, inhpar); toc;
timevarname{count} = ['HSPtout_' num2str(count)];
datavarname{count} = ['HSPfout_' num2str(count)];
eval([timevarname{count} '=HSPtout;']);
eval([datavarname{count} '=HSPfout;']);

if count == 1
    save('ParamSensData.mat', 'pertvar', 'pert', timevarname{count}, ...
datavarname{count});
else
    save('ParamSensData.mat', timevarname{count}, datavarname{count}, ...
'-append');
end
clear('HSPtout', 'HSPfout', timevarname{count}, datavarname{count})
end

```

Appendix F.5 ParamFit.m – a Matlab m-file script that estimates parameters for the model. Uses the cost function HSP90_error.m. Optimizes using the sqp algorithm in the fmincon function.

```

% ParamFit.m
%%%%%%%%%%%%%%%%%%%%%%%%%%%%%%%%%%%%%%%%%%%%%%%%%%%%%%%%%%%%%%%%%%%%%%%%
% This m-file estimates parameters for the HSP90-IKK model.

```

```

% 1) It defines parameters and initial conditions.
% 2) It defines bounds for parameter(s) being fitted.
% 3) It uses the fmincon function to search for parameters that minimize
% the error between the simulation and data published by Werner et. al.
% This error is computed by the cost function "HSP90_error."
% 4) It returns the optimized parameters and runs a simulation with the
% optimized parameters and compares the simulated output to the Werner
% data.
%
% Created: 4/13/12
% By: Samuel Shimp
%%%%%%%%%%%%%%%%%%%%%%%%%%%%%%%%%%%%%%%%%%%%%%%%%%%%%%%%%%%%%%%%%%%%%%%%

clear all; clc; clf;

%% 1) Define Parameters and initial conditions

% IKK Synthesis/Degradation reactions
kdeg = 1.250e-4;    kprod = 1.25e-7;

% HSP90_IKK Binding
k1a = 1.0e-2;      k1b = 1.0e-3;
k1a = 3e-3; %fmincon result
k1a = 5e-3; %fitted (3rd round)

% IKK Activation with HSP90
k2a = 1.0e-2;
k2a = 7.3e-2;    %fmincon result

% Phtase reaction parameters
k4a = 1.0e-2;    % IKK deactivation by phosphatase
k4a = 9.9e-3;    %fitted (3rd round)

% HSP90 inhibitor
k5a = 1.0e-1;      k5b = 5.0e-2;

%IKKKp
ki3kphtase = 0.0001;    ki3k = 0.01;
ki3k = 7.3e-2;    % fmincon result
ki3k = 0.001;    % fmincon result when tried with a20
ki3k = 0.000848;% fmincon result when tried with a20

%A20 and IKK interaction
ka20 = 0.1;
% fmincon result when tried with ki3k, stayed here on second attempt
ka20 = 0.001;

% Ikb params
a1 = 0.5;      a2 = 0.2;      a3 = 1;
t1 = 0.1;      i1 = 0.0025;    i1a = 0.001;
e1a = 0.005;    e2a = 0.01;

% A20 parameters
c1 = 5e-7;      c2 = 0.0;      c3 = 0.0004;
c4 = 0.5;      c5 = 0.0005;    c5a = 0.0001;
c6a = 0.00002;

```

```

params = [kprod,kdeg,k1a,k1b,k2a,k4a,k5a,k5b,ki3kphtase,ki3k,...
          ka20,a1,a2,a3,t1,i1,ila,ela,e2a,c1,c2,c3,c4,c5,c5a,c6a];

% Time delay
tau = 30*60;

% Initial Conditions
IKKi_0 = 0.001;      IKKp_0 = 0;
HSP90_0 = 9.9;      HSP90_IKK_0 = 0.1;
IKKK_0 = 0.5;      IKKKp_0 = 0;
NFkBcyto_0 = 0;    NFkBnuc_0 = 0;

A20_0 = 0;          A20t_0 = 0;
IkBa_0 = 0.009;    IkBanuc_0 = 0.001;
IkBap_0 = 0;       I kBat_0 = 0;
inhib = 0;         HSP90_inhib = 0;

IkBa_NFkB_0 = 0.85; IkBa_NFkBnuc_0 = 0.01;  IkBap_NFkB_0 = 0;

IC = [IKKi_0,IKKp_0,HSP90_0, HSP90_IKK_0,IKKK_0,IKKKp_0,...
      NFkBcyto_0,NFkBnuc_0,...
      A20_0,A20t_0,IkBa_0,IkBanuc_0,IkBap_0,IkBat_0,inhib,HSP90_inhib,...
      IkBa_NFkB_0,IkBa_NFkBnuc_0,IkBap_NFkB_0];

%% 2) Define parameter bounds
% define the initial parameter guess and search bounds

% x0 = [ki3k ka20];
% ub = x0.*[1e1 1e1];
% lb = x0.*[1e-1 1e-3];

x0 = [k1a k4a];
ub = x0.*[1e2 0.2e1];
lb = x0.*[5e-1 1e-2];

% x0 = [k1a k2a ki3k];
% ub = x0 .* [1e2 1e1 5];          % lower bound
% lb = x0 .* [1e-2 1e-1 1e-2];    % upper bound

if length(x0) == 1
    % lb1 = {'k2a'};
    lb1 = {'tau'};
end
if length(x0) == 2
    lb1 = {'ki3k','ka20'};
    lb1 = {'k1a','k4a'};
end
if length(x0) == 3
    lb1 = {'k1a','k2a','ki3k'};
end
if length(x0) == 4
    lb1 = {'k1a','k2a','ki3k','tau'};
end

```

```

end

%% 3) Search for Parameters
% prepare for the optimization
options = optimset(...
    'Display','iter',... % want to display lots of results
    'MaxFunevals',1000*length(x0),... % maximum number of iterations
    'TolCon',1e-12,... % termination tolerance for constraint violation
    'TolFun',1e-8,... % termination tolerance for f
    'TolX',1e-6,... % termination tolerance for x
    'Algorithm','sqp');
% Load Werner et. al. data
load IKKdata; % Loads data as two variables, t and IKKmeas.

% find the optimal parameter vector
xopt = fmincon('HSP90_error',x0,[],[],[],[],lb,ub,[],...
    options,tau,params,IKKmeas,t);

%% 4) Display optimized parameters and run a simulation for comparison

% display the results
fmt = '%s: %g < %g < %g';
for i = 1:length(xopt),
    disp(sprintf(fmt,lbl{i},lb(i),xopt(i),ub(i)))
end

% assign the optimized parameter values
if length(xopt) < 2
    % k2a = xopt;
tau = xopt;
end
if length(xopt) == 2
    % ki3k = xopt(1); ka20 = xopt(2);
    k1a = xopt(1); k4a = xopt(2);
end
if length(xopt) == 3
    k1a = xopt(1); k2a = xopt(2); ki3k = xopt(3);
end
if length(xopt) > 3
    k1a = xopt(1); k2a = xopt(2); ki3k = xopt(3);
    tau = xopt(4);
end

% Simulate model response
% LPS & HSP90 inhib functions
LPS_0 = 0;
stmtm = 2*3600; % Stimulate with LPS at time point
LPSmax = 1; % 0 or 1
dur = 45*60;
LPSpar = [stmtm,LPSmax,dur];

trtcon = 0;
trttm = 60*60;
inhpar = [trttm, trtcon];

% Simulate for steady-state

```

```

LPSpar(2) = 0; % set stimulation to 0 for steady state
[HSPtout,HSPfout] = ode15s(@HSP90_TD_ODE,[0,1200*3600],IC,[],...
    tau,params,LPSpar,inhpar);

IC = HSPfout(end,:);
clear HSPtout HSPfout

% Simulate with LPS activation
LPSpar(2) = LPSmax; % set stimulation to 1 for activation
[HSPtout,HSPfout] = ode15s(@HSP90_TD_ODE,t,IC,[],...
    tau,params,LPSpar,inhpar);

% Plot Response
mt = 'none'; lw = 2;
figure(1);
h = plot(HSPtout./3600,HSPfout(:,2)*1000+1,...
    t./3600,IKKmeas);
set(h,'LineWidth',lw,'Marker',mt);
set(h(1),'LineStyle','-','LineWidth',lw);
set(h(2),'LineStyle','none','Marker','o');
title('IKK activation profiles: Simulated and Measured in MEFs');
legend({'Simulated','Measured'});

save('ParamFitData1.mat','HSPtout','HSPfout','xopt')

```

Appendix F.6 HSP90_error.m – The function that calculates the cost function for estimating parameters in the model.

```

function e = HSP90_error(xopt,tau,params,IKKmeas,t)
%%%%%%%%%%%%%%%%%%%%%%%%%%%%%%%%%%%%%%%%%%%%%%%%%%%%%%%%%%%%%%%%%%%%%%%%
% This function simulates the HSP90_IKK model and computes the error
% (difference) between simulated IKKp and measured IKKp.
%
% Created: 4/13/12
% By: Samuel Shimp
%%%%%%%%%%%%%%%%%%%%%%%%%%%%%%%%%%%%%%%%%%%%%%%%%%%%%%%%%%%%%%%%%%%%%%%%
%% Simulate model response for HSP90_ODE with TNF stimulation

% This simulates the cellular response for the HSP90_ODE
% model under the with LPS stimulation.

% LPS function
stmtm = 2*3600; % Stimulate with LPS at time point
LPSmax = 1; % 0 or 1
dur = 45*60; % Duration of stimulation in experimental data
LPSpar = [stmtm,LPSmax,dur];

% HSP90 inhibitor function
trttm = 60*60;
trtcon = 0;
inhpar = [trttm, trtcon];

%% Simulate HSP90_ODE

```

```

% assign the optimized parameter values
if length(xopt) < 2
%     params(5) = xopt; %k2a
    tau = xopt;
end
if length(xopt) == 2
%     params(10) = xopt(1);    params(11) = xopt(2);    %ki3k and ka20
    params(3) = xopt(1);    params(6) = xopt(2);
end
if length(xopt) == 3
    params(3) = xopt(1);    params(5) = xopt(2);    params(10) = xopt(3);
    %k1a                    k2a                    ki3k
end
if length(xopt) > 3
    params(3) = xopt(1);    params(5) = xopt(2);    params(10) = xopt(3);
    %k1a                    k2a                    ki3k
    tau = xopt(4);
end

% Initial Conditions
IKKi_0 = 0.001;    IKKp_0 = 0;
HSP90_0 = 9.9;    HSP90_IKK_0 = 0.1;
IKKK_0 = 0.5;    IKKKp_0 = 0;
NFkBcyto_0 = 0;    NFkBnuc_0 = 0;

A20_0 = 0;    A20t_0 = 0;
IkBa_0 = 0.009;    IkBanuc_0 = 0.001;
IkBap_0 = 0;    I kBat_0 = 0;

inhib = 0;    HSP90_inhib = 0;

IkBa_NFkB_0 = 0.85; IkBa_NFkBnuc_0 = 0.01;    IkBap_NFkB_0 = 0;

IC = [IKKi_0,IKKp_0,HSP90_0, HSP90_IKK_0,IKKK_0,IKKKp_0,...
    NFkBcyto_0,NFkBnuc_0,...
    A20_0,A20t_0,IkBa_0,IkBanuc_0,IkBap_0,IkBat_0,inhib,HSP90_inhib,...
    IkBa_NFkB_0,IkBa_NFkBnuc_0,IkBap_NFkB_0];

% Simulate for steady-state
inhpar(2) = 0;
LPSpar(2) = 0; % set stimulation to 0 for steady state
[HSPtout,HSPfout] = ode15s(@HSP90_TD_ODE,[0,1200*3600],IC,[],...
    tau,params,LPSpar,inhpar);

IC = HSPfout(end,:);
clear HSPtout HSPfout

% Simulate for LPS activation
LPSpar(2) = LPSmax; % set stimulation to 1 for activation
[HSPtout,HSPfout] = ode15s(@HSP90_TD_ODE,t,IC,[],...
    ,tau,params,LPSpar,inhpar);

% Normalize Simulated data
% HSPfout = HSPfout(:,2).*1000+1;
HSPfout = HSPfout(:,2).*1500+1; % for last run

```

```

e = (HSPfout-IKKmeas);

e = sum(e .* e);

return

```

Appendix F.7 HSP90_inhib_Model_InhibParams.m – A Matlab m-file script that runs model simulations for multiple values of the inhibitor parameters and for multiple concentrations ratios of inhibitor.

```

% HSP90_inhib_Model_InhibParams

%%%%%%%%%%%%%%%%%%%%%%%%%%%%%%%%%%%%%%%%%%%%%%%%%%%%%%%%%%%%%%%%%%%%%%%%
% This m-file simulates the response of the HSP90_TD_ODE model with and
% without inhibitor treatment. It allows for variation of parameter
% specified by the user and saves the outputs for later plotting.
%
% The file performs the following tasks
% 1) Defines parameters, initial conditions, and inputs for LPSfun and
% INHfun.
% 2) Iteratively performs simulations with each iteration using a different
% value for the selected parameter. Each iteration runs a 1200 hour
% equilibration simulation and then an LPS stimulation run with inhibitor.
% On the first iteration the NT/S solution is computed just before the T/S
% solution. All LPS stimulation solutions are saved for later plotting.
%
% Created: 4/18/12
% By: Samuel Shimp
%%%%%%%%%%%%%%%%%%%%%%%%%%%%%%%%%%%%%%%%%%%%%%%%%%%%%%%%%%%%%%%%%%%%%%%%

clear all; clc; clf;

%% Define Parameters

% Stage 2 Parameters values

% IKK Synthesis/Degradation reactions
kdeg = 1.250e-4;    kprod = 1.25e-7;

% HSP90_IKK Binding
k1a = 5e-3;    k1b = 1.0e-3;    % k1a fitted

% IKK Activation with HSP90
k2a = 7.3e-2;    % fitted

% Phtase reaction parameters
k4a = 9.9e-3;    % fitted

% HSP90 inhibitor
k5a = 1.0e-1;    k5b = 1.0e-3;
% k5b = 0;

```

```

%IKKKp
ki3kphatase = 0.0001;    ki3k = 8.48e-4;    % ki3k fitted

%A20 and IKK interaction
ka20 = 0.001;    % fitted

% Ikb params
a1 = 0.5;    a2 = 0.2;    a3 = 1;
t1 = 0.1;    i1 = 0.0025;    i1a = 0.001;
e1a = 0.005;    e2a = 0.01;

% A20 parameters
c1 = 5e-7;    c2 = 0.0;    c3 = 0.0004;
c4 = 0.5;    c5 = 0.0005;    c5a = 0.0001;
c6a = 0.00002;

% Initial Conditions
IKKi_0 = 0.001;    IKKp_0 = 0;
HSP90_0 = 9.9;    HSP90_IKK_0 = 0.1;
IKKK_0 = 0.5;    IKKKp_0 = 0;
NFkBcyto_0 = 0;    NFkBnuc_0 = 0;

A20_0 = 0;    A20t_0 = 0;
IkBa_0 = 0.009;    IkBanuc_0 = 0.001;
IkBap_0 = 0;    IkBat_0 = 0;
inhib_0 = 0;    HSP90_inhib_0 = 0;

IkBa_NFkB_0 = 0.85; IkBa_NFkBnuc_0 = 0.01;    Ikbap_NFkB_0 = 0;

% HSP90 inhibitor Concentration function
trttm = 1*3600; % Treat with inhibitor 1 hour into stimulation
trtcon = 1;    % Treatment concentration, 0 or 1
INHpar = [trttm trtcon];

% LPS function
tau = 30*60;    % 30 minutes (in unit sof seconds)
stmtm = 2*3600; % Stimulate with LPS at time point
LPS_max = 1;    % 0 or 1
dur = 6*3600;    % Once LPS on, stimulate for entire simulation
LPSpar = [stmtm,LPS_max,dur];

%% Parameter sensitivity
kval = 'k5a';
rat = 0.9;
krange = [10,1,0.1] .* k1a;
% k5b = k1a*krange(3)*1e-1;

% Cycle through parameter values
for iter = 1:length(krange)
    IC = [IKKi_0,IKKp_0,HSP90_0, HSP90_IKK_0,...
          IKKK_0,IKKKp_0,NFkBcyto_0,NFkBnuc_0,...
          A20_0,A20t_0,IkBa_0,IkBanuc_0,IkBap_0,IkBat_0,...
          inhib_0,HSP90_inhib_0,IkBa_NFkB_0,IkBa_NFkBnuc_0,Ikbap_NFkB_0];

    % Simulate for steatdy state initials
    disp('Now computing Steady State ICs'); tic

```

```

% Redefine parameter vector
eval([kval, '=krange(iter);']);
%   k5b = k5a*1e1; k5b=0;
params = [kprod, kdeg, k1a, k1b, k2a, k4a, k5a, k5b, ...
ki3kptase, ki3k, ka20, a1, a2, a3, t1, i1, i1a, e1a, e2a, ...
c1, c2, c3, c4, c5, c5a, c6a];

% Simulate
LPSpar(2) = 0; % set concnetration to zero for steady state
INHpar(2) = 0; % set concentration to zero for steady state
tspan = [0 1200*3600]; % spanning 1200 hours

[HSPtout, HSPfout] = ode15s(@HSP90_TD_ODE, tspan, IC, [], ...
    tau, params, LPSpar, INHpar); toc;

% Define new ICs
IC = HSPfout(end, :)' ;
clear HSPtout HSPfout

%%%%%%%%%%%%%%%%%%%%%%%%%%%%%%%%%%%%%%%%%%%%%%%%%%%%%%%%%%%%%%%%%%%%%%%%
% Simulate for with HSPO90 inhibition and LPS Stimulation
if iter < 2
    disp('Now computing solution for LPS Stimulation Only'); tic

    LPSpar(2) = LPS_max; % redefine to turn on LPS
    INHpar(2) = 0; % redefine to turn on inhibitor treatment
    tspan = linspace(0, 6*3600, 100); % span 6 hours
    [HSPtout HSPfout] = ode15s(@HSP90_TD_ODE, tspan, IC, [], ...
        tau, params, LPSpar, INHpar); toc;

    % Record for plotting
    tNTS = HSPtout;
    fNTS = HSPfout;
    if rat < 0.95; sim = '1'; end
    if rat >= 0.95 && rat < 1.05; sim = '2'; end
    if rat >= 1.05; sim = '3'; end
    savefile = ['InhParDat' sim '.mat'];
    save(savefile, 'kval', 'krange', 'tNTS', 'fNTS', 'rat');
    clear HSPtout HSPfout
end

% Begin Simulation WITH HSP90 inhibitor & LPS stimulation
disp(['Now computing Solution for Treatment & LPS Stimulation for '...
    'iteration number ' num2str(iter)]); tic;

LPSpar(2) = LPS_max; % redefine to turn on LPS
% redefine trtcon to turn on inhibitor treatment
INHpar(2) = rat*trtcon*sum(IC(3:4));
tspan = linspace(0, 6*3600, 100); % span 6 hours
[HSPtout HSPfout] = ode15s(@HSP90_TD_ODE, tspan, IC, [], ...
    tau, params, LPSpar, INHpar); toc;

% Record for plotting
tTSnm{iter} = ['HSPtout_' num2str(iter)];
fTSnm{iter} = ['HSPfout_' num2str(iter)];
temp = ['trtcon_' num2str(iter)];

```

```

eval([tTSnm{iter} '=HSPtout;']);
eval([fTSnm{iter} '=HSPfout;']);
eval([temp '=INHpar(2);']);

save(savefile,tTSnm{iter},fTSnm{iter},temp,'-append');
clear('HSPtout','HSPfout',tTSnm{iter},fTSnm{iter},temp);

end

```

Appendix F.8 Validate.m – An m-file script that runs model simulations and compares the simulation data to the measured NF- κ B data.

```

% Validate.m

%%%%%%%%%%%%%%%%%%%%%%%%%%%%%%%%%%%%%%%%%%%%%%%%%%%%%%%%%%%%%%%%%%%%%%%%

%
% Created: 4/13/12
% By: Samuel Shimp
%%%%%%%%%%%%%%%%%%%%%%%%%%%%%%%%%%%%%%%%%%%%%%%%%%%%%%%%%%%%%%%%%%%%%%%%

clear all; clc; clf;

%% 1) Define Parameters and initial conditions

% IKK Synthesis/Degradation reactions
kdeg = 1.250e-4;    kprod = 1.25e-7;

% HSP90_IKK Binding
k1a = 1.0e-2;      k1b = 1.0e-3;
k1a = 3e-3; %fmincon result
k1a = 5e-3; %fitted (3rd round)

% IKK Activation with HSP90
k2a = 1.0e-2;
k2a = 7.3e-2; %fmincon result

% Phtase reaction parameters
k4a = 1.0e-2; % IKK deactivation by phosphatase
k4a = 9.9e-3; %fitted (3rd round)

% HSP90 inhibitor
k5a = 1e-2;      k5b = 1.0e-3;

%IKKKp
ki3kphtase = 0.0001;    ki3k = 0.01;
ki3k = 7.3e-2; % fmincon result
ki3k = 0.001; % fmincon result when tried with a20
ki3k = 0.000848;% fmincon result when tried with a20

%A20 and IKK interaction
ka20 = 0.1;

```

```

% fmincon result when tried with ki3k, stayed here on second attempt
ka20 = 0.001;

% IkB params
a1 = 0.5;      a2 = 0.2;      a3 = 1;
t1 = 0.1;      i1 = 0.0025;   i1a = 0.001;
e1a = 0.005;   e2a = 0.01;

% A20 parameters
c1 = 5e-7;     c2 = 0.0;      c3 = 0.0004;
c4 = 0.5;      c5 = 0.0005;   c5a = 0.0001;
c6a = 0.00002;

params = [kprod, kdeg, k1a, k1b, k2a, k4a, k5a, k5b, ki3kphtase, ki3k, ...
          ka20, a1, a2, a3, t1, i1, i1a, e1a, e2a, c1, c2, c3, c4, c5, c5a, c6a];

% Time delay
% tau = 86030*60;
tau = 4*60;

% Initial Conditions
IKKi_0 = 0.001;      IKKp_0 = 0;
HSP90_0 = 9.9;      HSP90_IKK_0 = 0.1;
IKKK_0 = 0.5;      IKKKp_0 = 0;
NFkBcyto_0 = 0;     NFkBnuc_0 = 0;

A20_0 = 0;          A20t_0 = 0;
IkBa_0 = 0.009;     IkBanuc_0 = 0.001;
IkBap_0 = 0;        I kBat_0 = 0;
inhib = 0;          HSP90_inhib = 0;

IkBa_NFkB_0 = 0.85; IkBa_NFkBnuc_0 = 0.01;  IkBap_NFkB_0 = 0;

IC = [IKKi_0, IKKp_0, HSP90_0, HSP90_IKK_0, IKKK_0, IKKKp_0, ...
      NFkBcyto_0, NFkBnuc_0, ...
      A20_0, A20t_0, IkBa_0, IkBanuc_0, I kBap_0, I kBat_0, inhib, HSP90_inhib, ...
      IkBa_NFkB_0, IkBa_NFkBnuc_0, I kBap_NFkB_0];

%% 2) Run a simulation for comparison

% Simulate model response
% LPS & HSP90 inhib functions
LPS_0 = 0;
stmtm = 2*3600; % Stimulate with LPS at time point
LPS_max = 1; % 0 or 1
dur = 45*60;
LPSpar = [stmtm, LPS_max, dur];

trtcon = 1;
trttm = 60*60;
INHpar = [trttm, trtcon];

% Simulate for steady-state
LPSpar(2) = 0; % set stimulation to 0 for steady state

```

```

INHpar(2) = 0; % Set inhibitoin to 0 for steady state
[HSPtout,HSPfout] = ode15s(@HSP90_TD_ODE,[0,1200*3600],IC,[],...
    tau,params,LPSpar,INHpar);

IC = HSPfout(end,:);
clear HSPtout HSPfout

% Load experimental data
load NFkBdata

% Simulate for with HSP90 inhibition and LPS Stimulation
disp('Now computing solution for LPS Stimulation Only'); tic

LPSpar(2) = LPS_max; % redefine to turn on LPS
INHpar(2) = 0; % redefine to turn on inhibitor treatment
% tspan = linspace(0,2*3600,100); % span 2 hours
[tNTS fNTS] = ode15s(@HSP90_TD_ODE,t,IC,[],...
    tau,params,LPSpar,INHpar); toc;

% Begin Simulation WITH HSP90 inhibitor & LPS stimulation
disp('Now computing Solution for Treatment & LPS Stimulation'); tic;

LPSpar(2) = LPS_max; % redefine to turn on LPS
% redefine trtcon to turn on inhibitor treatment
INHpar(2) = 2*trtcon*sum(IC(3:4));
% tspan = linspace(0,2*3600,100); % span 6 hours
[HSPtout HSPfout] = ode15s(@HSP90_TD_ODE,t,IC,[],...
    tau,params,LPSpar,INHpar); toc;

% Record for plotting
savefile = 'validata';
save(savefile,'tNTS','fNTS','HSPtout','HSPfout');

% Plot Response
mt = 'none'; lw = 2;
figure(1);
h = plot(tNTS./60,fNTS(:,8)*1.5+1,HSPtout./60,HSPfout(:,8)*1.5+1,...
    t./60,NFkBmeas(1,:),t./60,NFkBmeas(2,:));
set(h,'LineWidth',lw,'Marker',mt);
set(h(1),'LineStyle','-','LineWidth',lw);
set(h(2),'LineStyle','--','LineWidth',lw);
set(h(3),'LineStyle','-','Marker','o','LineWidth',lw/2);
set(h(4),'LineStyle','-','Marker','^','LineWidth',lw/2);
title('NF-{\kappa}B in J774s');
legend({'Simulated LPS CTRL','Simulated 17-DMAG','Measured LPS CTRL',...
    'Measured 17-DMAG'},'Location','NorthWest');

```